RESPONSES TO
U.S. NRC COMMENTS

REGARDING THE

Topical Safety Analysis Report for the NAC Storable Transport Cask for use at an Independent Spent-Fuel Storage Installation

Project No. M-55

November 1990

Nuclear Assurance Corporation
6251 Crooked Creek Road
Norcross, Georgia 30092
Telephone: (404) 447-1144
Telex: 6827020, 6827114
Facsimile: (404) 447-1797

2.2.5 Combined Load criteria

U.S. NRC Comment:

(a) In Tables 2.2-1 and 2.2-2, is S_m the ASME allowable stress intensity as defined in ASME Boiler and Pressure Vessel Code Section III, Appendix I. Is the definition of S_m different for the stainless steel, aluminum, and bolting materials?

(b) Since the accident condition stress limits in Tables 2.2-1 and 2.2-2 allow plastic deformation to occur, the presence of plastic deformation needs to be addressed in cask components essential for fuel removal. After an accident, the fuel rods may not be easily removed if permanent plastic deformation has occurred in the components around the rods.

(c) In Table 2.2-1, no margin of safety is built into the bolt allowable stresses. Yielding of the bolts should not be allowed. It is suggested that the ASME allowable stress intensity be used, where S_m is 1/3 of the yield stress. The average stress intensity is limited to 2 S_m, or 2/3 of the yield stress, while the maximum stress intensity in a bolt is not allowed to exceed 3 S_m, or the yield stress. Table 2.2-2 has a more restrictive stress criteria for the noncontainment bolts than Table 2.2-1 has for the containment bolts. Containment bolts are more critical to the cask performance and should have the more restrictive criteria.

(d) In Table 2.2-2, should the allowable stress condition be "the less of" the listed values instead of "the greater of" the two? It is unusual to define a design limit using the less restrictive of two values.

(e) In Table 2.2-2, no margin of safety is built into the allowable stress limits for primary stress under normal conditions. Yielding should not be allowed in any material under normal primary stress. Moreover, it is not reasonable to use the yield stress as the stress limit for both primary membrane and primary membrane plus primary bending stress categories.

NAC Response

(a) In Tables 2.2-1 and 2.2-2, S_m is the allowable stress intensity as defined in the ASME Boiler and Pressure Vessel Code, Section III, Appendix I. This definition of S_m applies to stainless steel and bolting materials. The ASME Boiler and Pressure Vessel Code does not define S_m values for aluminum alloys. Aluminum alloy components comprise the NAC-STC fuel basket; the allowable stress for these components is defined as the material yield strength at normal operating temperature (refer to Sections 3.4.10.3 and 11.2.4.7.2). Tables 2.2-1 and 2.2-2 will be revised to include definitions of S_m (allowable stress intensity), S_y (material yield strength), and S_u (material ultimate strength).

(b) No significant plastic deformation occurs in the NAC-STC cask body for any load condition, except for the outer shell during the pin puncture event. Since the allowable stress limit is the material yield strength, S_y, for all load conditions, no plastic deformation occurs in the fuel basket for any load condition. It is also noted that according to "Dynamic Impact Effects on Spent Fuel Assemblies", by hun, R., Witte, M., and Schwartz, M., UCID-21246, Lawrence Livermore National Laboratory, October 1987, damage is not likely to occur to the Westinghouse 17 x 17 fuel assembly for a 63g side drop or an 82g end drop loading. (Of the fuel assemblies examined, the Westinghouse 17 x 17 assembly had the "weakest" structural parameters.) It is, thus, concluded that the fuel in the NAC-STC may be removed with minimal difficulty following the hypothetical accident event. This conclusion was verified by the results of a NAC-STC quarter-scale model 30-foot side drop, which inadvertently produced an impact force equal to 5.5 times the design impact force (1200g quarter-scale = 300g full scale), but produced essentially no deformation of the support disks in the basket. (One support disk did incur significant local deformation due to direct compression loading by deformation through the outer and inner shells.) All of the quarter-scale model "dummy" fuel assemblies were removed without difficulty. (Refer to Section 2.10.6, NAC-STC SAR).

(c) An inherent margin of safety exists in the bolt allowable stresses because they are based on minimum specified material strengths; actual material strengths always exceed the specified minimums, often by a significant amount.

Because the bolts in the NAC-STC that are important to safety are preloaded in excess of their maximum calculated load for any loading condition, a constant maximum tensile stress state exists in the bolts throughout the period of their installation; for this well-defined, constant bolt load condition, the allowable bolt stress intensity is limited to approximately 70 percent of the material yield strength, 0.7 S_y, according to NAC's standard design practice for storage and transport casks even though the stated design criteria for the allowable bolt stress intensity is the material yield strength; this NAC design practice essentially reflects the suggested ASME allowable stress intensity criteria for bolts. Yielding of bolts is not permitted and does not occur since a significant margin of safety against material yield strength exists.

NAC agrees that containment bolts are more critical to the cask performance and should have the more restrictive stress criteria; Table 2.2-2 will be corrected to reflect a stress criteria for noncontainment bolts that is equal to, or less restrictive, than the containment bolt stress criteria.

(d) The definition of the allowable stress condition as "the Greater of" for normal and off-normal conditions for noncontainment structures reflects a previously established criteria to cover a wide variety of materials and structures. Since this broad, general criteria is not necessary for typical noncontainment component materials and structures for casks, the allowable stress limits for normal and off-normal conditions in Table 2.2-2 will be revised to be S_y, the material yield strength ($0.6S_y$ for pure shear).

(e) As discussed in Paragraph (c), an inherent margin of safety exists in the allowable stress limits because they are based on minimum specified material strengths, and fabrication experience has shown that actual material strengths exceed the specified minimums by more than ten percent. Yielding is not permitted in any material for any stress category for any load condition and none occurs because the calculated maximum stress intensity is limited to be less than, or equal to, the specified minimum material yield strength.

The material yield strength is conservatively defined as the allowable stress intensity limit for both the primary membrane and the primary membrane plus primary bending stress categories to ensure that yielding does not occur anywhere in the noncontainment components of the NAC-STC for the normal and off-normal load conditions; thus, elastic analysis methods are appropriate throughout the TSAR.

2.3.4.2 Error Contingency Criteria

U.S. NRC Comment

In the list of criticality analyses criterion, what is meant by: "(4) no structural material present in the assembly?" The components in the basket are considered structural since they support the fuel rods?

NAC Response

The term "assembly" refers only to the fuel assembly. It does not refer to the basket assembly, which includes the circular support disks, tubes, and connecting rods. The statement "no structural material present in the assembly" refers to the assumption that no spacer grids or end fittings are present.

2.3.6 Fire and Explosion Protection
(Table 2.3-1, Manufacturing Acceptance Leak Test Criteria)

U.S. NRC Comment

What are the minimum preload and gasket seating load required to meet the leak test criteria given in Table 2.3-1?

NAC Response

The metallic o-rings and the reinforced TFE o-rings are subjected to the manufacturers' specified compressions, rather than predetermined preloads, to meet the leak criteria given in Table 2.3-1. The Helicoflex metallic o-ring in the inner lid, for example, has to be compressed from its original 0.375-inch diameter to a height of 0.295 inch to meet the leakage criteria of 1×10^{-6} to 1×10^{-9} std-cm^3/sec, at one atmosphere differential pressure. The inner lid bolts are subjected to a preload sufficient to resist the applied external forces to ensure that the specified compression is maintained. The specified compression force is 2400 pounds per inch of circumference of the metallic o-ring. The 0.210-inch diameter Shambam TFE o-ring has a specified compressed height for sealing of 0.186 inch, which requires a compression force of 40 pounds per linear inch of its circumference.

3.1.2.2.1 Cask Body and Lids

U.S. NRC Comments

Inconsistency with Tables 2.2-1 and 2.2-2 concerning the stress limit for primary membrane plus primary bending stress intensity. The tables list that the stress limit is 1.5 S_m, while this section states that the limit is S_m.

Since the SCANS bending stress is constant over the local cross-section, the stress values calculated by SCANS are primary membrane stresses, not primary membrane plus bending. Therefore, the use of S_m as the limit for SCANS bending stress is appropriate and not over conservative.

NAC Response

Section 3.1.2.2.1 will be revised to use S_m as the stress limit for the primary membrane stress intensities that are calculated by the SCANS computer program. This makes the stress limit consistent with Tables 2.2-1 and 2.2-2.

3.1.2.2.5 Fuel Basket

U.S. NRC Comments

(a) The limit state of 2/3 yield strength applies only to ductile failure modes. While no authoritative code or standard has been cited for this structural criterion, it appears to reflect NRC Regulatory Guide 7.6. If such is the case, this criterion is only applicable to materials listed in Appendix I of the ASME code or those covered by an ASTM standard that specifies a minimum value for the yield strength. It should also be pointed out that the allowable stress is the lesser of the 2/3 yield strength and 1/3 ultimate tensile strength.

(b) The 1.5 factor of safety for the noncontainment basket components is inconsistent with the 1.0 factor (greater of S_m or S_y) listed in Table 2.2-2.

(c) The reference to Section 11.2.13.3 seems to be in error since the last section in Chapter 11 is 11.2.13.2. Further information about the structural evaluation criteria for the basket components would be useful.

NAC Response

(a) The second sentence of the first paragraph in Section 3.1.2.2.5 is erroneous information and will be deleted. The allowable stress criteria for the fuel basket components is properly stated in the third paragraph of Section 3.1.2.4.2.

(b) As noted in Part (a), this erroneous data will be deleted.

(c) The correct section number should be 11.2.4.7. As noted in Part (a), the allowable stress criteria for the fuel basket components is defined in the third paragraph of Section 3.1.2.4.2.

3.1.2.4.2 Non-Confinement Structures

U.S. NRC Comment

The specification of yield strength as the allowable stress for aluminum alloys is in contradiction with section 3.1.2.2.5 which limits the stresses to 2/3 of yield at the normal operating temperature. A yield strength limit under accident conditions is conservative for a ductile failure mode but may not be for a brittle fracture failure mode.

NAC Response

The allowable stress limit for the aluminum alloy fuel basket components is correctly stated in Section 3.1.2.4.2 as the material yield strength determined at operating temperature. As noted in the response to Comment 3.1.2.2.5, the second sentence of the first paragraph in Section 3.1.2.2.5 is erroneous in information.

Based on the information presented in the last paragraph in Section 3.1.2.5.1, the aluminum alloy components of the fuel basket possess adequate fracture toughness to preclude a brittle fracture failure mode; thus, the material yield strength is a conservative allowable stress limit for all loading conditions.

3.1.2.5.1 Brittle Fracture

U.S. NRC Comment

The analysis intended to demonstrate the brittle fracture resistance of bolts is not applicable to bolts. The methods of NUREG/CR-1815 apply only to plates and only to cases involving arrest of a moving crack that penetrates the thickness of the plate. The application to bolting is meaningless since bolt diameters cannot be equated to plate thicknesses.

NAC Response

NAC agrees that the brittle fracture analysis presented in this section is not applicable to bolts and so states in the last paragraph on Page 3.1.2-7 of the TSAR. The analysis is presented only to demonstrate that the bolt material possesses a level of resistance to brittle fracture that is comparable to the other cask component materials. Current standard practice for engineering evaluation of bolt materials requires no brittle fracture evaluation, since bolts are not considered as fracture-critical components because multiple load paths exist and because bolted systems are designed to be redundant. The TSAR will be revised to further clarify the intent of the brittle fracture evaluation that is presented in this section.

3.1.2.5.2.1 Cask Body

U.S. NRC Comment

(a) Justification is needed for the stress concentration factor of 3. Why is this value conservative? Regulatory Guide 7.6 suggests a value of 4.

(b) The evaluation of the number of fatigue cycles to failure is incomplete and incorrect if NRC Regulatory Guide 7.6 was used. If the stress concentration factor is unknown then a value of 4 should be assumed (Paragraph 3d). Also, it must show that S_n (the range of primary and secondary stress under normal conditions) is less than 3 S_m before the calculated or assumed peak stress is used to read the number of cycles to failure directly from the fatigue curve. If S_n is greater than 3 S_m the peak stress must be multiplied by the appropriate K_e factor defined in Paragraph 4b of Regulatory Guide 7.6 prior to reading the number of cycles to failure from the curve.

NAC Response

(a) Regulatory Guide 7.6 suggests the use of a value of 4 for stress concentration factors "in regions where this factor is unknown". A stress concentration factor of 4 is a relatively high value that represents an acute structural discontinuity. The NAC-STC has been carefully designed to include generous radii and/or tapers at locations of structural discontinuity and to locate holes in regions of massive material/low stress. The classical stress concentration factor for screw threads and small holes is 3. Therefore, the assumption of a stress concentration factor of 3 for the NAC-STC is reasonable and conservative. Rigorous finite element analyses using the ANSYS computer program have been performed for the NAC-STC; based on the ANSYS results for the 30-foot end, side, corner, and oblique drops, the maximum stress concentration factor in the cask body and lids is 2.0 (holes and bolt threads are not modelled).

(b) As discussed in (a), the stress concentrations in the NAC-STC have been minimized to the extent possible by good engineering design practice and the stress concentration factors are known throughout the cask; thus, a stress concentration factor of 3 is reasonable and conservative.

Table 3.4-7 demonstrates that for the bounding Normal Operation load conditions, Heat and Col, the range of primary plus secondary stresses is much less than the 3.0 s_m stress limit; thus, the use of a K_e factor is not appropriate and the evaluation of the number of fatigue cycles to failure is complete and correct using the methods of Regulatory Guide 7.6.

3.1.2.5.2.3.1 Inner Lid Bolts

U.S. NRC Comment

(a) A typical value of the torque coefficient is 0.2, not 0.085. Please explain or provide justification for the low value and the possible effects of over estimating the preload.

(b) The preload, P, and tensile stress, S_t, calculated in this section differ slightly from the P and S_t values calculated in 3.4.6.6.1.

(c) Under an applied load, the bolt load can be slightly greater than the preload. In addition, the preload cannot be expected to be precisely applied and controlled. For these reasons, using the yield stress as the limit for the preload will expose the design to the risk of plastically deformed closure bolts. Please review.

NAC Response

(a) NAC agrees that the torque coefficient should be 0.20 as given in Shigley, Page 246. The TSAR will be revised to reflect the torque coefficient of 0.20. (For standard screw threads, a torque coefficient of 0.20 reflects a coefficient of friction of 0.15).

(b) For consistency with the revision of Paragraph (a), the coefficient of friction in Section 3.4.6.6.1 is revised from the value of 0.06 to value of 0.15. Then for the 1-1/2 - 8 UNC bolt, the torque coefficient calculated using the Roehrich equation is 0.189. The slight difference in the calculated values of the bolt preload and tensile stresses in Sections 3.1.2.5.2.3.1 and 3.4.6.6.1 are due to the difference in the values of the torque coefficient used 0.20 versus 0.189. This difference is insignificant and the specified bolt torque load for installation exceeds the higher of the two values anyway.

(c) The inner lid closure bolt analysis has been reviewed. NAC agrees that the specified bolt preload may not be precisely applied and controlled due to various factors. However, the specified installed bolt torque is calculated to provide a bolt preload that exceeds the maximum applied bolt load. The total bolt stress, applied preload plus differential thermal expansion, is approximately 76 percent of the bolt material yield strength at temperature; for the total bolt stress to reach the bolt material yield strength, the applied bolt torque would have to exceed the specified bolt torque by 33 percent. This margin is sufficiently high to preclude yielding of the bolts considering that standardized procedures are used for lubrication and installation of the bolts.

3.1.2.5.2.3.2 Outer Lid Bolts

U.S. NRC Comment

The preload, P, and tensile stress, S_t, calculated in this section differ from the P and S_t values calculated in 3.4.6.6.2.

NAC Response

Referring to the NAC Response to Comment 3.1.2.5.2.3.1, the preload and torque calculations for the Outer Lid Bolts are revised similarly to those for the Inner Lid Bolts. Again, the slight difference in preload and torque values for the Outer Lid Bolts between Sections 3.1.2.5.2.3.2 and 3.4.6.6.2 are due to the variation in the torque coefficients for the two calculations. Also, note that the specified installed bolt torque and preload exceed the higher of the two values.

3.1.2.6 Impact Limiter Deformation Limits

U.S. NRC Comment

Please see comment and questions listed after Section 2.2.5 concerning Tables 2.2-1 and 2.2-2. They also apply for Tables 3.1.2-1 and 3.1.2-2.

NAC Response

Although numbered 3.1.2.6, NAC interprets this comment to actually apply only to Tables 3.1.2-1 and 3.1.2-2.

The responses to Comment 2.2.5 concerning Tables 2.2-1 and 2.2-2 are applicable to Tables 3.1.2-1 and 3.1.2-2, which will be revised accordingly.

3.3.1 Discussion

U.S. NRC Comment

The aluminum in the construction of the basket was assumed to have no significant structural requirements. Under normal conditions of storage with the fuel assemblies in a vertical position, the loads on the basket are negligible. Under accident conditions, such as a cask drop or tipover, the loads were transmitted through the aluminum tubes uniformly supported along their entire length in previous designs. In this design, however, the borated aluminum tubes are not so supported and in fact must transmit loads to the ring sections that are spaced six inches on center. Since the load applied by the fuel assembly is not uniformly distributed over the tubes, the tubes between supports can experience considerable stress and would, in fact, need to fulfill a structural requirements. Since such a structural requirement is indicated it will be necessary to demonstrate the structural capability of the borated aluminum. This will involve, at least, citing a standard that governs the fabrication of this material and compiling sufficient data describing its mechanical properties to assure that the possibility of either brittle or ductile failure under accident conditions is extremely remote.

NAC Response

Currently no code, standard, or specification that governs the fabrication of "borated aluminum alloy" exists. This is the reason that the Transportation Branch of the U.S. NRC requires that no credit be taken for the strength of "borated aluminum alloy" components in a spent fuel transport cask or basket. (Refer to comment 11.2.4.7.2 and NAC's response.) However, it is agreed that a "borated aluminum alloy" does possess some considerable strength.

Based on NAC's specifications for a "borated aluminum alloy" tube, Eagle-Picher Industries, Inc. undertook a research and development program to fabricate such tubes on a production basis using a readily available, standard aluminum alloy. Initial efforts with "borated" 6061-T6 aluminum alloy were unsatisfactory because it required a cold-quenc'ı that distorted the tubes beyond the required tolerance on straightness or twist. Upon the recommendation of Taber Metals, "borated" 6351-T54 aluminum alloy was used because it requires an air-quench or a mist-quench and, thus, distortions are minimal or nonexistent. As shown in the attached letter-report, strength data was obtained by Eagle-Picher from four press runs using metal from seven heats for a production run of "borated" 6351-T54 aluminum alloy tubes as follows:

Temperature (°F)	Average S_u ksi	Average S_y ksi	Average Elongation (%)
75	27.8	18.7	15.7
300	21.3	18.0	17.2
350	19.3	15.7	21.9
400	18.1	17.4	19.0
450	15.0	12.9	26.6

As shown in Table 3.3.5-2, the typical mechanical properties of 6351-T54 aluminum alloy (unborated) are:

Temperature (°F)	S_u ksi	S_y ksi	Elongatio. (%)
70	30.0	20.0	10.0 (Minimum)
360	16.8	11.4	
500	4.8	3.0	

Since the strength properties of "borated" 6351-T54 aluminum alloy are comparable to those of the standard "unborated" alloy and the elongation of the "borated" alloy significantly exceeds the minimum requirements of the standard "unborated" alloy, it can be concluded that the possibility of either brittle or ductile failure under accident conditions of the "borated" 6351-T54 aluminum alloy is no greater than for the standard "unborated" alloy.

According to The Metals Handbook, page 62, aluminum alloys are used for structural components operating at temperatures as low as -452°F. As the metal temperature decreases, the aluminum alloy strength increases, while ductility and toughness remain constant or increase similarly to the strength. Aluminum alloys have no ductile-to-brittle transition with change in temperature according to Kaufman and Holt (ALCOA Technical Paper No. 18) and The Metals Handbook. Consequencly, neither ASTM nor ASME specifications require low-temperature Charpy of Izod tests of aluminum alloys. The attached unpublished ALCOA report - Four Extrusion Alloys: 6061, 6063, 6351, 6005 by Jack P. Willard, May 1971 - also verified the toughness characteristics of 6351 aluminum alloy on pages 4, 8, 22 and 23.

elongation of the "borated" alloy significantly exceeds the minimum requirements of the standard "unborated" alloy, it can be concluded that the possibility of either brittle or ductile failure under accident conditions of the "borated" 6351-T54 aluminum alloy is no greater than for the standard "unborated" alloy.

According to The Metals Handbook, page 62, aluminum alloys are used for structural components operating at temperatures as low as -452°F. As the metal temperature decreases, the aluminum alloy strength increases, while ductility and toughness remain constant or increase similarly to the strength. Aluminum alloys have no ductile-to-brittle transition with change in temperature according to Kaufman and Holt (ALCOA Technical Paper No. 18) and The Metals Handbook. Consequently, neither ASTM nor ASME specifications require low-temperature Charpy of Izod tests of aluminum alloys. The attached unpublished ALCOA report - Four Extrusion Alloys: 6061, 6063, 6351, 6005 by Jack P. Willard, May 1971 - also verified the toughness characteristics of 6351 aluminum alloy on pages 4, 8, 22 and 23.

Eagle-Picher Industries, Inc.

SPECIALTY MATERIALS DIVISION
BORON DEPARTMENT

P.O. Box 798 Quapaw, Oklahoma 74363 FAX 918-673-1052 918-673-2201

September 12, 1990

Alan H. Wells Ph.D.
Nuclear Assurance Corporation
6251 Crooked Creek Road
Norcross, GA 30092

Dear Alan:

My apologies for the delay on this letter. If I had a good excuse I would sure use it.

The extruded aluminum tubes which were made for NAC's storage cask were developed over several years. Although earlier data is available the enclosed is more "real" in that it was generated in a manufacturing mode rather than the laboratory.

The alloy is a basic 6351 aluminum with an addition of boron. This boron is chemically bonded with the aluminum and is evenly dispersed throughout the matrix. This has been shown not only with photo micrographs but also with neutron radiographs. The chemistry for the tubes was as follows:

B	Si	Mn	Fe	Zn	Others	Al
1.22	1.27	.580	.154	.04	.01	Bal

Following extrusion the tubes were press quenched with an air/water mist and aged 8 hours at 350 degrees F. The result is a T5 heat condition. The attached is a summary of strength data obtained from four press runs using metal from seven heats.

If this is not what you are looking for let me know.

Sincerely,

EAGLE-PICHER INDUSTRIES, INC.
Specialty Materials Division

Marvin Y. Wachs
Special Projects Engineer
Boron Department

MYW/en

EAGLE PICHER

EAGLE PICHER IND., INC.
TUBE STRENGTH DATA SUMMARY
9/12/1990

DATE	TEMP DEG F	UTS, KSI	YIELD, KSI	% ELONG.	COMMENTS
20 DEC 88 TABER METALS, 6351+1.25%B HOLLOW EXTRUSIONS					
B-6	75	32.2	24.5	12.0	RUN #1. BILLET 3423BN
N-6	75	30.7	22.5	14.0	9" X 9" HOLLOW TUBE
M-6	75	31.5	24.1	13.0	DATA BY TABER
B-5	75	31.7	23.9	14.0	
11 JAN 89					
B-8	75	28.3	15.6	21.0	RUN #2, BILLET 3424BN
B-8	75	32.9	23.4	15.0	AIR/MIST PRESS QUENCH
B-8	75	28.1	21.9	21.0	B-8 DATA BY TABER
B-8	75	25.7	13.8	20.0	
B-8	75	29.2	22.2	14.5	NEXT 5 DATA BY WMTR
B-8	300	21.3	18.0	17.2	
B-8	350	21.7	19.0	22.7	
B-8	400	18.1	17.4	19.0	
B-8	450	17.1	15.8	20.5	
N-9	75	26.2	12.8	20.0	NEXT 4 DATA BY TABER
N-9	75	27.0	15.7	16.0	
N-9	75	25.4	17.8	13.0	
N-9	75	24.1	11.8	18.0	
11 APR 89					
B-11	75	28.9	18.4	15.0	RUN #3, BILLET 3425BN
29 APR 89 TABER METALS, 6351+1.25%B-10 HOLLOW EXTRUSIONS					
N-15	75	24.0	16.2	15.3	RUN #4, BILLETS 3426 TO 3429
(TUBE #)	350	18.5	14.4	19.0	
	450	13.6	11.1	30.7	THESE WERE THE ENRICHED TUBES
B-16	75	30.3	22.6	12.0	WE HAVE CHEMISTRY, PRESS DATA
B-18	75	25.3	15.9	15.0	EVEN CONDUCTIVITY DATA ON
N-19	75	24.1	16.2	15.3	THESE TUBES. FOUR HEATS ARE
	350	17.7	13.6	24.0	REPRESENTED HERE.
	450	14.2	11.8	28.7	
B-20	75	29.1	20.3	17.0	
N-17	75	25.3	16.8	14.0	
B-13	75	24.6	15.8	15.0	

Four Extrusion Alloys: 6061, 6063, 6351, 6005

ALCOA

May 1971

by

Jack P. Willard

Aluminum Company of America
Application Engineering Division
New Kensington, Pennsylvania

NOT RELEASED FOR PI'BLICATION

FOUR EXTRUSION ALLOYS: 6061, 6063, 6351, 6005

INTRODUCTION

The 6XXX extrusion alloys are generally characterized by good extrudability (resulting in low cost), formability, resistance to corrosion, weldability, and finishing qualities, combined with medium strength. Four alloys dominate this picture: 6061, 6063, 6351, and 6005. All are aluminum-silicon-magnesium compositions, but significant differences exist among them. The intent of this Green Letter is to help the designer select the alloy best suited to his needs.

CHEMICAL COMPOSITIONS

The composition limits for all four alloys are shown in Table I.

TEMPER DESIGNATIONS

F	As fabricated
0	Annealed
T1	Cooled from an elevated temperature shaping process and naturally aged to a substantially stable condition.
T4	Solution heat treated and naturally aged to a substantially stable condition.
T5 & T5X	Cooled from an elevated temperature shaping process and then artificially aged.
T6 & T6X	Solution heat treated and then artificially aged.*

When two digits (e.g. T52, T69) are used in a temper designation, they represent variations to the thermal treatment in order to achieve a special level of properties or a particular characteristic, such as formability.

The following TX510 and TX511 designations may be used in addition to one of the above to indicate a subsequent stress-relieving operation:

TX510	Stress-relieved by stretching (1-3% permanent set), no subsequent straightening.
TX511	Stress-relieved by stretching (1-3% permanent set), straightened to comply with standard tolerances.

TYPICAL PHYSICAL AND TENSILE PROPERTIES

Table II gives typical tensile properties, modulus of elasticity and physical properties of the four alloys in one or more of the standard tempers.

MECHANICAL PROPERTIES

Table III gives minimum mechanical properties, including tensile, compressive and bearing strengths and elongation for all four alloys in several tempers and thicknesses.

FATIGUE PROPERTIES

The smooth specimen fatigue properties of the 6XXX series alloys are summarized in Figures 1 and 2 for sheet-flexure and axial-stress loadings, respectively. In each figure, a band is shown representing data for all four alloys and a variety of quenching procedures. There are not large differences among the fatigue properties of these materials. Certain trends appear, however, that might be noted: Data for relatively low strength alloy 6063 and for 6005 generally fall along the low side of the respective bands, while data for 6351 and 6061 generally fall along the high side of the respective bands regardless of the procedures by which the alloys are heat treated and quenched.

*With these alloys, T6 properties can often be achieved by an alternate heat treat method involving press quenching followed by artificial aging. Because of the length of time this method of heat treatment has been common practice, it is often accepted in lieu of separate solution heat treatment by many suppliers and fabricators.

FRACTURE CHARACTERISTICS

The four 6XXX series alloys, as a group, are rather tough compared to many of the higher strength alloys used in critical aerospace applications, as shown by the comparisons in Figure 3. These alloys are tough enough that linear elastic fracture mechanics is of little value in describing fracture conditions; overstressing, even in the presence of rather large flaws, generally results in net section yielding. As a result, merit rating tests such as tear and notch-tensile tests provide the most meaningful indices of relative toughness. See Reference 2.

There are some significant differences, however, and these are illustrated by the results of tear tests on specimens from identical channels of each of the four alloys, in which the quench rate following heat treatment was varied. The type of quench ranged from a still air quench from the die to a rapid cold water quench after furnace heat treatment. The results are illustrated in the bar graph in Figure 4, which shows the range of unit propagation energies developed with the different quench procedures. Of the four, lower strength alloy 6063 consistently developed high unit propagation energies, regardless of type of quench. Of the other three alloys, 6351 exhibited significantly less variability in toughness related to quenching than 6005 and 6061. The latter two alloys showed much wider ranges in toughness dependent upon quench rate, with the slower air quenches resulting in appreciably lower toughness than water quenches; of these two alloys, 6061 consistently rated higher.

These results are interpreted to indicate that 6351 should be utilized in applications where the maximum combination of strength and toughness, with the least variability due to quench rate, is required. Alloy 6061 can be used in similar design situations, but only when control on quench rate is possible. Where toughness, not strength, is required, 6063 is adequate. Consideration should be given to 6005 in air-quenched tempers where strength, not toughness, is a design criterion.

STRENGTH OF WELDS

All of the 6XXX series alloys are readily weldable with either 4043 or 5356 filler. Weldments made with the former are heat-treatable, and thus 4043 is used when relatively high strengths are required and a thermal treatment after welding is feasible. The latter, 5356, is recommended when post-weld heat treatment is not performed, and particularly when high toughness (see below) and ductility are important requirements. It is not generally subjected to post-weld thermal treatment because of possible sensitization to stress-corrosion cracking.

Significantly higher weld strengths can be obtained by the use of sophisticated welding procedures, e.g., high-speed automatic welding and specialized cooling techniques. The weld properties listed below are minimums, based on the handiwork of average welders under average conditions.

The expected minimum tensile and yield strengths of 4043 and 5356 butt welds in these alloys are as follows:

	4043					5356	
	As-Welded Strengths, KSI		Heat-Treated and Aged Strengths, KSI			As-Welded Strengths, KSI	
Alloy	Tensile	Yield	Tensile	Yield	Alloy	Tensile	Yield
6005, 6061, 6351	24	20*	38	35	6005, 6061, 6351	24	20
6063	17	11					

Yield strength values determined on a 10-inch gage length.

*This value is for sections ≤ 3/8-in. thick; for sections > 3/8-in. thick, the value is 15 ksi.

TOUGHNESS OF WELDS

It is important to note that in welded structures of 6XXX alloys, the filler alloy has a marked effect on fracture toughness across the welds. Whether post-weld heat treatment is employed or not, 5356 filler alloy consistently yields weldments of much higher toughness than 4043 filler alloy.

The average values and ranges of unit propagation energies for the two filler metals in welds on 6061-T651 test panels in both the as-welded condition and heat treated and aged after welding are as follows:

Subsequent Thermal Treatment	Unit Propagation Energy, in.-lb./in.^{2} 4043 Filler Metal Average	Range	5356 Filler Metal Average	Range
No	365	250-445	1080	1050-1110
Yes	250	80-530	935	930- 940

ELEVATED TEMPERATURE PROPERTIES

Tables IV, V, VI, VII, VIII, and IX show elevated temperature properties for all four alloys, including two different tempers for 6351 and 6063.

STRESS STRAIN CURVES

Figures 5, 6, 7, and 8 show stress-strain curves for each of the four alloys.

BUCKLING FORMULA CONSTANTS

Buckling formula constants are shown as Table X. See The Aluminum Association's "Specifications for Aluminum Structures," November 1967, Table 3.3.4b.

CORROSION RESISTANCE

The 6XXX-series alloys exhibit excellent resistance to atmospheric corrosion in a wide variety of environments. This has been demonstrated not only by service experience with alloys 6061 and 6063 but also by long-term field corrosion tests of products of these alloys in various tempers. Data, such as that shown in Figures 9 and 10, illustrate the "self-limiting" characteristic of atmospheric corrosion of these alloys. The 6XXX-series alloys also have good resistance to corrosion in sea water. Relatively short time tests of newer alloys 6005 and 6351 indicate a high resistance to corrosion similar to that of 6061.

Service experience and extensive laboratory tests also have shown that the 6XXX-series alloys are virtually immune to the problems of stress-corrosion cracking and exfoliation corrosion.

Welding the 6XXX-series alloys by any of the various methods does not adversely affect the resistance to corrosion or to stress-corrosion of the parent metal. This has been demonstrated in exposure tests ranging up to eleven years in sea water and twenty years in an industrial environment.

FINISHING CHARACTERISTICS

The 6XXX-series alloys are among the best with regard to finishing characteristics. Mechanical finishes, such as scratch-brushing, buffing, grinding, polishing, and others, are readily applicable to these alloys, and provide highly satisfactory results. Electroplating can be applied to all these alloys. Chemical finishes, including both alkaline and acid etches, bright dips, and chemical conversion coatings, can be applied with ease to 6XXX-series alloys, and the surfaces thus obtained are generally uniform in appearance and suitable for further finishing operations. The electrochemical finish, anodizing, is often used with these alloys. Several types of anodic coatings are available: Natural or impregnated color Alumilite* is used for both decorative and protective finishes produced by conventional techniques, while Alumilite* Hard Coatings are especially thick, dense, hard coatings, used for the protection of aluminum parts against wear, abrasion, erosion and corrosion. A higher purity version of 6063 alloy, designated 6463, can be used where the optimum in chrome-like appearance is desired following bright dip and anodize.

Integral-colored anodic coatings, produced by the Duranodic* 300 Process, are special finishes which employ organic acid electrolytes to develop colors ranging from bronze to gray to black from the alloy itself; no dyes are required. In order to obtain the best color match with the Duranodic* 300 Process, Alcoa's special Anociad* alloys should be employed. These alloys, primarily for architectural applications, are carefully controlled with regard to chemical composition, fabricating and aging. The following colors are available with the specific alloy listed:

Colors	Alloy
Bronzes and Black	Anociad* Type 11-T52 (6063 Type)
Grays and Black	Anociad* Type 12-T54 (6351 Type)

*Trade name of Aluminum Company of America

A satisfactory commercial black finish can be achieved in small lots by using extrusions of 6061 alloy. In larger lots, Anoclad* alloys should be used to guarantee consistent color match throughout.

Paint and other organic coatings can be applied to the 6XXX-series alloys with excellent results. In order to achieve a tightly adherent coating, preparation of the surface by degreasing and etching is suggested, followed by a conversion coating or wash primer. For severe service conditions, a zinc chromate primer is recommended. Whether for decorative or protective purposes, painting is a satisfactory method of finishing these alloys of aluminum.

Porcelain enamel coatings, too, may be applied to 6XXX-series alloys but, as in integral-colored anodic coatings, a special variation of a 6XXX alloy has been developed especially for this application. It is designated No. 1 PEX, and it resembles 6061 alloy.

FORMING

Formability of extruded tubes or shapes in the 6XXX-series alloys is generally considered "excellent." Any one of the more widely used methods of bending can be applied to these alloys. Draw and compression bending are normally employed for the smaller tubes and extruded shapes, while larger items can be formed by ram or press benders. Heavy-walled tube or shapes are best formed on a roll bender. For complex extruded shapes, or for particularly difficult bends, stretch forming is most likely to achieve satisfactory results.

The minimum radius to which a tube or extruded shape of a particular alloy can successfully be bent without failure is an indicator of the formability of that alloy. In a recent bend test of a .094" thick, 6-inch wide extruded strip, a 90° bend made with the grain in four different alloy/temper combinations resulted in the following minimum bend radii:

Alloy/Temper	Minimum Bend Radius
6063-T6	3/8"
6061-T6	1/2"
6351-T5	1/2"
6005-T5	3/4"

All four of these alloys were given an air quench in the preparation of the extruded samples. There is some evidence to indicate that quen... appreciable effect on the latter thr... list above. A faster quench rate ... 6351, and particularly 6005 appears ... minimum bend radius which therefor... formability. A designer who wishes ... ability in a 6XXX extrusion alloy sh... an Alcoa Sales Engineer in order ... the temper called out will includ...

MACHINING

The 6XXX-series extrusion ... of the favorable characteristics o... tributed to aluminum alloys in gener... ing speeds and feed, low tool we... However, the relatively high duct... alloys tends to cause continuous ... during machining operations rath... desirable broken chips, which are m... from the cutting area. It is recomm... tools used with these alloys be design... chip breakers or chip control gro... direct the chip away from the wor...

Close tolerance machining o... can sometimes be made more diff... stresses, which can be caused eith... process itself, or the subsequent h... quenching. Residual stresses are mini... temperature stretching operatio... for this stress-relieved temper ar... TX511, as described on page 3. T... temper is recommended when clos... chining work is contemplated.

FUSION WELDING – INERT GAS AR...

The four 6XXX extrusion alloys ar... to be highly weldable and are more w... welded structures than any of the oth... alloys. When joint strength is not an im... weldments in all four alloys may ... welded condition. To improve joint ... 6061, 6351, and 6005 can be weld... and then subsequently heat treate... aged. A slight improvement ... achieved by welding in the T4 cond... a post-weld age. Higher as-welded ... brought about by keeping heat input ... to a minimum, particularly in secti... low 1/4".

*Trade name of Aluminum Company of America.

Filler material is required for satisfactory welding of these alloys. Alloy 5356 filler is recommended where strength and ductility are required but no post-weld thermal treatment is performed. If post-weld heat-treatment is employed, 4043 filler wire is recommended. When salt water corrosion resistance is a consideration, 4043 filler is desirable because it possesses an electrical potential close to that of the base material. In situations requiring good color match after anodizing, 5356 filler is recommended.

RESISTANCE WELDING

The 6XXX-series extrusion alloys are considered to be readily weldable by the resistance method of welding. Some care must be exercised in machine settings to accomplish satisfactory spot and seam welds, but the 6XXX-series alloys are not as prone to cracking as some of the high strength 2XXX and 7XXX alloys. Of paramount importance are degreasing and other chemical or mechanical cleaning to obtain consistent quality welds.

Resistance welds on the 6XXX-series alloys become somewhat more difficult if material is in the O (annealed) temper. Softer materials are much more susceptible to excessive indentation and electrode pickup, and show wider variation in weld strength.

BRAZING

The 6XXX-series alloys are commonly used in brazed assemblies. Brazing of alloys 6061 and 6351 can be done at 1100° to 1105° F maximum temperature. Alloys 6005 and 6063 are more brazeable by virtue of their higher solidus temperatures which allow brazing at higher temperature and more latitude in temperature deviation in production facilities.

The temperatures employed for brazing these alloys are somewhat higher than those generally used for their heat treatment, thus essentially annealing the material to a low strength level. In order to restore mechanical properties, the brazing cycle followed by quenching and aging will nearly duplicate properties obtained by the regular heat treatment. Care should be taken that the rapid cooling does not distort the finished assemblies. Brazed assemblies of these alloys can also be normally heat-treated, quenched and aged, but again, distortion must be controlled.

SOLDERING

The soldering of alloys 6061, 6351, 6063, and 6005 can be done with low temperature lead-tin type solders using Alcoa No. 64 Soldering Flux. High temperature zinc type solders may be used with Alcoa No. 66A or 67 Soldering Flux to obtain stronger joints with improved corrosion performance.

COMPARISON WITH OTHER EXTRUSION ALLOYS

The main advantage of the 6XXX-series extrusion alloys is the versatility they exhibit. Relatively low in initial cost, extrusions of these alloys can be formed, joined and finished with a minimum of difficulty or special care, and still maintain a respectable level of mechanical properties.

In comparison, many other alloys have individual advantages over the 6XXX-series, but exhibit disadvantages as well:

1. The softer alloys, such as 1100 and 3003, may be easily formed, joined and finished. Their relatively low mechanical properties, however, may result in problems of structural integrity and resistance to deformation.

2. The 2XXX alloys, such as 2014, 2219 and 2024, have good mechanical properties and fracture toughness. Extrusion of these alloys is more difficult than 6XXX alloys, though, and therefore their initial cost is higher. They are more difficult to form and they tend to finish poorly. Welding of 2014 and 2024, in particular, requires extreme care and special procedures not usually compatible with production practice. (The exception to this is 2219, which welds well to itself but not as well to other alloys.) Resistance to corrosion of these alloys is not as good as that of the 6XXX-series. Both 2014 and 2024 are susceptible to stress-corrosion cracking and exfoliation corrosion under certain circumstances where the 6XXX-series is practically immune.

3. The 5XXX alloys extrude with medium difficulty, and require stretching or other forms of cold working to achieve higher than annealed mechanical properties. They weld well, and offer high as-welded strength and toughness. Finishing characteristics are good, and resistance to corrosion is excellent.

4. The 7XXX-series alloys can be separated into

two groups, those which contain appreciable amounts of copper (e.g., 7075, 7178) and those which do not (e.g., 7005, 7039). The Al-Zn-Mg-Cu alloys are difficult to extrude, and are therefore expensive. Although they possess very high mechanical properties, they are extremely difficult to weld and do not form easily. They do not have good corrosion resistance, and in addition, they can be highly susceptible to stress-corrosion cracking and exfoliation unless special tempers are employed. The Al-Zn-Mg alloys extrude fairly easily and are not as expensive as their copper-bearing counterparts. They are generally more expensive than 6XXX-series alloys, but they can be welded easily, and provide the highest as-welded strength in the aluminum alloy system. Their general resistance to corrosion is similar to that of the 6XXX-series alloys, but they can be susceptible to stress-corrosion cracking under some conditions. Although all 7XXX-series alloys can be given a variety of finishing treatments, the results are not always as uniformly satisfactory as the 6XXX-series alloys.

CONCLUSIONS AND RECOMMENDED APPLICATIONS

To summarize, the 6XXX-series extrusion alloys covered in this Green Letter are 6061, 6063, 6351, and 6005. All four extrude easily, thus the initial cost is low. They offer good corrosion resistance and can be finished by a variety of mechanical, chemical, and electrochemical methods. These alloys lend themselves well to production fabrication, including forming, machining and joining. Good strength can be achieved, depending upon alloy and temper, as shown in Table III.

In the area of fracture toughness, careful attention should be paid to alloy and temper selection. In particular, the method of quenching from the elevated temperature of extrusion (T5, T5X) is important, as it determines the quench rate. The quench rate, as shown earlier in Figure 4, can have a dramatic effect upon the unit propagation energy (UPE) of an alloy. UPE is one of the most reliable indices for differentiating among alloys/tempers with regard to fracture toughness.

When selecting an alloy/temper combination for a particular design situation, a determination should be made as to the importance of fracture toughness. If an assembly is required to have high resistance to impact loading and "catastrophic" failure, but needs only nominal static strength, 6063 would be a good choice because of its relative insensitivity to quench rate. On the other hand, if a high static strength is required in a structure not expected to experience impact or overloading, 6005 in an air quenched temper would be quite satisfactory despite its relatively low toughness.

Before choosing an alloy/temper combination in an application where fracture toughness is important, an Alcoa Sales Engineer should be contacted.

The 6XXX-series extrusion alloys can be used in virtually any application where low cost, corrosion resistance, fabricability and medium strength are of paramount importance. In the transportation industry, both structural and trim components of trucks, trailers, vans, and railroad and rapid transit cars are extrusions of these alloys. Many consumer durable items, including pleasure and sporting goods as well as tools and household equipment, take advantage of the low cost and ease of fabrication and finishing which are characteristic of 6XXX alloy extrusions. The machinery and equipment industries are heavy users of these extrusion alloys for pipelines, supports, towers, heat exchanger tubes, textile equipment and other applications where low cost, ease of fabrication and limited maintenance in industrial environments are important.

Requests for additional information or design assistance in the use of the 6XXX-series extrusion alloys should be directed to the nearest Alcoa Sales Office. A list of these offices is provided inside the back cover of this Green Letter.

REFERENCES

1. Aluminum
   Vol. I – *Properties, Physical Metallurgy and Phase Diagrams*
   Vol. II – *Design and Application*
   Vol. III – *Fabrication and Finishing*
   American Society for Metals, 1967 – Edited by Dr. K. R. Van Horn

2. *Fracture Characteristics of Aluminum Alloys*, J. G. Kaufman and Marshall Holt, Alcoa Research Laboratories, Technical Paper No. 18, 1965

3. *Fatigue Resistance of Aluminum and Its Products*, G. A. Butz and G. E. Nordmark, Aluminum Company of America, SAE Reprint, No. 893E, September 1964

4. *Welding Aluminum*, The Aluminum Association, 1967

5. *Forming Alcoa Aluminum*, Aluminum Company of America, 1962

6. *Brazing Alcoa Aluminum*, Aluminum Company of America, 1967

7. *Soldering Alcoa Aluminum*, Aluminum Company of America, 1965

8. *Specifications for Aluminum Structures*, The Aluminum Association, November 1967

TABLE I

LIMITS – % BY WEIGHT

(maximum unless shown as a range)

Alloy	Si	Fe	Cu	Mn	Mg	Cr	Zn	Ti	Other, Each	Others Total
6061	0.40-0.8	0.70	0.15-0.40	0.15	0.8 -1.2	0.04-0.35	0.25	0.15	0.05	0.15
6063	0.20-0.6	0.35	0.10	0.10	0.45-0.9	0.10	0.10	0.10	0.05	0.15
6351	0.7 -1.3	0.50	0.10	0.40-0.8	0.40-0.8	—	0.20	0.20	0.05	0.15
6005	0.6 -0.9	0.35	0.10	0.10	0.40-0.6	0.10	0.10	0.10	0.05	0.15

TABLE II

TYPICAL TENSILE PROPERTIES, MODULUS OF ELASTICITY AND PHYSICAL PROPERTIES OF 6005, 6061, 6063 AND 6351 EXTRUDED SHAPES

	6005		6061			6063				6351			
	O	T5	O	T4, T451	T6, T651	O	T4	T5	T6	O	T5	T51	T6
Tensile Strength, ksi	18	44	18	35	45	13	25	32	36	18	45	42	48
Yield Strength, ksi	8	39	8	21	40	7	13	28	32	8	41	37	45
Elongation in 2 in., %	25	12	25	22	12	25	24	16	13	25	11.5	12	11
Modulus of Elasticity, ksi x 10^3	10												
Specific Gravity	2.70												
Density, lb/in.^{3}	0.098												
Melting Range, °F	1120-1205		1080-1200			1140-1205				1105-1205			
Thermal Conductivity at 25°C, CGS Units	.51	.45	.48	.41	.44	.52	.46	.48	.48	.47	.42	.42	.42
Electrical Conductivity at 20°C, CGS Units	56	49	57	45	48	57	50	53	53	52	46	46	46
Average Coefficient of Thermal Expansion, per °F x 10^{-6}													
68-212°F	13.0		13.0			13.0				13.0			
68-392°F	13.5		13.5			13.6				13.5			
68-512°F	14.1		14.1			14.1				14.1			

Alcoa Research Laboratories
April 1x, 1971

TABLE III

DESIGN (EXPECTED-MINIMUM) MECHANICAL PROPERTIES OF 6005, 6061, 6063 AND 6351 EXTRUDED SHAPES

Alloy		6005	6061	6063			6351		
Condition		T5	T6, T6510, T6511	T5		T6, T62	T5	T51	T6
Thickness, in.		≤0.500	≤1.000	≤0.500	0.501-1.000	≤1.000	≤1.000	0.125-1.000	≤0.249
Mechanical Property:									
F_{tu}, ksi	L	38	38	22	21	30	38	36	42
	LT	37	37	21	20	29	37	35	41
F_{ty}, ksi	L	35	35	16	15	25	35	33	37
	LT	33	33	16	15	24	33	31	35
F_{cy}, ksi	L	35	35	16	15	25	35	33	37
	LT	35	35	16	15	25	35	33	37
F_{su}, ksi		25	25	15	14	20	25	23	25
F_{bru}, ksi	(e/D=1.5)	61	61	34	33	46	61	58	67
	(e/D=2.0)	80	80	46	44	63	80	76	88
F_{bry}, ksi	(e/D=1.5)	52	52	22	21	35	52	49	55
	(e/D=2.0)	58	58	27	25	42	58	54	61
e, per cent L		(≤0.124) 8 (≥0.125) 10	(≤0.249) 8 (≥0.250) 10	8	8	(≤0.124) 8 (≥0.125) 10	(≤0.249) 8 (≥0.250) 10	10	(≤0.124) 8 (≥0.125) 10

Alcoa Research Laboratories
April 16, 1971

TABLE IV

6061-T6**, -T651, -T6511

ALCOA

ALCOA RESEARCH LABORATORIES
TYPICAL MECHANICAL PROPERTIES AT VARIOUS TEMPERATURES

NOT RELEASED FOR PUBLICATION

Temperature	Time at Temp, hr	TENSILE PROPERTIES: At Temperature Indicated: Tensile Strength, ksi	Yield Strength, ksi	Elong. in 2", %	Modulus of Elas*, 10^3 ksi	At Room Temp After Heating: Tensile Strength, ksi	Yield Strength, ksi	Elong. in 2", %
[illegible]		[illegible]	[illegible]	[illegible]				
[illegible]		[illegible]	[illegible]	[illegible]				
[illegible]		[illegible]	[illegible]	[illegible]	11.1			
[illegible]		[illegible]	[illegible]	[illegible]	[illegible]			
[illegible]		[illegible]	[illegible]	[illegible]	[illegible]			
75°F		45	40	17	9.9	45	40	17
212°F	0.1	[illegible]	[illegible]	[illegible]		[illegible]	[illegible]	[illegible]
	0.5	[illegible]	[illegible]	[illegible]		[illegible]	[illegible]	[illegible]
	10	[illegible]	[illegible]	[illegible]		[illegible]	[illegible]	[illegible]
	100	[illegible]	[illegible]	[illegible]	9.5	[illegible]	[illegible]	[illegible]
	1 000	[illegible]	[illegible]	[illegible]		[illegible]	[illegible]	[illegible]
	10 000	[illegible]	[illegible]	[illegible]		[illegible]	[illegible]	[illegible]
	100 000	[illegible]	[illegible]	[illegible]		[illegible]	[illegible]	[illegible]
300°F	0.1	[illegible]	[illegible]	[illegible]		[illegible]	[illegible]	[illegible]
	0.5	[illegible]	[illegible]	[illegible]		[illegible]	[illegible]	[illegible]
	10	[illegible]	[illegible]	[illegible]		[illegible]	[illegible]	[illegible]
	100	[illegible]	[illegible]	[illegible]	9.1	[illegible]	[illegible]	[illegible]
	1 000	[illegible]	[illegible]	[illegible]		[illegible]	[illegible]	[illegible]
	10 000	[illegible]	[illegible]	[illegible]		[illegible]	[illegible]	[illegible]
	100 000	[illegible]	[illegible]	[illegible]		[illegible]	[illegible]	[illegible]
350°F	0.1	[illegible]	[illegible]	[illegible]		[illegible]	[illegible]	[illegible]
	0.5	[illegible]	[illegible]	[illegible]		[illegible]	[illegible]	[illegible]
	10	[illegible]	[illegible]	[illegible]		[illegible]	[illegible]	[illegible]
	100	[illegible]	[illegible]	[illegible]	8.9	[illegible]	[illegible]	[illegible]
	1 000	[illegible]	[illegible]	[illegible]		[illegible]	[illegible]	[illegible]
	10 000	[illegible]	[illegible]	[illegible]		[illegible]	[illegible]	[illegible]
	100 000	[illegible]	[illegible]	[illegible]		[illegible]	[illegible]	[illegible]
400°F	0.1	[illegible]	[illegible]	[illegible]		[illegible]	[illegible]	[illegible]
	0.5	[illegible]	[illegible]	[illegible]		[illegible]	[illegible]	[illegible]
	10	[illegible]	[illegible]	[illegible]		[illegible]	[illegible]	[illegible]
	100	[illegible]	[illegible]	[illegible]	8.6	[illegible]	[illegible]	[illegible]
	1 000	[illegible]	[illegible]	[illegible]		[illegible]	[illegible]	[illegible]
	10 000	[illegible]	[illegible]	[illegible]		[illegible]	[illegible]	[illegible]
	100 000	[illegible]	[illegible]	[illegible]		[illegible]	[illegible]	[illegible]
450°F	0.1	[illegible]	[illegible]	[illegible]		[illegible]	[illegible]	[illegible]
	0.5	[illegible]	[illegible]	[illegible]		[illegible]	[illegible]	[illegible]
	10	[illegible]	[illegible]	[illegible]		[illegible]	[illegible]	[illegible]
	100	[illegible]	[illegible]	[illegible]	[illegible]	[illegible]	[illegible]	[illegible]
	1 000	[illegible]	[illegible]	[illegible]		[illegible]	[illegible]	[illegible]
	10 000	[illegible]	[illegible]	[illegible]		[illegible]	[illegible]	[illegible]
	100 000	[illegible]	[illegible]	[illegible]		[illegible]	[illegible]	[illegible]
500°F	0.1	[illegible]	[illegible]	[illegible]		[illegible]	[illegible]	[illegible]
	0.5	[illegible]	[illegible]	[illegible]		[illegible]	[illegible]	[illegible]
	10	[illegible]	[illegible]	[illegible]		[illegible]	[illegible]	[illegible]
	100	[illegible]	[illegible]	[illegible]	[illegible]	[illegible]	[illegible]	[illegible]
	1 000	[illegible]	[illegible]	[illegible]		[illegible]	[illegible]	[illegible]
	10 000	[illegible]	[illegible]	[illegible]		[illegible]	[illegible]	[illegible]
	100 000	[illegible]	[illegible]	[illegible]		[illegible]	[illegible]	[illegible]
600°F	0.1	[illegible]	[illegible]	[illegible]		[illegible]	[illegible]	[illegible]
	0.5	[illegible]	[illegible]	[illegible]		[illegible]	[illegible]	[illegible]
	10	[illegible]	[illegible]	[illegible]		[illegible]	[illegible]	[illegible]
	100	[illegible]	[illegible]	[illegible]	6.8	[illegible]	[illegible]	[illegible]
	1 000	[illegible]	[illegible]	[illegible]		[illegible]	[illegible]	[illegible]
	10 000	[illegible]	[illegible]	[illegible]		[illegible]	[illegible]	[illegible]
	100 000	[illegible]	[illegible]	[illegible]		[illegible]	[illegible]	[illegible]
700°F	0.1	8.5	[illegible]	[illegible]		[illegible]	[illegible]	[illegible]
	0.5	[illegible]	[illegible]	[illegible]		[illegible]	[illegible]	[illegible]
	10	[illegible]	[illegible]	[illegible]		[illegible]	[illegible]	[illegible]
	100	[illegible]	[illegible]	[illegible]	5.5	[illegible]	[illegible]	[illegible]
	1 000	[illegible]	[illegible]	[illegible]		[illegible]	[illegible]	[illegible]
	10 000	[illegible]	[illegible]	[illegible]		[illegible]	[illegible]	[illegible]
	100 000	[illegible]	[illegible]	[illegible]		[illegible]	[illegible]	[illegible]
800°F	0.1	[illegible]	[illegible]	[illegible]				
	0.5	[illegible]	[illegible]	[illegible]				
900°F		2.2	1.6	[illegible]				
1000°F		1.5	1.2	[illegible]				

Temperature	Time Under Stress, hr	CREEP-RUPTURE AND CREEP PROPERTIES: Stress, ksi, for Rupture and Creep in Time Indicated: Rupture	1.0% Creep	0.5% Creep	0.2% Creep	0.1% Creep	STRESS-RELAXATION: Time Under Strain‡, hr	Loss in Stress, %	FATIGUE PROPERTIES†: No. of Cycles	Stress, ksi
75°F	0.1	[illegible]	[illegible]	[illegible]	[illegible]	[illegible]	0.1		[illegible]	[illegible]
	1	[illegible]	[illegible]	[illegible]	[illegible]	[illegible]	1	[illegible]	[illegible]	[illegible]
	10	[illegible]	[illegible]	[illegible]	[illegible]	[illegible]	10	[illegible]	[illegible]	[illegible]
	100	[illegible]	[illegible]	[illegible]	[illegible]	[illegible]	100	[illegible]	[illegible]	[illegible]
	1 000	[illegible]	[illegible]	[illegible]	[illegible]	[illegible]	1 000	[illegible]	[illegible]	[illegible]
	10 000						10 000	[illegible]	[illegible]	[illegible]
	100 000						100 000		[illegible]	[illegible]
212°F	0.1	[illegible]	[illegible]	[illegible]	[illegible]	[illegible]	0.1			
	1	[illegible]	[illegible]	[illegible]	[illegible]	[illegible]	1	[illegible]	[illegible]	
	10	[illegible]	[illegible]	[illegible]	[illegible]	[illegible]	10	[illegible]	[illegible]	
	100	[illegible]	[illegible]	[illegible]	[illegible]	[illegible]	100	[illegible]	[illegible]	
	1 000	[illegible]	[illegible]	[illegible]	[illegible]	[illegible]	1 000	[illegible]	[illegible]	
	10 000						10 000	[illegible]	[illegible]	
	100 000						100 000		[illegible]	
300°F	0.1	[illegible]	[illegible]	[illegible]	[illegible]	[illegible]	0.1			
	1	[illegible]	[illegible]	[illegible]	[illegible]	[illegible]	1	[illegible]	[illegible]	
	10	[illegible]	[illegible]	[illegible]	[illegible]	[illegible]	10	[illegible]	[illegible]	
	100	[illegible]	[illegible]	[illegible]	[illegible]	[illegible]	100	[illegible]	[illegible]	
	1 000	[illegible]	[illegible]	[illegible]	[illegible]	[illegible]	1 000	[illegible]	[illegible]	
	10 000						10 000	[illegible]	[illegible]	
	100 000						100 000		[illegible]	
350°F	0.1	[illegible]	[illegible]	[illegible]	[illegible]	[illegible]	0.1			
	1	[illegible]	[illegible]	[illegible]	[illegible]	[illegible]	1	[illegible]	[illegible]	
	10	[illegible]	[illegible]	[illegible]	[illegible]	[illegible]	10	[illegible]	[illegible]	
	100	[illegible]	[illegible]	[illegible]	[illegible]	[illegible]	100	[illegible]	[illegible]	
	1 000	[illegible]	[illegible]	[illegible]	[illegible]	[illegible]	1 000	[illegible]	[illegible]	
	10 000						10 000	[illegible]	[illegible]	
	100 000						100 000		[illegible]	
400°F	0.1	[illegible]	[illegible]	[illegible]	[illegible]	[illegible]	0.1			
	1	[illegible]	[illegible]	[illegible]	[illegible]	[illegible]	1	[illegible]	[illegible]	
	10	[illegible]	[illegible]	[illegible]	[illegible]	[illegible]	10	[illegible]	[illegible]	
	100	[illegible]	[illegible]	[illegible]	[illegible]	[illegible]	100	[illegible]	[illegible]	
	1 000	[illegible]	[illegible]	[illegible]	[illegible]	[illegible]	1 000	[illegible]	[illegible]	
	10 000						10 000	[illegible]	[illegible]	
	100 000						100 000		[illegible]	
450°F	0.1	[illegible]	[illegible]	[illegible]	[illegible]	[illegible]	0.1			
	1	[illegible]	[illegible]	[illegible]	[illegible]	[illegible]	1		[illegible]	
	10	[illegible]	[illegible]	[illegible]	[illegible]	[illegible]	10		[illegible]	
	100	[illegible]	[illegible]	[illegible]	[illegible]	[illegible]	100		[illegible]	
	1 000	[illegible]	[illegible]	[illegible]	[illegible]	[illegible]	1 000		[illegible]	
	10 000						10 000		[illegible]	
	100 000						100 000		[illegible]	
500°F	0.1	21	21	[illegible]	[illegible]	[illegible]	0.1			
	1	[illegible]	[illegible]	[illegible]	[illegible]	[illegible]	1		[illegible]	
	10	[illegible]	[illegible]	[illegible]	[illegible]	[illegible]	10		[illegible]	
	100	[illegible]	[illegible]	[illegible]	[illegible]	[illegible]	100		[illegible]	
	1 000	7.5	[illegible]	[illegible]	[illegible]		1 000		[illegible]	
	10 000						10 000		[illegible]	
	100 000						100 000		[illegible]	
600°F	0.1	[illegible]	[illegible]	[illegible]	[illegible]	[illegible]	0.1		[illegible]	
	1	9.5	[illegible]	[illegible]	[illegible]	[illegible]	1		[illegible]	
	10	[illegible]	[illegible]	[illegible]	[illegible]	[illegible]	10		[illegible]	
	100	[illegible]	[illegible]	[illegible]	[illegible]	[illegible]	100		[illegible]	
	1 000	[illegible]	[illegible]	[illegible]	[illegible]	[illegible]	1 000		[illegible]	
	10 000	[illegible]	[illegible]	[illegible]	[illegible]	[illegible]	10 000		[illegible]	
700°F	0.1						0.1		[illegible]	
	1						1		[illegible]	
	10						10		[illegible]	
	100						100		[illegible]	
	1 000						1 000		[illegible]	
									[illegible]	

* The modulus of elasticity in compression is about 2 per cent greater than in tension.

† Based on results of rotating-beam tests at room temperature and cantilever-beam (rotating-load) tests at elevated temperatures.

‡ Stressed in tension to 60% of the tensile yield strength at the stressing temperature. Strain held constant during exposure.

** Except sheet and rolled-and-drawn products.

TABLE V

6063-T5 EXTRUSIONS

ALCOA

ALCOA RESEARCH LABORATORIES

TYPICAL MECHANICAL PROPERTIES AT VARIOUS TEMPERATURES

NOT RELEASED FOR PUBLICATION

Temperature	Time at Temp., hr	Tensile Properties – At Temperature Indicated: Tensile Strength, ksi	Yield Strength, ksi	Elong. in 4D, %	Modulus of Elas*, 10^3 ksi	At Room Temp After Heating: Tensile Strength, ksi	Yield Strength, ksi	Elong. in 4D, %
-452°F -423°F -320°F -112°F -18°F								
75°F		32	26	[illegible]		32	26	[illegible]
212°F	0.1 0.5 10 100 1 000 10 000 100 000	[illegible]	[illegible]	[illegible]		[illegible]	[illegible]	[illegible]
300°F	0.1 0.5 10 100 1 000 10 000 100 000	[illegible]	[illegible]	[illegible]		[illegible]	[illegible]	[illegible]
350°F	0.1 0.5 10 100 1 000 10 000 100 000	[illegible]	[illegible]	[illegible]		[illegible]	[illegible]	[illegible]
400°F	0.1 0.5 10 100 1 000 10 000 100 000	[illegible]	[illegible]	[illegible]		[illegible]	[illegible]	[illegible]
450°F	0.1 0.5 10 100 1 000 10 000 100 000	[illegible]	[illegible]	[illegible]		[illegible]	[illegible]	[illegible]
500°F	0.1 0.5 10 100 1 000 10 000 100 000	[illegible]	[illegible]	[illegible]		[illegible]	[illegible]	[illegible]
600°F	0.1 0.5 10 100 1 000 10 000 100 000	[illegible]	[illegible]	[illegible]		[illegible]	[illegible]	[illegible]
700°F	0.1 0.5 10 100 1 000 10 000 100 000	[illegible]	[illegible]	[illegible]		[illegible]	[illegible]	[illegible]
800°F	[illegible]	[illegible]	[illegible]	[illegible]				
900°F	[illegible]	[illegible]	[illegible]	[illegible]				
1000°F	[illegible]	[illegible]	[illegible]	[illegible]				

Temperature	Creep-Rupture and Creep Properties: Time Under Stress, hr	Stress, ksi, for Rupture and Creep in Time Indicated: Rupture	1.0% Creep	0.5% Creep	0.2% Creep	0.1% Creep	Stress-Relaxation: Time Under Strain‡, hr	Loss in Stress, %	Fatigue Properties†: No. of Cycles	Stress, ksi
75°F	0.1 1 10 100 1 000 10 000 100 000	[illegible]	[illegible]	[illegible]	[illegible]	[illegible]	0.1 1 10 100 1 000 10 000 100 000		[illegible]	
212°F	0.1 1 10 100 1 000 10 000 100 000	[illegible]	[illegible]	[illegible]	[illegible]	[illegible]	0.1 1 10 100 1 000 10 000 100 000		[illegible]	
300°F	0.1 1 10 100 1 000 10 000 100 000	[illegible]	[illegible]	[illegible]	[illegible]	[illegible]	0.1 1 10 100 1 000 10 000 100 000		[illegible]	
350°F	0.1 1 10 100 1 000 10 000 100 000	[illegible]	[illegible]	[illegible]	[illegible]	[illegible]	0.1 1 10 100 1 000 10 000 100 000		[illegible]	
400°F	0.1 1 10 100 1 000 10 000 100 000	[illegible]	[illegible]	[illegible]	[illegible]	[illegible]	0.1 1 10 100 1 000 10 000 100 000		[illegible]	
450°F	0.1 1 10 100 1 000 10 000 100 000	[illegible]	[illegible]	[illegible]	[illegible]	[illegible]	0.1 1 10 100 1 000 10 000 100 000		[illegible]	
500°F	0.1 1 10 100 1 000 10 000 100 000	[illegible]	[illegible]	[illegible]	[illegible]	[illegible]	0.1 1 10 100 1 000 10 000 100 000		[illegible]	
600°F	0.1 1 10 100 1 000 10 000	[illegible]	[illegible]	[illegible]	[illegible]	[illegible]	0.1 1 10 100 1 000 10 000		[illegible]	
700°F	0.1 1 10 100 1 000						0.1 1 10 100 1 000		[illegible]	

* The modulus of elasticity in compression is about 2 per cent greater than in tension.

† Based on results of rotating-beam tests at room temperature and cantilever-beam (rotating-load) tests at elevated temperatures.

‡ Stressed in tension to 60% of the tensile yield strength at the stressing temperature. Strain held constant during exposure.

January 18, 1971

ALCOA

TABLE VI

6063-T6 EXTRUSIONS

ALCOA RESEARCH LABORATORIES
TYPICAL MECHANICAL PROPERTIES AT VARIOUS TEMPERATURES

NOT RELEASED FOR PUBLICATION

TENSILE PROPERTIES

Temperature	Time at Temp, hr	At Temperature Indicated: Tensile Strength, ksi	At Temperature Indicated: Yield Strength, ksi	At Temperature Indicated: Elong. in 4D, %	At Temperature Indicated: Modulus of Elas*, 10^3 ksi	At Room Temp After Heating: Tensile Strength, ksi	At Room Temp After Heating: Yield Strength, ksi	At Room Temp After Heating: Elong. in 4D, %
-452°F								
-423°F								
-320°F								
-112°F								
-18°F								
75°F		36	32	18		36	32	18
212°F	0.1	33	30	19				
	0.5	33	30	19		36	32	18
	10	33	30	19		36	32	18
	100	33	31	19		36	33	18
	1 000	35	32	18		37	34	15
	10 000	34	32	18		37	34	15
	100 000							
300°F	0.1	30	28	22				
	0.5	30	28	22		36	32	18
	10	31	29	21		37	33	17
	100	31	29	19		37	34	16
	1 000	28	26	19		32	29	16
	10 000	21	17	24		26	20	19
	100 000							
350°F	0.1	28	27	23				
	0.5	28	27	23		36	32	17
	10	28	27	20		36	33	17
	100	24	23	21		31	26	18
	1 000	18	16	24		26	20	19
	10 000	16	12	28		22	16	26
	100 000							
400°F	0.1	26	25	23				
	0.5	26	25	21		35	32	18
	10	20	19	25		30	26	20
	100	16	14	27		25	19	21
	1 000	14	12	30		21	14	22
	10 000	11	8.5	35		17	10	25
	100 000							
450°F	0.1	23	22	21				
	0.5	22	21	19		32	29	20
	10	16	14	25		25	19	22
	100	13	11	29		21	15	24
	1 000	11	8	35		19	11	26
	10 000	7.5	5.5	55		13	6.5	55
	100 000							
500°F	0.1	18	17	20				
	0.5	15	14	21		27	22	21
	10	12	10	30		21	14	23
	100	10	8	40		18	10	25
	1 000	6.5	5	55		13	6.5	40
	10 000	5	3.5	70		12	5	40
	100 000							
600°F	0.1	9.5	8.5	35				
	0.5	8.5	7.3	46		20	12	24
	10	6.5	5.5	55		16	8	30
	100	4.2	3.5	75		13	5.5	40
	1 000	3.4	2.8	90		12	4.5	40
	10 000	3.1	2.4	90		12	4	40
	100 000							
700°F	0.1	4.5	4	65				
	0.5	4	3.5	70		18	9	26
	10	2.7	2.4	80		14	7.5	40
	100	2.5	2.1	100		12	6.2	40
	1 000	2.2	2	100		11	3.7	40
	10 000	2	1.7	100		10	3.2	40
	100 000							
800°F	0.1	2.1	1.8	110				
	0.5	[illegible]	[illegible]	110				
900°F	[illegible]	[illegible]	[illegible]	[illegible]				
	[illegible]	[illegible]	[illegible]	[illegible]				
1000°F	[illegible]	[illegible]	[illegible]	[illegible]				
	[illegible]	[illegible]	[illegible]	[illegible]				

Temperature	Creep-Rupture: Time Under Stress, hr	Stress, ksi, for Rupture and Creep in Time Indicated: Rupture	1.0% Creep	0.5% Creep	0.2% Creep	0.1% Creep	Stress-Relaxation: Time Under Strain‡, hr	Loss in Stress, %	Fatigue Properties†: No. of Cycles	Fatigue Properties†: Stress, ksi
75°F	0.1						0.1			
	1						1		10^4	
	10						10		10^5	
	100						100		10^6	
	1 000						1 000		10^7	
	10 000						10 000		10^8	
	100 000						100 000		5×10^8	
212°F	0.1						0.1			
	1						1		10^4	
	10						10		10^5	
	100						100		10^6	
	1 000						1 000		10^7	
	10 000						10 000		10^8	
	100 000						100 000		5×10^8	
300°F	0.1						0.1			
	1						1		10^4	
	10						10		10^5	
	100						100		10^6	
	1 000						1 000		10^7	
	10 000						10 000		10^8	
	100 000						100 000		5×10^8	
350°F	0.1						0.1			
	1						1		10^4	
	10						10		10^5	
	100						100		10^6	
	1 000						1 000		10^7	
	10 000						10 000		10^8	
	100 000						100 000		5×10^8	
400°F	0.1						0.1			
	1						1		10^4	
	10						10		10^5	
	100						100		10^6	
	1 000						1 000		10^7	
	10 000						10 000		10^8	
	100 000						100 000		5×10^8	
450°F	0.1						0.1			
	1						1		10^4	
	10						10		10^5	
	100						100		10^6	
	1 000						1 000		10^7	
	10 000						10 000		10^8	
	100 000						100 000		5×10^8	
500°F	0.1						0.1			
	1						1		10^4	
	10						10		10^5	
	100						100		10^6	
	1 000						1 000		10^7	
	10 000						10 000		10^8	
	100 000						100 000		5×10^8	
600°F	0.1						0.1		10^4	
	1						1		10^5	
	10						10		10^6	
	100						100		10^7	
	1 000						1 000		10^8	
	10 000						10 000		5×10^8	
700°F	0.1						0.1		10^4	
	1						1		10^5	
	10						10		10^6	
	100						100		10^7	
	1 000						1 000		10^8	
									5×10^8	

* The modulus of elasticity in compression is about 2 per cent greater than in tension.

† Based on results of rotating-beam tests at room temperature and cantilever-beam (rotating-load) tests at elevated temperatures.

‡ Stressed in tension to 60% of the tensile yield strength at the stressing temperature. Strain held constant during exposure.

October 13, 1970

ALCOA

TABLE VII

6351-T5 EXTRUSIONS

ALCOA RESEARCH LABORATORIES
TYPICAL MECHANICAL PROPERTIES AT VARIOUS TEMPERATURES

NOT RELEASED FOR PUBLICATION

TENSILE PROPERTIES

Temperature	Time at Temp., hr	At Temperature Indicated: Tensile Strength, ksi	Yield Strength, ksi	Elong. in 2-in. or 4D, %	Modulus of Elas.*, 10^3 ksi	At Room Temp After Heating: Tensile Strength, ksi	Yield Strength, ksi	Elong. in 2-in., %
-452°F								
-423°F								
-320°F		59	47	17				
-112°F		51	44	10.5				
-18°F		48	43	11				
75°F		45	41	11.5		45	41	11.5
212°F	0.1	40	38	13		45	41	11.5
	0.5	40	38	13		45	41	11.5
	10	40	39	14		45	41	11.5
	100	41	39	15		45	41	11
	1 000	41	39	13		46	42	10
	10 000	41	39	12		45	42	10
	100 000							
300°F	0.1	36	34	15		45	40	11.5
	0.5	36	34	15		45	40	11.5
	10	35	35	14		45	40	11
	100	36	35	14		44	40	10
	1 000	30	28	15		38	34	11
	10 000	25	22	18		33	26	13
	100 000							
350°F	0.1	33	32	15		44	40	11
	0.5	33	32	15		45	41	12
	10	33	32	14		44	40	12
	100	28	27	15		36	31	11
	1 000	22	20	19		33	24	14
	10 000	17	14	26		25	18	16
	100 000							
400°F	0.1	30	29	17		44	39	11
	0.5	31	30	14		44	39	12
	10	27	29	18		36	30	12
	100	20	18	21		35	23	14
	1 000	15	13	24		29	15	19
	10 000	9.5	7	35		17	9	30
	100 000							
450°F	0.1	27	27	13		42	36	12
	0.5	25	25	12		38	33	12
	10	19	15	16		31	29	14
	100	15	13	25		25	16	17
	1 000	9	7.5	30		19	10	24
	10 000							
	100 000							
500°F	0.1	21	21	16		36	30	12
	0.5	19	18	19		33	26	14
	10	12	11	22		29	15	17
	100	8	6.5	29		18	8.5	28
	1 000	5.5	4.8	40		16	6.5	35
	10 000							
	100 000							
600°F	0.1	11	11	19		30	24	14
	0.5	10	10	23		23	14	18
	10					17	7	26
	100					16	6	35
	1 000					16	5.5	35
	10 000							
	100 000							
700°F	0.1					23	12	17
	0.5					20	8	21
	10							
	100							
	1 000							
	10 000							
	100 000							
800°F								
900°F								
1000°F								

CREEP-RUPTURE AND CREEP PROPERTIES / STRESS-RELAXATION / FATIGUE PROPERTIES

Temperature	Time Under Stress, hr	Stress, ksi, for Rupture and Creep in Time Indicated: Rupture	1.0% Creep	0.5% Creep	0.2% Creep	0.1% Creep	Stress-Relaxation: Time Under Strain*, hr	Loss in Stress, %	Fatigue Properties*: No. of Cycles	Stress, ksi
75°F	0.1 1 10 100 1 000 10 000 100 000						0.1 1 10 100 1 000 10 000 100 000		10^4 10^5 10^6 10^7 10^8 5×10^8	
212°F	0.1 1 10 100 1 000 10 000 100 000						0.1 1 10 100 1 000 10 000 100 000		10^4 10^5 10^6 10^7 10^8 5×10^8	
300°F	0.1 1 10 100 1 000 10 000 100 000						0.1 1 10 100 1 000 10 000 100 000		10^4 10^5 10^6 10^7 10^8 5×10^8	
350°F	0.1 1 10 100 1 000 10 000 100 000						0.1 1 10 100 1 000 10 000 100 000		10^4 10^5 10^6 10^7 10^8 5×10^8	
400°F	0.1 1 10 100 1 000 10 000 100 000						0.1 1 10 100 1 000 10 000 100 000		10^4 10^5 10^6 10^7 10^8 5×10^8	
450°F	0.1 1 10 100 1 000 10 000 100 000						0.1 1 10 100 1 000 10 000 100 000		10^4 10^5 10^6 10^7 10^8 5×10^8	
500°F	0.1 1 10 100 1 000 10 000 100 000						0.1 1 10 100 1 000 10 000 100 000		10^4 10^5 10^6 10^7 10^8 5×10^8	
600°F	0.1 1 10 100 1 000 10 000						0.1 1 10 100 1 000 10 000		10^4 10^5 10^6 10^7 10^8 5×10^8	
700°F	0.1 1 10 100 1 000						0.1 1 10 100 1 000		10^4 10^5 10^6 10^7 10^8 5×10^8	

* The modulus of elasticity in compression is about 2 per cent greater than in tension.
* Based on results of rotating-beam tests at room temperature and cantilever-beam (rotating-load) tests at elevated temperatures.
* Stressed in tension to 60% of the tensile yield strength at the stressing temperature. Strain held constant during exposure.

TABLE VIII

6351-T6 EXTRUSIONS

ALCOA

ALCOA RESEARCH LABORATORIES
TYPICAL MECHANICAL PROPERTIES AT VARIOUS TEMPERATURES

NOT RELEASED FOR PUBLICATION

Temperature	Time at Temp., hr	Tensile Properties – At Temperature Indicated: Tensile Strength, ksi	Yield Strength, ksi	Elong. in 2-in., %	Modulus of Elas.*, 10^3 ksi	At Room Temp After Heating: Tensile Strength, ksi	Yield Strength, ksi	Elong. in 2-in., %
-452°F								
-423°F								
-320°F		63	53	14				
-112°F		54	48	10.5				
-18°F		51	47	10.5				
75°F		48	45	11		48	45	11
212°F	0.1	43	42	13		48	45	11
	0.5	43	42	13		48	45	11
	10	43	42	14		48	45	11
	100	43	42	15		48	46	11
	1 000	43	42	13		50	47	10
	10 000	43	42	12		48	45	10
	100 000							
300°F	0.1	39	38	15		48	45	11
	0.5	39	38	15		48	45	11
	10	39	38	14		49	46	11
	100	38	37	14		48	45	10
	1 000	37	33	15		41	38	11
	10 000	27	24	18		35	30	13
	100 000							
350°F	0.1	36	36	15		48	45	11
	0.5	36	36	15		48	45	12
	10	35	35	14		47	44	12
	100	30	29	15		41	37	11
	1 000	25	24	19		35	30	14
	10 000					28	21	16
	100 000							
400°F	0.1	33	33	17		48	45	11
	0.5	33	33	14		47	44	12
	10	26	26	18		40	35	12
	100	22	20	21		34	28	14
	1 000	17	15	24		28	21	19
	10 000							
	100 000							
450°F	0.1	29	29	13		46	44	12
	0.5	28	28	12		42	39	12
	10	21	20	16		34	29	14
	100	17	15	25		28	21	17
	1 000					20	12	24
	10 000							
	100 000							
500°F	0.1	23	23	16		40	37	12
	0.5	21	20	14		36	30	14
	10	16	14	22		28	20	17
	100	12	10	29		21	17	28
	1 000					17	7	34
	10 000							
	100 000							
600°F	0.1					34	28	14
	0.5	11	[illegible]	21		30	22	16
	10					19	9	26
	100					18	7	35
	1 000							
	10 000							
	100 000							
700°F	0.1					26	16	17
	0.5					21	9.5	21
	10							
	100							
	1 000							
	10 000							
	100 000							
800°F								
900°F								
1000°F								

Temperature	Creep-Rupture and Creep Properties: Time Under Stress, hr	Stress, ksi, for Rupture and Creep in Time Indicated: Rupture	1.0% Creep	0.5% Creep	0.2% Creep	0.1% Creep	Stress-Relaxation: Time Under Strain‡, hr	Loss in Stress, %	Fatigue Properties†: No. of Cycles	Stress, ksi
75°F	0.1						0.1			
	1						1		10^4	
	10						10		10^5	
	100						100		10^6	
	1 000						1 000		10^7	
	10 000						10 000		10^8	
	100 000						100 000		5×10^8	
212°F	0.1						0.1			
	1						1		10^4	
	10						10		10^5	
	100						100		10^6	
	1 000						1 000		10^7	
	10 000						10 000		10^8	
	100 000						100 000		5×10^8	
300°F	0.1						0.1			
	1						1		10^4	
	10						10		10^5	
	100						100		10^6	
	1 000						1 000		10^7	
	10 000						10 000		10^8	
	100 000						100 000		5×10^8	
350°F	0.1						0.1			
	1						1		10^4	
	10						10		10^5	
	100						100		10^6	
	1 000						1 000		10^7	
	10 000						10 000		10^8	
	100 000						100 000		5×10^8	
400°F	0.1						0.1			
	1						1		10^4	
	10						10		10^5	
	100						100		10^6	
	1 000						1 000		10^7	
	10 000						10 000		10^8	
	100 000						100 000		5×10^8	
450°F	0.1						0.1			
	1						1		10^4	
	10						10		10^5	
	100						100		10^6	
	1 000						1 000		10^7	
	10 000						10 000		10^8	
	100 000						100 000		5×10^8	
500°F	0.1						0.1			
	1						1		10^4	
	10						10		10^5	
	100						100		10^6	
	1 000						1 000		10^7	
	10 000						10 000		10^8	
	100 000						100 000		5×10^8	
600°F	0.1						0.1		10^4	
	1						1		10^5	
	10						10		10^6	
	100						100		10^7	
	1 000						1 000		10^8	
	10 000						10 000		5×10^8	
700°F	0.1						0.1		10^4	
	1						1		10^5	
	10						10		10^6	
	100						100		10^7	
	1 000						1 000		10^8	
									5×10^8	

* The modulus of elasticity in compression is about 2 per cent greater than in tension.

† Based on results of rotating-beam tests at room temperature and cantilever-beam (rotating-load) tests at elevated temperatures.

‡ Stressed in tension to 50% of the tensile yield strength at the stressing temperature. Strain held constant during exposure.

TABLE IX

6005-T5 EXTRUSIONS

ALCOA

ALCOA RESEARCH LABORATORIES
TYPICAL MECHANICAL PROPERTIES AT VARIOUS TEMPERATURES

NOT RELEASED FOR PUBLICATION

Temperature	Time at Temp., hr	TENSILE PROPERTIES: At Temperature Indicated — Tensile Strength, ksi	Yield Strength, ksi	Elong. in 2-in., %	Modulus of Elas*, 10^3 ksi	At Room Temp After Heating — Tensile Strength, ksi	Yield Strength, ksi	Elong. in 2-in., %
[illegible]								
75°F		[illegible]	[illegible]	12		[illegible]	[illegible]	12
212°F	0.1, 0.5, 10, 100, 1 000, 10 000, 100 000	[illegible]	[illegible]	[illegible]		[illegible]	[illegible]	[illegible]
300°F	0.1, 0.5, 10, 100, 1 000, 10 000, 100 000	[illegible]	[illegible]	[illegible]		[illegible]	[illegible]	[illegible]
350°F	0.1, 0.5, 10, 100, 1 000, 10 000, 100 000	[illegible]	[illegible]	[illegible]		[illegible]	[illegible]	[illegible]
400°F	0.1, 0.5, 10, 100, 1 000, 10 000, 100 000	[illegible]	[illegible]	[illegible]		[illegible]	[illegible]	[illegible]
450°F	0.1, 0.5, 10, 100, 1 000, 10 000, 100 000	[illegible]	[illegible]	[illegible]		[illegible]	[illegible]	17
500°F	0.1, 0.5, 10, 100, 1 000, 10 000, 100 000	20, 17	[illegible]	12, 20		[illegible]	25	17
600°F	0.1, 0.5, 10, 100, 1 000, 10 000, 100 000	[illegible]	10, 8.5	[illegible]		[illegible]	[illegible]	[illegible]
700°F	0.1, 0.5, 10, 100, 1 000, 10 000, 100 000					21	11	17
800°F								
900°F								
1000°F								

Temperature	CREEP-RUPTURE AND CREEP PROPERTIES: Time Under Stress, hr	Stress, ksi, for Rupture and Creep in Time Indicated — Rupture	1.0% Creep	0.5% Creep	0.2% Creep	0.1% Creep	STRESS-RELAXATION: Time Under Strain‡, hr	Loss in Stress, %	FATIGUE PROPERTIES†: No. of Cycles	Stress, ksi
75°F	0.1, 1, 10, 100, 1 000, 10 000, 100 000						0.1, 1, 10, 100, 1 000, 10 000, 100 000		10^5, 10^6, 10^7, 10^8, 5×10^8	
212°F	0.1, 1, 10, 100, 1 000, 10 000, 100 000						0.1, 1, 10, 100, 1 000, 10 000, 100 000		10^5, 10^6, 10^7, 10^8, 5×10^8	
300°F	0.1, 1, 10, 100, 1 000, 10 000, 100 000						0.1, 1, 10, 100, 1 000, 10 000, 100 000		10^5, 10^6, 10^7, 10^8, 5×10^8	
350°F	0.1, 1, 10, 100, 1 000, 10 000, 100 000						0.1, 1, 10, 100, 1 000, 10 000, 100 000		10^5, 10^6, 10^7, 10^8, 5×10^8	
400°F	0.1, 1, 10, 100, 1 000, 10 000, 100 000						0.1, 1, 10, 100, 1 000, 10 000, 100 000		10^5, 10^6, 10^7, 10^8, 5×10^8	
450°F	0.1, 1, 10, 100, 1 000, 10 000, 100 000						0.1, 1, 10, 100, 1 000, 10 000, 100 000		10^5, 10^6, 10^7, 10^8, 5×10^8	
500°F	0.1, 1, 10, 100, 1 000, 10 000, 100 000						0.1, 1, 10, 100, 1 000, 10 000, 100 000		10^5, 10^6, 10^7, 10^8, 5×10^8	
600°F	0.1, 1, 10, 100, 1 000, 10 000						0.1, 1, 10, 100, 1 000, 10 000		10^5, 10^6, 10^7, 10^8, 5×10^8	
700°F	0.1, 1, 10, 100, 1 000						0.1, 1, 10, 100, 1 000		10^5, 10^6, 10^7, 10^8, 5×10^8	

* The modulus of elasticity in compression is about 2 per cent greater than in tension.
† Based on results of rotating-beam tests at room temperature and cantilever-beam (rotating-load) tests at elevated temperatures.
‡ Stressed in tension to 60% of the tensile yield strength at the stressing temperature. Strain held constant during exposure.

July 22, 19[illegible]

TABLE X

BUCKLING FORMULA CONSTANTS

Alloy and Temper	Thickness Range, in.	Compression in Columns B_c, ksi	D_c, ksi	C_c	Compression in Flat Plates B_p, ksi	D_p, ksi	C_p	Compression in Round Tubes B_t, ksi	D_t, ksi	C_t	Bending in Round Tubes B_{tb}, ksi	D_{tb}, ksi	C_{tb}	Bending in Rectangular Bars B_b, ksi	D_b, ksi	C_b	Shear in Flat Plates B_s, ksi	D_s, ksi	C_s
6005-T5	Up thru 0.500	39.4	0.246	66	45.0	0.301	61	43.2	1.558	141	64.8	4.458	55	66.8	0.665	67	25.8	0.131	81
6061-T6, T6510, T6511	Up thru 1.000	39.4	0.246	66	45.0	0.301	61	43.2	1.558	141	64.8	4.458	55	66.8	0.665	67	25.8	0.131	81
6063-T5	Up thru 0.500	17.3	0.072	99	19.5	0.086	93	19.2	0.529	275	28.8	1.513	95	28.3	0.183	103	11.0	0.036	124
6063-T5	0.501 - 1.000	16.2	0.065	102	18.2	0.078	96	18.0	0.484	289	26.9	1.384	99	26.4	0.165	107	10.4	0.033	128
6063-T6, T62	Up thru 1.000	27.6	0.145	78	31.4	0.175	73	30.5	0.978	188	45.7	2.800	70	46.1	0.381	81	17.6	0.074	98
6351-T5	Up thru 1.000	39.4	0.246	66	45.0	0.301	61	43.2	1.558	141	64.8	4.458	55	66.8	0.665	67	25.8	0.131	81
6351-T51	0.125 - 1.000	37.0	0.224	68	42.3	0.274	63	40.6	1.436	148	60.9	4.110	58	62.6	0.603	69	24.5	0.120	83
6351-T6	Up thru 0.749	41.7	0.268	64	47.8	0.329	60	45.8	1.682	134	68.6	4.815	53	71.0	0.729	65	27.2	0.141	79

Refer to Table 3.3.4b, The Aluminum Association's "Aluminum Construction Manual - Specifications for Aluminum Structures," November, 1967.

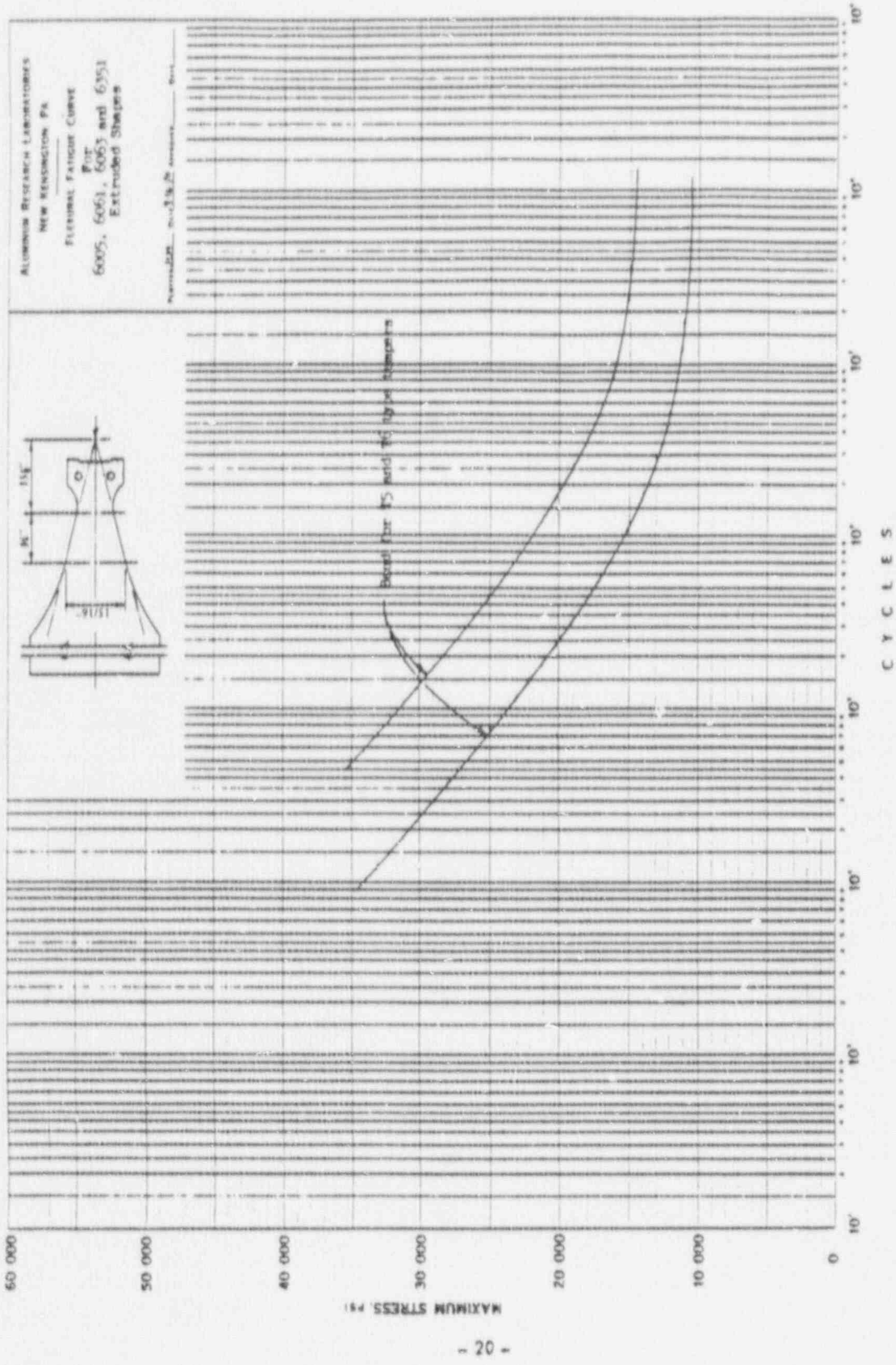
Aluminum Research Laboratories
New Kensington Pa
Flexural Fatigue Curve
For
6005, 6061, 6063 and 6351
Extruded Shapes
60 000
50 000
40 000
30 000
20 000
10 000
0
MAXIMUM STRESS, PSI
CYCLES

FIGURE 1

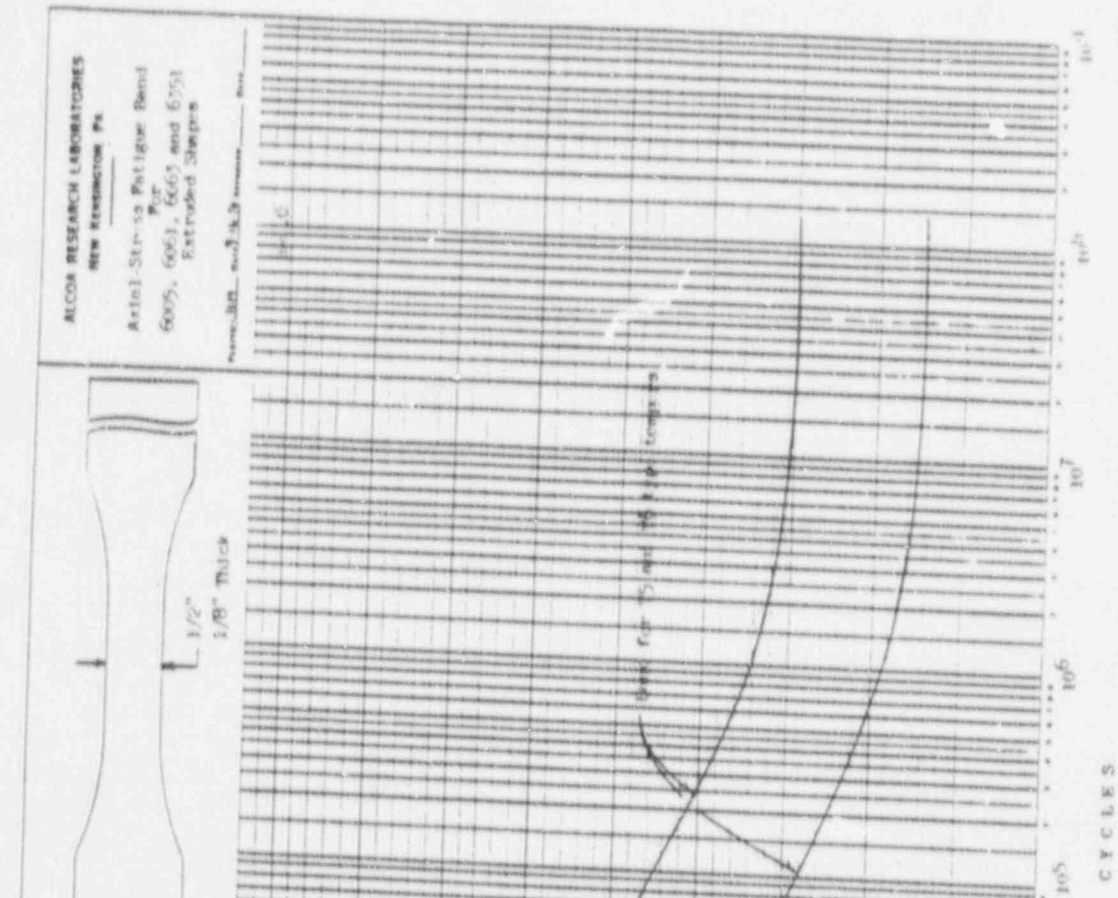
ALCOA RESEARCH LABORATORIES
NEW KENSINGTON PA
Axial-Stress Fatigue Band For 6005, 6061, 6063 and 6351 Extruded Shapes
1/2"
1/8" Thick
MAXIMUM STRESS, psi
120 000
100 000
80 000
60 000
40 000
20 000
0
10^2
10^3
10^4
10^5
10^6
10^7
10^8
10^9
CYCLES

FIGURE 2

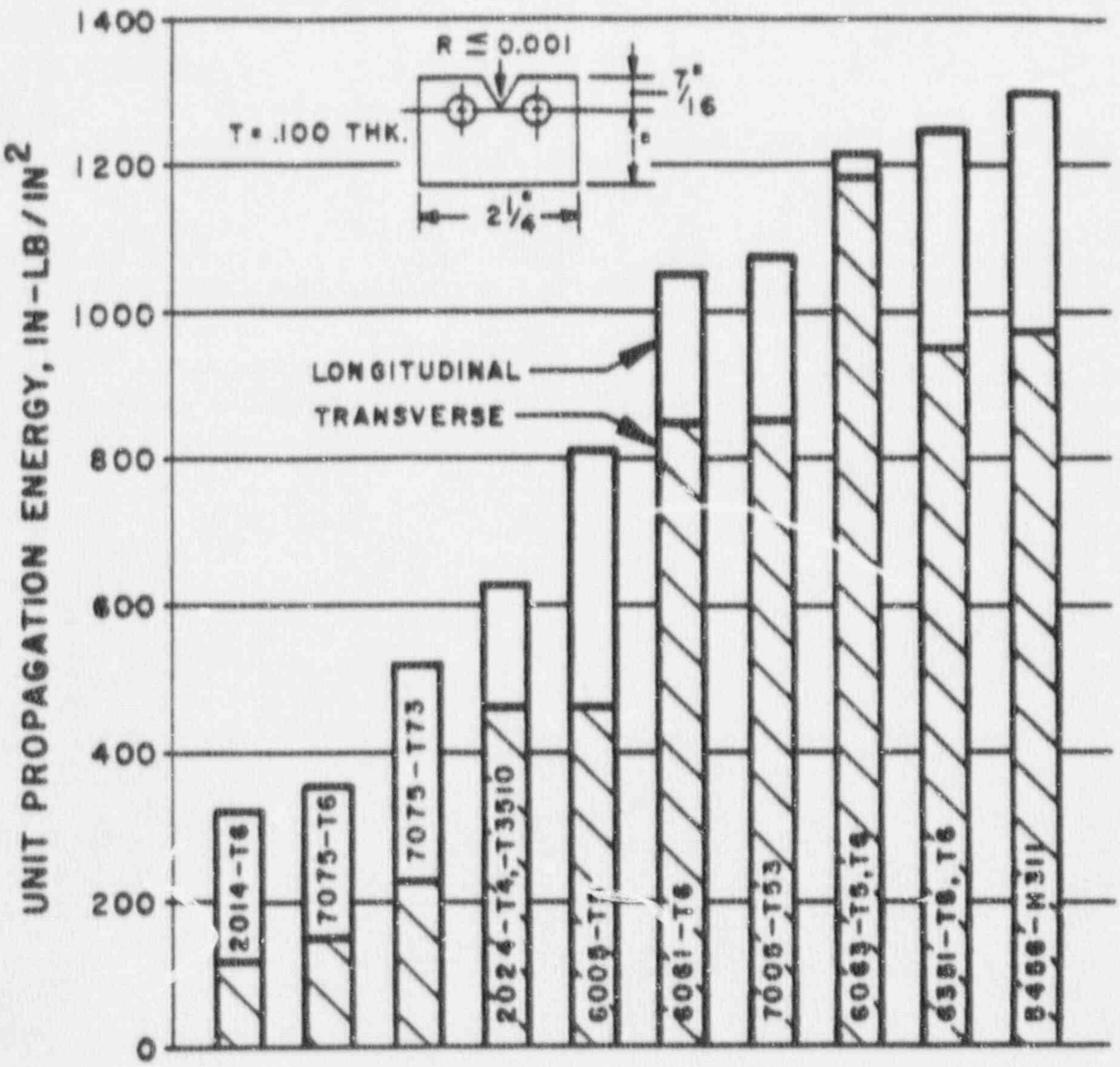

ALCOA RESEARCH LABORATORIES

UNIT PROPAGATION ENERGIES* OF SOME ALUMINUM ALLOYS

.100 THICK

*See Reference 2 for details of this test

FIGURE 3

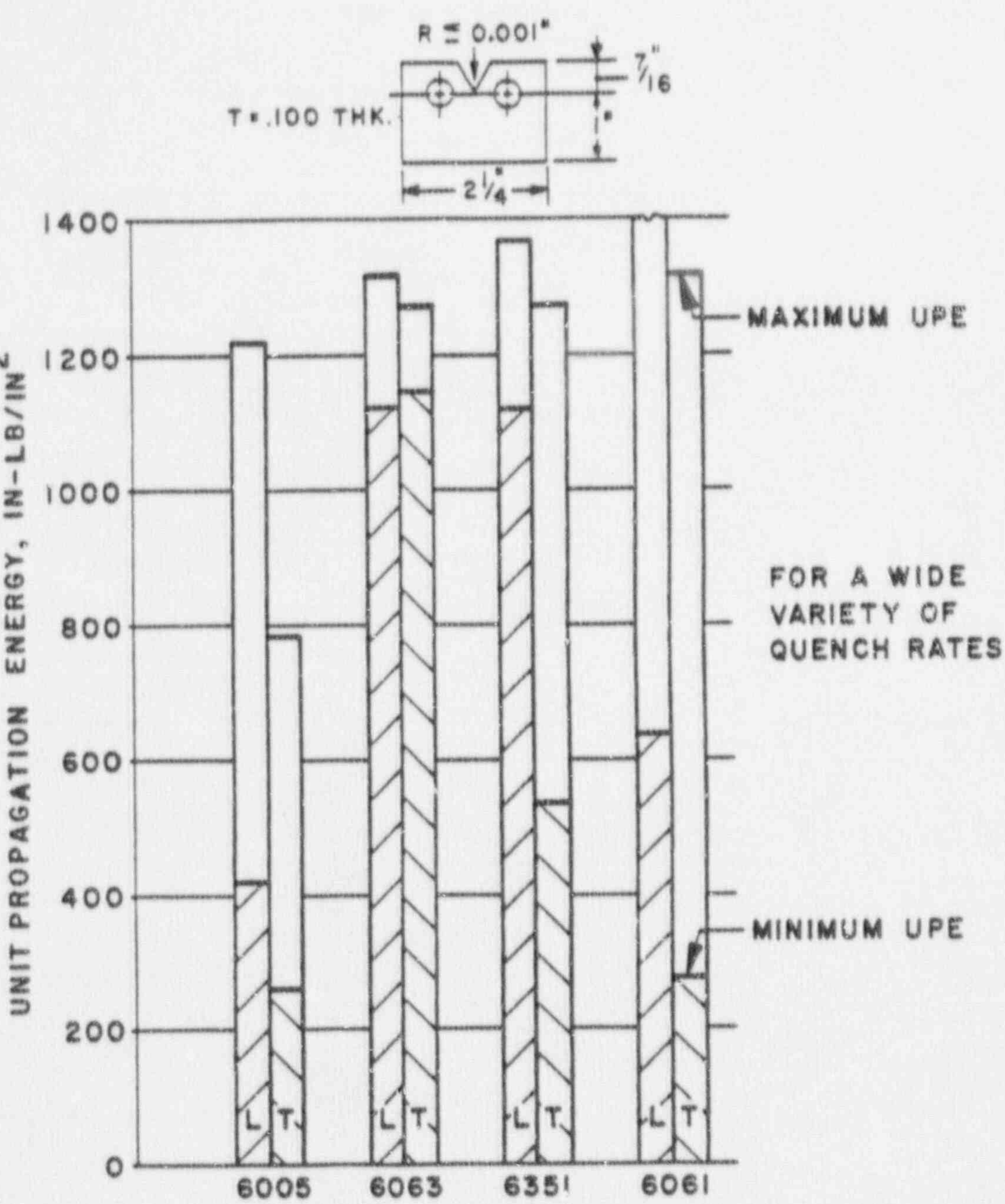

ALCOA RESEARCH LABORATORIES

UNIT PROPAGATION ENERGIES* OF SOME ALUMINUM ALLOYS .100 THICK

*See Reference 2 for details of this test.

FIGURE 4

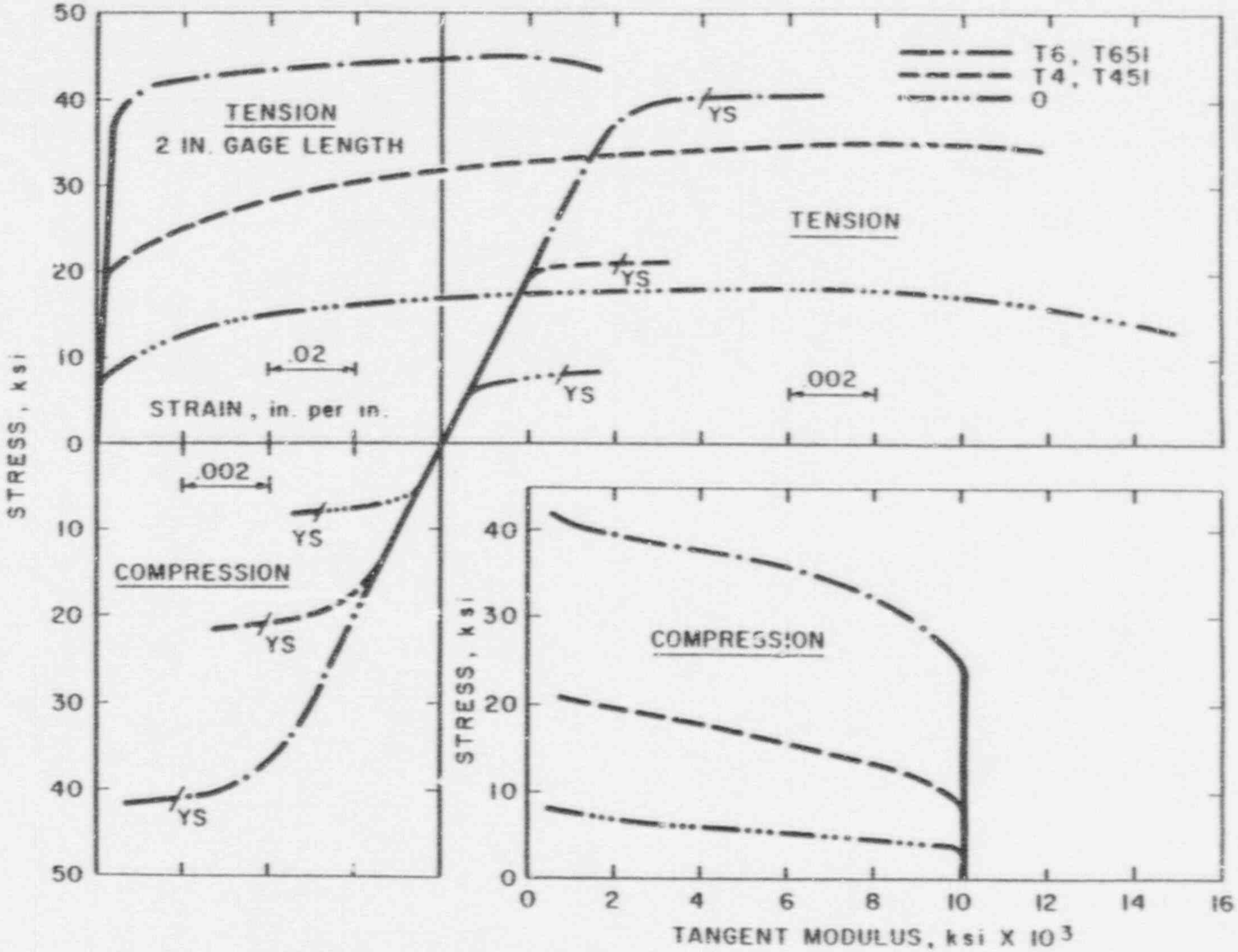

TENTATIVE TYPICAL STRESS - STRAIN CURVES FOR
6061-0, -T4, -T451, -T6 AND -T651 EXTRUSIONS

FIGURE 5

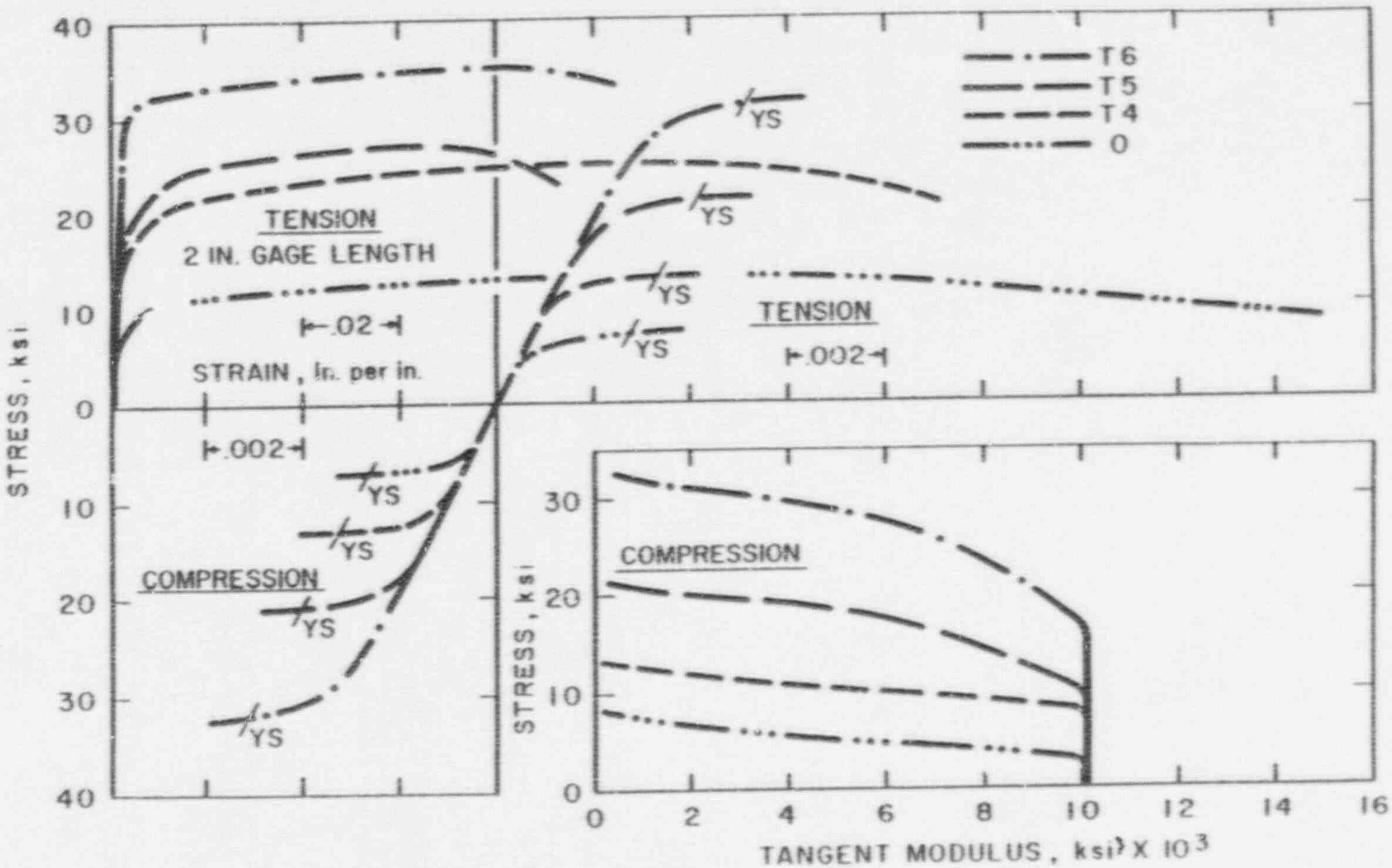

TENTATIVE TYPICAL STRESS – STRAIN CURVES
FOR 6063-0, -T4, -T5 AND -T6 EXTRUSIONS.

FIGURE 6

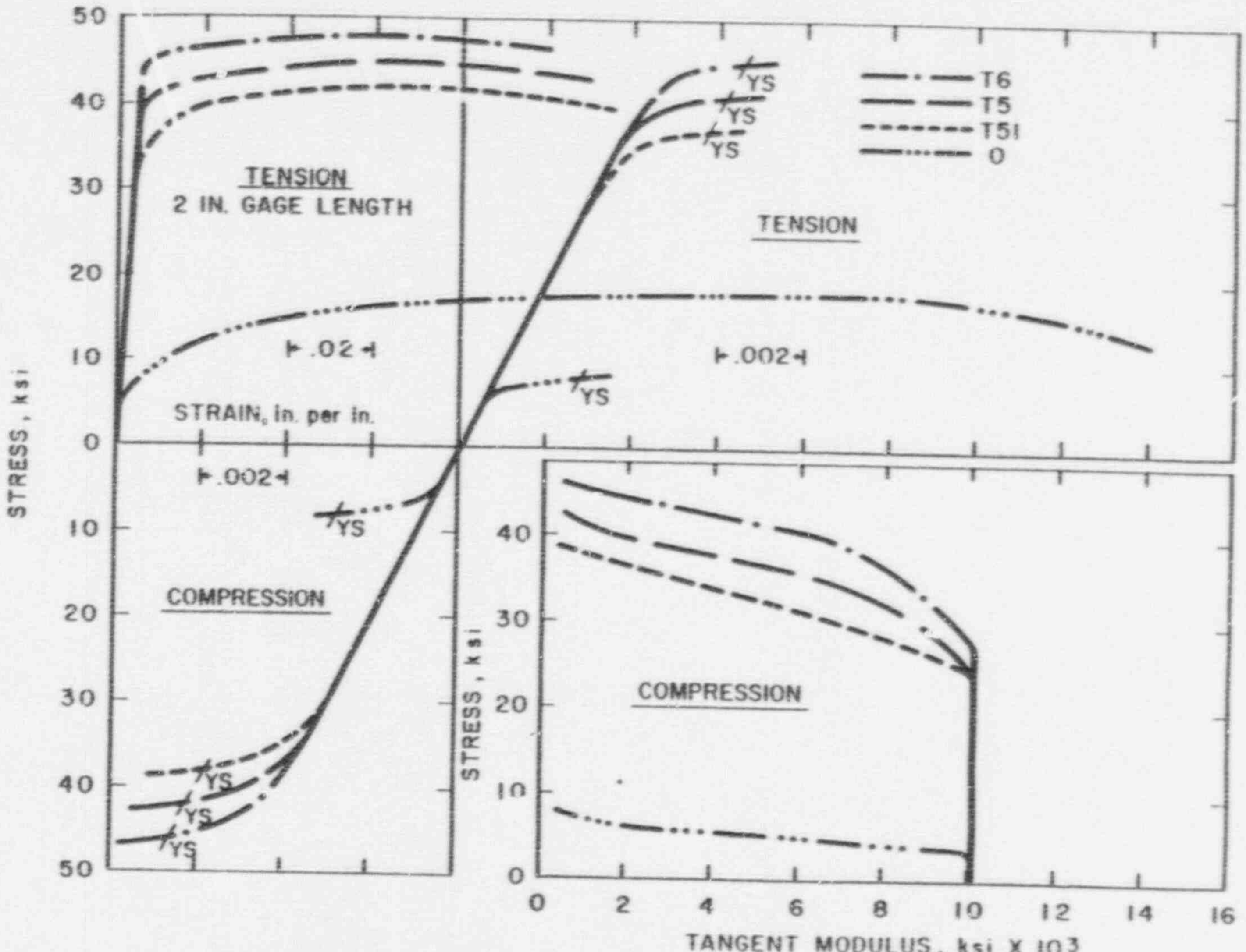

TENTATIVE TYPICAL STRESS–STRAIN CURVES FOR 6351-O, -T5, -T51 AND-T6 EXTRUSIONS.

FIGURE 7

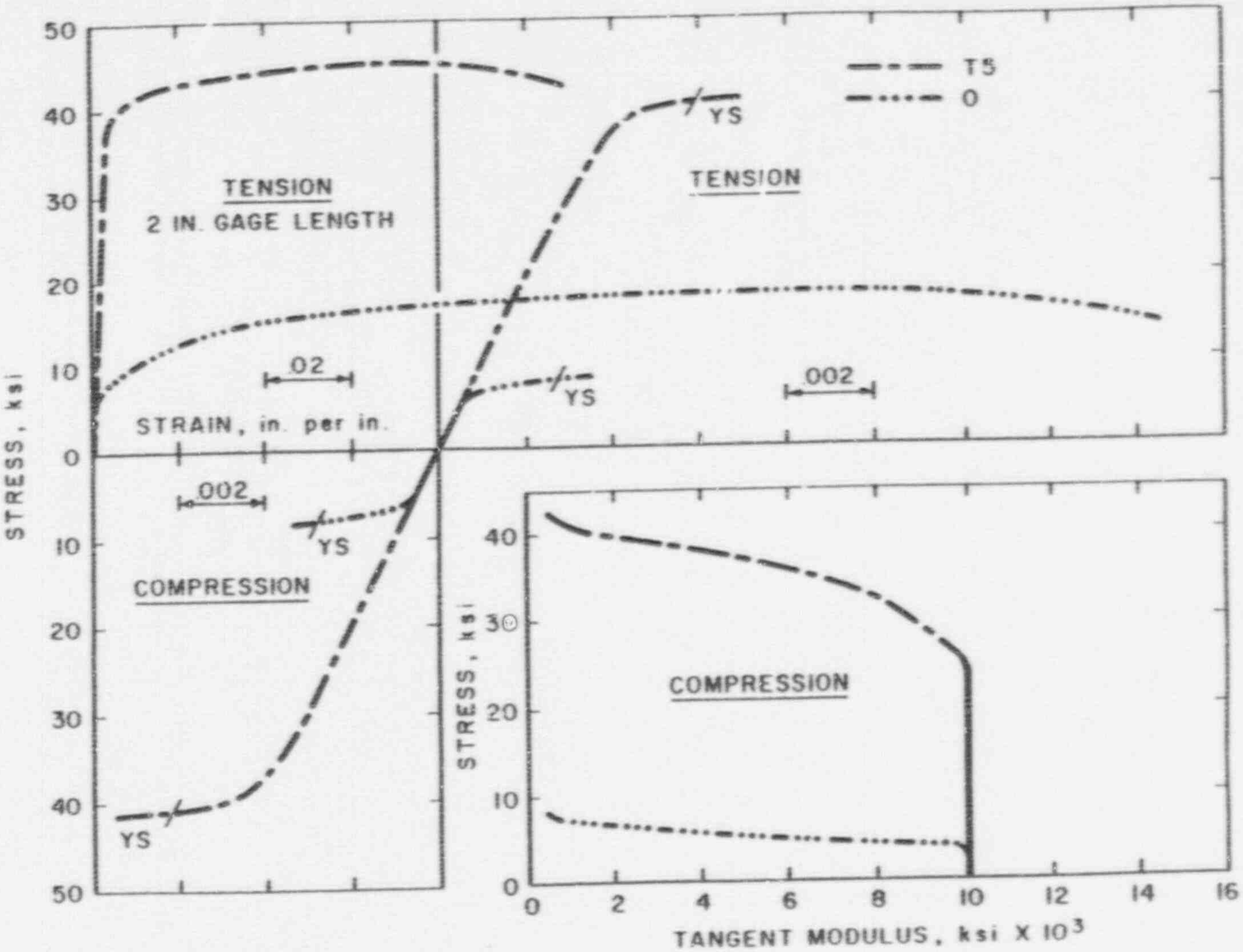

TENTATIVE TYPICAL STRESS-STRAIN CURVES FOR
6005-O,-T5 EXTRUSIONS

FIGURE 8

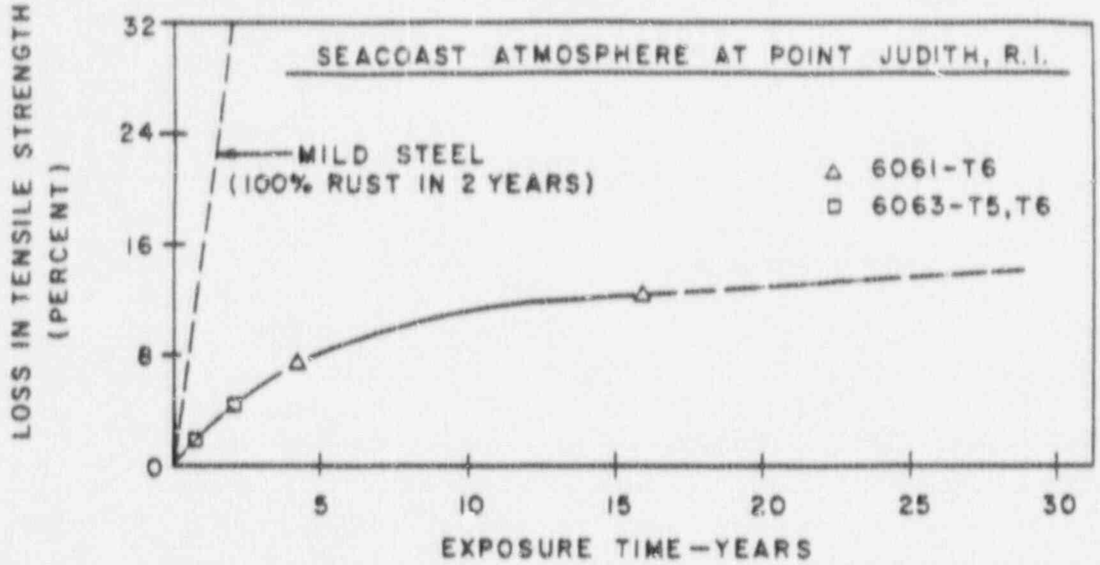

LOSS IN TENSILE STRENGTH OF 6XXX ALLOYS
(TENSION SPECIMEN 0.064 THICK)

FIGURE 9

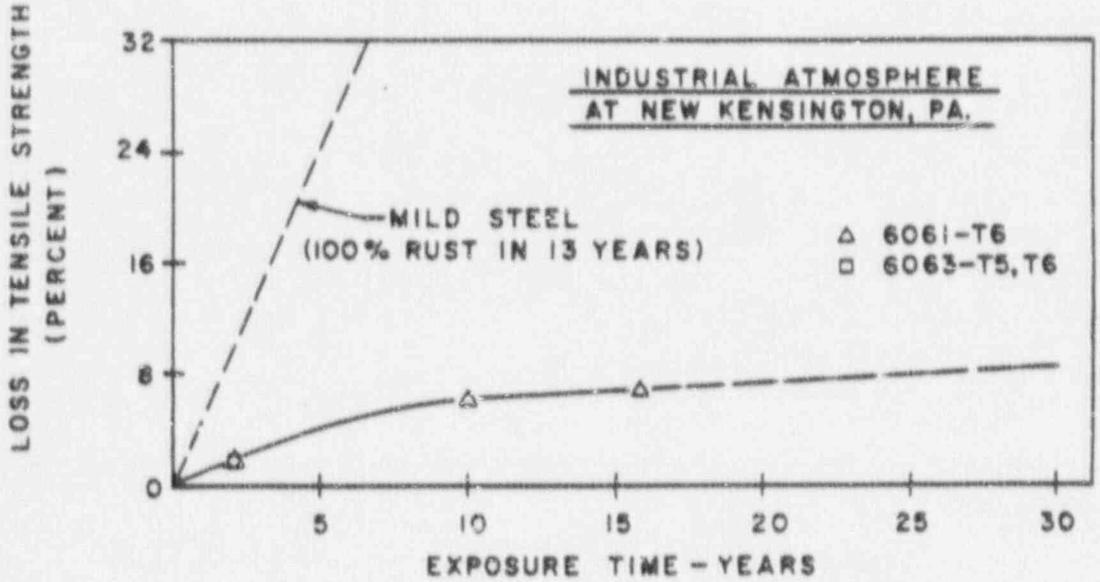

LOSS IN TENSILE STRENGTH OF 6XXX ALLOYS
(TENSION SPECIMEN 0.064 THICK)

FIGURE 10

3.3.5 Aluminum Alloys

U.S. NRC Comment

What S_m values are used for the aluminum basket material? Are they obtained from the minimum yield strength and ultimate tensile strength according to the ASME formulas for S_m of pressure vessel materials? Please list the S_m values in Tables 3.3.5-1, 3.3.5-2 and 3.3.5-3.

NAC Response

As stated in the response to Paragraph (a) of the Comment on Section 2.2.5, the ASME Boiler and Pressure Vessel Code does not define S_m values for aluminum alloys.

The allowable stress value used for the aluminum alloy basket materials is the minimum material yield strength determined at operating temperature. Thus, S_m values are not listed in Tables 3.3.5-1, 3.3.5-2, and 3.3.5-3.

3.3.6.1 Chemical Lead

U.S. NRC Comments

(a) In Tables 3.3.6-1 and 3.3.6-2, the listed values of the elastic modulus of elasticity are only valid for stress levels below 500 to 1000 psi. The modulus of elasticity of lead, the slope of the stress-strain curve, at stress levels above 1000 psi has a value much lower than 2×10^6 psi and is closer to the value of 27,750 psi used for the SCANS impact model.

(b) In Table 3.3.6-2, the listed values of 5000 ksi for the lead yield strength are too high. Are the units psi as in Table 3.3.6-1?

(c) The yield strengths listed in Table 3.3.6-2 cannot be found in the cited references.

NAC Response

(a) An extensive study was made on the cask structural assessments using both the analytical method and experimental verification. Comparisons of stress results were prepared between the completed drop-test results and the analytical solutions using the SCANS program. These comparisons provide a basis to determine an appropriate value of the lead modulus, which should be used in the cask structural analysis using the SCANS program as well as the other finite element programs, such as ANSYS. In attached Table 1, stresses are presented at different locations on the cask outer shell for the 30-foot top end drop condition. The SCANS evaluations were carried out using a dynamic method with a consideration of unbonded lead-and-shell interfaces. Two different lead moduli, 2,280 ksi and 27.75 ksi, were used in the SCANS-A and SCANS-B evaluations, respectively. The NAC-STC quarter-scale model cask drop test results were used to compare with the above-mentioned SCANS calculations. Strain gauges were placed at nine locations on the exterior surface of the cask outer shell. Columns 1 and 2 in Table 1 specify the locations of those strain gages. Strains were measured in the cask longitudinal and circumferential directions at those selected locations during the drop test. The drop test stress results were then determined from the strain-time-history diagrams, which are the graphic presentations of the test data.

The comparison between the SCANS-A and test results show a very close agreement in the longitudinal and circumferential stresses, which occur during a 30-foot top end drop condition, as illustrated in Table 1. The favorable comparison between the SCANS-A evaluation and the experimental results justifies the use of a lead modulus value of 2,280 ksi in the cask structural analysis.

The same statement cannot be made for the comparison of the drop test results and the SCANS-B solution, which considers a lead modulus of 27.75 ksi. As illustrated in Table 1, the SCANS-B evaluation significantly over-predicts the cask outer shell stresses, especially, the circumferential (hoop) stresses resulting from lead slump pressures.

Table 1 Summary of 30-Foot Top End Drop Stress Results on the Outer Shell of the NAC-STC (SCANS vs Drop-Test)

Location[1]			Stress (ksi)		
Longitudinal (inch)	Circumferential (degree)		SCANS-A[3] (51.4g)	Test (57.5g)	SCANS-B[3] (51.4g)
36.0	0	Sz[2]	-2.70	-1.86	-2.31
		St[2]	0.35	1.42	4.47
	90	Sz	-2.70	-1.79	-2.31
		St	0.35	1.49	4.47
	180	Sz	-2.70	-1.67	-2.31
		St	0.35	1.56	4.47
96.0	0	Sz	-5.00	-4.74	-3.00
		St	1.28	1.76	18.00
	90	Sz	-5.00	-4.54	-3.00
		St	1.28	1.42	18.00
	180	Sz	-5.00	-3.95	-3.00
		St	1.28	1.71	18.00
156.96	0	Sz	-7.17	-8.27	-3.33
		St	1.88	1.68	26.91
	90	Sz	-7.17	-5.66	-3.33
		St	1.88	1.04	26.91
	180	Sz	-7.17	-5.88	-3.33
		St	1.88	2.01	26.91

Note:

1. Locations where the strain gauges positioned for the NAC-STC drop tests. Longitudinal location measured from the cask bottom; Circumferential location is around the cask circumference. Note that a circumferential location of 0° orientation is equivalent to a 180° position in the specification of gauge location.

2. Sz (longitudinal) and St (circumferential) are normal stresses.

3. Lead modulus 2,280 ksi was used in the SCANS-A dynamic evaluation. Lead modulus 27.75 ksi was used in the SCANS-B dynamic evaluation.

(b) In Table 3.3.6-2, the listed value of the lead yield strength was mistyped as 5000 ksi. It should be 5000 psi. Table 3.3.6-2 will be revised.

(c) The reference about the lead dynamic yield strength was not properly cited. The values of the dynamic yield strength for the chemical lead are determined using the following formula:

$$(S_y)_{DYN.} = (S_y)_{STA.} \times \left[(S_y)_{DYN.\ (70°)} / (S_y)_{STA.\ (70°)} \right]$$

Where

$(S_y)_{DYN.}$ = dynamic yield strength of chemical lead at a selected temperature

$(S_y)_{DYN.\ (70°)}$ = dynamic yield strength of chemical lead at 70°F temperature

= 5000 psi, Deformation Yield Strength from Shappert, L.R., "Cask Designers Guide"

= 10,000 psi, from Shappert, L.R., "Cask Designers Guide"

$(S_y)_{STA.}$ = static yield strength of chemical lead at a selected temperature, as documented in Table 3.3.6-1, NAC-STC TSAR

$(S_y)_{STA.\ (70°)}$ = static yield strength of chemical lead at 70°F temperature

= 620 psi

Tables 3.3.6-1 and 3.3.6-2 will be revised to incorporate the values of 620 psi for static yield strength at 70°F and 10,000 psi for deformation yield strength of 70°F.

3.3.7 Impact Limiter Materials

U.S. NRC Comments

(a) Please provide further details about the storage impact limiters. Specifically, information is needed about the manner in which the force-deflection curves were obtained; either by experiment or theoretical calculations. Where is the 30 percent crush point on the force-deflection curves and are the impact limiters used beyond that point? Drawings which show the details of the impact limiters and their particular attachments will be useful.

(b) Why are the redwood force-deflection curves included in Section 11.2.4, but not in the impact limiter materials section?

(c) A table is needed which summarizes under which conditions, or drop cases, the different types of impact limiters are used and the respective maximumg levels of the cask and contents under those conditions.

(d) In Figures 3.3.7-3 and 3.3.7-4, provide an explanation for the dip of the force-deflection curve beneath the zero-force line.

(e) In Figures 3.3.7-5 and 3.3.7-6, why is the tipover equivalent to a 58-inch side drop? A tipover accident includes rotational effects which are not present in the side drop.

NAC Response

(a) The details of the NAC-STC storage impact limiters are presented in Section 3.4.9 of the TSAR. For further information regarding the manner in which the force-deflection curves for the storage impact limiters is obtained, please refer to the NAC response to Comment 3.4.9.5. It is assumed that the "30 percent crush point" refers to the point where the depth of the compressed impact limiter is 30 percent of the initial depth of the impact limiter (the assumed maximum crush depth of aluminum honeycomb); this point is not depicted on any of the force-deflection curves except figure 3.3.7-4, because the cask is stopped before that point is reached; thus, the impact limiters are not used beyond that point. In Figure 3.3.7-4 (6.0-Foot Corner Drop with "Nominal - 10 percent" crush strength), the point of assumed maximum crush depth ("stacked height") is the second to last point plotted. The calculated crush depths (displacements) for each of the drop accidents analyzed are tabulated in Table 3.4.9-1 of the TSAR. For the load condition, 6.0-Foot Corner Drop with "Nominal - 10 percent" crush strength depicted in Figure 3.3.7-4, the initial impact limiter depth is 17.75/cos 24° - 19.43 inches where 17.75 inches is the thickness of the aluminum honeycomb in the storage bottom impact limiter and 24° is the corner drop angle. From Table 3.4.9-1 the maximum crush depth for this load condition is 13.75 inches, or 71 percent of 19.43 inches; thus, only a small region of the aluminum honeycomb at the extreme bottom corner of the impact limiter is compressed beyond its assumed "stacked height" (The force-deflection curve in Figure 3.3.7-4, as calculated by RBCUBED, represents this extreme corner of aluminum honeycomb material). This condition is acceptable, since the associated impact force is less than 26 percent of the design impact force for the NAC-STC. The details of the storage impact limiters and their attachments are shown in drawings 423-538 and 423-539, which are included in the NAC-STC TSAR Section 1.5.2.

(b) The storage impact limiters for the NAC-STC utilize aluminum honeycomb as the energy-absorbing material, while the transport impact limiters utilize redwood and balsa wood as the energy-absorbing materials. Since the NAC-STC TSAR considers only the loading conditions associated with a spent fuel storage cask, only the storage impact limiters are included in the TSAR, that is, the aluminum honeycomb in Section 3.3.7. The cask drop analyses presented in Section 11.2.4 conservatively consider the 30-foot drop load conditions that are specified for transport casks. The force-deflection curves for the redwood/balsa wood transport impact limiters for the NAC-STC are included in Section 11.2.4 only to document these loads applied to the cask for the drop analyses.

(c) Table 3.4.9-1 summarizes the drop conditions and the associated impact forces that are applicable to the NAC-STC Cask "storage configuration", which includes only the aluminum honeycomb impact limiters that are defined and evaluated in Section 3.4.9. The redwood/balsa wood impact limiters designed for the "transport configuration" of the NAC-STC are only included in the TSAR as part of the very conservative 30-foot drop analyses (described in Response Paragraph (b)) that verify the structural adequacy of the cask (Section 11.2.4). The impact limiter types, load conditions, and impact forces are summarized as follows:

Aluminum Honeycomb Impact Limiters (Storage Configuration)

6-Foot End Drop: $F_I = 10.1 \times 10^6$ lbs. (40.4g)

6-Foot Corner Drop: $F_I = 3.52 \times 10^6$ lbs. (14.1g)

Tipover: $F_I = 2.94 \times 10^6$ lbs. (11.8g)

*Redwood/Balsa Wood Impact Limiters (Transport Configuration)

*Included in TSAR for analysis purposes only.

30-Foot End Drop: $F_I \cdot 10.1 \times 10^6$ lbs. (40.4g)

30-Foot Corner Drop: $F_I = 10.35 \times 10^6$ lbs. (41.4g)

30-Foot Side Drop: $F_I = 13.6 \times 10^6$ lbs. (54.3g)

(d) Prior to corner drop impact of the NAC-STC, with its bottom limiter attached, the only force acting on the cask is equal to its weight (W). The force on the cask is -W, giving it an acceleration of -1g (downward acceleration), which is the acceleration of a freely falling body. Immediately after the initial impact of the limiter, the contact area between the impact limiter and the unyielding surface is a very small area, with a correspondingly small force exerted by the unyielding surface on the impact limiter. The net force acting on the cask influencing its motion is the sum of all forces, that is, the vector sum of the mass of the cask (downward direction) and the force exerted by the unyielding surface on the limiter (upward direction). Because the force exerted by the unyielding surface of the impact limiter is small in the early stages of the impact, the net force acting on the cask remains in the downward direction (negative). The velocity of the cask continues to increase, until the time when the contact area between the impact limiter and the unyielding surface is large enough such that the unyielding surface exerts a force on the cask that is larger than its own weight. With the net force acting on the cask in the upward direction (positive), the velocity of the cask starts to decrease until it becomes zero. The energy absorption ignored by starting the force-deflection curve with zero force instead of -W is small and is neglected in the RBCUBED analysis.

(e) The height of the center of gravity of the NAC-STC during a tipover of the cask is maximum when the center of gravity is directly over the corner of the cask and minimum when the cask is lying at rest on its side. (The cask is assumed lying at rest supported by the neutron shield, which has a diameter of 98.2 inches.) The center of gravity of the package during storage is 97.49 inches from the bottom of the cask. The radius of the bottom of the cask is 43.35 inches. The maximum height of the center of gravity from the unyielding surface is $(97.49^2 + 43.35^2)$ 0.5 = 106.7 inches. The minimum height of the center of gravity from the unyielding surface is 98.2/2 = 49.1 inches. The maximum change in height of the center of gravity of the cask is 106.7 - 49.1 = 57.6 inches (rounded off to 58 inches). The total change in potential energy of the cask when the center of gravity is lowered by 58 inches during tipover is (58)(250000) = 14.5×10^6) inch/pounds. This is equal to the kinetic energy of the 250000-pound NAC-STC dropped on its side from the height of 58 inches. The total kinetic energy is absorbed by only one impact limiter during a tipover - the upper side storage impact limiter located near the top of the cask. Since the RBCUBED program assumes for a side drop that two identical impact limiters absorb the total kinetic energy of the cask, a height of 2(58) = 116 inches was used in the RBCUBED analysis to obtain the equivalent energy absorption in one impact limiter.

3.4.3.1.3 Trunnion Base

U.S. NRC Comments

Please identify in Figure 3.4.3-1 the trunnion base cantilever as depicted on page 3.4.3-7. Are the parameters, F_{ty} and F_{tz}, forces or moments (units given in lb-in)? Further description of f_{pl} and f_v is needed.

NAC Response

The component of the lifting trunnion shown in Figure 3.4.3-1 referred to as trunnion base in Section 3.4.3.1.3 is the 10.75-inch diameter, 2.5-inch thick section welded inside a 2-inch deep cavity in the outer surface of the cask upper forging. The trunnion base cantilever length is (10.75 - 6.50)/2 = 2.125 inches.

The parameter, F_{ty}, is the reaction force per unit length acting on the outer perimeter of the 10.75-inch diameter trunnion base. It is the reaction opposing the force acting on the shaft of the trunnion, and is acting in the direction parallel to the longitudinal axis of the cask. The parameter, F_{tz}, is the reaction force per unit length acting on the outer perimeter of the trunnion base, It resists the moment on the trunnion (force acting on midpoint of the shaft of the trunnion times its distance from the midplane of the trunnion base). F_{tz} is acting in the direction parallel to the longitudinal axis of the shaft of the trunnion. The pound-inch units are typographical error and will be corrected to pound/inch.

The parameter, f_{pl}, is the maximum fiber stress in the trunnion base plate due to the combined effect of the compressive force, F_{ty}, and the moment of the shear force, F_{tz}, defined above. The point on the trunnion base plate with the maximum fiber stress is located at the intersection of the outer surface of the trunnion base plate and the perimeter of the trunnion shaft.

The parameter, f_v, is the shear stress through the thickness of the trunnion base plate due to the shear force, F_{tz}, defined above.

3.4.4.1 Summary of Pressures and Temperatures

U.S. NRC Comments

Is the internal pressure of 50 psia an assumed or calculated value?

NAC Response

The internal pressure value of 50 psia is assumed based on previous design experience for similar casks. The actual calculated internal pressure is 33.67 psi. (Section 4.4.4), so the assumed pressure is conservatively bounding.

3.4.5.1 Summary of Pressures and Temperatures

U.S. NRC Comments

Is the internal pressure of 12 psia an assumed or a calculated value?

NAC Response

The internal pressure value of 12 psia is assumed based on previous design experience for similar casks. The actual calculated internal pressure is 13.9 psia, so the assumed pressure is conservatively bonding.

3.4.6.4 Loading Conditions

U.S. NRC Comments

How does the impact limiter response differ between the corner drop and the side or end drops. The crush strengths and characteristics are given in the axial or radial directions. What are their values in arbitrary impact directions which occur in a corner drop?

NAC Response

The aluminum honeycomb energy-absorbing material in the NAC-STC storage impact limiters is described in Section 3.3.7 of the TSAR. The aluminum honeycomb material in the bottom storage impact limiter is a multidirectional type that has essentially equal crush strength in the radial (cask side impact) direction, the axial (cask end impact) direction, and any oblique (between radial and axial) direction, including the corner orientation. Tests documented in the NAC LWT SAR have verified the oblique direction crush strength of this aluminum honeycomb. The aluminum honeycomb material in the upper side storage impact limiter is a unidirectional type with its primary crush strength oriented in the radial (cask side impact) direction because it is only loaded by a tipover side impact.

NOTE: The following information is provided for information only, since the transport impact limiters are not a part of the NAC-STC TSAR nor the "storage configuration" of the NAC-STC.

The redwood/balsa wood energy-absorbing material in the NAC-STC transport impact limiters is described in the following Sections of the NAC-STC SAR: 2.3.7, 2.6.7.4, 2.10.6.3, and 2.10.7. Redwood, which possesses a high crush strength parallel to its grain direction, comprises the majority of the transport impact limiters and its grain direction is oriented radially (perpendicular to the longitudinal axis of the cask) throughout. Low crush strength balsa wood comprises the remainder of the transport impact limiters - a 1.5-inch thick layer with radial grain orientation on the end of the impact limiter and an adjoining exterior annular ring with its grain direction oriented 24 degrees from the longitudinal axis of the cask. All strength properties of wood vary with its orthotropic axes in a manner which is approximated by Hankinson's Formula (Baumeister and Marks, Standard Handbook for Mechanical Engineers, Seventh Edition, Page 6-157). Therefore, the crush strength of the redwood, balsa wood, and the impact limiter for any crush direction is:

$$N = \frac{PQ}{P\sin^2\theta + Q\cos^2\theta}$$

where,

N = Crush strength in a loading direction at an angle to the grain direction

P = Crush strength parallel to the grain direction

Q = Crush strength perpendicular to the grain direction

θ = angle between the load direction and the grain direction

Tests described in the referenced sections of the NAC-STC SAR have verified the oblique angle crush strengths of the wood.

3.4.6.6.1 Inner Lid Bolts

U.S. NRC Comments

(a) relate compression forces to the o-ring material specifications and provide manufacturer specification which lists the design factor, D_f, of the o-rings.

(b) Why is F4 estimated while F3 is strictly determined?

(c) A typical value of a friction coefficient is 0.15, not 0.06. Please explain and provide justification for the low value and the possible effects of overestimating the preload.

(d) The bolt force during cask operation can be higher than the preload, sometimes by as much as 10 percent. Was this considered in the analyses? The preload cannot be precisely applied and controlled. Due to the uncertainties associated with applying a specified preload torque, the actual load of the bolt may be greater or less than 30 percent of the specified value. Since the calculated margin of safety is only 0.31 and the stress limit is the yield stress, the bolts may be overstressed. For these reasons, using the yield stress as the limit for the preload will expose the design to the risk of plastically deformed closure bolts.

(e) Please address the shear stress in the bolt. Does this stress exceed the allowable ASME shear strength?

NAC Response

(a) The compression force and design factor, D_f, for the Helicoflex metallic o-rings were designed based on Fluorocarbon Components Division (now Helicoflex Company) Bulletin 101C. The TFE o-ring in the inner lid was designed based on Shamban Seals Division Bulletin SD150-C. The design compression force was provided by the Shamban technical staff. The reinforced-TFE o-rings in the outer lid were designed based on the Fluorocarbon Omniseal Design Handbook. The pertinent pages of these manufacturer specifications are included as a part of this response.

(b) The TSAR will be revised to show the calculation of F4 using a total compression force of 40 pounds per linear inch as obtained from page 12 of the Fluorocarbon Omniseal Design Handbook (Pressure Load of 14 pounds/inch + average spring load of 26 pounds/inch = 40 pounds/inch). The calculated value is F4 = 10,130 pounds.

(c) As discussed in the NAC Response to Comment 3.1.2.5.2.3.1, the torque calculations in the TSAR will be revised to use a value of 0.15 for the coefficient of friction.

(d) The inner lid bolt load during cask operation is a conservatively calculated maximum value that includes the dynamic loading of the weight of the inner lid, outer lid, and cavity contents during a 30-foot drop top corner or top end impact, even though these are not credible load cases for a storage cask; the specified preload for the inner lid bolts exceeds the maximum calculated operation load. It is extremely unlikely that any storage operation load for the NAC-STC inner lid bolts would ever approach the specified bolt preload. As discussed in Paragraph (c) of the NAC Response to Comment 3.1.2.5.2.3.1, NAC agrees that uncertainties do exist in the application of the specified bolt torque; however, since the total design stress (preload + differential thermal expansion) for the NAC-STC inner lid bolts is only 76 percent of the material yield strength at operating temperature and a 33 percent increase in the specified bolt torque would be required to just reach the material yield strength, it is reasonable to conclude that plastic deformation of the inner lid bolts will not occur.

(e) The maximum shear stress of 17,620 psi in the NAC-STC inner lid bolts occurs for the 30-foot side drop transport accident and results from the weight of the inner and outer lids multiplied by the 55g impact loading. This shear stress does not approach the Level D shear stress limit of the ASME Boiler and Pressure Vessel Code, Section III, Appendix F, i.e. $0.4S_u = 66.2$ ksi or $0.6S_y = 67.2$ ksi. Since the bolt tensile stress is 83,817 psi (based on the revised bolt torque calculations), the combined shear and tensile stress is evaluated as $(83{,}817/111{,}400)^2 + (17{,}620/66{,}200)^2 = 0.832 < 1.0$. Since the maximum side impact loading for the NAC-STC for storage is only 11.8g for the tipover condition, the shear stress in the inner lid bolts is approximately $(17{,}620)(11.8/55.0) = 3{,}767$ psi for storage operation.

Helicoflex

Components Division
P.O. Box 9889
Columbia, South Carolina 29290
Telephone (803) 783-1880
FAX (803) 783-4279

February 1, 1990

Dear Valued Customer:

This letter is to advise you that the Metallic O-Ring product line of Fluorocarbon Components Division has been acquired by the Helicoflex Company. Helicoflex is maintaining the business in the same factory where the Metallic O-Rings have been designed and manufactured since 1977, and the entire O-Ring team has been retained. We will continue to manufacture O-Rings with the same people, equipment, procedures, and to the same high standards that were developed and employed by Fluorocarbon.

Our complete name, address, telephone number and FAX number are as follows:

Helicoflex Company
Components Division
P.O. Box 9889
Columbia, SC 29290

(803) 783-1880 Telephone
(803) 783-4279 FAX

All correspondence concerning Metal O-Rings should be directed to the above address. If you need customer service, or technical information, please contact Ken Morales, Rusty Glasscock, or the undersigned, for help.

We will be publishing a new catalog in the near future, and will forward you a copy. Our part numbering system and drawings will not change. In addition, all customer files will be retained and you may continue to place orders for the same part numbers as previously.

Also, in the near future we will be adding complementary metallic sealing product lines to our South Carolina operation. We are extremely pleased with this broadening of our capabilities and will be providing you with further details as they become available.

We look forward to working with you in the future. If you have any questions regarding this merging, please feel free to contact me.

Very truly yours,

Jim Powell
Sales Manager, Helicoflex Components

Bulletin 101C

UNITED METALLIC O-RINGS

Static, metal-to-metal seals
for confining gases or liquids
under adverse conditions of
pressure/temperature/ambience

FLUOROCARBON
COMPONENTS DIVISION

United Metallic O-Rings

United Metallic O-Rings are designed to prevent leakage of gases or liquids under adverse sealing conditions. These static, metal-to-metal seals can withstand pressures from high vacuum to 100,000 psi (6,804 atm). They can endure continuous temperatures from −425° F. up to 1,800° F. (−269° C. to 982° C.), or intermittent temperatures up to 3,000° F. (1,650° C.). They resist radiation, chlorides, corrosives, and other hostile environments. They will not deteriorate with age, either in use or in storage.

Design, Materials, Coatings, Sizes

United Metallic O-Rings, designated MOR, are made of metal tubing (or solid rod) which is formed into circular or other shapes and the two ends welded together. The O-Ring metal is stainless steel or other alloys. The O-Ring can be electroplated with silver, copper, indium, nickel, gold, lead or other metals, or it can be coated with Teflon. The flow of the finish material improves the sealing, especially under high pressure and/or vacuum. Since tensile strength and resilience of the seal are determined in part by metal temper, Fluorocarbon Components offers a choice of heat treating to material specification or tempering to customer specifications. Tubular or solid wire rings can be manufactured in sizes ranging up to 25 feet (7.6 m) or more in diameter, or as small as .250 inches (6.4 mm) OD.

Application Characteristics

The typical application places a Metallic O-Ring in axial compression between parallel faces which are square to the fluid passage or vessel axis. The seal is usually located in an open or closed groove in one face. It can also be located in a retainer, which eliminates the need for machining a groove (see description of retainers on page 8).

Upon compression to a predetermined fixed height, the seal tubing buckles slightly, resulting in two contact areas on the seal face and maximum contact stress between the seal and the mating faces. When the flange faces are closed, the O-Ring is under compression and tends to spring back against the flanges, thus exerting a positive sealing force. If the O-Ring is the self-energizing type, the pressure of the gas or liquid on the vented side energizes the seal and further increases the sealing force by pushing the seal against the flange face.

Types of Metallic O-Rings

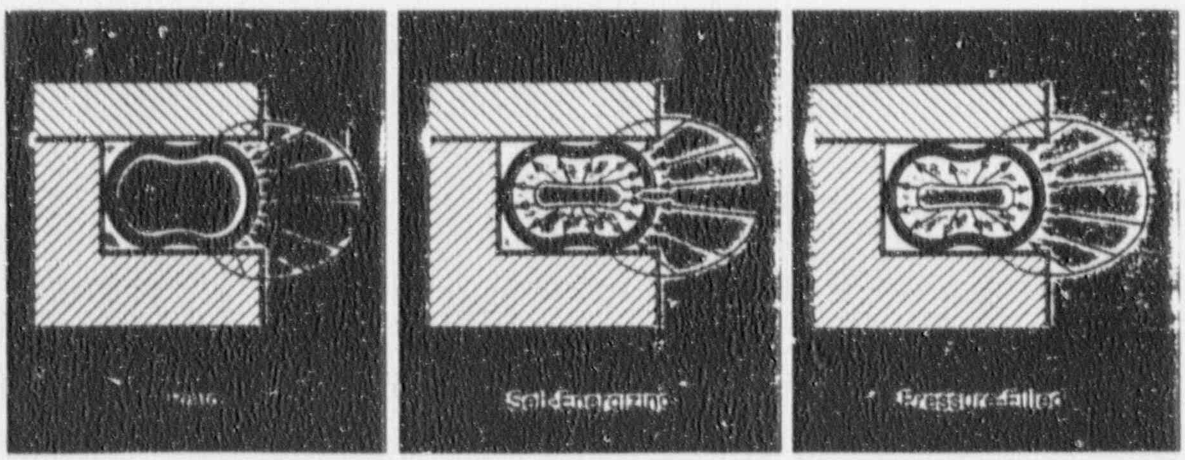

Plain

(Not Self-Energizing or Pressure-Filled)
Made of metal tubing (or solid rod) in most metals. This type is the most economical O-Ring. It is designed for low to moderate pressure and vacuum conditions.

Self-Energizing

The inner periphery of the O-Ring is vented by small holes or a slot. The pressure inside the ring becomes the same as in the system. Increasing the internal pressure increases sealing effectiveness.

Pressure-Filled

Pressure-filled O-Rings are designed for a temperature range of 800° F. to 2,000° F. (425° C. to 1093° C.). They cannot tolerate pressures as high as the self-energizing type. The ring is filled with an inert gas at about 600 psi (41 atm). At elevated temperatures, gas pressure increases, offsetting loss of strength in tubing and increasing sealing stress.

Typical Applications

Metallic O-Rings have been used successfully in vacuum and high pressure systems, and in critical systems for hydraulic and lubricating oil, jet engine fuel, gasoline, rocket fuels, steam, liquid metals and combustion gas. They also provide positive, leak-proof seals in piping systems for chemical, petrochemical, oil and gas, and refining industries. Many reciprocating engines, gas turbines, compressors, heat exchangers, pressure vessels, injection molding machines, high pressure filters and other components rely on Metallic O-Rings for permanent, metal-to-metal seals. Several common applications are shown in the following illustrations.

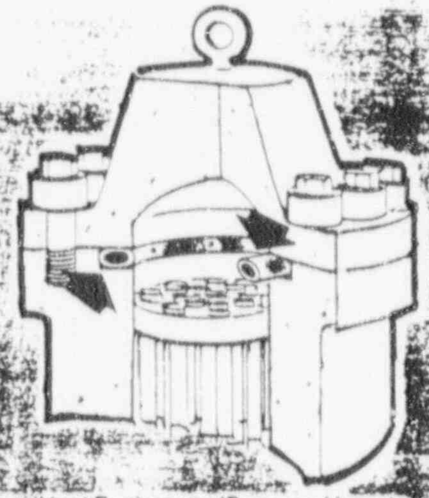

Heat Exchanger/Pressure Vessels

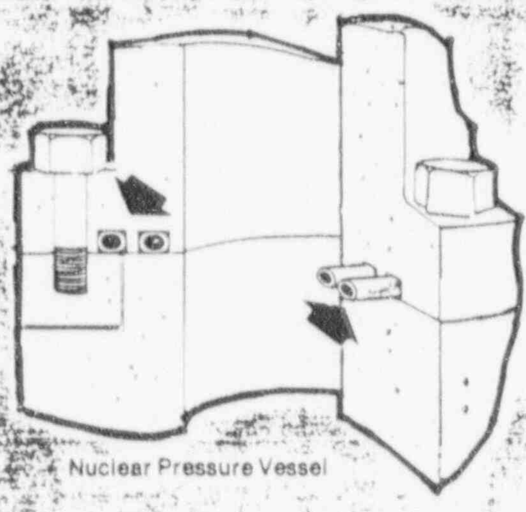

Nuclear Pressure Vessel

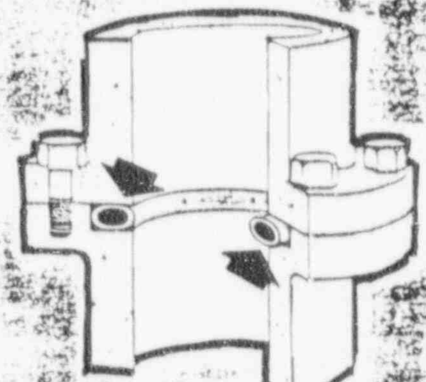

Bolted Flange

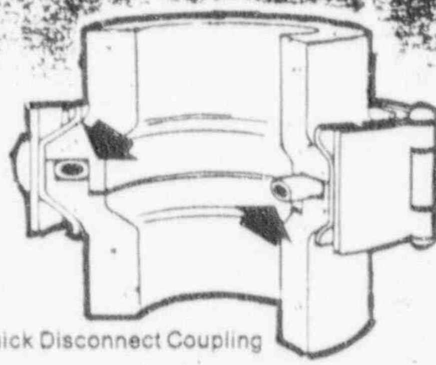

Quick Disconnect Coupling

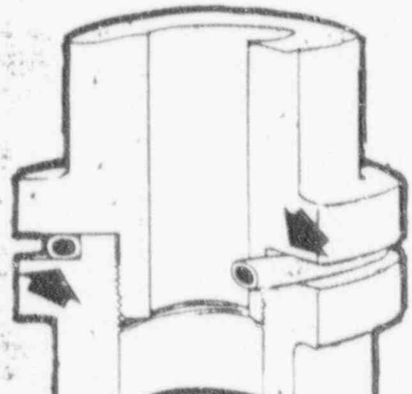

External Pressure (Thread Joint)

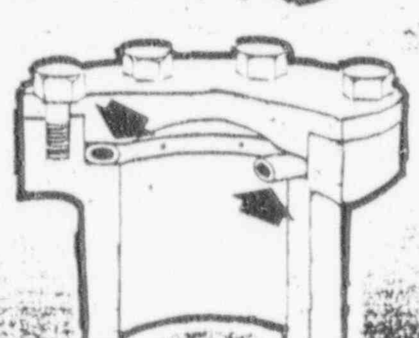

Bolted Cap

Metallic O-Ring Selection Guide

To select the proper Metallic O-Ring for a particular application, it is necessary to determine system pressure, temperature, and kind of fluid to be sealed.

1. O-Ring Type

Pressure determines if O-Ring should be self-energizing.

Pressure	O-Ring Type
Vacuum to 100 psi (6.81 atm)	Self-energizing not required
100 psi (6.81 atm and above)	Self-energizing desirable

2. O-Ring Material

Temperature determines basic O-Ring material.

Temperature	O-Ring Material
Cryogenics to 500° F (260° C)	321 Stainless steel
to 800° F (427° C)	Alloy 600
to 1800° F (982° C)	Alloy X-750
above 1800° F (982° C)	Consult Factory

3. O-Ring Size

Tubing diameter is determined by ring OD, compression force desired, and available space. See complete data for O-Ring size selection on pages 6 and 7.

4. Seal Load vs. Seal Ring Diameter

Curves on page 7 show the seal load vs. seal ring diameter to various tubing outer diameters and wall thickness for stainless steel tubing. For tubing made of Alloy 600, multiply loads shown by 1.1. For Alloy X-750, multiply by 1.4.

5. O-Ring Wall Thickness

The wall thickness should be selected to provide the proper yield under compression. The data on pages 6 and 7 include the practical wall thickness dimensions that may be used for each tube diameter. If plating is used, wall thickness for seals made with .125 inch (3.2mm) tubing and smaller should cause yielding of the plating at a load of 400 lb/in (7.14 kg/mm). For tubing over .125 inch (3.2mm) diameter, 800 lb/in (14.28 kg/mm) should be required. Teflon coatings on rings will yield at 100 lb/in (1.78 kg/mm).

6. Groove Dimensions

The proper dimensions and surface finish of the groove are as important in achieving a seal as the O-Ring itself. As a general guide in the preparation of joint surfaces, the recommended groove dimensions for internal and external pressure applications are shown on page 5.

Should you need further guidance and our recommendations, submit the following information regarding your application: 1. Temperature and pressure ranges. 2. Space available. 3. Material. 4. Medium to be sealed. 5. Available compression load. 6. Sketch of proposed application.

7. Coating or Plating

Coating or plating of the O-Ring will provide adherence and ductility (softness) to conform to microscopic groove or flange irregularities.

For unplated seals, liquid leakage can be estimated by the following expression:

$$Q = \frac{5.0 \times 10^{-6} P}{\mu}$$

(Q = leakage cc/sec; P = pressure difference psi; and μ = liquid viscosity at operating conditions, centipoise.) If the resulting calculated leakage is 10^{-3} to 10^{-4} or less, actual leakage may be zero because of surface tension. If leakage occurs, it should be proportional to seal diameter, and in the above expression, multiplied by D/2. D = seal diameter. Actual leakage will probably be less than predicted.

For coated or plated seals, helium-leaktight joints may be made with proper O-Ring and coating or plating selections. Test results range from 10^{-6} to 10^{-9} cc/sec. and lower at one atmosphere differential. Recommended coating or plating materials are:

Temperature	Plating or Coating
Cryogenic to 500° F (260° C)	Teflon
to 1800° F (982° C)	Silver
to 2200° F (1186° C)	Nickel

See page 12 for other coatings and plating

8. Sealing Surface Finish

The groove and mating flange face must have a surface finish of 16 μin. rms (0.4 μmm) for bare rings, and 32-100 μin. rms (0.8 μ-2.54 μmm) for plated or coated rings.

For gas, vacuum and light liquid (water), a finish of 16 μin. (0.4 μmm) rms is recommended. For medium liquids (hydraulic oils) and heavy liquids (tar or polymers) a finish of 32 μin. (0.8 μmm) rms is recommended. Machining tool marks on groove or flange face must be concentric.

Seal surfaces should be free of dirt, grit or other foreign materials.

9. Other Design Considerations

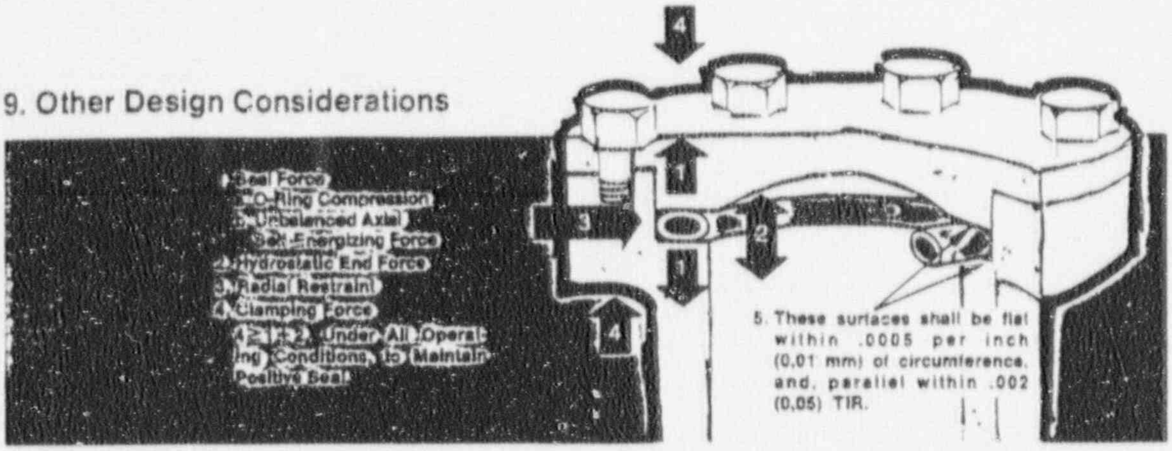

Recommended Groove Dimension

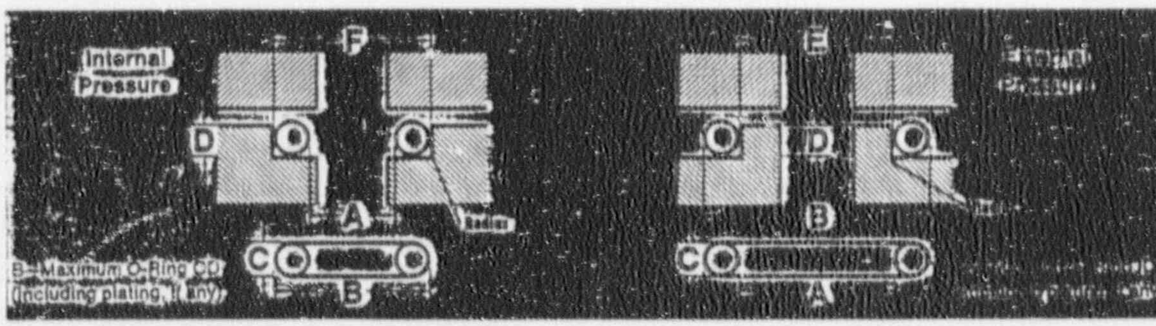

	Internal Pressure			External Pressure		
C Tube Diameter inches/mm	F Groove OD inches/mm	D Groove Depth inches/mm	Ring Tolerance A − +.000 B + −.000 inches/mm	E Groove ID inches/mm	Minimum Groove Width inches/mm	Springback* inches/mm
.031	B+.004/.006	.020/.022	0.003	A−.004/.006	.042	.002
0.8	B+0.10/0.15	0.50/0.56	0.076	A−0.10/0.15	1.07	0.05
.063	B+.004/.006	.042/.045	0.003	A−.004/.006	.085	.002
1.6	B+0.10/0.15	1.07/1.14	0.076	A−0.10/0.15	2.16	0.05
.093	B+.005/.009	.065/.069	0.004	A−.005/.009	.112	.002
2.4	B+0.13/0.23	1.65/1.75	0.102	A−0.13/0.23	2.80	0.05
.125	B+.007/.012	.090/.095	0.005	A−.007/.012	.144	.003
3.2	B+0.18/0.30	2.29/2.41	0.127	A−0.18/0.30	3.66	0.08
.156	B+.008/.014	.115/.120	0.006	A−.008/.014	.182	.004
4.0	B+0.20/0.36	2.92/3.05	0.152	A−0.30/0.36	4.46	0.10
.188	B+.009/.015	.145/.150	0.007	A−.009/.015	.220	.004
4.8	B+0.23/0.38	3.68/3.8	0.178	A−0.23/0.38	5.59	0.10
.250	B+.011/.019	.195/.200	0.008	A−.011/.019	.290	.005
6.4	B+0.28/0.48	4.95/5.08	0.203	A−0.28/0.48	7.37	0.13
.375	B+.014/.029	.295/.300	0.012	A−.014/.029	.445	.009
9.5	B+0.36/0.74	7.49/7.62	0.305	A−0.36/0.74	11.3	0.23
.500	B+.020/.038	.415/.425	0.016	A−.020/.038	.645	.013
12.7	B+0.51/0.97	10.54/10.8	0.406	A−0.51/0.97	16.7	0.33
.625	B+.020/.038	.520/.530	0.016	A−.020/.038	.780	.017
15.9	B+0.51/0.97	13.21/13.46	0.406	A−0.51/0.97	19.8	0.43

Dimensions in table above are for unplated rings. Increase groove depth for .031 inch (0.8mm) cross section rings by 2 times the plating or coating thickness of plated or coated rings.

Do not increase groove depth on plated or coated rings for cross section of .063 inch (1.6mm) and larger.

*Springback figures for tube diameters up to .250 inch (6.4 mm) are for stainless steel. Springback for .375, .500 and .625 inch (9.5, 12.7 and 15.9 mm) tube diameters are for precipitation hardened Alloy 718. Other values for different materials are available.

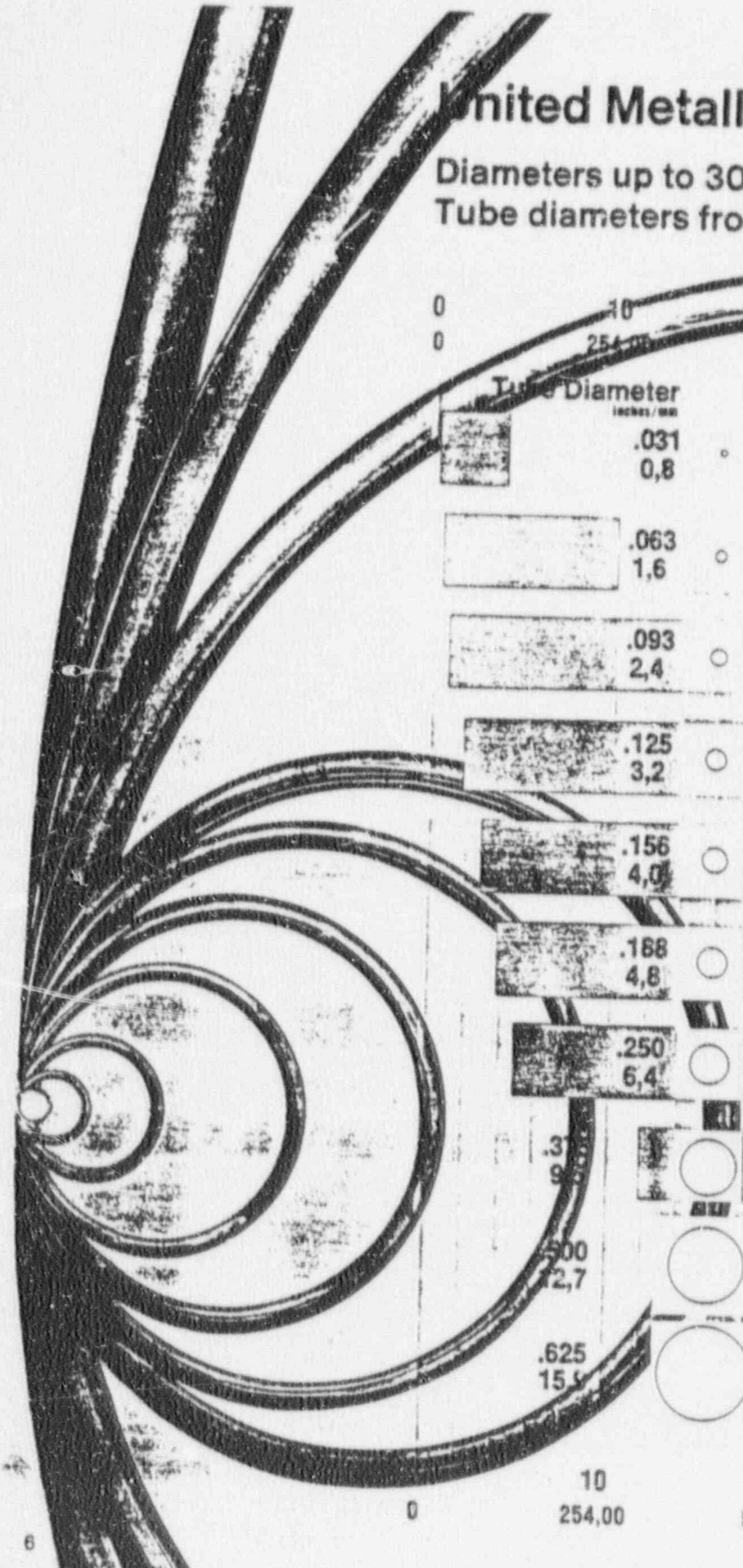

United Metallic O-Rings

Diameters up to 300 inches (7620 mm)*
Tube diameters from .031 to .625 inches (0,8 to 15,9 mm)*

0 10 20 30 40
0 254,00 508,00 762,00 1016,00

Tube Diameter inches/mm	Wall Thickness inches/mm				
.031 0,8	.005 0,13	.010 0,25	.012 0,30		
.063 1,6	.006 0,15	.010 0,25	.012 0,30	.014 0,36	
.093 2,4	.006 0,15	.010 0,25	.012 0,30	.018 0,46	
.125 3,2	.006 0,15	.010 0,25	.012 0,30	.020 0,51	.025 0,64
.156 4,0	.010 0,25	.020 0,51	.025 0,64		
.188 4,8	.012 0,30	.020 0,51	.032 0,81		
.250 6,4	.012 0,30	.025 0,64	.032 0,81	.049 1,24	
.3[illegible] 9[illegible]	.035 0,89	.049 1,24			
.500 12,7	.050 1,27	.065 1,65			
.625 15,[illegible]	.063 .063				

10 20 30 40
0 254,00 508,00 762,00 1016,(

Table I

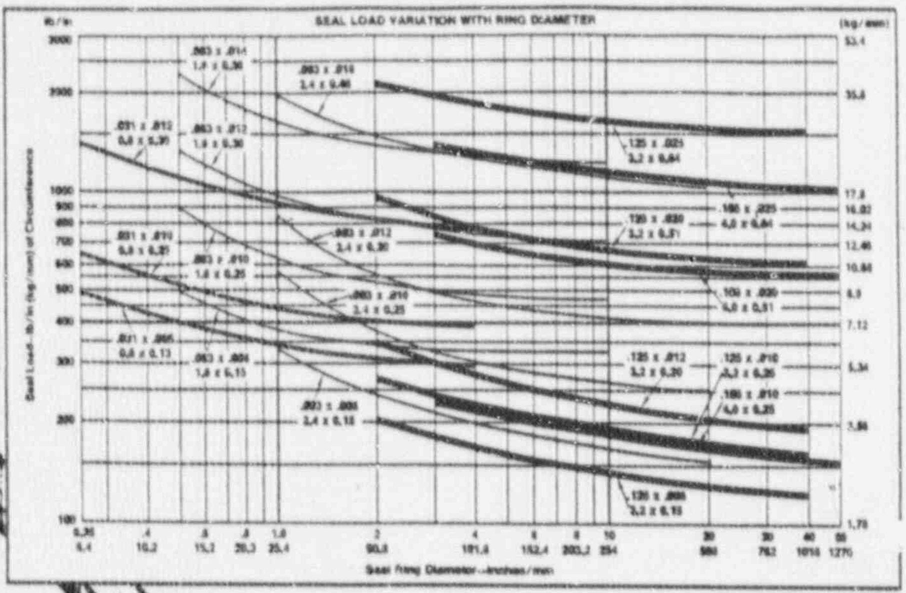

Tables I and II are for 321 stainless steel tubing.

For tubing made of Alloy 600, multiply loads shown by 1.1. For Alloy X-750, multiply by 1.. For Alloy 718, multiply by ..0.

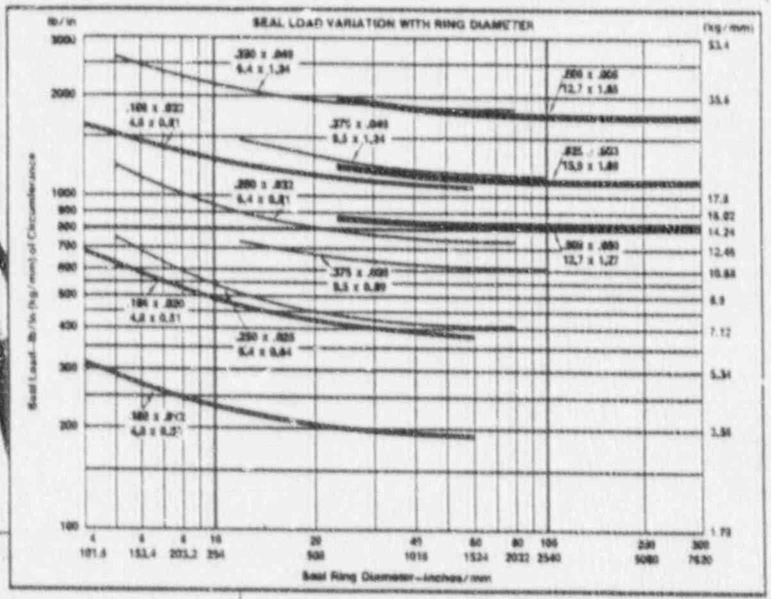

Table II

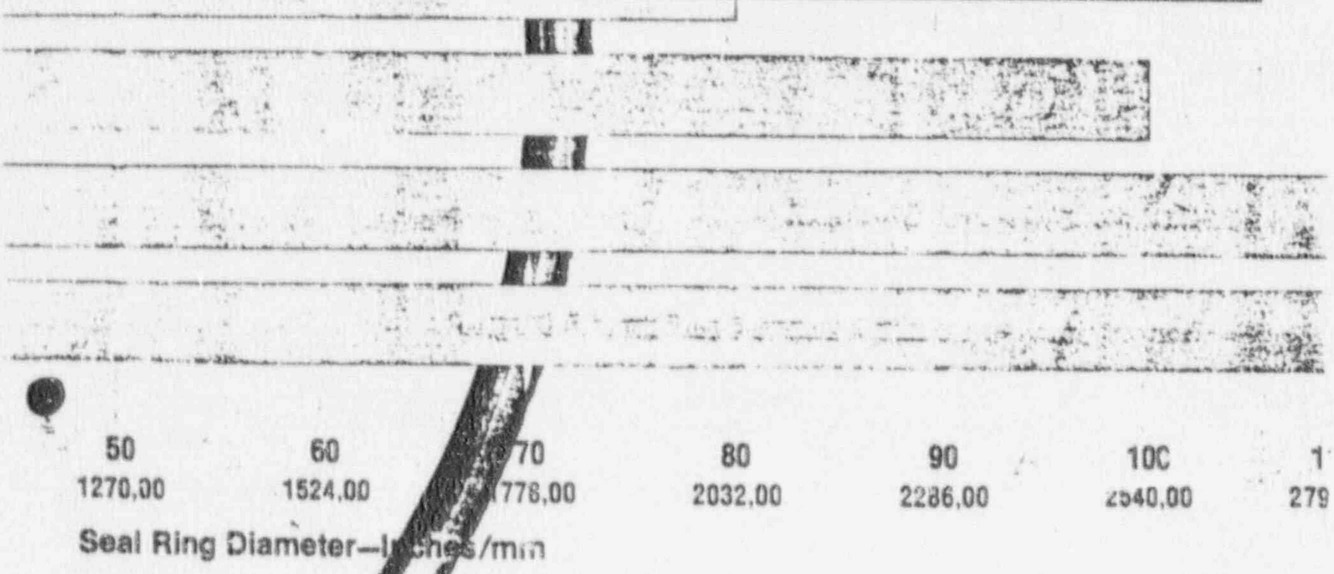

Retainer Assemblies

Metallic O-Rings can be used with a metal retainer plate for mechanical back-up that serves the same function as the machined groove wall in conventional installations. Retainer assemblies may incorporate several Metallic O-Rings into one all metallic assembly. The O-Rings are press-fitted without cross-section distortion, are secured against dropout and are easily handled during field assignment or retrofit programs. The retainer plate furnishes the O-Ring compression limit, controls hoop tension of the O-Ring, simplifies surface finish operation, permits interchangeability of flanges, and applies to single or multiple O-Ring requirements. A selection of several standard assemblies is described below:

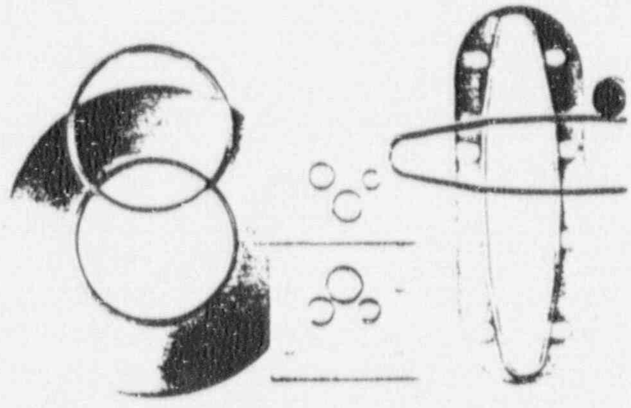

ASA/API Pipe Flange Seals

Metallic O-Rings offer static seal reliability and safety for installation or maintenance of piping. Over long periods of time, the all-metal construction of Fluorocarbon tubular Metallic O-Rings and retainer plates make them less susceptible to relaxation of sealing stresses – as compared to partially non-metallic gaskets.

In addition to their natural resilience characteristics, Metallic O-Rings provide the stability of a metal-to-metal pipe joint seal.

The natural springback of thin-wall metal tubing, and unique self-energizing design feature, create a balance of inside and outside forces which prevent collapse of the tube under pressure cycling. These same features allow Metallic O-Rings to respond to variations in sealing surface deflections without creep or cold flow, and to accommodate high and low temperature cycling. For process plant piping, they withstand temperatures from cryogenic to 1,800° F (982° C) and pressures from vacuum to 50,000 psi (3402 atm).

To maintain seal reliability, tubular Metallic O-Rings require less bolt stress than solid, fiber, flat metal, spiral wound or jacketed gaskets. Lower seal loads allow a greater bolt and flange safety factor for a given installation.

O-Rings and retainer plates are available for .250" to 24" (6.4 to 609.6 mm) pipe in all sizes of 150 to 2500 psi (10.2 to 170.1 atm) flat or raised face flanges.

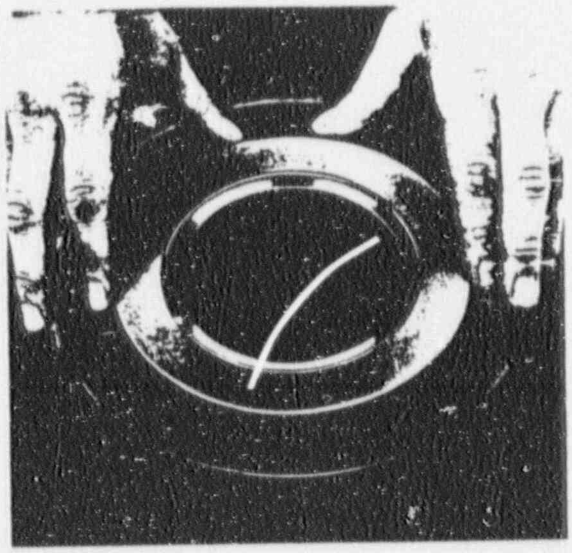

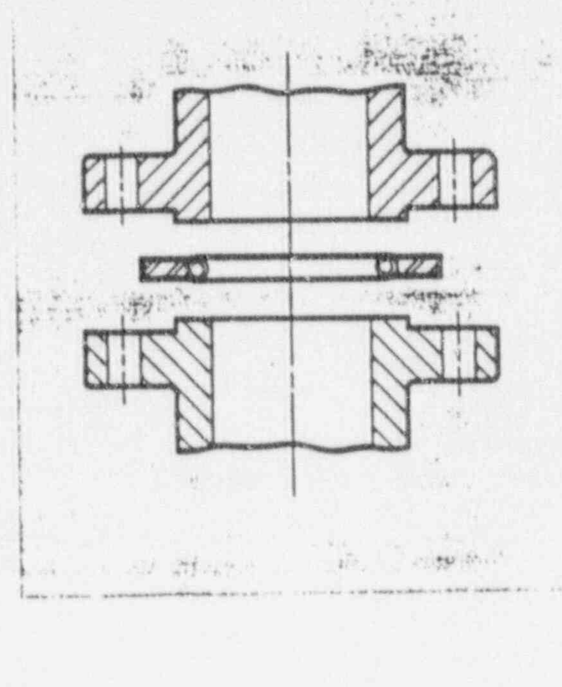

Boss Seals

United Metallic FIT-O-SEAL for boss joints combines a stainless steel retainer and a press fit Metallic O-Ring. The unit is self-positioning, controls ring compression, and can be reused. It won't deteriorate with age and is not affected by environment. Existing boss can be easily retrofitted. It can seal fuels and chemicals from high vacuum to 10,000 psi (680 atm) or higher, and will endure continuous temperatures of −452° F. (−269° C.) to 1,800° F. (982° C.). Standard seal assembly available for MS33656 fitting to MS33649 boss. Modifications available.

Flange-O-Seal

The Metallic O-Ring is semi-fastened into the metal retainer. The assembly is used for sealing jet engine fuel lines and exotic missile fuel lines from −452° F. (−269° C.) to 1,800° F. (982° C.).

It can be used for steel fittings MS20757 thru MS20762 and MS33786 fitting installation. The following assemblies are available from stock:

Part No U-700490	Part No U-700520	A Dia. Inches/mm ± .035 (0.89)	B Inches/mm ± .005 (0.13)	C Inches/mm ± .005 (0.13)
—12	—12	.863 21.92	1.156 29.36	.210 5.33
—16	—16	1.113 28.27	1.312 33.32	.210 5.33
—17	—17	1.113 28.27	1.414 35.92	.271 6.88
—20	—20	1.425 36.2	1.656 42.06	.271 6.88
—24	—24	1.613 40.97	1.812 46.02	.271 6.88
—32	—32	2.300 58.42	2.375 60.33	.333 8.46

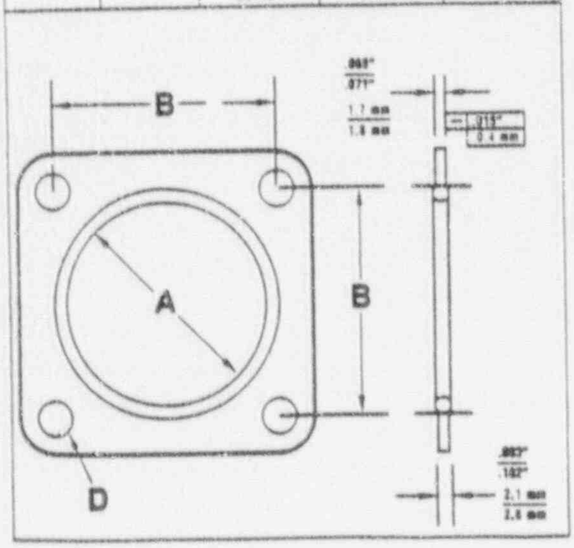

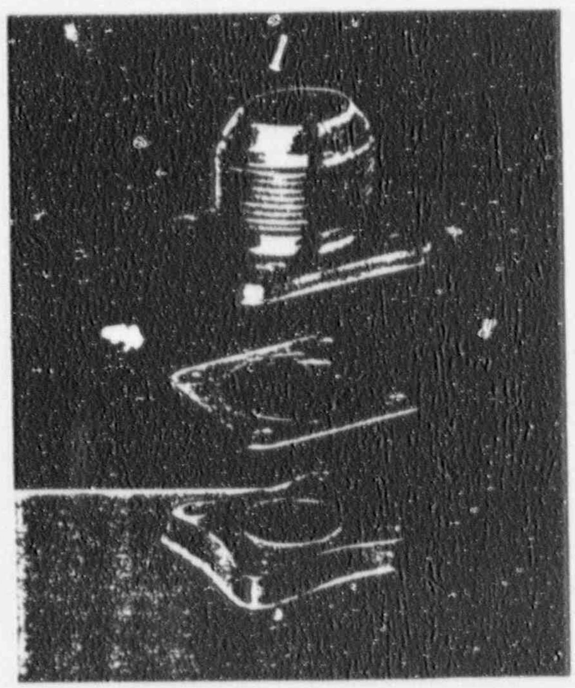

Nuclear Pressure Vessel Seals

The principal application of United Metallic O-Rings in nuclear power plants is the sealing of reactor pressure vessel heads. They are also specified for sealing applications on valves, steam generators, condensers, pumps, piping and other equipment components throughout the nuclear flow chart.

United O-Rings can easily meet the three major requirements of nuclear applications: high temperature ratings, high pressure ratings, and larger than average ring diameters (see Page 2 for specifics). United Metallic O-Rings offer other significant advantages in nuclear applications: they are not normally affected by damaging environments or corrosives; they don't deteriorate with age, even in storage, and they resist radiation and chlorides.

TABLE 1 O-Ring—Alloy 718—DEFLECTION and SPRINGBACK—Inches (mm)

Load Force Unrestrained /linear inch ◆	.375 dia. x .038 wall (9.5 x 0.95)		.500 dia. x .050 wall (12.7 x 1.27)		.625 dia. x .063 wall (15.9 x 1.60)	
	2500 lb/in (45 kg/mm)		2500 lb/in (45 kg/mm)		4000 lb/in (71.5 kg/mm)	
Percentage	Deflection	Min. Springback	Deflection	Min. Springback	Deflection	Min. Springback
8%	.030 (0.76)	.009 (0.23)	.040 (1.02)	.013 (0.33)	.050 (1.27)	.017 (0.43)
10%	.037 (0.94)	.009 (0.23)	.050 (1.27)	.013 (0.33)	.062 (1.57)	.017 (0.43)
12%	.045 (1.14)	.009 (0.23)	.060 (1.52)	.013 (0.33)	.075 (1.91)	.017 (0.43)
16%*	**.060 (1.52)**	**.009 (0.23)**	**.080 (2.03)**	**.013 (0.33)**	**.100 (2.54)**	**.017 (0.43)**
17%	.064 (1.63)	.009 (0.23)	.085 (2.16)	.013 (0.33)	.106 (2.69)	.017 (0.43)

*Optimum compression percentage. 8 to 17% compression may be utilized with UAP Inconel 718. Load forces may vary slightly below 17% inch compression.

Media to be Sealed

Media in the nuclear power plant which United O-Rings can successfully seal include: ordinary (light) water, heavy water, boiling water, steam, borated water, carbon dioxide, helium, nitrogen, liquid metals including sodium, terphenyl and other phenyl fluids, and acids including boric acid.

Flange and Groove Details

United Metallic O-Rings do not require expensive groove preparation and, being flexible, are easily installed. On pressure vessel head seals, a machined groove is required, the groove diameter being determined by the location of vessel rings so that minimum lift-off exists.

The O-Ring OD must be sufficiently large so that upon compression, the ring will expand and contact the groove outer wall. This limits hoop tension of the ring and provides a backup that restricts radial outward movement of the ring when the vessel is pressurized. Groove should be sufficiently wide so that the O-Ring ID does not contact the inside wall when the ring is compressed. Groove depth controls the amount of compression and the amount of load required to seat the ring. Table 1 shows the amount of flange load required to seat the seal.

The O-Ring and groove dimensions for internal and external pressure applications may be determined from the data on page 5.

Materials and Plating

Alloy 718 is the O-Ring material of choice on most nuclear sealing applications. Inconel 706 is also available. Alloy 718 used in United O-Rings is annealed and age hardened, offers optimum strength and springback, and resists chlorides, radiation and corrosion. Type 304 stainless steel O-Rings are also offered for applications that are less critical and where a less expensive material will suffice.

Both Alloy 718 and Type 304 stainless steel O-Rings are available with silver plating of .004" – .006" (0.10 mm – 0.15 mm) thickness. Ring OD can be controlled to .010" (0.25 mm) total tolerance after silver plating. The silver plating assures good adherence and ductility (softness) to conform to groove irregularities. Nickel plating is recommended when sealing sodium.

O-Ring Fabrication

United Metallic O-Rings are fabricated by bending straight metal tubing into circular or other desired shapes. The two ends are welded together and the weld ground flush.

Where the proposed size of the fabricated O-Ring would prohibit shipping, the company offers on-site welding fabrication that meets the same quality standards as fabrication performed in our plant.

Tube and Ring Dimensions

The three most common tube diameters used for nuclear applications are shown below with the recommended relationship of tube diameter and wall thickness to the O-Ring diameter. Other tube diameters are also available for nuclear applications. See pages 6 and 7.

TABLE 2

Tube Diameter inches/mm	Wall Thickness inches/mm	O-Ring Diameter inches/mm
.375 9.5	.038 1.0	Up to 180 Up to 4572
.500 12.7	.050 1.3	120 to 260 3048 to 6604
.625 15.9	.063 1.6	220 and up 5580 and up

TABLE 3

O-RING DIAMETER inches (mm)	No. Slots or Holes *
Up to 144 (3657.6)	8
144 (3657.6) and up.	12

*unless otherwise specified

TABLE 4

SLOT or HOLE DIMENSIONS inches (mm)

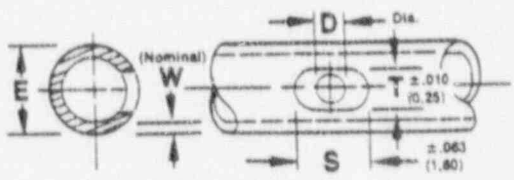

E	.375 (9.5)	.500 (12.7)	.625 (15.9)
W	.038 (1.0)	.050 (1.3)	.063 (1.6)
S	.281 (7.1)	.375 (9.5)	.438 (11.1)
T	.125 (3.2)	.205 (5.2)	.256 (6.5)
D	.070 (1.8)	.093 (2.4)	.125 (3.2)

STYLE A STYLE B STYLE C

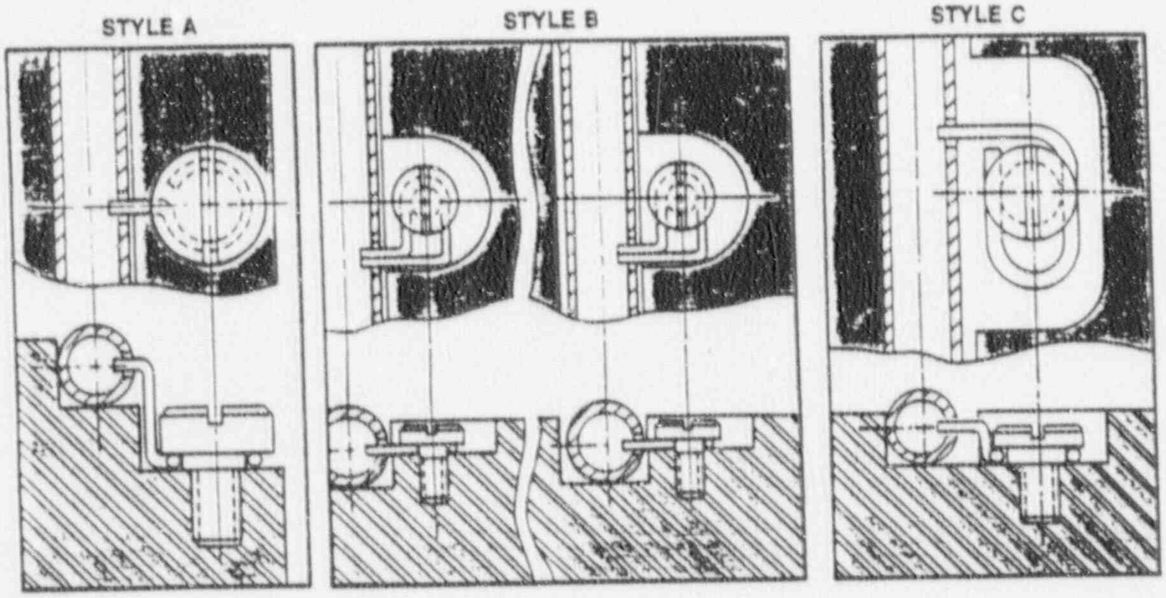

Retainer Clips

On nuclear pressure vessel heads, the rings are installed to the underside of the flange on the head. This requires clips to hold the rings in proper place and alignment during assembly of the head to the vessel. Slots are provided in the O-Ring to receive the retainer clips. In some instances the retainer clips are welded to the O-Ring. Instead of slots for retainer clips, drilled holes with additional self-energizing holes can be provided. The number of slots or holes and their size varies in relation to the ring and tube diameters (see Tables 3 and 4). The data shown assures installation without excessive O-Ring buckling in the groove and without endangering O-Ring strength. Different clipping methods are available, depending on vessel design, for both single and double ring applications (see drawings above—styles A, B and C).

How to Specify O-Rings

Denotes Metallic O-Ring | Tubing OD (Thirty-Seconds) | Wall Thickness (Thousandths)

U 2 3 12—03 625 SE A

Materials

1—Alloy 718	7—Stainless Steel 304
2—Stainless Steel 321	8—Stainless Steel 316
3—Aluminum	9—Stainless Steel 347
4—Copper	X—As Specified
5—Alloy 600	
6—Alloy X-750	

Metallic O-Ring OD (Inches) (Thousandths)

Type

SE—Self-energized on ID
PF—Pressure filled
NP—Not self-energized, not pressure filled
SO—Self-energized on OD
SX—Self-energized as spec.

Coatings

A—Silver	.001/.002 (0.03/0.05)	N—None	
B—Silver	.002/.003 (0.05/0.08)	P—Lead	.001/.002 (0.03/0.05)
D—Teflon	.001/.003 (0.03/0.08)	R—Indium	.001/.002 (0.03/0.05)
E—Teflon	.003/.004 (0.08/0.10)	T—Nickel	.001/.002 (0.03/0.05)
L—Copper	.001/.002 (0.03/0.05)	V—Gold	.0005/.001 (0.02/0.03)
X—As Specified			

Example:

U2312-03625SEA

The above example, U2312-03625SEA, indicates a type 321 stainless steel O-Ring, 3/32" (2.38 mm) tube size, .012 (0.30 mm) wall thickness, 3.625" (92.08 mm) OD, self-energized (ID) and .001-.002" (0.03/0.05 mm) silver coating.

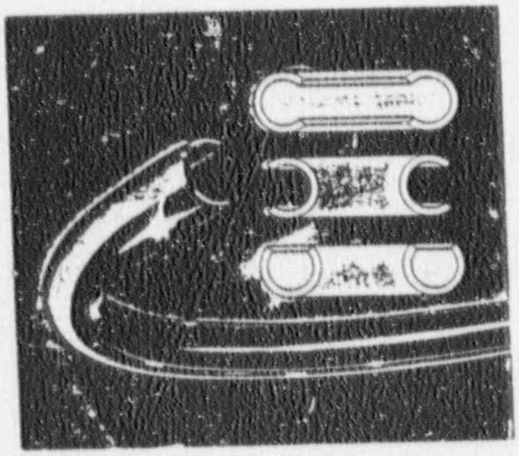

United Metallic C-Rings

United Metallic C-Rings (designated MCR) are designed for static sealing on machinery or equipment and are available for internal pressure, external pressure, or axial pressure ID/OD applications. Because C-Rings are designed with an open side on the pressure side of the installation, the seal is self-energizing. United C-Rings are offered in round or irregular shapes in a broad range of sizes from .126" (3,2 mm) OD x .032" (0,81 mm) free height to over 300" (7620 mm) OD x 2" (50,80 mm) free height. They are available in a wide variety of metal alloys and metallic or Teflon coatings. Sealing application temperature range is from cryogenic to 3,000° F. (1650° C.); pressure tolerances are from 10^{-10} torr to 100,000 psi (6,804 atm). Where customer requirements are large, the C-Ring provides the lowest unit price of any high performance seal on the market. Request **Bulletin 102C.**

FLUOROCARBON COMPONENTS DIVISION
Post Office Box 9889/Columbia, South Carolina 29290
Phone: 803/783-1880 Telex: 57-3334

SD150-C

SHAMBAN

SEALS DIVISION

Shamban P/N S11732	AS568A Dash No.	AN6227B AN6230B Part No.	O-ring Size (Inches) I.D.	±	W.	±	Nominal I.D.	Nominal O.D.	Nominal W.
313	-313	....	.662	.005	.210	.005	11/16	1 1/16	3/16
314	-314	....	.725	.005	.210	.005	3/4	1 1/8	3/16
315	-315	....	.787	.006	.210	.005	13/16	1 3/16	3/16
316	-316	....	.850	.006	.210	.005	7/8	1 1/4	3/16
317	-317	....	.912	.006	.210	.005	15/16	1 5/16	3/16
318	-318	....	.975	.006	.210	.005	1	1 3/8	3/16
319	-319	....	1.037	.006	.210	.005	1 1/16	1 7/16	3/16
320	-320	....	1.100	.006	.210	.005	1 1/8	1 1/2	3/16
321	-321	....	1.162	.006	.210	.005	1 3/16	1 9/16	3/16
322	-322	....	1.225	.006	.210	.005	1 1/4	1 5/8	3/16
323	-323	....	1.287	.006	.210	.005	1 5/16	1 11/16	3/16
324	-324	....	1.350	.006	.210	.005	1 3/8	1 3/4	3/16
325	-325	AN6227B-28	1.475	.010	.210	.005	1 1/2	1 7/8	3/16
326	-326	AN6227B-29	1.600	.010	.210	.005	1 5/8	2	3/16
327	-327	AN6227B-30	1.725	.010	.210	.005	1 3/4	2 1/8	3/16
328	-328	AN6227B-31	1.850	.010	.210	.005	1 7/8	2 1/4	3/16
329	-329	AN6227B-32	1.975	.010	.210	.005	2	2 3/8	3/16
330	-330	AN6227B-33	2.100	.010	.210	.005	2 1/8	2 1/2	3/16
331	-331	AN6227B-34	2.225	.010	.210	.005	2 1/4	2 5/8	3/16
332	-332	AN6227B-35	2.350	.010	.210	.005	2 3/8	2 3/4	3/16
333	-333	AN6227B-36	2.475	.010	.210	.005	2 1/2	2 7/8	3/16
334	-334	AN6227B-37	2.600	.010	.210	.005	2 5/8	3	3/16
335	-335	AN6227B-38	2.725	.015	.210	.005	2 3/4	3 1/8	3/16
336	-336	AN6227B-39	2.850	.015	.210	.005	2 7/8	3 1/4	3/16
337	-337	AN6227B-40	2.975	.015	.210	.005	3	3 3/8	3/16
338	-338	AN6227B-41	3.100	.015	.210	.005	3 1/8	3 1/2	3/16
339	-339	AN6227B-42	3.225	.015	.210	.005	3 1/4	3 5/8	3/16
340	-340	AN6227B-43	3.350	.015	.210	.005	3 3/8	3 3/4	3/16
341	-341	AN6227B-44	3.475	.015	.210	.005	3 1/2	3 7/8	3/16
342	-342	AN6227B-45	3.600	.015	.210	.005	3 5/8	4	3/16
343	-343	AN6227B-46	3.725	.015	.210	.005	3 3/4	4 1/8	3/16
344	-344	AN6227B-47	3.850	.015	.210	.005	3 7/8	4 1/4	3/16
345	-345	AN6227B-48	3.975	.015	.210	.005	4	4 3/8	3/16
346	-346	AN6227B-49	4.100	.015	.210	.005	4 1/8	4 1/2	3/16
347	-347	AN6227B-50	4.225	.015	.210	.005	4 1/4	4 5/8	3/16
348	-348	AN6227B-51	4.350	.015	.210	.005	4 3/8	4 3/4	3/16
349	-349	AN6227B-52	4.475	.015	.210	.005	4 1/2	4 7/8	3/16
350	-350	....	4.600	.015	.210	.005	4 5/8	5	3/16
351	-351	....	4.725	.015	.210	.005	4 3/4	5 1/8	3/16
352	-352	....	4.850	.015	.210	.005	4 7/8	5 1/4	3/16
353	-353	....	4.975	.015	.210	.005	5	5 3/8	3/16
354	-354	....	5.100	.023	.210	.005	5 1/8	5 1/2	3/16
355	-355	....	5.225	.023	.210	.005	5 1/4	5 5/8	3/16
356	-356	....	5.350	.023	.210	.005	5 3/8	5 3/4	3/16
357	-357	....	5.475	.023	.210	.005	5 1/2	5 7/8	3/16

SHAMBAN
SEALS DIVISION • FORT WAYNE INDIANA

2531 BREMER DRIVE
P.O. BOX 176
FORT WAYNE INDIANA 46801
(219) 749-9631 TELEX 22-8480
TELEFAX 219-749-0066

INDUSTRIAL PRODUCTS GROUP
2531 BREMER DRIVE
P.O. BOX 176
FORT WAYNE, INDIANA 46801
219-749-9631 TELEX 22-8480
TELEFAX 219-749-0066

AEROSPACE PRODUCTS GROUP
1855 CENTINELA AVE P.O. BOX 2141
SANTA MONICA CALIFORNIA 90404
213-829-9926 TELEX 18-2025
TELEFAX 213-829-9931

Printed in USA

FLUOROCARBON

Components Division
2620 The Boulevard
Columbia Industrial Park
Columbia, South Carolina 29209
803/783-1880

KENNETH A. MORALES
Marketing Manager

FURON

Dan Grey
Sales Engineer
4011 S. Peninsula Drive
Daytona Beach, FL 32019
904.761.6000
Fax 904.761.2794

4412 Corporate Center Drive
Los Alamitos, California 90720
714.995.1518
213.594.0941
TWX 910.341.7672
FAX 714.761.1270/213.431.6389

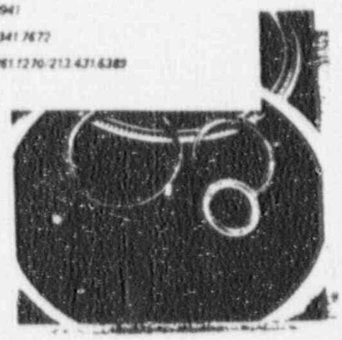

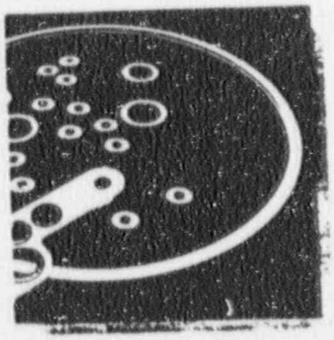

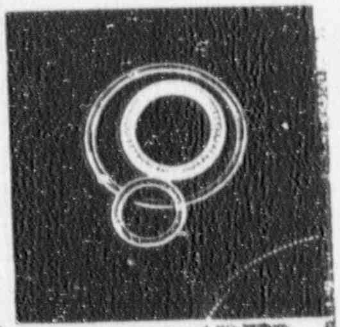

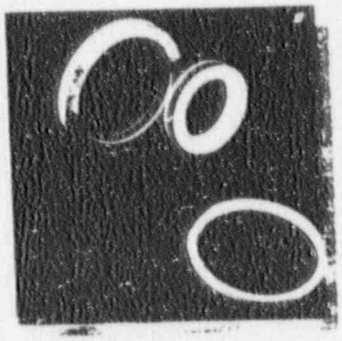

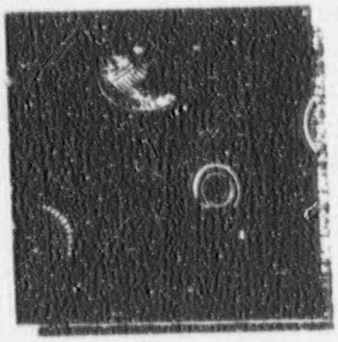

Omniseal® Design Handbook

Table of Contents

How Omniseals Work

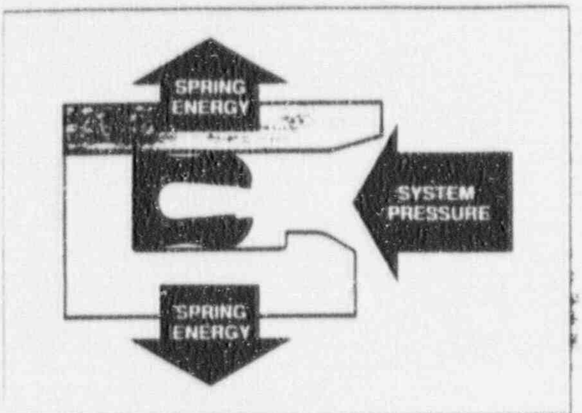

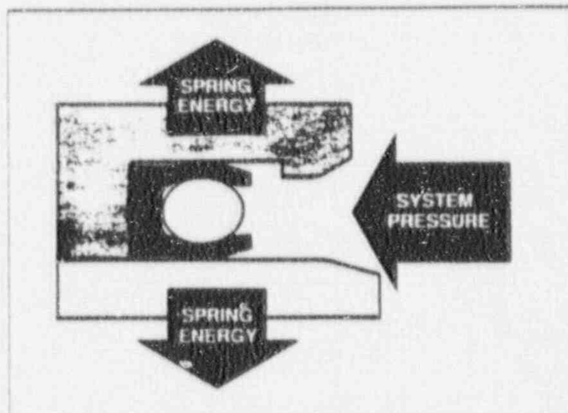

The Omniseal is a spring actuated, pressure assisted sealing device consisting of a Teflon (or other polymer) jacket or cover partially encapsulating a corrosion resistant metal spring energizer.

When the Omniseal is seated in the gland, the spring is under compression forcing the jacket lips against the gland walls thereby creating a leak-tight seal. The spring provides permanent resilience to the seal jacket and compensates for jacket wear and hardware misalignment or eccentricity. System pressure also assists in energizing the seal jacket. Spring loading assisted by system pressure provides effective sealing at both low and high pressures.

Omniseal jackets are precision machined from Teflon (PTFE), filled Teflon composites and other high performance polymers. Omniseals of Teflon are serviceable at temperatures ranging from cryogenic to 650° F. and are resistant to virtually all chemicals except molten alkali metals, fluorine gas at high temperatures and chlorine trifluoride (ClF_3).

Omniseals are available with a variety of spring energizers, each having characteristics to meet specific requirements. Spring loading can be tailored to meet critical low friction requirements in dynamic applications, or extremely high loading often required for cryogenic sealing. Springs are fabricated from corrosion resistant metals such as 300 Series and 17-7 PH stainless steels, Hastelloy, Inconel and Cobalt Nickel alloys. Omniseals with elastomer O-Rings used as energizers (nitrile, silicone, Viton®, etc.) are also available by contacting the factory.

The geometry of the Omniseal installed in the gland provides positive resistance to torsional or spiral failures. Omniseals (with metal springs) have unlimited shelf life and are not subject to age controls normally imposed on elastomeric seals.

†Viton is a registered trademark of DuPont Corporation

Omniseal Spring Designs


Spring Ring II

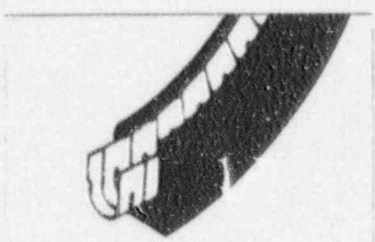
Omniseal 400A

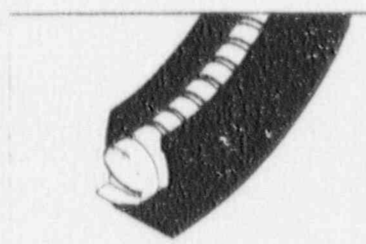
Omniseal 103A

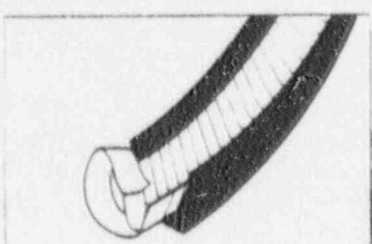
Omniseal RP II


Omniseal 1100A

Seal Selection Guide

This Omniseal Design Handbook is organized to allow you to quickly and accurately determine which Omniseal to use in your application, or to determine if you require a custom sealing solution from our Engineering Department. It is important to follow the steps below which will help you consider the appropriate seal design, size and materials.

Whether or not the solution is a standard or special Omniseal, we welcome your call to let us assist you with the selection. Take a moment to fill out the Application Data Form on page 16 and then call us at: 1-800-544-0080

Selecting Standard Omniseals

STEP 1

Familiarize yourself with the Omniseal part numbering system shown on Page 17 and note the difference between military and industrial glands.

Determine seal type (radial or face seal) and design (static or dynamic) from the Seal Function And Motion section on Page 10 and 11.

STEP 2

Determine the optimum seal configuration based on the following:

A. Design variations for radial seals on Pages 17 through 21 (military or industrial) and face seals on Pages 30 and 31.
B. Temperature/Pressure/Extrusion Gap Page 13.
C. Frictional Considerations Page 12.
D. Hardware Design Considerations Page 22, 23, 28 and 31.

You have now determined the design of the seal to use in your application. This selection will determine the first element of the seal part number.

XXX - XXX - XXXX
Basic Seal Design

STEP 3

Select a seal size from the charts on pages 24 through 27 for a radial seal or pages 32 through 35 for a face seal. If the desired size does not appear on the charts, call our Technical Service Department for assistance.
Caution: Do not intermix military and industrial gland dimensions shown on Page 24 through 27.

The selection of the seal size dash number will determine the second component of the seal part number.

XXX - **XXX** - XXXX
Seal Size Dash Number

STEP 4

Select a seal jacket material from Page 14 based on the following:

A. Friction Page 12.
B. Temperature Capabilities Page 13 and 14.
C. Pressure Capabilities Page 13.
D. Media Compatibility Page 14.

The seal jacket material selection will determine the third component of the seal part number.

XXX - XXX - **XX**XX
Seal Jacket Material

STEP 5

Select a seal energizer material from the information on Page 15. This will determine the fourth and final component of the seal part number.

XXX - XXX - XX**XX**
Seal Spring Material

Note: For additional Part Number information see Page 17.

Special Sizes

In addition to the standard sizes listed in this catalog, sizes in between those shown, larger sizes and metric sizes are also available. Since Omniseals are machined rather than molded, no special tooling charges are involved in producing non-standard sizes.

Custom Designs

Fluorocarbon specializes in custom engineered designs to meet specific applications. If your application is of a particularly critical nature not covered in this catalog, we invite you to send complete details for review and recommendations by our Engineering Department.

Seal Function And Motion

Static Seals & Dynamic Seals

The two basic types of sealing devices are STATIC SEALS and DYNAMIC SEALS. In static sealing there is essentially no relative motion between the seal and the hardware members. An example would be the seal clamped between bolted flanges.

In dynamic sealing there is relative motion between the two sealing surfaces. A typical example would be the rod and piston seals in a hydraulic cylinder.

There are two directions of motion in dynamic sealing, reciprocating or linear motion, and rotary (including oscillating) motion. Occasionally there may be a combination of both.

An additional factor to be considered is the orientation of the seal in the hardware. Seals that are compressed in a radial direction are called RADIAL Seals, again using rod and piston seals as examples. Radial Seals are usually dynamic, although may occasionally be static.

Seals that are compressed in a direction parallel to the axis are called FACE Seals, the flange gasket being a typical example. Face Seals are usually, but not always, static.

Examples of these basic seal types are shown below and on Page 11. Typical installations are also shown on Page 37.

Selecting An Omniseal Design

The Mechanical Seal Division of the Fluorocarbon Company manufactures and markets a variety of basic styles of spring energized Teflon (or other plastics) seals. Several of these designs can be used interchangeably in the same gland. Further, there are overlap and gray areas where several different designs may be used in the same application.

The recommendations below are intended as a general guide and should be used together with the tables and charts that appear on the following pages. Should you require additional assistance, we invite you to contact our Technical Service Department.

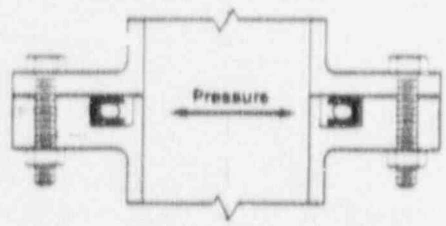

Inside Face Seal

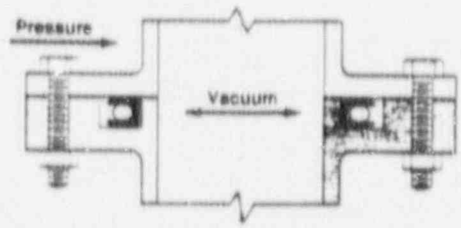

Outside Face Seal


Omniseal 400A


Omniseal 103A


Omniseal 1100A

Face Seals In Static Service

Omniseal 103A, Page 30, is generally the first choice for most static face seal applications. This series has moderate to high load spring, and is capable of sealing effectively over a wide temperature and pressure range.

Because of its very high spring loading, the Omniseal 1100A, Page 31, is particularly recommended for extreme sealing conditions, cryogenic temperatures, ultra-high vacuum and positive sealing of helium and other thin gases.

The Omniseal 400A, Page 30, may also be used as a static face seal when very light spring loading is essential. However, sealing ability may not be as effective under extreme conditions as can be obtained with either the Omniseal 103A or the 1100A due to the relatively light spring load. Optional springs are available from the factory.

Face Seals In Rotary Motion

The Omniseal 400A, Page 30, is recommended for rotary face seal applications at slow to moderate rotary speeds. Low spring loading keeps friction to a minimum. For ultra-low friction or high surface speeds it is suggested that the factory be contacted for guidance.

In oscillatory or slow, intermittent rotary applications, where high rotational torques are available, the Omniseal 1100A, Page 31, is recommended. Such applications include swivels and loading arm pivot joints. Because of its exceptionally high spring load, the Omniseal 1100A is also an excellent choice when maximum sealability is mandatory in thin liquids and gases, and sealing at cryogenic temperatures.

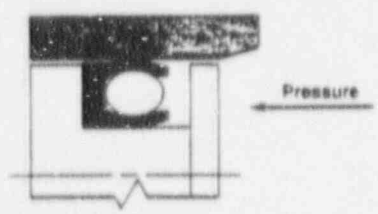

Piston Seal

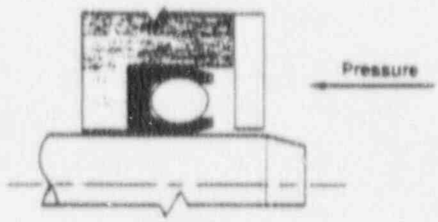

Rod Seal

Radial Seals In Static Service

While most of the Omniseal designs can be used as static radial seals, the Omniseal 103A, Page 20, is generally recommended for this service. Its moderate to high spring load provides positive sealing under most static sealing conditions.

Radial Seals In Reciprocating Motion

Reciprocating radial seals are the most common Omniseal applications. For rod and piston sealing and similar applications the Omniseal 400A, Page 19, is recommended for general purpose sealing at low to moderate pressures. This series has a low load, high deflection spring which provides low friction sealing and compensates for minor hardware eccentricity or misalignment.

For more severe dynamic conditions the Omniseal 103A, Page 20, is recommended. The higher spring load provides positive sealing but with some increase in seal friction. Particularly suitable for medium to high pressure service. Excellent rod seal for positive sealing.

The Omniseal RP II, page 21, is a very rugged design for severe operating conditions. This seal utilizes a unique wrapped and formed stainless steel ribbon spring which is highly resilient with wide deflection capabilities. Its almost indestructible spring and rugged jacket design make the Omniseal RP II an excellent choice for heavy duty sealing applications and long wear life.

The Spring Ring II, Page 18, is an economical alternative to the Omniseal 400A for high production applications requiring low cost, small size seals. It is manufactured by automated methods and is offered only in a limited number of sizes (.125 I.D. to .875 I.D.). Design and sealing characteristics are similar to the Omniseal 400A.

Radial Seals In Rotary Motion

All of the Omniseal designs can be used in slow to moderate speed rotary or oscillatory applications at low pressure.

In rotary shaft applications the flanged design is recommended. The flange is clamped in the hardware to prevent the seal from turning with the shaft. This can sometimes occur with the standard designs due to thermal and other effects. The flange provides positive retention of the seal in the gland.

The flanged Omniseal 400A, Page 19, and Spring Ring II, Page 18, are recommended for most rotary/oscillatory applications. The light spring load minimizes friction, and at pressure under 20 PSI, permits surface speeds in the range of 200 - 300 ft/min. At higher pressures the surface speed must be reduced to prolong seal wear life. The resilient U-shaped spring allows for minor shaft run-out or misalignment.

For very slow (under 50 ft/min.) and intermittent rotary/oscillatory motion at higher pressures, the flanged Omniseal 103A, Page 20, and Omniseal RP II, Page 21, are recommended. The Omniseal RP II has a very resilient spring that can tolerate shaft run-out and misalignment.

For applications requiring ultra-low friction, high pressures or high surface speeds we suggest that you consult with our Technical Service Department for recommendations.

Fluorocarbon's Components Division, in Columbia, South Carolina, designs and manufactures a complete line of rotary lip seals for high speed and/or high pressure rotary applications, see Page 43

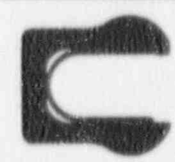
Spring Ring II

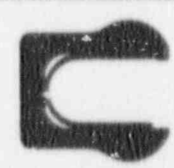
Omniseal 400A

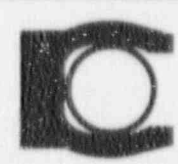
Omniseal 103A


Omniseal RP II


400A With Flange

Step 2 Step 4

Friction And Rotary Motion

Friction

Friction, a measurement of the resistance to sliding between a seal and hardware surfaces, is directly related to seal material coefficient of friction and the total load. Some other factors affecting friction are lubrication, temperature and hardware surface finishes. An approximate friction value for non-lubricated conditions can be calculated using the charts and formulas on this page. Lubrication provided by the media may produce lower friction results.

It is difficult to predict how the running and break-out friction values will differ without testing under actual existing conditions. In many cases, these differences are insignificant.

Fluorocarbon manufactures a variety of springs with lower or higher loads than shown below. Also, special springs can be developed when required.

Contact our Technical Service Department for assistance with applications where friction is critical.

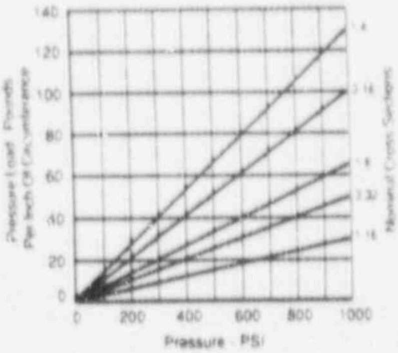

The total load of an Omniseal can be calculated by adding the pressure load found in the above chart to the average spring load shown below.

F = total load - pounds per inch of circumference (pressure load + spring load)

D = diameter of dynamic surface

R = $\frac{D}{2}$ (radius)

μ = material coefficient of friction

Linear Friction (pounds) = $F \times D \times \pi \times \mu$

Frictional Torque (inch - pounds) = $F \times D \times \pi \times \mu \times R$

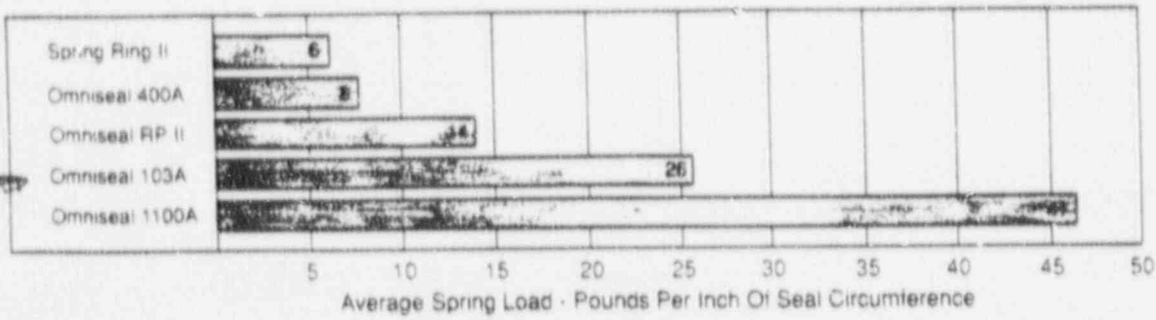

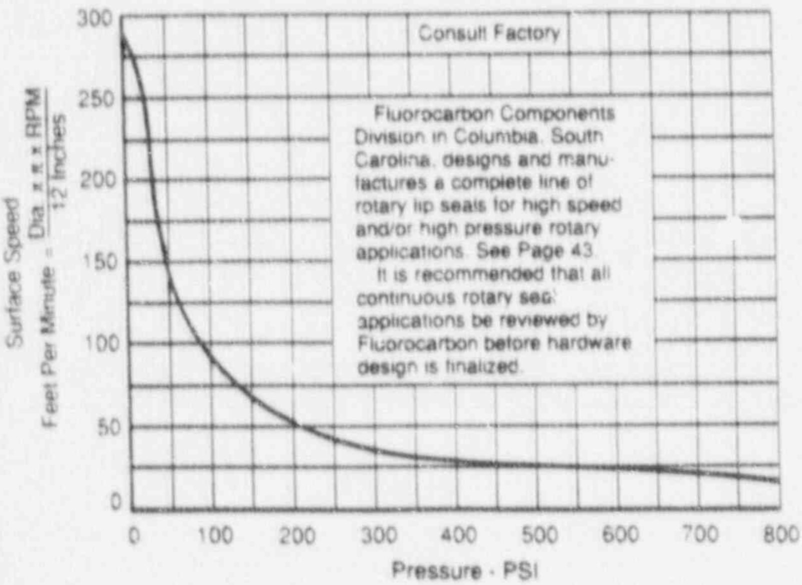

Rotary Motion

Use the adjacent chart to qualify Omniseals for continuous rotary applications.

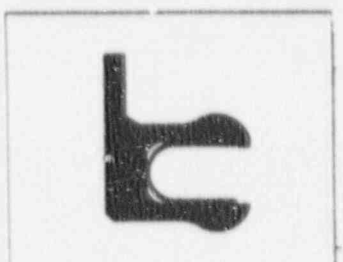

400A With Flange

The flanged seal design allows entrapment of the seal by the hardware to prevent seal rotation. See Page 11 for seal design recommendations.

Temperature - Pressure - Extrusion Gap

Maximum Recommended Extrusion Gap

(Omniseal 103A shown for illustration only)	Material (See Page 14)	A	B	C	[illegible]
 G. Width	Unfilled	.004	.003	.002	
	Filled	.006	.004	.003	
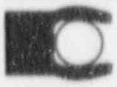 G. Width	Unfilled	.006	.004	.003	
	Filled	.008	.006	.004	
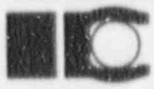 G. Width	Filled Back-up	.008	.006	.004	
	Fluoroloy 55 Back-up	.010	.008	.006	[illegible]
 G. Width	Filled Back-up	.010	.008	.006	
	Fluoroloy 55 Back-up	.014	.010	.008	[illegible]

See Back-up Rings, Page 21

Temperature Vs. Pressure And Seal Design

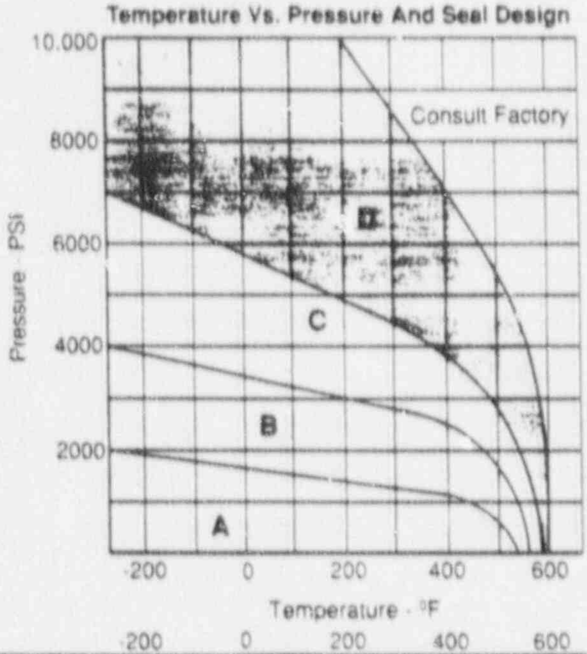

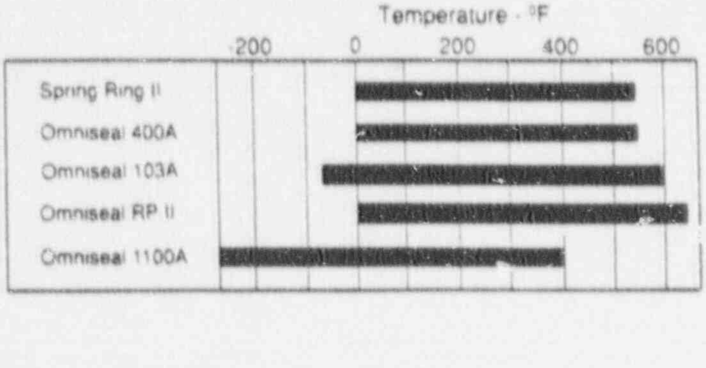

When sealing high pressures and/or high temperatures, the amount of the extrusion gap behind the seal becomes critical. This extrusion gap is the clearance between the hardware members. Hardware designs without bearing or centering devices must consider the diametral clearance as the maximum extrusion gap. At high pressures and/or high temperatures an excessive clearance can allow the seal jacket to be extruded into the gap causing premature seal failure.

The extrusion gap should be held to the minimum practical, and should not exceed the values shown on the table at the left. Increasing the heel thickness of the seal improves resistance to extrusion. Also, the extrusion gap can be bridged by the use of a separate back-up ring arrangement.

Generally, the back-up ring should be of a harder material than the seal material. A high filled Teflon compound, or a high modulus plastic, such as Fluoroloy 55, is recommended. See materials shown on Page 14. Additional back-up ring details are shown on Page 21.

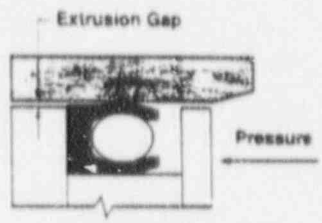

Cryogenic Sealing

Cold temperatures below -40° F will cause Teflon and other Fluorocarbon sealing materials to shrink and harden. These additional forces may compromise the spring load and frictional characteristics of the Omniseal.

Although face seals are less affected than radial seals, we recommend you consult our Technical Service Department before selecting an Omniseal for any cryogenic application.

Seal Design Vs. Temperature

In general, seal jacket materials become somewhat harder at cold temperatures and tend to soften to some extent at high temperatures (see material list on Page 14 for temperature ranges). The spring energizer compensates for these conditions. If your seal design selection does not agree with the graph at the left, consult our Technical Service Department.

Seal Jacket Materials

Fluorocarbon Seal Jacket Materials

Fluorocarbon's seal materials are compounded and processed for optimum seal performance in a wide variety of sealing environments. The materials listed below are our most commonly recommended compounds, and are suitable for most applications.

Over the years Fluorocarbon has developed over 80 different materials for seal use. These additional compounds are available should they be required in special cases. If in doubt about selection, contact our Technical Service Department for guidance. 1-800-544-0080

Code No.	Name and Description	Color	Application	Temperature Range Degrees °F.	Coefficient of Friction Nominal	Relative Cost 1 = Low, 5 = High
01	Fluoroloy 01 Virgin PTFE	White	Excellent for light to moderate dynamic and static service. Limited wear and heat resistance. Low gas permeability. Good cryogenic properties. Moderate to hard vacuum service. FDA approved	+400° To -450°	.09	1
02	Fluoroloy S Premium PTFE	Yellow	Modified PTFE with similar properties to Fluoroloy 01 material but with substantially improved wear resistance	+400° To -450°	.09	2
03	Fluoroloy SL Carbon/Graphite Filled PTFE	Grey	Excellent general purpose material for heat and wear resistance. Recommmended for dry and poorly lubricated applications. Particularly suitable for water and steam service	+600° To -450°	.09	3
06	Fluoroloy 06 Glass/Moly Filled PTFE	Grey	Tough, long wearing, heat resistant. Recommended for high pressure hydraulic service, steam and water. Caution: Can be abrasive running against soft metals at high surface speeds	+550° To -450°	.09	1
08	Fluoroloy G Proprietary UHMWPE	Gold	Extremely tough, long wearing, but limited heat and chemical resistance. Particularly suitable for abrasive media. Recommended for long wear life under severe conditions	+180° To -450°	.11	4
10	Fluoroloy K Ekonol® Filled PTFE	Tan	Proprietary plastic reinforced (filled) PTFE. Superior heat and wear resistance. Non-abrasive. Recommended for moderate to high speed dynamic service running against soft metals	+550° To -450°	.15	3
12	Fluoroloy 12 Graphite Filled PTFE	Black	Excellent general purpose material with good heat and wear resistance. Non-abrasive. Compatible with all hydraulic fluids and most chemicals. Good in water and non-lubricating fluids	+600° To -450°	.09	2
14	Fluorogold Premium Glass Filled PTFE	Yellow	Proprietary fiber glass filled PTFE with excellent heat, wear and chemical resistance. Good cryogenic properties. Caution: Can be abrasive running against soft metals at high surface speeds. Excellent material for back-up rings	+550° To -450°	.09	3
23	Fluoroloy 23 Virgin Tefzel®	Clear	Thermoplastic with superior resistance to nuclear radiation, but limited heat and wear resistance. Not recommended for general purpose sealing	+300° To -150°	.50	5
24	Fluoroloy B Carbon/Graphite Filled PTFE	Black	Similar to Fluoroloy SL material but increased hardness and wear resistance. Excellent in steam and water under severe conditions. Improved creep and extrusion resistance at higher temperatures. Good for back-up rings	+550° To -450°	.10	4
33	Fluoroloy 33 Premium Filled PTFE	Black	Excellent wear material for higher temperatures, pressures and speeds. Excellent in water and water base solutions. Superior in dry or poorly lubricated applications. Can be abrasive running against soft metals	+600° To -450°	.09	3
34	Fluoroloy 34 Polyester Elastomer	Cream	Elastomeric material with good wear and abrasion resistance but limited chemical and temperature resistance. Excellent in hydraulic oils and water. Not recommended for steam	+300° To -150°	.18	4
36	Fluoroloy 36 Glass/Moly Filled PTFE	Grey	Similar to Fluoroloy 06 material but somewhat softer for improved sealing at low pressure. Can be abrasive running against soft metals	+600° To -450°	.09	1
49	Fluorowhite Proprietary UHMWPE	White	Proprietary composite with extremely good wear and abrasion resistance, but limited heat and chemical resistance. Meets FDA requirements	+180° To -450°	.11	4
55	Fluoroloy 55 Virgin Peek	Tan	A high modulus material with excellent high temperature resistance. Recommended for back-up rings only	+550° To -100°	N/A	5

[1] Ekonol is a registered trademark of SOHIO Co.

®Tefzel is a registered trademark of DuPont Corporation

Spring Energizer Materials

Spring Energizer Materials

Omniseals are offered with the following spring energizers. Because of the almost infinite variety of fluid media that may be encountered by the seals, no attempt is made to make specific recommendations. The various stainless steels listed are compatible with most fluids. If you are in doubt about media compatibility, consult Fluorocarbon's Technical Service Department.

Code No.	Description	Relative Cost 1 = Low, 5 = High	Spring Ring II	Omniseal 400A	Omniseal 103A	Omniseal RP II	Omniseal 1100A
							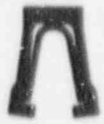
			Page 18	Page 19 & 30	Page 20 & 30	Page 21	Page 31
01	301 Stainless Steel	1	**Standard**	Optional All Sizes		**Standard**	**Standard**
02	718 Inconel	4					Optional All Sizes
03	Cobalt Nickel Allo, (Equivalent To Elgiloy)	4		Optional All Sizes	Optional All Sizes		Optional All Sizes
04	304 Stainless Steel	1		**Standard**	Optional All Sizes		
05	Elgiloy®	5		Optional All Sizes	Optional All Sizes		
06	316 Stainless Steel	2	Optional All Sizes	Optional All Sizes	Optional All Sizes		
07	17-7PH Stainless Steel	2			**Standard**		
08	C276 Hastelloy	3		Optional All Sizes	Optional All Sizes	Optional All Sizes	

® Elgiloy is a registered trademark of the Elgiloy Company

All Fluorocarbon spring and seal materials are of the highest quality and are traceable to their origin. Material certifications are available at no extra charge.

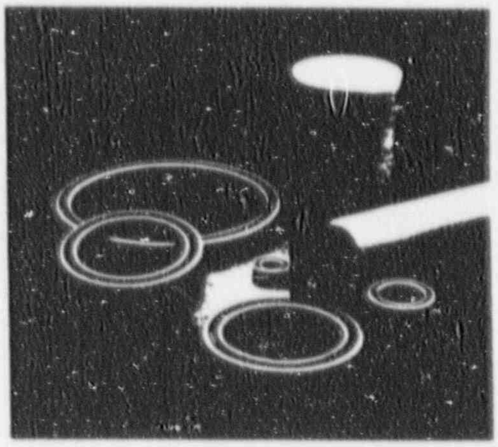

16

Application Data Form

Sample Work Sheet - Do Not Remove!

Name ______________________ Title ______________

Company ______________________________

Address ______________________________

City ______________ State ______ Zip ______________

Phone No. ______ ______ FAX No. ______________

Product Name ______________________ ☐ In Test

Application ______________________ ☐ In Production

Present Seal ______________________ ☐ In-House Equipment

No. Seals/Unit ______________ No. Seals/Year ______________

☐ Static ☐ Rod Seal Stroke Length ______________

☐ Reciprocating ☐ Piston Seal Strokes Per Min. ______________

☐ Rotary ☐ Inside Face Seal RPM ______________

☐ Oscillating ☐ Outside Face Seal Friction Req'd. ______________

Media ______________________ ☐ Liquid ☐ Gaseous

Temperature: Operating ________ Min. ________ Max. ________

Pressure: Operating ________ Min. ________ Max. ________

Gland O.D. ______ / ______ Gland I.D. ______ / ______

Material ______________ Material ______________

Hardness ______________ Hardness ______________

Finish ______________ Finish ______________

Gland Width ______ / ______ Can gland be changed? ______________

Extrusion Gap ______ / ______ Will seal be stretched? ______________

Will seal pass by sharp edges? ______ Sealing grit or abrasives? ______

INDICATE PRESSURE SIDE

TEMPERATURE CONVERSION

°F	°C	°R	°K
602	316.6	1061.7	589.8
572	300.0	1031.7	573.2
542	283.3	1001.7	556.5
512	266.6	971.7	539.8
482	250.0	941.7	523.2
452	233.3	911.7	506.5
422	216.6	881.7	489.8
392	200.0	851.7	473.2
362	183.3	821.7	456.5
332	166.6	791.7	439.8
302	150.0	761.7	423.2
272	133.3	731.7	406.5
242	116.6	701.7	389.8
212	100.0	671.7	373.2
182	83.3	641.7	356.5
152	66.6	611.7	339.8
122	50.0	581.7	323.2
92	33.3	551.7	306.5
62	16.6	521.7	289.8
32	0.0	491.7	273.2
2	-16.6	461.7	256.6
-28	-33.3	431.7	239.9
-58	-50.0	401.7	223.9
-88	-66.6	371.7	206.6
-118	-83.3	341.7	189.6
-148	-100.0	311.7	173.2
-178	-116.6	281.7	156.6
-208	-133.3	251.7	139.9
-238	-150.0	221.7	123.2
-268	-166.6	191.7	106.6
-298	-183.3	161.7	89.9
-328	-200.0	131.7	73.2
-358	-216.6	101.7	56.6
-388	-233.3	71.7	39.9
-418	-250.0	41.7	23.2
-448	-266.6	11.7	6.6
-459.7	-273.2	0	0

$F = \frac{9}{5}C + 32$ $K = C + 273.2$

$C = \frac{5}{9}(F - 32)$ $R = F + 459.7$

POUNDS PER SQUARE INCH (PSI)
VERSUS KILOGRAMS PER SQUARE CENTIMETER
(KG/CM^2)

PSI	$KG./CM^2$	PSI	$KG./CM^2$	PSI	$KG./CM^2$
100	7.03	2,600	182.84	5,200	365.68
200	14.06	2,700	189.87	5,400	379.75
300	21.10	2,800	196.90	5,600	393.81
400	28.13	2,900	203.94	5,800	407.88
500	35.16	3,000	210.97	6,000	421.94
600	42.19	3,100	218.00	6,200	436.01
700	49.23	3,200	225.03	6,400	450.07
800	56.26	3,300	232.07	6,600	464.14
900	63.29	3,400	239.10	6,800	478.20
1,000	70.32	3,500	246.13	7,000	492.26
1,100	77.35	3,600	253.16	7,200	506.33
1,200	84.39	3,700	260.20	7,400	520.39
1,300	91.42	3,800	267.23	7,600	534.46
1,400	98.45	3,900	274.26	7,800	548.52
1,500	105.48	4,000	281.29	8,000	562.59
1,600	112.52	4,100	288.33	8,200	576.65
1,700	119.55	4,200	295.36	8,400	590.72
1,800	126.58	4,300	302.39	8,600	604.78
1,900	133.61	4,400	309.42	8,800	618.85
2,000	140.65	4,500	316.46	9,000	632.91
2,100	147.68	4,600	323.49	9,200	646.98
2,200	154.71	4,700	330.52	9,400	661.04
2,300	161.74	4,800	337.55	9,600	675.11
2,400	168.78	4,900	344.58	9,800	689.17
2,500	175.81	5,000	351.62	10,000	703.23

1 2

Omniseal Part Numbering System

Important Note About Part Numbers

Standard part numbers listed in this catalog should not be used for source control drawings or when special handling of any kind is required. This includes special dimensional or material control requirements, inspection procedures or packaging not normally covered by standard catalog part numbers. Special part numbers are assigned by the factory to cover any out-of-the-ordinary requirements. These special numbers are assigned to your specific application and provide precise, permanent control of your parts. Contact our Technical Service Department, 1-800-544-0080

Seal Design	Seal Size	Jacket Material	Energizer Material
230	348	01	07

Seal Design (230):
- **Spring Ring II** Page 18
- **Omniseal 400A** Page 19 & 30
- **Omniseal 103A** Page 20 & 30
- **Omniseal RP II** Page 21
- **Omniseal 1100A** Page 31
- **Back-up Rings** Page 21

Seal Size (348):
- **Radial Seals** Page 24 - 27
- **Face Seals** Page 32 - 35

Jacket Material (01): Page 14

Energizer Material (07): Page 15 (Not required for back-up rings.)

Part Number Can Be Written As *2303480107 or 230-348-0107*

Boss Seal part number shown on Page 36.

Basic P/N	
Mil. 230	

Mil. = Military Glands
Ind. = Industrial Glands

Military Versus Industrial Glands
Radial Omniseals and back-up rings can be supplied to fit either Mil-G-5514F military O-Ring glands, or industrial, (fractional) glands. Unless conformance to the military specification is required, it is recommended that the industrial gland dimensions be used. See Page 24 through 27 for gland diameters.

Seal Design Variations

Skived Lip
All Omniseal designs except Omniseal RP II can be supplied with a sharp edge on either the I.D. or O.D. sealing lip. This edge provides a scraper/wiper action for sealing abrasive or viscous media. May also be used as an environmental excluder.

Extended Heel
Omniseals can be supplied with an extended heel section for improved resistance to extrusion at high temperatures and/or high pressures. See Page 13 for selection guidance.

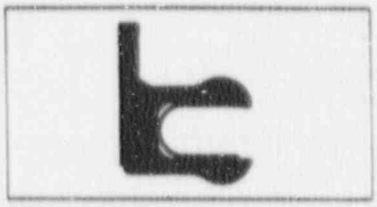

Flanged Heel
The flanged heel design is recommended for rotary/oscillatory shaft applications. The flange is clamped in the seal housing to prevent the seal from turning with the shaft. See comments on Page 11 and 12.

Quality Control

The Fluorocarbon Mechanical Seal Division Quality System is based on the requirements of MIL-I-45208. This system also conforms to NASA Spec. NHB5300.4 and Federal Regulation 10CFR50, Appendix B. Our facility is equipped to provide complete inspection, test and certification needs. Our Quality Department will represent the customer interest in all areas of contract administration, documentation control and manufacturing functions.

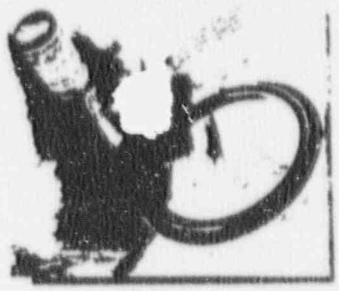

Omniseal 103A

Omniseal Series 103A

The Omniseal 103A is a refinement of the original spring energized seal design. The helical wound flat spring offers a moderate to high spring load for static and slow to moderate speed dynamic sealing. It has higher friction than the 400A Series, but better sealing of thin liquids and gases. Available in all MIL-G-5514F and industrial sizes.

Elastomeric Energizers

Omniseal 103A seals may be ordered with optional elastomeric O-Ring energizers in place of the metallic spring. A wide variety of elastomers (nitrile, Viton®, silicone, etc.) are available. Contact our Technical Service Department for details.

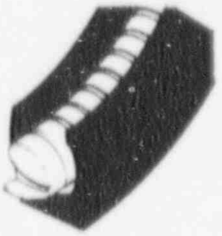

Nominal Seal Dimensions (For Reference Only)

[illegible]	Nominal Cross Section	M	Mil. N	Ind. N	R	X	W	T	(1) Seal I.D. = Gland B Dia.
[illegible]	1/16	.082	.067	.073	.110	.104	.118	.021	Minus .011
[illegible]	3/32	.122	.102	.107	.160	.150	.149	.028	Minus .013
[illegible]	1/8	.160	.140	.144	.210	.185	.196	.033	Minus .019
[illegible]	3/16	.245	.215	.218	.300	.240	.296	.038	Minus .029
[illegible]	1/4	.308	.277	.289	.413	.330	.384	.053	Minus .038

(1) See Pages 24 through 27 for Gland Dimensions

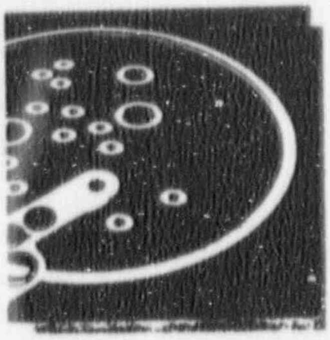

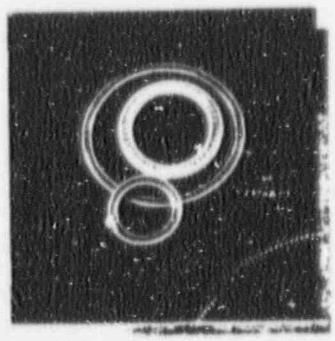

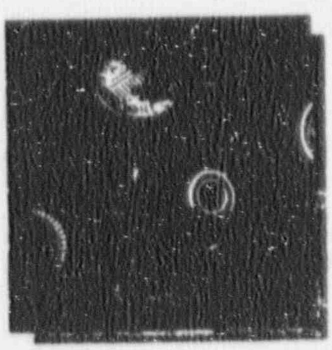

FLUOROCARBON

Dedicated To Excellence

MECHANICAL SEAL DIVISION
4412 Corporate Center Drive
P.O. Box 520
Los Alamitos, CA 90720
(213) 594-0941 (714) 995-1818
FAX (714) 761-1270
TWX 910-341-7672

3.4.6.6.2 Outer Lid Bolts

U.S. NRC Comment

Please address the shear stress in the bolt. Does this stress exceed the allowable ASME shear strength?

NAC Response

The maximum shear stress of 20,090 psi in the NAC-STC outer lid bolts occurs for the 30-foot side drop transport accident and results from the weight of the outer lid multiplied by the 55g impact loading. This shear stress does not approach the Level D shear stress limit of the ASME Boiler and Pressure Vessel Code, Section III, Appendix F, that is, $0.4S_u = 54.0$ ksi or $0.6S_y = 59.3$ ksi. Since the bolt tensile stress is 46,090 psi (based on the revised bolt torque calculations), the combined shear and tensile stress is evaluated as $(46{,}090/97{,}100)^2 + (20{,}090/54{,}000)^2 = 0.364 < 1.0$. Since the maximum side impact loading for the NAC-STC for storage is only 11.8g for the tipover condition, the shear stress in the outer limit bolts is approximately (20,090)(11.8/55.0) = 4,130 psi for storage operation.

3.4.7.1 Port Cover Bolts

U.S. NRC Comment

Why is the engagement length not checked in the other bolt analyses?

NAC Response

The engagement length of the threads on the port cover bolts is checked to ensure that the thread shear area is adequate to prevent a shear failure. This check is necessary for the port cover bolts because they are specially designed "captured" bolts so that they don't get lost when the port cover is removed from the cask. The "captured" design only permits a thread length of 1.5 x thread diameter. NAC's standard design practice is to use a thread length of 2.0 x thread diameter, which ensures adequate thread shear area, so no engagement check is necessary. The other bolts in the NAC-STC satisfy this criteria, so no engagement check is performed.

3.4.7.3 ANSYS Finite Element Analysis of the Port Cover

U.S. NRC Comment

(a) What is the justification for the 200 psi internal pressure?

(b) Please explain the ANSYS axisymmetric beam element.

(c) The ANSYS and classical method results differ considerably. Please explain the large difference

NAC Response

(a) The value of 200 psi is a typical, but conservative, internal pressure for NAC casks. The maximum calculated internal pressure for the NAC-STC is 107.3 psi for a 10 CFR 71 transport cask thermal fire accident scenario. Thus, the NAC-STC port cover analysis is conservative.

(b) The term "axisymmetric beam element" is used to describe an ANSYS two-dimensional beam element with effective sectional properties such that it represents a "360-degree" revolution of the element in a finite element analysis.

(c) The difference between the results of the ANSYS and the classical analysis methods is due to the methodology and boundary conditions used. The ANSYS evaluation uses an elastic-plastic consideration together with a specified degree of edge rotational restraint on the port cover structure. In contrast, the classical analysis method uses an elastic analysis approach and considers the port cover as a simply supported plate.

3.4.7.4.1 Classical Analysis

U.S. NRC Comment

How does the initial assumption of perfect elasticity make the classical analysis conservative? Elastic analyses usually under predict deflections.

NAC Response

NAC agrees that the elastic analysis method usually under-predicts deflections. The conservatism identified for this analysis refers to the assumption of a simply supported plate, rather than including some degree of constraint that is provided by the bolts; also, no shear stiffness of the plate is considered. Both of these analysis considerations contribute to the calculation of a conservatively high port cover deflection. The ANSYS finite element analysis of the port cover presented in Section 3.4.7.4.2 verifies the conservatism of the classical analysis.

3.4.8.2.1.2 Tipover Impact Analysis

U.S. NRC Comment

Is the assumed value of 55g shown to be conservative?

NAC Response

Yes, it is conservative to assume a 55g impact load for a tipover impact analysis. As documented in Section 3.4.9, the maximum lateral load on the NAC-STC is 2.94×10^6 pounds (11.75g) at the upper side impact limiter for a tipover side impact. The conservatism of the assumed 55g side impact is documented in Section 11.2.3 and further verified in the NAC Response to Comment 11.2.3.2

3.4.9.5 Method of Analysis

U.S. NRC Comment

(a) Besides information included in Section 3.6.2.3, please provide technical details about the manner in which RBCUBED calculates the force-deflection curves.

(b) Was sliding between the aluminum honeycomb and the stainless skin considered for the impact analyses? This sliding may adversely load the steel shell encasing the honeycomb.

(c) The structural strength of the impact limiter tabs needs to be addressed for the tipover condition. For the tipover, the shear force over the interface between the impact limiter and the cask bottom is high.

NAC Response

(a) RBCUBED utilizes quasi-static methodology. The impact of the cask package is frozen at an instant in time during which all calculations are performed. At any particular instant the deformation of the impact limiter is divided into a number of "zones". A zone is a three-dimensional body section of the impact limiter oriented normally to the unyielding surface. Only the zones directly compressed between the cask body and the unyielding surface are considered effective in absorbing the kinetic energy of the package. The deformation of each zone is determined and the associated strain is calculated by dividing that deformation by the original height of the zone. The stress in the zone is determined from the stress-strain data for the material, as previously defined in the input. The force in the zone is calculated by multiplying the area of the zone by the stress in the zone. The total force exerted by the impact limiter is the sum of all the forces in the effective zones. The iteration process is continued until all of the kinetic energy of the cask is absorbed and the velocity of the cask is reduced to zero. The force-deflection relationship for the impact limiter for a particular drop orientation is thus, calculated by RBCUBED.

(b) No sliding between the aluminum honeycomb and the stainless steel shell was considered in the analysis. The epoxy bonding the interfaces between the two materials sufficiently limits sliding between the materials so that deformation of the impact limiter proceeds as predicted. Previous quarter-scale model drop tests of the NAC LWT cask have verified the impact limiter behavior.

(c) As discussed in Section 11.2.4.1, tipover is evaluated as a credible occurrence for the NAC-STC during storage on the concrete pad. The cask is stored with its base on the concrete pad without the bottom impact limiter. Therefore, an analysis of the bottom impact limiter attachments is not applicable.

3.4.9.7.2 Upper Side Impact Limiter Attachment Analysis

U.S. NRC Comment

(a) Does Figure 3.4.9-1 provide the attachment details for the bottom and side impact limiters? Are the storage and transport impact limiters attached the same way?

(b) In Figure 3.4.9-1, what is the length between the side impact limiter and the top of the cask?

NAC Response

(a) Yes, Figure 3.4.9-1 provides the attachment details for the bottom and upper side storage impact limiters; additional attachment details are shown on Drawings 423-538 and 423-539 in Section 1.5.2 of the NAC-STC TSAR. The upper side impact limiter has eight equally spaced 1/4-inch plate mounting tabs that are bolted to the side of the cask body with 1/2-inch diameter SA-193, Grade B6, Type 410 stainless steel bolts. The bottom impact limiter has four equally spaced 1/4-inch plate mounting tabs that are bolted to the side of the cask body with 1/2-inch diameter, SA-193, Grade B6, Type 410 stainless steel bolts.

No, the storage and transport impact limiters are not attached to the cask in the same way. The upper and lower transport impact limiters for the NAC-STC are each attached to the ends of cask by 16 1-inch diameter bolts through the transport impact limiters.

(b) The top of the upper side impact limiter is 1.8 inches from the top of the cask. Figure 3.4.9-1 will be revised to clarify this.

3.4.10.4 Stress Evaluation of Gravity Effects

U.S. NRC Comment

(a) Please address the structural analysis of the rods and spacer nuts. Buckling of the rods is a critical concern.

(b) In the ANSYS model of the basket disk, what type of displacement restraints were assumed at the rod locations, hinged, fixed, or other?

(c) In Table 3.4.10-1, the formula for the Von Mises Stress is incorrect. Please address. If using ASME stress limits, the Tresca criteria should be used since the ASME code is based on that criteria. However, the resulting difference between the Von Mises criteria and Tresca criteria is small.

NAC Response

(a) As documented in the last paragraph of the NAC-STC TSAR Section 3.4.10.5, the threaded rods and spacer nuts are analyzed in Section 11.2.4.7.6.4 of the TSAR. In that section, the threaded rod stresses are calculated for the end drop condition. The buckling analysis of the threaded rods for the end drop condition and an evaluation of the side and corner drop conditions for the rods are addressed in the NAC response to Comment 11.2.4.7.6.4.

(b) In the ANSYS model of the support disk, roller-type displacement restraints were assumed at the threaded rod locations. To be specific, displacement is only restrained in the disk lateral direction (threaded rod axial direction). This is a conservative representation of the restraint provided by the threaded spacer nuts.

(c) The formula for the Von Mises stress is mistyped in table 3.4.10-1. However, the Von Mises stress calculations are based on the correct formula. The typo in footnote No. 2 in Table 3.4.10-1, will be revised as:

SIGE (Von Mises) Stress = $0.707\ [\ (Sx\text{-}Sy)^2 + Sx^2 + Sy^2 + 6(Sxy^2)\,]^{0.5}$

Note that the terms of Sz, Syz, and Sxz are zero for the two-dimensional stress analysis and, therefore, are not shown in the Von Mises stress formula.

4.4.1.1.1.3 Radial Neutron Shield

U.S. NRC Comment

(a) What is the UNS number of the copper heat conductor plates in the Neutron Shield Assembly?

(b) Is the thermal conductivity of the copper given in Table 4.2-7 (page 4.2-11) for copper with a purity > 99.99 percent appropriate for the actual copper used (UNS C1????) which, according to ASTM B152 has a purity <99.99 percent?

(c) What is the thermal contact resistance between the NS4FR and the metallic components of the radial neutron shield assembly and between the explosively bonded composite copper and stainless steel plates with 95 percent minimum bond area between the plates?

(d) The plate materials shown in the figure on page 4.4-4 are not consistent with the electric circuit diagram?

(e) What are the dimensions (length and area for example) of each of the five resistances shown in the electric circuit diagram on page 4.4-4, and are the thickness dimensions of the copper and stainless shell plates correct?

NAC Response

(a) The ASTM B152 copper alloy material has a UNS number of C11000.

(b) ASTM B152 copper allow has a minimum copper and silver content of 99.90 percent. Therefore, it is not entirely appropriate to use conductivity values for copper with a purity > 99.99 percent. However, the value of the effective thermal conductivity of the radial neutron shield used in the analysis (0.246 BTU/hr-in-°F) is conservative. The effective thermal conductivity of the neutron shield, based on stainless steel and copper fin thicknesses of 6 mm and 8 mm, respectively, is 0.261 BTU/hr-in-°F, based on a thermal conductivity of 18.11 BTU/hr-in-°F for the copper alloy at 300°F.

(c) The thermal contact resistance between the NS4FR and the metallic components of the radial neutron shield is negligible, due to the thermal expansion characteristics of the material. Under storage limiting thermal conditions, the NS4FR expands to fill any small air pockets formed between the NS4FR and the steel during fabrication, resulting in a continuous contact between either the outer shell or the neutron shield shell of the cask and the NS4FR material.

Explosion bonding produces a mechanical, metallic bond between the bonded materials. Therefore, there is no thermal contact resistance between the copper and stainless steel fin materials.

(d) The designations for stainless steel and copper in the figure on page 4.4-4 are incorrect. The stainless steel, not the copper, is in contact with the outer shell and the cask surface. The electric circuit diagram is correct.

(e) The length of the stainless steel fin and the NS4FR region is 5.5 inches. The length of the copper fin is 5.25 inches, leaving an 1/8-inch gap at each end of the fin. For analysis purposes, the thicknesses of the stainless steel and copper fins are 1/4 inch each. However, the fins are actually composed of 6-mm thick stainless steel and 8-mm thick copper, resulting in a higher effective thermal conductivity for the radial neutron shield.

4.4.1.1.3 Maximum Fuel Rod Cladding Temperature Model

U.S. NRC Comment

What is the reference for SCOPE and where is it documented?

NAC Response

SCOPE is referenced in Chapter 14 of the TSAR under the author's name (Bucholz). The reference is provided in the short description of the use of the SCOPE code given on page 4.1-2.

11.2 Accidents

U.S. NRC Comment

(a) Since quasi-static analyses were used for all the drop test analyses, an appropriate dynamic amplification factor (DAF), or dynamic load factor (DLF), needs to be specified and used. The choice of the DAF or DLF should be justified, or the conservative value of 2 is used. What is the DLF suggested by the comparison of the stress results between the SCANS quasi-static and dynamic analyses?

(b) Does SCANS predict the same g-levels as RBCUBED for the storage and transport impact limiters? Please show comparisons.

NAC Response

(a) The loadings used in the static analyses for ANSYS were factored by the maximum deceleration for each drop. For the side drop, which simulates a condition more severe than the tipover, the loadings in the static analyses were factored by 55 to correspond to the maximum deceleration of 54.2g's experienced only at the end of the impact.

Any additional amplification of loadings would be caused by dynamic excitation of the ~sk, either in a beam mode or in one of the fundamental shell modes. The duration of the cask impact based on the RBCUBED results for the side drop is approximately 0.035 seconds. The cask, if viewed as a beam for a free-free mode, has a first mode natural frequency on the order of 300 Hertz. This would allow the cask to experience 10 cycles during the loading and to follow the impact limiter force input. It can be shown that the excitation of the cask during the impact follows the impact limiter force curve and that the dynamic oscillations are about the force curve and are considered to be small.

(b) Yes, SCANS predicts the same G-loads as RBCUBED does for the storage and transport impact limiters. A comparison is provided between RBCUBED and the SCANS calculated g-loads for the NAC-STC transport impact limiters:

Loading Conditions	RBCUBED	SCANS
30-Foot Bottom End Drop	40.4	38.8
30-Foot Side Drop	54.4	54.4
30-Foot Bottom Corner Drop	41.4	41.4

11.2.3.2 Accident Analysis

U.S. NRC Comment

Even though the shear load in the 2.94×10^6 lb tipover accident is smaller than the shear load in the 13.75×10^6 side drop accident, is the shear load considered in the analysis? Are there cask cross-sections at which the combined moment and shear contributions are greater for the tipover accident than for the side drop accident?

NAC Response

Although not included in the analysis presented in Section 11.2.3.2, the magnitude of the shear loads and the shear diagrams for the NAC-STC for the tipover and for the 13.75×10^6-pound side drop accident conditions were considered in the preparation of that analysis. Since the maximum shear stresses on the inner and outer shells are less than one-half the maximum bending stresses on those shells, the comparison of the maximum bending moments for the two accident conditions was considered more significant than that of the shear forces and so, was presented in the tipover analysis.

It is important to remember that the maximum bending stress in the cask shells occurs at the extreme fiber location at 90-degrees to the neutral axis, while the maximum shear stress in the cask shells occurs at the neutral axis. The maximum bending moment on the cask for the tipover accident is only 0.33 of the maximum bending moment on the cask for the side drop accident and, likewise, the maximum shear on the cask for the tipover accident is only 0.43 of the maximum shear on the cask for the side drop accident. The shapes of the shear and moment diagrams for the cask for the tipover accident are nearly identical to those for the side drop accident, although their magnitudes are quite different. Thus, the combined shear and bending stresses at any location along the cask for the tipover accident and for the side drop accident will have essentially the same relationship as do the maximum bending moments or the maximum shear forces for those two load conditions. For the 30-foot side drop, the maximum outer shell bending stress is 15,998 psi at the midpoint of the cask. For the tipover, the maximum outer shell bending stress occurs 13.8 inches above the cask midpoint at the extreme top and bottom fibers and is 5,391 psi, while the maximum shear stress occurs at the location of the upper side impact limiter along the cask body at the neutral axis location of the cask cross-section and is 5,641 psi. Very conservatively assuming that the maximum bending and shear stresses for the tipover condition occur at the same point, the equivalent stress is $S_e = (S_b^2 + S_s^2)^{0.5} = 12,504$ psi. Since this equivalent stress is less than the "maximum bending stress only" for the 30-foot side drop, it is clear, then, that there are no cask cross-sections at which the combined moment and shear contributions are greater for the tipover accident than for the side drop accident.

11.: 3.2 Accident Analysis

U.S. NRC Comment

(a) This section contains the first mention of the redwood impact limiters. It would be helpful if these impact limiters were mentioned along with the introduction of the storage impact limiters.

(b) Please provide further details about the transport impact limiters. Specifically, information is needed about the manner in which the force-deflection curves are obtained; either by experiment or theoretical calculations. Drawings which show the details of the impact limiters and their particular attachments will be useful.

(c) The high modulus of elasticity (2280 ksi) for lead is valid only at stresses less than about 700 psi. For stresses higher than about 700 psi, a lower modulus is necessary for the structural analysis of lead.

(d) The lead modulus of 27,750 psi used in SCANS is appropriate and the SCANS prediction of hoop stress should be accurate. The SCANS results presented in the TSAR, which used a lead modulus near 2 x 10^6 psi, cannot be accepted as an adequate solution for the case with unbonded lead and steel shells. Please provide results of a detailed elastic-plastic analysis using the stress-strain curve in NUREG/CR-0481 to represent the elastic-plastic properties of the lead.

(e) SCANS does calculate the values of hoop stress, S_θ, for the lead/shell interfaces unbonded case, but these values were omitted in Table 11.2.4-1 and other similar tables. Please review.

(f) The shear stress calculated by SCANS is $S_{r\theta}$, at the beam neutral axis, not S_{rz}. Please review the impact of this change in the data presented in Table 11.2.4-4 and other similar tables.

NAC Response

(a) Refer to Paragraph (b) of the NAC Response to Comment 3.3.7. The transport impact limiters for the NAC-STC contain redwood and balsa wood as the energy absorbing materials; they are mentioned in the TSAR only to provide the basis for the 30-foot drop impact g-loads that are conservatively used to demonstrate the structural adequacy of the NAC-STC for impact accident conditions.

(b) Again, it is reiterated that the NAC-STC transport impact limiters are not a part of the storage cask license application, except to provide insight on the selection of the impact loads used in the drop accident analyses. The force-deflection curves for the NAC-STC transport impact limiters are calculated by the RBCUBED computer program based on experimental force-deflection data from redwood test specimens. Refer to the NAC Response to Paragraph (a) of Comment 3.4.9.5 for a description of RBCUBED's calculational techniques. Details of the transport impact limiters and their attachments are presented in Drawings 423-609 and 423-610 in Section 1.3.2 of the NAC-STC SAR, September 1990.

(c & d) Refer to the NAC Response to Paragraph (a) of Comment 3.3.6.1 for the discussion and documentation of the appropriate modulus of elasticity to be used in the analyses of the NAC-STC; a summary tabulation of calculational and experimental results is presented in that response.

(e & f) The SCANS analyses, beginning with the second paragraph of Section 11.2.4.2 and continuing through Section 11.2.4.5.3, will be deleted and replaced by the text which follows; the structural adequacy of the NAC-STC for the impact accident conditions is documented by the ANSYS finite element analyses that are presented in the NAC-STC SAR. The accuracy of the ANSYS analyses has been verified by comparison of the results to those from SCANS and from the quarter-scale model drop tests for the outer shell. For convenient reference, the pertinent pages from the NAC-STC SAR are included as a part of this response and appear as Appendix A of this document.

Rigorous finite element analyses using the ANSYS computer program have been performed for the NAC-STC. ANSYS evaluations include the 30-foot side, bottom end and bottom corner drop analyses, which were documented in detail in the Sections 2.7.1.0 through 2.7.1.3 of the NAC-STC SAR. Each ANSYS evaluation uses an equivalent-static elastic analysis method and considers that cask material properties are temperature dependent. Each ANSYS evaluation also calculates the effects of the lead slump stress and three-dimensional stress effects (including the Poisson's effect in the hoop direction) resulting from accident drop impact conditions.

A two-dimensional axisymmetric ANSYS computer model for the NAC-STC was used in the bottom end drop analysis, while two three-dimensional ANSYS models were employed for the side and corner drop evaluations. The two-dimensional (2-D) axisymmetric model is described in Section 2.10.2.1.1 of the NAC-STC SAR. ANSYS STIF3 (2-D beam), STIF12 (2-D gap), and STIF42 (2-D solid) elements are used to construct the 2-D model of the NAC-STC. The overall view of the model is shown in Figure 2.10.2-1 of the SAR. Detailed plots showing node numbering patterns and the mesh arrangements in the different regions of the model are included in Figures 2.10.2-2 through 2.10.2-7 of the SAR. The three-dimensional (3-D) models are described in Section 2.10.2.1.2 of the SAR. In order to reduce the overall problem size, two 3-D models are developed: 1) the bottom fine mesh model, to be used in the stress evaluations for the bottom half of the cask; and 2) the top fine mesh model, to be used in the stress evaluations for the top half of the cask. In fact, both models are complete representations of the cask, since the entire cask is modeled. Three-dimensional beam elements (STIF4), gap elements (STIF52), and solid elements (STIF45) are used in the construction of the two 3-D finite element models. The complete bottom and top fine mesh models are shown in Figures 2.10.2-9 and 2.10.2-20, respectively, of the NAC-STC SAR

Documentation procedures for the finite element stress calculations are described in Section 2.10.2.4 of the SAR and are briefly summarized here. First, cask components are defined so that the structural qualification of the cask can be performed on a component basis. The cask is divided into components based on the physical geometry of the cask, such that each component consists of a single material. The cask component identification is illustrated in Figure 2.10.2-33 of the SAR. Stress evaluations are performed at every feasible cross-section of the cask. Then, the most critical cross-section within each cask component is determined by searching, on a component basis, for the cross-section where the maximum stress intensity is located. Since the stress evaluations and the search are performed by a computer algorithm, every feasible cross-section is identified and evaluated, insuring that the maximum stress location within each component is found. Stress cables are then prepared to summarize the critical primary membrane (Pm), primary membrane plus primary bending (Pm + Pb), primary plus secondary stresses (Sn), and the margin of safety, of each cask component, for each loading condition. Stress intensity summaries are also prepared for the primary membrane, primary membrane plus primary bending, and primary plus secondary stresses at other selected representative sections on the cask. The representative section locations were chosen, based on the critical stress locations, in order to illustrate the overall structural behavior of the cask. The selected section locations are described in Section 2.10.2.4.2 and depicted in Figure 2.10.2-34 of the SAR.

The NAC-STC is evaluated for impact orientations in which the cask strikes the impact surface on its top end, top end oblique, side, bottom end, and bottom end oblique. Since only the side, bottom end, and bottom corner drop conditions are credible for the design of the storage cask, the stress results for these conditions are summarized in the following discussion.

ANSYS evaluations for the side, bottom end, and bottom corner drop conditions consider that the impact forces result from 30-foot accident drops. An impact load factor of 55g is used for both side and bottom corner drops and a factor of 56.1g is used for the bottom end drop. These impact load factors are significantly greater than the impact load factors for the cask for the 6-foot drop storage accident conditions. Impacts with the maximum and minimum weights of contents are considered. The environmental temperature for the drop is between -20°F and 100°F. Internal heat generation from the contents and solar heating are also considered. Regarding internal pressure, the maximum or minimum normal operating pressure is applied to produce the critical stress condition in conjunction with the other loads previously discussed. Closure lid bolt preload stresses are also considered.

For the 30-foot bottom end drop case, the critical (maximum) stress summary for all cask components are documented in Tables 2.10.4-124 and 2.10.4-125 of the SAR. These two tables document the critical primary membrane (Pm) and primary membrane plus primary bending (Pm+Pb) stresses in accordance with the criteria presented in Regulatory Guide 7.6. The allowable stresses are functions of the material strength at operating temperature. The maximum operating temperature within a given component is used to determine the allowable stresses for that component. Note that higher temperatures result in lower allowable stresses. The maximum calculated Pm stress in[illegible] ?.3 ksi and the maximum calculated Pm+Pb stress intensity is 22.7 ksi, which are produced by the combined loading condition: 30-foot bottom end drop impact, bolt preload, and internal pressure. As shown in Tables 2.10.4-124 and 2.10.4-125 of the SAR, the margins of safety are positive for the 30-foot end drop accident condition. The most critically stressed component in the system is the bottom forging. The minimum margin of safety for the bottom end drop condition is found to be <u>+1.8</u>, as documented in Table 2.10.4-125 of the SAR.

Likewise, the maximum Pm and Pm + Pb stress intensities for the 30-foot side drop are 36.0 ksi and 49.4 ksi, respectively, as documented in Tables 2.10.4-133 and 2.10.4-134 of the SAR. These two tables also show that the margins of safety are positive for the 30-foot side drop accident condition. The most critically stressed component in the system is the top forging. The minimum margin of safety for the side drop condition is <u>+0.3</u>, as documented in Table 2.10.4-134 of the SAR.

The maximum Pm and Pm + Pb stress intensities for the 30-foot bottom end corner drop are 23.5 ksi and 39.6 ksi, respectively, as documented in Tables 2.10.4-155 and 2.10.4-156 of the SAR. The minimum margin of safety is +0.7, as documented in Table 2.10.4-156 of the SAR.

Satisfaction of the extreme total stress intensity range limit is demonstrated in SAR Section 2.1.3.3. The documentation of the NAC-STC adequacy in satisfying the buckling criteria for the stresses of the accident drop conditions is presented in SAR Section 2.10.5.

The NAC-STC maintains its containment capability and is structurally adequate to withstand the 30-foot accident drop cases. Since the impact loads on the cask for the 6-foot drop storage accident conditions are less than the impact loads on the cask for the 30-foot drop accident condition, the NAC-STC is also structurally adequate for the 6-foot drop storage accident conditions.

Appendix A

Pertinent pages copied from the NAC-STC SAR for reference purposes.

2.7.1.0 Free Drop (30 Feet)

The NAC-STC is required by 10 CFR 71.73(c)(1) to demonstrate structural adequacy for a free drop through a distance of 30 feet onto a flat, unyielding, horizontal surface. The cask strikes the surface in an orientation that inflicts maximum damage. In determining which orientation produces the maximum damage, the NAC-STC is evaluated for impact orientations in which the cask strikes the impact surface on its top end, top end oblique, side, bottom end, and bottom end oblique. The impact limiters and the impact limiter attachments are evaluated in Section 2.6.7.4 for all loading conditions.

Impacts with the maximum and minimum weights of contents are considered. The environmental temperature for the drop is between -20°F and 100°F. Internal heat generation from the contents and solar heating are also considered. Regarding internal pressure, the maximum or minimum normal transport pressure is applied to produce the critical stress condition in conjunction with the other loads previously discussed. Closure lid bolt preload and fabrication stresses are also considered.

The following method and assumptions are adopted in all of the drop analyses:

1. The finite element method is utilized to do the impact analyses. The analyses are performed using the ANSYS computer program.

2. The analyses assume linearly elastic behavior of the cask.

3. The impact loads calculated in Section 2.6.7.4 are statistically applied to the impact surface of the cask. The dynamic wave propagation produced by the impact is assumed to spread throughout the cask body simultaneously.

4. The finite element model of the NAC-STC includes only the major structural components of the cask body; thus, the weight of the modeled cask body does not include the weight of the neutron

shield material, the neutron shield shell, nor the cavity contents. However, the applied loads on the cask model are based on a cask design weight of 250,000 pounds.

5. To account for the lead slump during the drops, and for the differential thermal expansion between the cask stainless steel shells and lead shell, gap elements are used in the finite element model.

The types of loading considered in the accident condition analyses include: (1) thermal, (2) internal pressure, (3) closure lid bolt preload, and (4) impact and inertial loads resulting from the impact event. These loadings and the boundary conditions, used in the finite element analyses, are discussed in Sections 2.7.1.1 through 2.7.1.4. Appendix 2.10 documents the procedures, analysis and stress results for the 30-foot drop accident conditions.

Note that the fabrication stresses are considered negligible as explained in Section 2.6.11.0. The puncture analysis is performed using classical hand calculations, as shown in Section 2.7.2.0.

2.7.1.1 Thirty-Foot End Drop

The NAC-STC is structurally evaluated for the hypothetical accident 30-foot end drop condition in accordance with the requirements of 10 CFR 71.73(c)(1). In this event, the NAC-STC (equipped with an impact limiter over each end) falls through a distance of 30 feet onto a flat, unyielding, horizontal surface. The cask strikes the surface in a vertical position; consequently, an end impact on the bottom end or top end of the cask occurs. The types of loading involved in an end drop accident are closure lid bolt preload, internal pressure, thermal, impact load, and inertial body load. There are six credible end impact conditions to be considered, according to Regulatory guide 7.8:

1. Top end drop with 100°F ambient temperature, maximum decay heat load, and maximum solar insolation.

2. Top end drop with -20°F ambient temperature, maximum decay heat load, and no solar insolation.

3. Top end drop with -20°F ambient temperature, no decay heat load, and no solar insolation.

4. Bottom end drop with 100°F ambient temperature, maximum decay heat load, and maximum solar insolation.

5. Bottom end drop with -20°F ambient temperature, maximum decay heat load, and no solar insolation.

6. Bottom end drop with -20°F ambient temperature, no decay heat load, and no solar insolation.

The finite element analysis method is utilized to perform the end drop stress evaluations for the NAC-STC. The end drop accident condition can be analyzed using a two-dimensional axisymmetric model, because of the symmetry of both the cask structure and the loads involved in the end drop case. The cask is modeled as an axisymmetric structure using ANSYS STIF42 isoparametric elements. A detailed description of the two-dimensional finite element model of the NAC-STC is provide in Section 2.10.2.1.1.

During an impact event, the cask body will experience a vertical deceleration. Considering the cask as a free body, the impact limiter will apply the load to the cask end to produce the deceleration. Since the deceleration represents an amplification factor for the inertial loading of the cask, the equivalent static method is adopted to perform the impact evaluations. The analyses consider the behavior of the cask to be linearly elastic. Additionally, the fabrication stresses are considered to be negligible (Section 2.6.11.0).

Five categories of load--closure lid bolt preload, internal pressure, thermal, impact, and inertial body loads--are considered on the cask:

1. Closure lid bolt preload - The required total bolt preloads on the inner lid bolts and the outer lid bolts are 4.87×10^6 pounds and 5.09×10^5 pounds, respectively, as calculated in Section 2.6.7.5. Bolt preload is applied to the model by imposing initial strains to the bolt shafts, as explained in Section 2.10.2.2.3. The initial strains applied to the bolts are 3.034×10^{-3} inch/inch and 8.863×10^{-4} inch/inch for the inner and outer lid bolts, respectively. The bolts are modeled as beam (ANSYS STIF3) elements.

2. Internal pressure - The cask internal pressure is temperature dependent and is evaluated in Section 3.4.4. Pressures of 50 psig and 12 psig are applied on the interior surfaces of the cask cavity for the hot ambient and cold ambient cases, respectively.

3. Thermal - The heat transfer analyses performed in Sections 3.4.2 and 3.4.3 determine the cask temperature distributions for the following three combinations of ambient temperature, heat load, and solar insolation:

Condition 1. 100°F ambient temperature, with maximum decay heat load, and maximum solar insolation.

Condition 2. -20°F ambient temperature, with maximum decay heat load, and no solar insolation.

Condition 3. -20°F ambient temperature, with no decay heat load, and no solar insolation.

The cask temperatures calculated for each of the three thermal conditions discussed above are used in the ANSYS structural analyses to determine the values of the temperature-dependent material properties, such as modulus of elasticity, density, and Poisson's ratio.

4. Impact loads - The impact loads are induced by the impact limiter acting on the cask end during an end drop condition. The impact loads are determined from the energy absorbing characteristics of the impact limiters, as described in Section 2.6.7.4. The impact load is expressed in terms of the design cask weight (loaded or empty), multiplied by appropriate deceleration factors (g's). For details, see Section 2.6.7.4.

   The impact limiter load is considered to be uniformly applied over the end surface of the finite element model of the cask. The calculation of impact pressure loads is documented in Section 2.10.2.2.2. The following is a summary of the impact pressures applied to the exterior surface of the impacting end, for the different loading scenarios, with the corresponding design deceleration (g) values.

LOADING CONDITION	IMPACT PRESSURE FOR 1 g	DECELERATION (g)
Top end impact with basket and fuel	42.48 psi	56.1
Top end impact with basket, no fuel	35.86 psi	45.9
Bottom end impact with basket and fuel	42.35 psi	56.1
Bottom end impact with basket, no fuel	35.74 psi	49.4

For the case of a bottom end impact, with basket and fuel, a uniform pressure of 2376 psi ([42.35 psi][56.1 g/1 g]) is applied on the exterior surface of the bottom end of the finite element model of the cask. This pressure value is calculated by dividing the total impact load ([56.1 g/1 g][250,000 lb] = 14.03×10^6 lb) by the impact area ($\pi \times (43.35)^2 = 5903.8\ in^2$), which is the bottom surface area of the cask. Note that the impact pressure for the top end impact is slightly higher than that of the bottom end impact. A small radial gap exists between the outer lid and the top forging, and therefore the impact surface area for the top end impacts is reduced by the amount of the gap surface area, as explained in Section 2.10.2.2.2.

It should be noted that the design weight of the cask is 250,000 pounds, which includes the weight of the empty cask (194,000 lb), plus the weight of the cavity contents (56,000 lb). For those load conditions for which the cask contains no fuel, the basket (design weight = 17,000 lb) is still considered to be in the cask, resulting in a weight of 211,000 pounds for the empty cask with basket.

5. Inertial body load - The inertial effects, which occur during the end impact, are represented by equivalent static forces, in accordance with D'Alembert's principle. Inertial body load includes the weight of the empty cask (194,000 lb) and the weight of the cavity contents (56,000 lb).

   Inertia loads resulting from the weight of the empty cask are imposed by applying an appropriate deceleration factor to the cask mass. The applied decelerations are determined by considering the crush strength and the geometry of the impact limiters, as explained in Section 2.6.7.4.

The inertial load resulting from the 56,000-pound contents design weight is represented as an equivalent static pressure load uniformly applied on the interior surface of the impacting end of the cask. For the load case with no fuel in the cavity, the basket (design weight = 17,000 lb) is considered to be in the cask; the weight of the basket is represented in the ANSYS finite element model in the same manner as that of the contents.

The following is a summary of the inertial body load for a 1-g deceleration and the design decelerations for the different loading scenarios. The calculations of content pressures is documented in Section 2.10.2.2.1.

LOADING CONDITION	IMPACT PRESSURE FOR 1 g	DECELERATION (g)
Top end impact with basket and fuel	14.14 psi	56.1
Top end impact with basket, no fuel	4.29 psi	45.9
Bottom end impact with basket and fuel	14.14 psi	56.1
Bottom end impact with basket, no fuel	4.29 psi	49.4

In the ANSYS analyses, the inertial body loads are considered together with the impact loads. The results of the two simultaneous loadings are documented as "impact loads".

The primary stresses throughout the cask body are calculated for individual and combined loading conditions. The individual primary loading conditions are: (1) internal pressure (including bolt preload); (2) top end impact (impact load only); and (3) bottom end impact (impact load only). The combined loading conditions for primary stress evaluations are the: (1) 30-foot top end impact with bolt preload and 50 psig internal pressure; (2) 30-foot top end impact with bolt preload and 12 psig internal pressure; (3) 30-foot top end impact (without contents) with bolt preload and 12 psig internal pressure; (4) 30-foot bottom end impact with bolt preload and 50 psig internal pressure;

(5) 30-foot bottom end impact with bolt preload 12 psig internal pressure; and (6) 30-foot bottom end impact (without contents) with bolt preload and 12 psig internal pressure.

Because axisymmetry exists in the cask geometry and in the end-drop loading conditions, axisymmetric boundary conditions are represented in the formulation of the isoparametric elements. A longitudinal support is imposed on the corner node located in the non-impacting end of the cask, to prevent rigid body motion. When the cask system is in equilibrium (i.e., the inertial body loads match the impact loads exactly), then the reaction force at this support will be zero. An examination of the magnitude of the reaction forces provides a check of the validity of the finite element evaluation for the 30-foot end drop condition. The reaction at the longitudinal support is 2582 pounds/radian for the 56.1 g top end drop load condition. This means that the unbalanced force of the cask model system is only $(2582)(2\pi)/56.1 = 289$ pounds. Compared to the cask design weight of 250,000 pounds, the unbalanced force is negligible, amounting to only 0.12 percent of the design weight of the cask.

The allowable stress limit criteria, for containment and noncontainment structures, are provided in Section 2.1.2. These criteria are used to determine the allowable stresses for each cask component, conservatively using the maximum operating temperature within a given component to determine the allowable stress throughout that component. Note that higher temperatures result in lower allowable stresses. A different set of cask component allowable stresses is determined for each of the temperature conditions. Tables 2.10.2-5 through 2.10.2-7 document the allowable stress values determined for each component, for each of the temperature conditions.

Stress results for the individual loading cases of internal pressure (including bolt preload) are documented in Tables 2.10.4-1 and 2.10.4-2. Stress results for the individual 30-foot top and bottom end drop impact loading cases are documented in Tables 2.10.4-13 and 2.10.4-14. These are nodal stress summaries obtained from the finite element analysis results. As described in Section 2.10.4, the nodal stresses are documented on the representative section cuts. Stress results for the combined loading conditions discussed above are documented in Tables 2.10.4-112 through 2.10.4-129. These tables document the primary, primary membrane (P_m), primary membrane plus primary bending ($P_m + P_b$), and critical P_m and $P_m + P_b$ stresses in accordance with the criteria presented in Regulatory Guide 7.6. As described in Sections 2.10.2.3 and 2.10.2.4, procedures have been implemented to document the nodal and sectional stresses as well as to determine the critical (maximum) stress summary for all cask components.

For the top end impact loading case, the maximum calculated membrane stress intensity is 12.6 ksi. The maximum calculated membrane plus bending stress intensity is 34.4 ksi. By comparison, for the combined loading case, including impact, bolt preload, and internal pressure; the maximum calculated primary membrane stress intensity is 16.4 ksi and the maximum calculated primary membrane plus primary bending stress intensity is 38.5 ksi. The maximum stress intensities due to impact alone are equal to 90 percent of the maximum primary stress intensities due to the combined loading. Therefore, it is concluded that the impact stresses are the governing factor for the 30-foot end drop condition.

For the 30-foot top end drop scenario, ANSYS analyses were performed at the three different temperature conditions. The results from those three analyses show that the maximum $P_m + P_b$ stress intensities are 37.1 ksi, 38.5 ksi, and 36.2 ksi.

These three stress results are essentially identical, with the difference between them being less than 6 percent. Since the allowable stress for a component is a function of the component temperature, with higher temperatures resulting in lower allowable stresses, the allowable stress will be lowest for temperature condition 1 because the highest component temperatures occur for condition 1. As a result, the margins of safety are smallest for the analysis for temperature condition 1. The minimum margins of safety for the three temperature conditions are +0.9, +0.9, +1.0, respectively. Therefore, it is concluded that the stress results from temperature condition 1 are the most critical for the end drop accident conditions.

A similar set of ANSYS analyses was performed for the 30-foot bottom end drop case. The stress results follow the same pattern as the top end drop. The maximum $P_m + P_b$ stress intensities for the 30-foot bottom end drop are 22.7 ksi, 23.1 ksi, and 21.7 ksi.

As shown in Tables 2.10.4-112 through 2.10.4-129, the margins of safety are positive for all of the end drop accident conditions. The most critically stressed component in the system is the inner lid, for the top end drop. The minimum margin of safety for the top end drop condition is found to be +0.9, as documented in Table 2.10.4-116. The minimum margin of safety for the bottom end drop condition is found to be +1.9, as documented in Table 2.10.4-125.

Satisfaction of the extreme total stress intensity range limit is demonstrated in Section 2.1.3.3. The documentation of the NAC-STC adequacy in satisfying the buckling criteria for the stresses of the end drop condition is presented in Section 2.10.5.

The NAC-STC maintains its containment capability and therefore satisfies the requirements of 10 CFR 71.73 for the hypothetical accident 30-foot end drop condition.

2.7.1.2 Thirty-Foot Side Drop

The NAC-STC is structurally evaluated for the hypothetical accident 30-foot side drop condition in accordance with the requirements of 10 CFR 71.73(c)(1). In this event the NAC-STC, equipped with an impact limiter over each end, falls through a distance of 30 feet onto a flat, unyielding, horizontal surface. The cask strikes the surface in a horizontal position; consequently, a side impact on the cask occurs. The types of loading involved in a side drop accident are closure lid bolt preload, internal pressure, thermal, impact load, and inertial body load. There are three credible side impact conditions to be considered, according to Regulatory Guide 7.8:

1. Side drop with 100°F ambient temperature, maximum decay heat load, and maximum solar insolation.

2. Side drop with -20°F ambient temperature, maximum decay heat load, and no solar insolation.

3. Side drop with -20°F ambient temperature, no decay heat load, and no solar insolation.

The finite element analysis method is utilized to perform the side drop stress evaluations for the NAC-STC. The side drop accident condition is analyzed using a three-dimensional structural model to accurately represent the non-axisymmetric loads involved in the side drop case. One-half of the cask is modeled as a three-dimensional structure with one plane of symmetry. The ANSYS STIF45 3-D solid element is the primary element type used in the model. In order to reduce the overall problem size to satisfy the limitations of the ANSYS program and the computer hardware, two three-dimensional models have been constructed--the top fine mesh model and the bottom fine mesh model. A detailed description of the three-dimensional finite element models of the NAC-STC is presented in Section 2.10.2.1.2. The top model contains a fine mesh region at the upper half of the cask with a relatively coarse mesh at the bottom end; the bottom model contains a fine mesh region at the bottom end with relatively coarse mesh at the top end. Both models are used in the side drop analyses to obtain the detailed stresses throughout the cask. The stress results from the fine mesh portion of each model are then used to form the final stress summary.

During an impact event, the cask body experiences a lateral deceleration. Considering the cask as a free body, the impact limiters apply the load to the side of the cask (in the impact limiter contact area) to produce the deceleration. Since the deceleration represents an amplification factor for the inertial loading of the cask, the equivalent static method is adopted to do the impact evaluations. The analyses consider the behavior of the cask to be linearly elastic. Additionally, fabrication stresses are considered to be negligible (Section 2.6.11.0).

Five categories of load--closure lid bolt preload, internal pressure, thermal, impact, and body inertia--are considered on the cask:

1. Closure lid bolt preload - The required total bolt preloads on the inner lid bolts and the outer lid bolts are 4.81×10^6 pounds and 5.09×10^5 pounds, respectively (Section 2.6.7.5). Bolt preload is applied to the model by imposing initial strains to the bolt shafts, as explained in Section 2.10.2.2.3. The initial strains applied to the bolts are 3.034×10^{-3} inch/inch and 8.863×10^{-4} inch/inch for the inner and outer lid bolts, respectively. The bolts are modeled as beam (ANSYS STIF4) elements.

2. Internal pressure - The cask internal pressure is temperature dependent and is evaluated in Section 3.4.4. Pressures of 50 psig and 12 psig are applied on the interior surfaces of the cask cavity for the hot ambient and cold ambient cases, respectively.

3. Thermal - The heat transfer analyses performed in Sections 3.4.2 and 3.4.3 determine the cask temperature distributions for the following three combinations of ambient temperature, heat load, and solar insolation:

   Condition 1. 100°F ambient temperature, with maximum decay heat load, and maximum solar insolation.

Condition 2. -20°F ambient temperature, with maximum decay heat load, and no solar insolation.

Condition 3. -20°F ambient temperature, with no decay heat load, and no solar insolation.

The cask temperatures calculated for each of the three thermal conditions discussed above are used in the ANSYS structural analyses to determine the values of the temperature-dependent material properties such as modulus of elasticity, density, and Poisson's ratio. These temperatures are also used to evaluate the thermal stress effect on the cask.

4. Impact loads - The impact loads are induced by the impact limiters acting on the cask during a side drop condition. The impact loads are determined from the energy absorbing characteristics of the impact limiters, as described in Section 2.6.7.4. The impact load is expressed in terms of the design cask weight (loaded or empty), multiplied by appropriate deceleration factors (g's). The 30-foot side drop evaluations conservatively consider a deceleration factor of 55 g; the calculated deceleration value is 54.1 g, as documented in Section 2.6.7.4.

   The impact limiter load is applied to the finite element model as a distributed pressure over the contact areas between the impact limiters and the cask. The contact area is defined based on the "crush" geometry of the impact limiter. The distribution of impact pressure is considered to be uniform in the longitudinal direction, and is considered to vary sinusoidally in the circumferential direction. A cosine-shaped pressure distribution is selected, which is peaked at the center, and spread over a 79.4-degree arc on either side of the centerline, around the circumference, as shown in Figure 2.10.2-32 of Section 2.10.2.2.1. The 79.4-degree arc is determined based on the impact limiter test results for a side drop crush geometry. The assumption of a "peaked" pressure distribution is a conservative, classical, stress analysis procedure. Since the center of gravity of the loaded cask is located within 1 inch of the cask middle plane, the impact load is considered to be evenly divided between the two limiters. The impact contact area for a side drop accident includes the 12.03-inch overlapping region between the impact limiter and the cask, at each end of the cask.

The calculation to determine the pressure applied to the finite element model is documented in Section 2.10.2.2.2. The calculation is based on a 1-g deceleration condition. The following is a summary of the lateral impact pressures for the eight circumferential sectors:

ARC (deg)	LATERAL IMPACT PRESSURE FOR 1 g (psi)	DECELERATION (g)
0 - 8.3	163.22	55
8.3 - 17.0	158.67	55
17.0 - 26.2	149.06	55
26.2 - 35.8	133.98	55
35.8 - 45.9	113.17	55
45.9 - 56.5	86.69	55
56.5 - 67.7	54.99	55
67.7 - 79.4	18.96	55

The impact pressures used in the 30-foot side drop analyses are determined by multiplying the pressure values above by the deceleration factor (55 g).

It should be noted that the design weight of the cask is 250,000 pounds, which includes the weight of the empty cask (194,000 lb), plus the weight of the cavity contents (56,000 lb). For those load conditions in which the cask contains no fuel, the basket (design weight = 17,000 lb) is still considered to be in the cask, resulting in a weight of 211,000 pounds for the cask with basket.

5. Inertial body load The inertial effects that occur during the impact are represented by equivalent static forces, in accordance with D'Alembert's principle. Inertial body load includes the weight of

the empty cask (194,000 lb) and the weight of the cavity contents (56,000 lb).

Inertia loads resulting from the weight of the empty cask are imposed by applying an appropriate deceleration factor to the cask mass. The applied deceleration is 55 g, and is applied as explained in the discussion of the impact loads.

The inertial load, resulting from the 56,000-pound contents weight, is represented as an equivalent static pressure applied on the interior surface of the cask. Specifically, the equivalent static pressure is applied with a uniform distribution along the cavity length, and with a cosine-shaped distribution in the circumferential direction. The calculation of the contents pressure, as documented in Section 2.10.2.2.1, uses the identical method as that used in the determination of the impact pressures. In the case of no fuel in the cavity, the design weight of the basket (17,000 lb) is considered, and is represented in the same manner as that of the contents design weight. The following is a summary of the contents pressures for a 1-g deceleration, for the eight circumferential sectors:

ARC (deg)	LATERAL CONTENTS PRESSURE FOR 1 g (psi)	DECELERATION (g)
0 - 8.3	6.51	55
8.3 - 17.0	6.33	55
17.0 - 26.2	5.95	55
26.2 - 35.8	5.34	55
35.8 - 45.9	4.51	55
45.9 - 56.5	3.46	55
56.5 - 67.7	2.19	55
67.7 - 79.4	0.76	55

The contents pressures considered in the 30-foot side drop analyses are determined by multiplying the pressure values above by the deceleration factor (55 g).

In the ANSYS analyses, the inertial body loads are considered together with the impact loads. The results of the two simultaneous loadings are documented as "impact loads".

The stresses throughout the cask body are calculated for individual and combined loading conditions. The individual loading conditions are (1) internal pressure (including bolt preload); and (2) 30-foot side impact (impact load only). The combined loading condition is the 30-foot side impact with bolt preload and 50 psig internal pressure. This is the most critical combined loading condition for the 30-foot side drop, as will be shown in a discussion later in this report.

The finite element model has one plane of symmetry in the cask geometry and in the side drop loading conditions. Symmetric boundary conditions are applied to the cask finite element model by restraining the nodes on the symmetry plane to prevent translations in the direction normal to the symmetry plane. In addition, two nodes at the outer cask radius on the top and bottom ends of the cask, opposite the points of impact, are restrained laterally (in the drop direction) and the node at the top is restrained in the longitudinal direction to prevent rigid body motion. When the cask system is in equilibrium (i.e., the inertial body loads match the impact loads exactly), then the reaction forces at these supports will be zero. An examination of the magnitude of the reaction forces provides a check of the validity of the finite element evaluation for the 30-foot side drop condition. The sum of reactions in the cask lateral direction for the bottom model is 9,465 pounds, for the application of a 55 g-load. This means that the unbalanced force of the cask model system is only 9465/55 = 172.1 pounds. Compared to one-half of the design weight of the cask (125,000 lb), the unbalanced force is negligible, amounting to only 0.1 percent of the design weight of the cask. A similar check done for the top model indicates that the unbalanced force is 0.5 percent of the design weight, which is also negligible.

The allowable stress limit criteria, for containment and noncontainment structures, are provided in Section 2.1.2. These criteria are used to determine the allowable stresses for each cask component, conservatively using the maximum operating temperature within a given component to determine the allowable stress throughout that component. Note that higher component temperatures result in lower allowable stresses. A different set of component allowable stresses is determined for each of the three temperature conditions. Table 2.10.2-5 documents the allowable stress values determined for each component, for temperature condition 1.

Stress results for the individual internal pressure loading conditions are documented in Tables 2.10.4-1 and 2.10.4-2. Stress results for the individual 30-foot side impact loading condition are documented in Table 2.10.4-15 . These are the nodal stress summaries obtained from the finite element analysis results. As described in Section 2.10.2.4.2 and Section 2.10.4, the nodal stresses are documented on the representative section cuts. Stress results for the combined loading condition are documented in Tables 2.10.4-130 through 2.10.4-140. These tables document the primary stresses--for the 0-degree circumferential location; the primary membrane (P_m) stresses for the 0-, 45.9-, 91.7-, and the 180-degree circumferential locations, the primary membrane plus primary bending (P_m + P_b) stresses for the 0-, 45.9-, 91.7-, and the 180-degree circumferential locations, and the critical P_m and critical P_m + P_b stresses--in accordance with the criteria presented in Regulatory Guide 7.6. The stress results on the 0-, 45.9-, 91.7-, and the 180-degree circumferential locations document the stress variation in the circumferential direction. The circumferential locations are illustrated in Figure 2.10.2-8. As described in Sections 2.10.2.3 and 2.10.2.4, procedures have been implemented to document the nodal and sectional stresses as well as to determine the critical stress summary for all cask components.

Each of the stress summary tables are prepared by considering the stress results of two analysis runs, the first using the top fine mesh model and the second using the bottom fine mesh model. The stress results from the fine mesh portion of each model are used to form the nodal and sectional stress summaries. For the critical stress summaries, stresses for the top forging, inner lid and outer lid are determined from the top fine mesh model results; stresses for the bottom plate and the bottom forging are calculated from the bottom fine mesh model results; stresses for the inner shell, the transition sections, and the outer shell are determined as the larger of the stress results from both models. In order to justify the use of stress results from both models for the side drop evaluation, comparisons are made on the combined loading (impact plus internal pressure) stress results from the two models, at the middle section of the cask (Sections L and M in Figure 2.10.2-34, axial location of 96.15 inches from cask bottom). On the 0-degree, 45-degree, and 90-degree circumferential locations, the stress results from the two models show good agreement, with a difference of less than 10 percent. On the 180-degree circumferential location, where stresses are lower, the stress results from the two models are still reasonably comparable, with a difference of less than 15 percent. An additional check is performed for sections J and K (axial location of 54.90 inches), and sections N and O (axial location of 137.40 inches), which are about 40 inches away from the center of the cask (Figure 2.10.2-34). The stress results from the two models also show good agreement at these sections, with a difference of less than 10 percent for the 0-degree, 45.9-degree and 90-degree circumferential locations. Therefore, it is concluded that the combined stress results from the top fine mesh model and the bottom fine mesh model for the 30-foot side drop condition are valid and conservative.

There are three temperature conditions to be considered in the side drop evaluation. In order to determine the most critical temperature condition, two parametric studies are performed for the NAC-STC, using the three-dimensional bottom fine mesh model. The first parametric study compares the stress results for temperature condition 1 and temperature condition 2. The combined loading stress results show that the maximum stress intensities for conditions 1 and 2 are 34.1 ksi and 34.0 ksi, respectively. Since allowable stress is a function of temperature, higher component temperatures result in lower allowable stresses. The minimum margins of safety for conditions 1 and 2 are +0.87 and +0.93, respectively. It is, therefore, concluded that condition 1 is more critical than condition 2. The second parametric study compares the stress results between the analyses of conditions 1 and 3. The stress results indicate that the minimum margins of safety for temperature conditions 1 and 3 are +0.87 and +1.67, respectively. Therefore, condition 1 is more critical than condition 3. It is concluded, from the stress results of the parametric studies, that condition 1 is the most critical for the side drop accident condition. Therefore, only the stress results for temperature condition 1 for the 30-foot side drop are provided in the stress tables of this section.

It is worthwhile to mention that the most critical stress for the impact loading condition and that for the primary loading condition are essentially identical, with a maximum difference of 3 percent. Therefore it is concluded that the impact stresses are the governing factor, for the 30-foot side drop condition.

As shown in the critical P_m and $P_m + P_b$ stress summaries (Tables 2.10.4-133 and 2.10.4-134), the critical stresses for most of the cask components occur on the 0-degree circumferential location, which contains the line of impact. It is also observed that, for the cask inner shell, the maximum calculated stresses are located on the circumferential locations in the 56.5- to 67.7-degree region. This is because the maximum shearing stresses are located near the 56.5-degree circumferential location.

As shown in Tables 2.10.4-133 and 2.10.4-134, the margins of safety are positive for all of the 30-foot side drop accident conditions. The most critically stressed component in the system is the top forging. The minimum margin of safety for the side drop condition is found to be +0.3, as documented in Table 2.10.4-134.

Satisfaction of the extreme total stress intensity range limit is demonstrated in Section 2.1.3.3.

The documentation of the adequacy of the NAC-STC to satisfy the buckling criteria for the stresses of the side drop condition is presented in Section 2.10.5.

The NAC-STC maintains its containment capability and, therefore, satisfies the requirements of 10 CFR 71.73 for the 30-foot side drop hypothetical accident condition.

This page intentionally left blank.

2.7.1.3 Thirty-Foot Corner Drop

The NAC-STC is structurally evaluated for the hypothetical accident 30-foot corner drop condition in accordance with the requirements of 10 CFR 71.73(c)(1). In this event the NAC-STC, equipped with an impact limiter over each end, falls through a distance of 30 feet onto a flat, unyielding, horizontal surface. The cask strikes the surface on its top or bottom corner. The cask center of gravity is directly above the initial impact point for the corner drop condition. For the NAC-STC, an angle of 24 degrees from vertical is calculated for the corner drop orientation. The types of loading involved in a corner drop accident are closure lid bolt preload, internal pressure, thermal, impact load, and inertial body load. There are six credible corner impact conditions to be considered, according to Regulatory guide 7.8:

1. Top corner drop with 100°F ambient temperature, maximum decay heat load, and maximum solar insolation.

2. Top corner drop with -20°F ambient temperature, maximum decay heat load, and no solar insolation.

3. Top corner drop with -20°F ambient temperature, no decay heat load, and no solar insolation.

4. Bottom corner drop with 100°F ambient temperature, maximum decay heat load, and maximum solar insolation.

5. Bottom corner drop with -20°F ambient temperature, maximum decay heat load, and no solar insolation.

6. Bottom corner drop with -2C F ambient temperature, no decay heat load, and no solar insolation.

The finite element analysis method is utilized to perform the corner drop stress evaluations for the NAC-STC. The corner drop accident conditions are analyzed using a three-dimensional structural model to accurately represent the non-axisymmetric loads involved in the corner drop case. One-half of the cask is modeled as a three-dimensional structure with one plane of symmetry. The ANSYS STIF45 3-D solid element type is used in the model. Two finite element models are constructed: a top fine mesh model and a bottom fine mesh model. Each model is a complete representation of the cask, with a fine mesh region at the impacting end and with a relatively coarse mesh at the opposite end. The fine element mesh is modeled at the impacting end of the cask to provide detailed results in that region. The stresses predicted by the coarse element mesh at the non-impacting end of the model are not critical, so less detail is required. The detailed descriptions of the three-dimensional finite element models of the NAC-STC are described in Section 2.10.2.1.2.

During an impact event, the cask body will experience a deceleration in the corner drop direction. Considering the cask as a free body, the impact limiter will apply the load to the cask impacting corner to produce the deceleration. Since the deceleration represents an amplification factor for the inertial loading of the cask, the equivalent static method is adopted to do the impact evaluations. The analyses consider the behavior of the cask to be linear elastic. Additionally, the fabrication stresses are considered to be negligible (Section 2.6.11.0).

Five categories of load -- closure lid bolt preload, internal pressure, thermal, impact, and body inertia -- are considered on the cask:

1. Closure lid bolt preload - The required total bolt preloads on the inner lid bolts and the outer lid bolts are 4.81×10^6 pounds and 5.09×10^5 pounds, respectively (Section 2.6.7.5). Bolt preload is applied to the model by imposing initial strains to the bolt shafts, as explained in Section 2.10.2.2.3. The initial strains applied to the bolts are 3.034×10^{-3} inch/inch and 8.863×10^{-4} inch/inch for the inner and outer lid bolts, respectively. The bolts are modeled as beam (ANSYS STIF4) elements.

2. Internal pressure - The cask internal pressure is temperature dependent and is evaluated in Section 3.4.4. Pressures of 50 psig and 12 psig are applied on the interior surfaces of the cask cavity for the hot ambient and cold ambient cases, respectively.

3. Thermal - The heat transfer analyses performed in Sections 3.4.2 and 3.4.3 determine the cask temperature distributions for the following three combinations of ambient temperature, heat load, and solar insolation:

Condition 1. 100°F ambient temperature, with maximum decay heat load, and maximum solar insolation.

Condition 2. -20°F ambient temperature, with maximum decay heat load, and no solar insolation.

Condition 3. -20°F ambient temperature, with no decay heat load, and no solar insolation.

The cask temperature distributions, calculated for each of the three thermal conditions, are used in the ANSYS structural analyses to determine the values of the temperature-dependent material properties such as modulus of elasticity, density, and Poisson's ratio. These temperatures are also used to evaluate the thermal stress effect on the cask.

4. Impact loads - The impact loads are produced by the impact limiter acting on the cask corner during a corner drop condition. The impact loads are determined from the energy absorbing characteristics of the impact limiters, as described in Section 2.6.7.4. The impact load is expressed in terms of the design cask weight (loaded or empty), multiplied by an appropriate deceleration factor (g's). The design deceleration factor of 55 g is used for both top and bottom corner drops. This compares to the actual deceleration factors of 41.4 g, and 40.4 g, as documented in Section 2.6.7.4.

The impact loads for the corner drop analyses have lateral and longitudinal components, which are calculated from the total impact loads. The lateral component is distributed as a pressure with a circumferential distribution (similar to the side drop pressure) over an arc of 0 to 79.4 degrees on each side of the impact centerline

(Section 2.10.2.2.2). The longitudinal component has a uniform distribution on a sector of the impacting end of the cask, over the same arc of 0 to 79.4 degrees on each side of the impact centerline.

Section 2.10.2.2.2 documents the impact pressures for a cask design weight of 250,000 pounds and an impact limiter contact length of 24.06 inches (12.03 inches at each end). In the corner drop case the impact energy is absorbed by only one impact limiter and, hence, the corner drop lateral impact pressures are determined by multiplying the side drop impact limiter by 2 (to account for only half as much impact limiter area), and by multiplying by the sine of the drop angle. For example, the corner drop lateral impact pressure, for the elements located between the 0- and 8.29-degree circumferential planes, is:

$$Press_1 = (163.22)(2)(\sin 24°) = 132.78 \text{ psi for 1 g}$$
$$Press_{55} = (132.78)(55 \text{ g}/1 \text{ g}) = 7303.0 \text{ psi for 55 g}$$

The following is a summary of the lateral impact pressures, for the elements at the various circumferential locations, for a 1-g deceleration:

ARC (deg)	LATERAL IMPACT PRESSURE FOR 1 g (psi)	DECELERATION (g)
0 - 8.3	132.78	55
8.3 - 17.0	129.07	55
17.0 - 26.2	121.26	55
26.2 - 35.8	108.99	55
35.8 - 45.9	92.06	55
45.9 - 56.5	70.52	55
56.5 - 67.7	44.73	55
67.7 - 79.4	15.42	55

The longitudinal impact pressure is calculated as the cosine component of the total impact load, divided by the sector area within the 0- to 79.4-degree arc. Therefore:

Weight $= 250{,}000$ lb
Area $= (79.4/180)(\pi)(43.35)^2 = 2604\ \text{in}^2$
$\text{Press}_1 = (250{,}000)(\cos 24°)/2604 = 87.70$ psi for 1 g
$\text{Press}_{55} = (87.70)(55\ \text{g}/1\ \text{g}) = 4824.0$ psi for 55 g

It should be noted that the design weight of the cask is 250,000 pounds, which includes the weight of the empty cask (194,000 lb) plus the weight of the cavity contents (56,000 lb).

5. Inertial body load - The inertial effects that occur during the impact are represented by equivalent static forces, in accordance with D'Alembert's principle. Inertial body load includes the weight of the empty cask (194,000 lb) and the weight of the cavity contents (56,000 lb).

Inertia loads resulting from the weight of the empty cask are imposed by applying an appropriate deceleration factor to the cask mass. The lateral and longitudinal components of inertial loading are determined in the same manner as for the impact loading.

The inertial load resulting from the 56,000-pound contents weight is represented as an equivalent static pressure load with both lateral and longitudinal components applied on the interior surface of the cask. The lateral component is applied to the cask model with the same circumferential distribution as that for the side drop pressure (over an arc of 0° to 79.4° on each side of the impact centerline). The lateral component pressure is determined by ratioing the side drop contents pressure values (Section 2.10.2.2.1) by the deceleration factor and by the sine of the drop orientation angle. The longitudinal component has a uniform distribution over the cask cavity end. The longitudinal component pressure is calculated by ratioing the end drop contents pressure by the deceleration factor and by the cosine of the drop orientation angle. The total deceleration factor is constant at 55 g for both the top and the bottom corner drops.

Section 2.10.2.2.1 contains the side drop contents pressures for a total contents weight of 56,000 pounds. The corner drop lateral contents pressure for the elements located between the 0- and 8.29-degree circumferential planes is therefore:

$$Press_1 = (6.51)(\sin 24°) = 2.65 \text{ psi for 1 g}$$
$$Press_{55} = (2.65)(55 \text{ g}/1 \text{ g}) = 146.0 \text{ psi for 55 g}$$

The following is a summary of the applied lateral contents pressures, for the elements at the various circumferential locations, for a 1-g deceleration.

ARC (deg)	LATERAL CONTENTS PRESSURE FOR 1 g (psi)	DECELERATION (g)
0 - 8.3	2.65	55
8.3 - 17.0	2.57	55
17.0 - 26.2	2.42	55
26.2 - 35.8	2.17	55
35.8 - 45.9	1.83	55
45.9 - 56.5	1.41	55
56.5 - 67.7	0.89	55
67.7 - 79.4	0.31	55

The longitudinal contents pressure is calculated from the longitudinal component of the total contents weight and the area over which it acts. Therefore:

$$Weight = 56{,}000 \text{ lb}$$
$$Area = (\pi)(35.5)^2 = 3959 \text{ in}^2$$
$$Press_1 = (56{,}000)(\cos 24°)/3959 = 12.92 \text{ psi for 1 g}$$
$$Press_{55} = (12.92)(55 \text{ g}/1 \text{ g}) = 711.0 \text{ psi for 55 g}$$

In the ANSYS analyses, the inertial body loads are considered together with the impact loads. The results of the two simultaneous loadings are documented as "impact loads".

The stresses throughout the cask body are calculated for individual and combined loading conditions. The individual loading conditions are: (1) internal pressure (including bolt preload); (2) 30-foot drop top corner impact (impact load only); and (3) 30-foot drop bottom corner impact (impact load only). The combined loading conditions are: (1) the 30-foot drop top corner impact with bolt preload and 50 psig internal pressure and (2) the 30-foot drop bottom corner impact with bolt preload and 50 psig internal pressure.

The model has one plane of symmetry in the cask geometry and in the corner drop loading conditions. Symmetric boundary conditions are applied to the cask finite element model by restraining the nodes on the symmetry plane to prevent translations in the direction normal to the symmetry plane. In addition, two nodes at the outer cask radius on the top and bottom ends of the cask opposite the point of impact are restrained laterally; a longitudinal restraint is applied at one of the nodes opposite the end of impact, i.e., a bottom corner drop is axially restrained at the top node, and vice-versa. These lateral and axial restraints are only to prevent rigid body motion; there should be no significant reaction forces associated with these restraints. When the cask system is in equilibrium (i.e., the inertial body loads match the impact loads exactly), then the reaction forces at these supports will be zero. However, it is difficult to balance the impact limiter pressure resultant with the contents pressure and inertial body load resultant. An eccentricity between the two resultants induces a moment on the cask model. Therefore, non-zero reactions are found at the restraints. The reaction forces cause very high localized stresses (or stress singularities) in the model at the supports. These stresses are unrealistic and do not exist in the real cask. The stress singularity effect is minimized by distributing the reaction forces over the nodes in the top and bottom regions of the model. For the bottom corner drop, the reactions at the supports are 612 pounds laterally and zero longitudinally, for the application of a 55-g deceleration. This means that the unbalanced force of the cask model system is only 612/55 = 11.1

pounds. Compared to one-half of the design weight of the cask (125,000 lb), the unbalanced force is negligible, amounting to only 0.009 percent of the design weight of the cask. For the top corner drop, the reactions at the supports are 511 pounds laterally and zero longitudinally, for the application of a 55-g deceleration. This means that the unbalanced force of the cask model system is only 511/55 = 9.3 pounds. Compared to one-half of the design weight of the cask (125,000 lb), the unbalanced force is negligible, amounting to only 0.007 percent of the design weight of the cask.

The allowable stress limit criteria, for containment and non-containment structures, are provided in Section 2.1.2. These criteria are used to determined the allowable stresses for each cask component, conservatively using the maximum transport temperature within a given component to determine the allowable stress throughout that component. Note that higher component temperatures result in lower allowable stresses. Table 2.10.2-5 documents the allowable stress values determined for each component, for temperature condition 1.

Stress results for the individual loading cases of internal pressure (including bolt preload) are documented in Tables 2.10.4-1 and 2.10.4-2A. Stress results for the individual 30-foot top and bottom corner drop impact loading cases are documented in Tables 2.10.4-16 and 2.10.4-41A. These are the nodal stress summaries obtained from the finite element analysis results. As described in Section 2.10.2.4.2 and Section 2.10.4, the nodal stresses are documented on the representative section cuts. Stress results for the combined loading conditions discussed above are documented in Tables 2.10.4-141 and 2.10.4-152. All of the corner drop analyses are performed at temperature condition 1. The results from Sections 2.7.1.1 and 2.7.1.2 indicate that the stresses associated with temperature condition 1 yield the smallest margins of safety due to the effect of higher temperatures upon the allowable stresses.

These tables document the primary, primary membrane (P_m), primary membrane plus primary bending ($P_m + P_b$), and critical P_m and $P_m + P_b$

stresses in accordance with the criteria presented in Regulatory Guide 7.6. As described in Section 2.10.2.3 and 2.10.2.4, procedures have been implemented to document the nodal and sectional stresses as well as to determine the critical stress summary for all cask components.

The P_m and the $P_m + P_b$ stresses documented in Tables 2.10.4-142 through 2.10.4-151 and 2.10.4-146 through 2.10.4-162 are stress results on the 0-, 45.9-, 91.7-, and the 180-degree circumferential locations. They indicate that the stress variations in the circumferential direction are similar between the top and the bottom corner drops. Furthermore, it is observed that the maximum calculated stresses are located on the circumferential locations in the 45.9- to 67.7-degree region. This is because the maximum shearing stresses are located near the 56.5-degree circumferential location. This shear stress, which is in the axial to circumferential location, is caused by the cantilever support from the impact limiter pressures and is compounded by the uneven distribution of the impact limiter and of the contents pressure loading.

The top corner drop cases result in higher maximum stress intensities than the bottom corner drop cases. For the individual impact loading cases, the maximum calculated membrane stress intensity for the top corner drop is 33.7 ksi. The maximum calculated membrane plus bending stress intensity is 52.8 ksi. By comparison, for the combined loading case, including impact, bolt preload, and internal pressure, the maximum calculated P_m stress intensity is 33.4 ksi and the maximum calculated $P_m + P_b$ stress intensity is 51.8 ksi. The maximum stress intensity due to impact alone is 1.9 percent greater than the maximum stress intensities due to the combined loading. Therefore it is concluded that the impact case is the governing one for the 30-foot corner drop condition.

As shown in Tables 2.10.4-141 through 2.10.4-152, the margins of safety are positive for all of the corner drop accident conditions. The most critically stressed component is the inner lid for the top corner drop, and is the bottom forging for the bottom corner drop. The minimum margin of safety for the top corner drop condition is found to be <u>+ 0.4</u>, as documented in Table 2.10.4-145. The minimum margin of safety for the bottom corner drop condition is found to be <u>+ 0.8</u>, as documented in Table 2.10.4-156.

Satisfaction of the extreme total stress intensity range limit is demonstrated in Section 2.1.3.3.

The documentation of the adequacy of the NAC-STC to satisfy the buckling criteria for the stresses of the corner drop condition is presented in Section 2.10.5.

The NAC-STC maintains its containment capability and, therefore, satisfies the requirements of 10 CFR 71.73 for the 30-foot corner drop hypothetical accident condition.

2.10.0 Appendices

2.10.1 Computer Program Descriptions

The structural evaluation of the NAC-STC body, closure lids, basket and impact limiters is accomplished using two computer codes, ANSYS and RBCUBED. Each program is described in the following sections.

2.10.1.1 ANSYS

The structural analysis of the main body, the closure lids, and the basket of the NAC-STC is performed by the finite element analysis method using the ANSYS structural analysis computer program. The ANSYS computer program is a large-scale, general purpose computer program for the solution of several classes of engineering analyses that include: static and dynamic; elastic, plastic, creep and swelling; buckling; and small and large deflections. The matrix displacement method of analysis based on finite element idealization is employed throughout the program. The large variety of element types available gives ANSYS the capability of analyzing two-dimensional and three-dimensional frame structures, piping systems, two-dimensional plane and axisymmetric solids, three-dimensional solids, flat plates, axisymmetric and three-dimensional shells, and nonlinear problems, including gap element interfaces. A two-dimensional axisymmetric model and two three-dimensional models, a top fine model and a bottom fine model, are used in the analysis of the NAC-STC. The interface gap elements provide the capability of realistic modeling and evaluation of the interactions between the lead layer and the surrounding stainless steel shells; between the top forging, inner lid, and outer lid; and between the neutron shield material and the steel in the inner lid and in the bottom of the cask.

Typically, the ANSYS program is run by sequential implementation of three options: pre-processing (or model building); analysis (calculation of stiffness matrix, displacements and reaction forces solution, element stresses); and post-processing (selection of analysis results). Each option may be run in the interactive or batch mode computer environment.

The ANSYS preprocessing routine (PREP7) is used to construct the finite element mesh, describe each cask component material (temperature-dependent) property, assign unique identifiers for cask components, model displacement boundary conditions and prescribe temperature, point loads, or surface tractions of appropriate element faces or nodes. The PREP7 graphics option is a valuable tool that permits the user to check the model for completeness. The ANSYS analysis option uses the PREP7 file to generate a solution file and to provide a user-oriented printout of the solution phase. In general, each solution provides a complete echo of the model input data, model displacement solution, element stresses, nodal forces, reaction forces, and any warnings or errors related to the analysis.

A variety of ANSYS post-processors (for example, Post1) utilize the solution file to sort, print, or plot selected results from the ANSYS analysis. The post-processors can provide many useful features including a maximum set of variables (such as stress components or displacements) or sectional stresses along a designated path. Additionally, the structural behavior can be viewed by model displacement and stress contour plots.

2.10.1.2 RBCUBED - A Program to Calculate Impact Limiter Dynamics

RBCUBED is an impact limiter analysis computer program developed by NAC (Hardeman) and used in the NAC-STC impact limiter analyses. RBCUBED utilizes quasi-static methodology; that is, each iteration freezes an instant in time during which all calculations are performed, and then, proceeds to the next time increment. The methodology employed in the program sizes the impact limiter and calculates the deceleration forces used to calculate the stresses imposed on the cask structure, but does not implement any load factor. There are several assumptions that are attendant to this methodology:

1. Gravity is the only force that acts on the cask during free fall. While falling, the cask is translating vertically and continues to do so until the initial (first) impacting end has been brought to rest.

In oblique and side drop cases, after the first end has been stopped, the cask rotates until the second limiter strikes the unyielding surface and absorbs the remaining kinetic energy.

2. There is no sliding or lateral motion of the cask at any time during the impact(s).

3. The cask weight includes the impact limiters, but the length of the cask does not.

4. The deceleration force generated during crushing of the isotropic energy absorption material acts at the centroid of the area engaged in crushing for that increment in time.

5. Crushing of the energy absorption material occurs from the outside toward the cask body.

6. The component of the cask weight acting downward and the crush force acting upward are assumed to act colinearly. The magnitude of the weight component is very small compared to the crush force.

7. The impact limiter material that is not between the cask and the unyielding surface does not absorb any kinetic energy. The extraneous limiter material is ineffective for the purposes of this impact limiter analysis.

RBCUBED is capable of analyzing any cask impact orientation from vertical (0°) to horizontal (90°).

The input data for RBCUBED includes the following: (1) height of drop; (2) weight of cask system; (3) cask length; (4) impact orientation angle; (5) deflection increment; (6) material crush properties (stress-strain curve or force deflection curve); and (7) impact limiter geometry. Geometric modeling of the impact limiter is performed using combinatorial geometry based on the MORSE-CG computer program.

The output data from RBCUBED includes the following: (1) a verbatim input return; (2) a processed input of general problem parameters and material properties; (3) the results of the RBCUBED execution--deflection; (4) resultant force; (5) remaining kinetic energy; (6) velocity; (7) elapsed time since the beginning of impact; (8) area currently involved in crushing; and (9) a series of crush "footprints" at crush intervals of one inch.

The computer program, RBCUBED--A Program to Calculate Impact Limiter Dynamics, was benchmarked for validity by comparison of analysis results to manual calculations using crush areas determined by drafting methods.

A two-dimensional axisymmetric model is used for the axisymmetric loading cases, which include internal pressure, thermal heat load, end drop on top, and end drop on the bottom. The two-dimensional axisymmetric model is described in Section 2.10.2.1.1.

The other two models are three-dimensional, so that they can properly analyze non-axisymmetric loading conditions, which include gravity (with the cask in the horizontal position), the side drop impact, the corner drop impacts, and the oblique drop impacts. The three-dimensional models are described in Section 2.10.2.1.2.

2.10.2.1.1 Two-Dimensional Axisymmetric Model

The ANSYS PREP7 routine is used to generate the finite element model of the NAC-STC. Dimensions used in the development of the model are obtained from Nuclear Assurance Corporation Cask Assembly Drawings 423-602 through 423-605. Because of the axisymmetric geometry of the cask, several of the loading conditions can be effectively analyzed using a two-dimensional axisymmetric model. These conditions include bolt preload, internal pressure, thermal expansion, and drops on both the bottom and the top ends of the cask.

The two-dimensional finite element model of the NAC-STC is constructed of 3083 nodes and 2842 elements. Care is taken when developing the model to maintain adequate mesh density and aspect ratio for the elements in order to minimize any numerical inaccuracies that might result from the finite element method.

The cask components that are considered in the ANSYS model include the inner lid, the outer lid, the bolting for each of the lids, the top forging, the inner shell, the transition sections, and the outer shell, the lead shell, the bottom forging, the bottom plate, and the BISCO NS4FR material in the bottom and in the inner lid.

ANSYS STIF3, STIF12, and STIF42 elements are used to construct the two-dimensional finite element model of the NAC-STC. The overall view of the model is shown in Figure 2.10.2-1. Detailed plots showing node numbering

2.10.2 Finite Element Analysis

2.10.2.1 Model Descriptions

The finite element analysis technique is well suited for the evaluation of the axisymmetric cask body structure, especially with respect to the following: (1) the interaction between the lead layer and the stainless steel shells; (2) the interaction between the internal neutron shield layers and the surrounding steel in the inner lid and the bottom forging; (3) the discontinuity effects at the shell and bottom forging intersections; and (4) the interaction of the top forging and the bolted lids in the vicinity of the closure. Furthermore, finite element analysis must consider (1) the stresses in the inner and outer shells induced by the lateral pressure loading from the lead during the 30-foot drop conditions; (2) the differential thermal expansion of the lead layer and the stainless steel shells under both hot and cold temperature conditions; and (3) the fact that no physical bonding exists between the lead and the surrounding stainless steel.

The finite element models of the NAC-STC body are generated utilizing the ANSYS PREP7 routine. The aspect ratio of finite elements and the density of the geometric mesh is carefully arranged, especially at the locations of geometric discontinuities and force boundaries, to minimize the possibility of numerical inaccuracies in the finite element method.

The cask components considered in the finite element models include the cask inner lid and outer lids; the top forging; the BISCO NS4FR neutron shield layer in the inner lid; the inner shell, transition sections, and outer shell; the lead layer; the bottom forging; the bottom plate; and the BISCO NS4FR neutron shield layer in the bottom.

Due to the complexity of the cask geometry and the loading conditions, it is apparent that one model is not sufficiently accurate to characterize all loading conditions and still be of a manageable size for available computer resources; therefore, three separate models are used to perform the analysis of the NAC-STC.

patterns and the mesh arrangements in the different regions of the model are included in Figures 2.10.2-2 through 2.10.2-7.

ANSYS STIF42 elements, which are two-dimensional, axisymmetric, isoparametric solid elements, are used to model all of the cask components except the bolts, the interfaces between the lead and the steel, and the interfaces between the neutron shield material and the steel. The bolts are modeled using ANSYS STIF3 elements, which are two-dimensional beam elements. The section properties of the bolts are entered on a "per radian" basis. The bolt preload is included in the model by applying an initial strain to the bolt shaft, which connects the bolt head to the threaded portions of the cask. The initial strain for the inner lid bolts is 3.034×10^{-3} inch/inch. The initial strain for the outer lid bolts is 8.8633×10^{-4} inch/inch. Beams representing the bolt heads and the portion of the bolts threaded into the cask do not have an initial strain applied. For a detailed description of how the bolts are modeled, and how the initial strain is determined, see section 2.10.2.2.3.

The "gap" element, STIF12, represents two surfaces that may maintain or break physical contact and may slide relative to each other. Such surfaces exist between: (1) the lead shell and the inner and outer stainless steel shells, (2) the neutron shield and the cask bottom, (3) the neutron shield and the inner lid, (4) the inner lid, and the outer lid, (5) the inner lid and the cask, and (6) the outer lid and the cask. Note that the gap element is only capable of supporting compression in the direction normal to the surfaces and friction in the tangential direction.

Gap elements completely surround the lead shell in the cask wall. If there is contact between the lead and the stainless steel surfaces, the gap elements transmit compressive load, but permit no tensile load between the lead and the stainless steel. This means that the gap elements allow the lead to move freely inside the space surrounded by the stainless steel. When a deceleration is imposed on the entire mass of the cask model to simulate the inertial effect of a drop impact condition, the deceleration causes the lead to slump and, consequently, creates a lateral pressure on the inner and the outer shells along the lead/shell interfaces.

Similarily, since the lead has a higher coefficient of thermal expansion than the stainless steel, the lead will incur larger thermal expansions and contractions than the stainless steel inner and outer shells; and thus, may be restrained by those shells. The gap element again allows the lead to move freely inside the annulus between the inner and the outer shells. Pressures resulting from the thermal expansion restraints develop wherever the lead contacts the stainless steel shells.

Thus, accurate modeling is achieved for the lead slump during an impact load condition and for the differential thermal expansions and contractions during temperature excursions.

In Figure 2.10.2-1, the elements representing the lead shell and the neutron shield layers are intentionally not shown, in order to improve the clarity of the mesh in the stainless steel components.

A gap element stiffness of 3.0×10^8 psi approximately 10 times greater than the cask stiffness, is specified to maintain the boundaries between the lead/steel and neutron shield/steel surfaces. Similar gap elements are used to model the interfaces between the lids and the top forging. The initial radial gap between the lead shell and the outer shell is calculated to be 0.0428 inch.

The neutron shield that is located around the outer shell of the cask along the length of the cask cavity is not modeled because its structural rigidity is conservatively ignored in the structural analyses of the cask. However, its weight effects are included in the model by using an increased effective density in the region of the cask between the top of the bottom forging and the bottom of the inner lid. Modification of the density of this portion of the cask allows the overall weight of the empty cask to be adjusted to the proper value. Minor density changes are also made to the bottom end forging and bottom plate to allow for proper center of gravity location. The mass of the upper impact limiter is distributed to the top end of the cask by increasing the density of the lids and top forging. The mass of the lower impact limiter is distributed to the cask bottom by increasing the density of the bottom forging and bottom plate. The resulting cask total weight (including impact limiters) and center of gravity are then verified by an ANSYS check run.

The material properties used in the stress analyses include the elastic modulus, the Poisson's ratio, the density and the coefficient of thermal expansion. The elastic modulii and coefficients of thermal expansion are functions of temperature. They are represented by a table of material property values at various temperatures. The material property evaluation for each element is performed by linear interpolation of the tabular data at the element average or integration point temperatures. Thermal expansion is computed relative to a reference temperature (assumed to be 70°F for this analysis). The material property values used are given in Section 2.3.

The temperature distributions used are those computed in Sections 3.4.2 and 3.4.3. The nodal temperatures in the structural model are determined from the results of the thermal analysis which is performed using the HEATING5 computer program. The temperature distribution is considered to to be constant around the circumference.

Stability of the finite element analysis requires that one node on the model be restrained in the cask longitudinal (axial) direction to prevent any vertical rigid body motion. Node 7332, located at the top outside corner, is axially restrained for the pressure, thermal, and bottom end impact cases (see Figure 2.10.2-6). Node 360, located at the bottom outside corner, is axially restrained for the top end impact case (see Figure 2.10.2-2).

2.10.2.1.2 <u>Three-Dimensional Finite Element Models</u>

There are a number of loading conditions that can only be characterized by a three-dimensional finite element analysis. In order to reduce the overall problem size, two three-dimensional models are developed:

(1) the top fine mesh model, to be used in the stress evaluations for the top half of the cask; and (2) the bottom fine mesh model, to be used in the stress evaluations for the bottom half of the cask. In fact, both models are complete representations of the cask, since the entire cask is modeled. The top fine mesh model contains a very detailed representation of the top end of the cask, while the bottom end of the cask is modeled using a coarser mesh density. The top fine mesh model is used in those analyses that are expected to produce larger stresses in the top half of the cask. Similarily, the bottom fine mesh model contains a very detailed representation of the bottom end region of the cask, while the upper end of the cask is modeled with a coarser mesh density. The bottom fine mesh model is used in those analyses that are expected to produce larger stresses in the bottom half of the cask.

For the side drop analysis, both the top and bottom fine mesh models are used separately to obtain the detailed stresses in the upper and lower portions of the NAC-STC, respectively. The stress summary for the entire cask combines the results of the two runs. The oblique drop analyses use the fine mesh model for the impacting end of the cask.

The two three-dimensional models are constructed by first creating a mesh representing a two-dimensional plane of the cask, and then revolving that mesh 180 degrees around the axis of symmetry of the cask to create a model of one-half of the cask. This half-model of the cask is adequate for the drop analyses, because the cask geometry and the imposed loads are also symmetric about the midplane of the cask. The plane of symmetry is chosen to pass through the line of impact in the side, corner, and oblique drop cases. Symmetry boundary conditions (i.e., no translations normal to the plane of symmetry), are imposed on all nodes on the plane of symmetry.

Mesh adequacy in the circumferential direction is ensured by first reviewing the ANSYS reference manual for a recommended mesh size, then adapting a non-uniform circumferential element size to accurately capture the high stresses in the impact region. Finally, a parametric study of mesh density is performed to verify the validity of the chosen mesh arrangement.

The ANSYS reference manual recommends a 15-degree circumferential mesh increment for shell structures. A minimum of twelve (180/15) circumferential elements would be required to model a 180-degree surface, according to this criteria. Since the region of impact will have much higher stresses than the region of the cask remote from the impact, a non-uniform circumferential element spacing is chosen. A very fine mesh near the region of impact varies to a coarse mesh on the side of the cask opposite the impact region. The largest circumferential element size was chosen to be twice that of the smallest, with the element size varying linearly in between. Figure 2.10.2-8 illustrates the resulting non-uniform angular locations of each row of nodes. Table 2.10.2-1 documents the angular location of each plane of nodes, and the circumferential element size for each row of elements. The arc length of the smallest elements, those along the line of impact, is 8.3 degrees. The arc length increases to 16.6 degrees for the elements farthest away from the impact.

A series of parametric studies were performed, which considered a thick-walled cylinder subject to a gravity loading in the lateral direction, in order to examine the results of using different mesh densities. Circumferential mesh densities of 28 uniformly spaced elements and of 15 uniformly spaced elements were considered. The results of the parametric study indicated that maximum stresses as determined by the mesh with 28 circumferential elements were within 1 percent of those determined by the mesh with 15 elements. Therefore, it is concluded that the 15 element non-uniform mesh is adequate to model the structural behavior of the cask. The parametric studies also considered the effects of varying the number of elements through the wall thickness and of varying the element aspect ratio.

Three-dimensional beam elements (STIF4), solid elements (STIF45), and gap (STIF52) elements are used in the construction of the two three-dimensional finite element models. All cask components (forgings, lids, lead shell, shielding, inner and outer shells, etc.) are modeled using the STIF45 element. The STIF45 element is an eight-node, three-dimensional, parametric solid element having three degrees of freedom at each node (translations in X, Y, and Z directions).

Connections and interfaces between the components of the cask are modeled using the ANSYS STIF52 gap element. The STIF52 gap element is a three-dimensional interface element that represents two surfaces that may maintain or break physical contact, and may slide relative to each other. The use of this element is required in areas where contact between adjacent surfaces is not guaranteed by the geometry or loading. Such locations include the lead/steel shell interfaces and lid top forging interfaces. The disadvantage of the STIF52 element is that, because it is a nonlinear element, the solution procedure becomes an iterative one and can substantially increase solution run times. The cask lid bolts are modeled using the ANSYS beam element (STIF4). The STIF4 is a three-dimensional, uniaxial element with tension, compression, torsion, and bending capabilities. The element has six degrees of freedom at each node (translations in the nodal X, Y and Z directions and rotations about the nodal X, Y, and Z axes).

The material properties required by ANSYS for the three-dimensional analyses are those identified in Section 2.10.2.1.

2.10.2.1.2.1 Bottom Fine Mesh Model

The bottom fine mesh model of the NAC-STC is constructed of 13,597 nodes and 10,050 elements. The maximum in-core wavefront size is 794. The maximum in-core wavefront size is used as a measurement of the size of an ANSYS analysis. The Root Mean Square (RMS) wavefront size is 507.

The complete bottom fine mesh model is shown in Figure 2.10.2-9. A two-dimensional view of the model is shown in Figure 2.10.2-10. The node numbering patterns and mesh arrangement in different regions of the model are provided in Figures 2.10.2-11 through 2.10.2-19. The node numbers shown in these figures are for the 0-degree circumferential plane. A circumferential node number increment of 2000 is used to determine the node numbers on the remaining circumferential planes. The bottom half of the cask contains the finer mesh density. The structural components have a mesh density of at least three elements through their thicknesses in areas of structural discontinuities to ensure detection of stress gradients in those regions. The lead shell and the neutron shield end layers are modeled with one element through their thickness, which is sufficient to distribute their loads to the surrounding structure. In Figure 2.10.2-10, the elements representing the lead layer and the neutron shield layers are intentionally not shown in order to improve the clarity of the mesh used in modeling the stainless steel components.

The bottom fine mesh model is constructed by first building a two-dimensional mesh of the cask, and then revolving that mesh 180 degrees around the longitudinal axis of the cask to get a three-dimensional model of one-half of the cask.

All of the cask components - cask body, lead, shielding, lids, etc.-- are modeled with the three-dimensional solid elements (STIF45). Interaction between the components is modeled by the use of three-dimensional gap elements (STIF52). The cask components which are enclosed by stainless steel, including the lead and the end neutron shields, are surrounded radially and axially by gap elements. Just as for the two-dimensional model, a gap element stiffness of 3.0×10^8 psi is specified to maintain the boundaries between the surfaces. The initial radial gap between the lead layer and the outer shell is set to 0.0428 inches.

The mass densities of some of the cask components are modified to distribute the impact limiter masses onto the cask ends and to distribute the mass of the external neutron shield material to the region between the top of the bottom forging and the bottom of the inner lid, as described in Section 2.10.2.1.1.

2.10.2.1.2.2 Top Fine Mesh Model

The top fine mesh model of the NAC-STC is comprised of 12,601 elements and 15,261 nodes. The maximum in-core wavefront size is 1338, as compared to the maximum permissible wavefront size of 1439, which is based on ANSYS program limitations. The maximum in-core wavefront size is used as a measurement of the ANSYS analysis size. The RMS wavefront size is 664.

The three-dimensional model is generated by first creating a mesh for a two-dimensional plane and then revolving the mesh 180 degrees around the longitudinal axis of the cask to create a half model, as described in Section 2.10.2.1.2.

The complete top fine mesh model is shown in Figure 2.10.2-20. The upper half of the model is shown at a larger scale in Figure 2.10.2-21. Figure 2.10.2-22 is a view of the 0-degree circumferential plane of the top fine mesh model. Figures 2.10.2-23 through Figure 2.10.2-31 show in detail the node numbering patterns and the mesh arrangement at different regions of the cask. The node numbers shown in these figures are for the 0-degree circumferential plane. The node numbers on the remaining circumferential planes can be determined by adding 2000 (unless otherwise noted on each plot) to the node numbers on each succeeding circumferential plane. In Figure 2.10.2-23, the elements representing the lead layer and the neutron shield layers are intentionally not shown, in order to improve the clarity of the mesh used in the stainless steel components.

All cask components (cask body, lead, shielding, lids, etc.) are modeled using the ANSYS STIF45 solid elements, as in the bottom fine mesh model. The structural components have a mesh density of at least three elements through their thickness near areas of structural discontinuities to ensure the detection of stress gradients in those regions. The lead shell and the neutron shield end layers are modeled with one element through their thicknesses, which is adequate to distribute their loads to the surrounding structure. The lids are modeled with two or more elements through their thickness near the center of the cask, where stresses are low, and with a finer mesh density near the outer radius of the cask, where the stresses are higher as a result of the bolt loads and the impact loads.

Interaction between the cask components is modeled by use of three-dimensional gap elements (STIF52). The cask components that are enclosed by stainless steel, including the lead and the end neutron shields, are surrounded radially and axially by gap elements. The interface between the inner lid and the cask top forging is modeled using STIF52 gap elements in the axial and radial directions. The outer lid interfaces also use STIF52 gap elements in the radial direction (between the outer lid and the cask top forging) and in the axial direction (between the outer lid and the inner lid and between the outer lid and the top forging). There are 0.03-inch radial gaps between the top forging and the inner lid outside diameter and 0.075-inch gaps between the top forging and the outer lid outside diameter. There is a 0.06-inch axial gap between the inner lid and the outer lid in the 50.0-inch diameter center region of the lids. Just as for the two-dimensional model, a gap element stiffness of 3.0×10^8 psi is used to maintain the boundaries between the surfaces.

The cask lead shielding is modeled using ANSYS STIF45 elements. The interface between the lead and the cask body is modeled using gap elements in the radial direction along its entire length. All runs are made with an initial gap specification of 0.00 inches at the inside diameter of the lead and 0.0428 inch at the outside diameter of the lead. At locations where the lead surface is angled, the gaps are oriented in such a way that they close in the direction perpendicular to the surface. This allows these gaps to support some axial load, as would be the case in the actual cask. The shielding at the bottom end of the cask is far enough removed from the area of interest for this model, that any gap element effects would be negligible. For this reason, the bottom end shielding is modeled using ANSYS STIF45 brick elements having common nodes with the cask body. The neutron shielding between the lids is also connected to the inner lid with common nodes. Since its modulus of elasticity is small compared to that of steel, the lid stresses are not significantly affected.

The mass densities of some of the cask components are modified to distribute the impact limiter masses onto the cask ends, and to distribute the external neutron shield mass to the region between the top of the bottom forging and the bottom of the inner lid, as described in Section 2.10.2.1.1.

A detailed analysis of the top end of the cask requires that the lids and their bolted connections to each other and to the cask be accurately modeled. This is difficult in this case because of the different circumferential bolt spacing on the inner (42 bolts) and outer (36 bolts) lids, and additionally because neither of these spacings are the same as the element circumferential spacing used in the ANSYS model. This problem is solved by "averaging" the effective bolt properties around the circumference.

The bolts are modeled using ANSYS STIF4 beam elements and are located on their appropriate radii (connecting the outer lid to the inner lid and connecting the inner lid to the cask top forging), on each circumferential plane location. Since there are 16 circumferential planes contained in the finite element model, this results in 16 equivalent bolts per lid. Each bolt consists of four elements--one element as the bolt shaft, one as the bolt thread, and two as the bolt head.

The effective properties of each bolt are determined by calculating the percentage of the 180-degree arc that each bolt affects, and multiplying that by an overall sum c the actual properties. Table 2.10.2-2 shows the calculated percentages of the 180-degree arc, determined by summing one-half of the angles of the arc of the two elements adjacent to a given node. Tables 2.10.2-3 and 2.10.2-4 document the calculated effective properties for all of the bolts in both lids, including the associated real constant numbers. Following are example calculations for the inner and outer lid bolt properties:

Inner Lid Bolts (42, 1 1/2 - 8 UN)

Tensile area of one bolt = $1.492\ in^2$

Total tensile area = $(42)(1.492) = 62.66\ in^2$

Bolt minor radius (R) = $1.3444/2 = 0.6722$ in

Moment of inertia (I) of one bolt = $\pi R^4/4 = 0.1604\ in^4$

Total moment of inertia = $(42)(0.1604) = 6.7368\ in^4$

Referring to Table 2.10.2-3, the inner lid bolt properties for circumferential plane location 4, real constant number 17, are:

Tensile area = $(0.0522)(62.66)(0.5) = 1.6354\ in^2$

I = $(0.0522)(6.7368)(0.5) = 0.1758$ in

Diameter for stress recovery = $[(1.492)(4)/\pi)]^{0.5} = 1.378$ in

Additionally, to determine the shear area of the bolt, a shear factor of 10/9 is applied to the bolt tensile area, as recommended by the ANSYS User's Manual, Section 4.0.5. In the ANSYS model, bolt head properties are taken to be 10 times the associated bolt shaft properties.

Outer Lid Bolts (36, 1 - 8 UNC)

Tensile area of one bolt = 0.606 in^2

Total tensile area = (36)(0.606) = 21.816 in^2

Bolt minor radius (R) = 0.8446/2 = 0.4223 in

Moment of inertia (I) of one bolt = $\pi R^4/4$ = 0.0250 in^4

Total moment of inertia = (36)(0.0250) = 0.900 in^4

Referring to Table 2.10.2-4, the outer lid bolt properties for circumferential plane location 8, real constant number 38, are:

Tensile area = (0.0639)(21.816)(0.5) = 0.697 in^2

I = (0.0639)(0.900)(0.5) = 0.02876 in

Diameter for stress recovery = $[(0.606)(4)/\pi)]^{0.5}$ = 0.878 in

Additionally, to determine the shear area of the bolt, a shear factor of 10/9 is applied to the bolt tensile area, as recommended by the ANSYS User's Manual, Section 4.0.5. In the ANSYS model, bolt head properties are taken to be 10 times the associated bolt shaft properties.

The bolt preload is calculated as shown in Section 2.6.7.5. The preload on the inner lid bolts is calculated to be 4,870,000 pounds for 42 bolts. The preload on the outer lid bolts is calculated to be 509,316 pounds for 36 bolts.

The bolt preload is accounted for in the ANSYS analysis by assigning to each bolt shaft an initial strain that will result in an axial stress equivalent to the bolt preload divided by the bolt area. The initial strain is applied to the element representing the portion of the bolt shaft that is not engaged in threads. The initial strain is calculated by applying an initial guess or unit strain to the bolt and running the model (with no other loads) iteratively, until convergence is reached between the resulting preload values and the required preload values. Section 2.10.2.2.3 contains a detailed description of the bolt preload calculation for both the inner and outer lids.

2.10.2.2 Loading Conditions

This section documents the methods of calculating contents pressure loads and impact pressure loads for the end drop, side drop, corner drop, and oblique drop scenarios. Additionally, the use of bolt initial strain to represent the bolt preload and the determination of the bolt initial strain are explained.

2.10.2.2.1 Contents Pressure Calculation

For the end drop analyses, the contents weight is assumed to be uniformly distributed on the cask end, over an area determined by the inside diameter of the cask. Therefore, the contents weight of 56,000 pounds, and the cask cavity inside radius of 35.5 inches are used to calculate a contact pressure of:

$$p = \frac{56{,}000}{(\pi)(35.5)^2} = 14.14 \text{ psi}$$

This pressure applies to a 1 g loading condition. Pressure values for the 1-foot and 30-foot end drop analyses are determined by ratioing this pressure by the g-load values applicable to the specific case, which are documented in Sections 2.6.7.1 and 2.7.1.1.

For the side drop condition, the basket stress analysis performed in Section 2.7.8.0 indicates that the contact area between the basket and the cask cavity is approximately 180 degrees (90 degrees on each side of the drop centerline), therefore, for the side drop analyses, the cask contents are conservatively assumed to contact the inner cask diameter on an arc of only 79.4 degrees on either side of the impact centerline. The inertial load produced by the 56,000-pound contents weight is represented as an equivalent static pressure applied on the interior surface of the cask. The pressure is uniformly distributed along the cavity length, and is varied in the circumferential direction as a cosine distribution. The maximum pressure occurs at the impact centerline; the pressure decreases to zero at locations that are 79.4 degrees either side of the impact centerline, as illustrated in Figure 2.10.2-32. The method used to determine the varying pressures on the elements within the 79.4-degree arc is presented in the following paragraphs.

Eight sectors of elements in the ANSYS model are defined within the 79.4-degree arc. The first sector of elements subtends the arc from the 0-degree circumferential plane to the 8.3-degree circumferential plane. The second sector subtends the arc from the 8.3-degree circumferential plane to the 17-degree circumferential plane. The remaining five sectors are defined in the same manner, by the 26.2-, 35.8-, 45.9-, 56.5-, and 67.7-degree circumferential planes, which are shown in Figure 2.10.2-8.

The following formula is used to determine the contents pressures for the side drop analyses, which vary around the circumference. This method uses a summation scheme to approximate the integration of the cosine-shaped pressure distribution:

$$F_{total} = \sum_{i=1}^{8} P_{max} A_i \cos(\theta_i) \cos(\theta_i')$$

where

F_{total} = 28,000 lb (cask contents weight is 56,000 lb: therefore, 28,000 lb for a half model)

P_{max} = maximum pressure (at impact centerline)

θ_i = average angle of subtended arc

i = i^{th} circumferential sector

θ_i' = normalized angle to peak at 0° and to be zero at 79.4°
= $\theta_i \left(\frac{90}{79.4}\right) = 1.1335(\theta_i)$

A_i = i^{th} circumferential area over which the pressure is applied

$= R\ (\Delta\theta_i)(\pi/180)\ L$

R = inner radius of cask = 35.5 in

L = cask cavity length = 165 in

Therefore,

$$A_i = (35.5)(\Delta\theta_i)(\pi/180)(165) = 102.23\ (\Delta\theta_i)$$

$$\Delta\theta_1 = 8.3 - 0 = 8.3°$$

$$\Delta\theta_2 = 17.0 - 8.3 = 8.7°$$

$$\Delta\theta_3 = 26.2 - 17.0 = 9.2°$$

$$\Delta\theta_4 = 35.8 - 26.2 = 9.6°$$

$$\Delta\theta_5 = 45.9 - 35.8 = 10.1°$$

$$\Delta\theta_6 = 56.5 - 45.9 = 10.6°$$

$$\Delta\theta_7 = 67.7 - 56.5 = 11.2°$$

$$\Delta\theta_8 = 79.4 - 67.7 = 11.7°$$

$$\theta_1 = \frac{0 + 8.3}{2} = 4.15°;\ \theta_1' = 4.15°(1.1335) = 4.70°$$

$$\theta_2 = \frac{8.3 + 17.0}{2} = 12.65°;\ \theta_2' = 12.65°(1.1335) = 14.34°$$

$$\theta_3 = \frac{17.0 + 26.2}{2} = 21.6°;\ \theta_3' = 21.6°(1.1335) = 24.48°$$

$$\theta_4 = \frac{26.2 + 35.8}{2} = 31°;\ \theta_4' = 31°(1.1335) = 35.14°$$

$$\theta_5 = \frac{35.8 + 45.9}{2} = 40.85°;\ \theta_5' = 40.85°(1.1335) = 46.30°$$

$$\theta_6 = \frac{45.9 + 56.5}{2} = 51.20°;\ \theta_6' = 51.20°(1.1335) = 58.04°$$

$$\theta_7 \quad \frac{\cdot 5 + 67.7}{2} = 62.10°;\ \theta_7' = 62.10°(1.1335) = 70.39°$$

$$\theta_8 = \frac{67.7 + 79.4}{2} = 73.55°;\ \theta_8' = 73.55°(1.1335) = 83.3$$

Define: $F_i = P_{max}\ A_i \cos(\theta_i) \cos(\theta_i')$

where $i = 1$ through 8

$$F_1 = P_{max}(102.23)(8.3°) \cos(4.15°) \cos(4.70°) = 843.4\ (P_{max})$$

$$F_2 = P_{max}(102.23)(8.7°) \cos(12.65°) \cos(14.34°) = 840.8\ (P_{max})$$

$$F_3 = P_{max}(102.23)(9.2°) \cos(21.6°) \cos(24.48°) = 795.9\ (P_{max})$$

$$F_4 = P_{max}(102.23)(9.6°) \cos(31°) \cos(35\ 14°) = 687.9\ (P_{max})$$

$$F_5 = P_{max}(102.23)(10.1°)\ \text{co}\ldots.85°) \cos(46.30°) = 539.6\ (P_{max})$$

$$F_6 = P_{max}(102.23)(10.6°) \cos(51.20°) \cos(58.04°) = 359.4\ (P_{max})$$

$$F_7 = P_{max}(102.23)(11.2°) \cos(62.10°) \cos(70.39°) = 179.8\ (P_{max})$$

$$F_8 = P_{max}(102.23)(11.7°) \cos(73.5\ldots) \cos(83.37°) = 39.11\ (P_{max})$$

$$F_{total} = 4286(P_{max})$$

Setting the total load (F_{total}) to 28,000 lb

$$4286(P_{max}) = 28,000$$

$$(P_{max}) = 6.533 \text{ psi}$$

P_{max} represents the contents pressure load which would occur along the drop centerline. Given P_{max}, the contents pressure loadings, which are applied to the eight sectors of elements, are calculated as follows:

$$P_1 = P_{max} \cos\theta_1' = 6.533 \cos(4.70°) = 6.51 \text{ psi}$$

$$P_2 = P_{max} \cos\theta_2' = 6.533 \cos(14.34°) = 6.33 \text{ psi}$$

$$P_3 = P_{max} \cos\theta_3' = 6.533 \cos(24.48°) = 5.95 \text{ psi}$$

$$P_4 = P_{max} \cos\theta_4' = 6.533 \cos(35.14°) = 5.34 \text{ psi}$$

$$P_5 = P_{max} \cos\theta_5' = 6.533 \cos(46.30°) = 4.51 \text{ psi}$$

$$P_6 = P_{max} \cos\theta_6' = 6.533 \cos(58.04°) = 3.46 \text{ psi}$$

$$P_7 = P_{max} \cos\theta_7' = 6.533 \cos(70.39°) = 2.19 \text{ psi}$$

$$P_8 = P_{max} \cos\theta_8' = 6.533 \cos(83.37°) = 0.76 \text{ psi}$$

The following is a summary of the side drop contents pressures applied to the finite element model in the eight circumferential sectors:

ARC (deg)	PRESSURE (psi)
0 - 8.3	6.51
8.3 - 17.0	6.33
17.0 - 26.2	5.95
26.2 - 35.8	5.34
35.8 - 45.9	4.51
45.9 - 56.5	3.46
56.5 67.7	2.19
67.7 - 79.4	0.76

The pressures are applied to the cask inner shell, over the length of the cask cavity for the side drop analyses. It should be noted that these pressures consider a 1 g deceleration condition. Pressures for the 1-foot and 30-foot side drop analyses are calculated by ratioing these pressure values by the appropriate deceleration g-loads, which are documented in Sections 2.6.7.2 and 2.7.1.2.

For the corner and oblique drop analyses, the contents pressure loading is a combination of the end drop pressure load and the side drop pressure load. The corner and oblique drop pressure loadings are determined by breaking up the contents pressure load into longitudinal and lateral components, based on the drop angle. The longitudinal component is applied to the cask end, and the lateral component is applied to the cask inner shell as described previously for the side drop case.

2.10 2.2.2 Impact Pressure Calculation

For the bottom end drop analysis, the impact pressure is assumed to uniformly contact the cask bottom end over an area determined by the outside diameter of the cask. Therefore, the cask weight (including contents) of 250,000 pounds and the cask outside radius of 43.35 inches are used to calculate a bottom end drop impact pressure of:

$$P = \frac{250,000}{(\pi)(43.35)^2} = 42.35 \text{ psi}$$

For cases when no contents are present, the weight of the empty cask plus basket is 211,000 pounds, therefore the bottom end drop impact pressure is:

$$P = \frac{211,000}{(\pi)(43.35)^2} = 35.74 \text{ psi}$$

These pressures apply to a 1 g loading condition. Pressure values for the 1-foot and 30-foot end drop analyses are determined by ratioing these pressure values by the g-loads applicable to the specific case, which are documented in Sections 2.6.7.1. and 2.7.1.1.

For the top end drop analysis, the impact pressure is assumed to uniformly contact the cask top end over an area determined by the outside diameter of the cask, less the area represented by the 0.075-inch radial gap between the outer lid and the top forging. Therefore, the cask weight (including contents) of 250,000 pounds, the cask outside radius of 43.35 inches, the top forging inside radius of 40.88 inches, and the outer lid outside radius of 40.805 inches, are used to calculate a bottom end drop impact pressure of:

$$P = \frac{250,000}{(\pi)(43.35)^2 - (\pi)[(40.88^2 - 40.805)^2]} = 42.48 \text{ psi}$$

For cases when no contents are present, the top end drop impact pressure is:

$$P = \frac{211,000}{(\pi)(43.35)^2 - (\pi)[(40.88^2 - 40.805)^2]} = 35.86 \text{ psi}$$

These pressures apply to a 1 g loading condition. Pressures for the 1-foot and 30-foot end drop analyses are calculated by ratioing these pressure values by the g-loads applicable to the specific case, which are documented in Sections 2.6.7.1 and 2.7.1.1.

For the side drop analyses, the impact pressure load is applied to the finite element model as a distributed pressure over the contact area between the impact limiters and the cask. Since the center of gravity of the loaded cask is located within 1 inch of the cask middle plane, the impact load is assumed to be evenly divided between the two limiters.

The distribution of impact pressure is assumed to be uniform, in the longitudinal direction, over the two 12.03-inch impact limiter contact areas. The distribution of impact limiter pressure is assumed to vary sinusoidally in the circumferential direction. A cosine-shaped pressure distribution is selected, which is "peaked" at the impact centerline, and is spread over a 79.4-degree arc on each side of the impact centerline, as shown in Figure 2.10.2-32. The region of applied pressure (a 158.8° arc) is defined based on the "crush" geometry of the impact limiter. The assumption of a peaked pressure distribution is a conservative, classical, stress analysis procedure since the applied pressure actually is spread over a 180-degree arc (90-degree half-cask arc).

The following calculation is performed to determine the pressure (P_i) to be applied to elements within the eight circumferential sectors defined in Section 2.10.2.2.1. The calculation is based on the weight of a half-model of the cask at 1 g. Pressure forces for the 1-foot and 30-foot side drop analyses are determined by ratioing these pressure forces by the g-load applicable to the specific case.

The following formula can be used to compute the maximum impact pressure. This method uses a summation scheme to approximate the integration of the cosine-shaped pressure distribution:

$$F_{total} = \sum_{i=1}^{8} P_{max} A_i \cos(\theta_i) \cos(\theta_i')$$

where

F_{total} = 125,000 lb (the cask design weight for a half model)

P_{max} = maximum impact pressure occuring at the impact centerline

θ_i = average angle of subtended arc

i = i^{th} circumferential sector

$\Delta\theta_i$ = arc length, in degrees, of sector i

θ_i' = Normalized angle to peak at 0° and to be zero at 79.4°
= θ_i (90/79.4) = 1.1335 θ_i

A_i = i^{th} circumferential area over which the pressure is applied
= $R(\Delta\theta_i)(\pi/180)L = 0.01745(\Delta\theta_i)(R)(L)$

R = outer radius of the cask at impact limiter contact points
= 43.35 in

L = Impact limiter contact length = 24.06 in (for two limiters, one on each end of the cask)

$\Delta\theta_1 = 8.3 - 0 = 8.3°$

$\Delta\theta_2 = 17.0 - 8.3 = 8.7°$

$\Delta\theta_3 = 26.2 - 17.0 = 9.2°$

$\Delta\theta_4 = 35.8 - 26.2 = 9.6°$

$\Delta\theta_5 = 45.9 - 35.8 = 10.1°$

$\Delta\theta_6 = 56.5 - 45.9 = 10.6°$

$\Delta\theta_7 = 67.7 - 56.5 = 11.2°$

$\Delta\theta_8 = 79.4 - 67.7 = 11.7°$

$\theta_1 = \frac{0 + 8.3}{2} = 4.15°$; $\theta_1' = 4.15°(1.1335) = 4.70°$

$\theta_2 = \frac{8.3 + 17.0}{2} = 12.65°$; $\theta_2' = 12.65°(1.1335) = 14.34°$

$$\theta_3 = \frac{17.0 + 26.2}{2} = 21.6°;\ \theta_3' = 21.6°(1.1335) = 24.48°$$

$$\theta_4 = \frac{26.2 + 35.8}{2} = 31°;\ \theta_4' = 31°(1.1335) = 35.14°$$

$$\theta_5 = \frac{35.8 + 45.9}{2} = 40.85°;\ \theta_5' = 40.85°(1.1335) = 46.30°$$

$$\theta_6 = \frac{45.9 + 56.5}{2} = 51.20°;\ \theta_6' = 51.20°(1.1335) = 58.04°$$

$$\theta_7 = \frac{56.5 + 67.7}{2} = 62.10°;\ \theta_7' = 62.10°(1.1335) = 70.39°$$

$$\theta_8 = \frac{67.7 + 79.4}{2} = 73.55°;\ \theta_8' = 73.55°(1.1335) = 83.37°$$

$$F_i = P_{max}\ A_i\ \cos(\theta_i)\ \cos(\theta_i')$$

$i = 1$ through 8

$$F_1 = P_{max}(0.01745)(R)(8.3°)(L)\cos(4.15°)\cos(4.70°)$$
$$= 0.1440\ (P_{max})(L)(R)$$

$$F_2 = P_{max}(0.01745)(R)(8.7°)(L)\cos(12.65°)\cos(14.34°)$$
$$= 0.1435\ (P_{max})(L)(R)$$

$$F_3 = P_{max}(0.01745)(R)(9.2°)(L)\cos(21.6°)\cos(24.48°)$$
$$= 0.1359\ (P_{max})(L)(R)$$

$$F_4 = P_{max}(0.01745)(R)(9.6°)(L)\cos(31°)\cos(35.14°)$$
$$= 0.1174\ (P_{max})(L)(R)$$

$$F_5 = P_{max}(0.01745)(R)(10.1°)(L)\cos(40.85°)\cos(46.30°)$$
$$= 0.0921\ (P_{max})(L)(R)$$

$$F_6 = P_{max}(0.01745)(R)(10.6°)(L)\cos(51.20°)\cos(58.04°)$$
$$= 0.0614\ (P_{max})(L)(R)$$

$$F_7 = P_{max}(0.01745)(R)(11.2°)(L)\cos(62.10°)\cos(70.39°)$$
$$= 0.0307\,(P_{max})(L)(R)$$

$$F_8 = P_{max}(0.01745)(R)(11.7°)(L)\cos(73.55°)\cos(83.37°)$$
$$= 0.0067\,(P_{max})(L)(R)$$

$$F_{total} = 0.7317\,(P_{max})(L)(R)$$

$$P_{max} = \frac{F_{total}}{(0.7317)(L)(R)}$$

The pressures to be applied to the finite element analysis can then be computed as follows:

$$P_i = \frac{F_{Total}\cos(\theta_i')}{(0.7317)(L)(R)}$$

where

F_{total} = 125,000 lb (for half model)

L = 24.06 in

R = 43.35 in

$P_i = 163.7918\cos(\theta_i')$

$P_1 = 163.7918\cos(4.70°) = 163.22$ psi

$P_2 = 163.7918\cos(14.34°) = 158.67$ psi

$P_3 = 163.7918\cos(24.48°) = 149.06$ psi

$P_4 = 163.7918\cos(35.14°) = 133.98$ psi

$P_5 = 163.7918\cos(46.30°) = 113.17$ psi

$P_6 = 163.7918\cos(58.04°) = 86.96$ psi

$$P_7 = 163.7918 \cos (70.39°) = 54.99 \text{ psi}$$

$$P_8 = 163.7918 \cos (83.37°) = 18.96 \text{ psi}$$

The following is a summary of the side drop impact pressures applied to the finite element model in the eight circumferential sectors:

ARC (deg)	PRESSURE (psi)
0 - 8.3	163.22
8.3 - 17.0	158.67
17.0 - 26.2	149.06
26.2 - 35.8	133.98
35.8 - 45.9	113.17
45.9 - 56.5	86.69
56.5 - 7	54.99
67.7 - 79.4	18.96

It should be noted that these pressures consider a 1 g deceleration condition. Pressures for the 1-foot and 30-foot side drop analyses are calculated by ratioing these pressure values by the appropriate deceleration or g values, which are documented in Sections 2.6.7.2 and 2.7.1.2.

For the corner and oblique drop analyses, the impact pressure loading is a combination of the end drop impact pressure load and the side drop impact pressure load. The corner and oblique drop impact pressure loadings are determined by breaking up the impact pressure load into longitudinal and lateral components, based on the drop angle. The longitudinal component is applied to the cask end, and the lateral component is applied to the cask inner shell as previously described for the side drop case.

2.10.2.2.3 Bolt Initial Strain Determination

The standard technique for applying bolt preload to a finite element model is employed. The bolts are modeled using beam elements, ANSYS STIF3 elements for the two-dimensional model and ANSYS STIF4 elements for the three-dimensional top fine mesh model. Each bolt is modeled by four beam elements, two that represent the bolt head and two that represent the bolt shaft. The two bolt head elements are defined by three nodes that are an integral part of the non-threaded plate. The bolt head elements are assigned a stiffness of 10 times the actual bolt stiffness. The first bolt shaft element connects the center node of the bolt head with a node located at the top of the threaded hole. This element represents the portion of the bolt that is not engaged in the threaded hole. This portion of the bolt will be in tension due to the bolt preload. The second bolt shaft element connects the node at the top of the threaded hole with a node at the bottom of the threaded hole. This element represents the portion of the bolt that is engaged in the threaded hole. The two bolt shaft elements are assigned material property values (area and stiffness) equal to the actual bolt properties.

The effect of bolt preload is imposed on the model by applying an initial strain to the bolt shaft. The initial strain is applied only to the beam element representing the portion of the bolt shaft not engaged in threads. The initial strain values, which result in the required preload values, are determined by first running ANSYS analyses of both the two- and three-dimensional models with a "trial" initial strain, applied to the bolt shaft element, as the only loading condition. The resulting beam element force (from the element representing the portion of the bolt shaft not engaged in threads), is then used to ratio the trial initial strain to a value that will result in a beam element force closer to the actual bolt preload. This procedure is performed iteratively until the beam element force is effectively equal to the actual bolt preload.

The trial initial strain values are first determined by performing hand calculations of the value of P/nAE for both the inner and the outer lid bolts. For the inner lid bolts, the calculation considers a required total bolt preload (P) of 4,870,000 pounds for 42 bolts, a quantity (n) of 42 bolts, a bolt cross-sectional area (A) of 1.492 square inches per bolt, and a Young's modulus (E) of 31.0×10^6 psi. For the outer lid bolts, the calculation considers a required total bolt preload (P) of 509,316 pounds for 36 bolts, a quantity (n) of 36 bolts, a bolt cross-sectional area (A) of 0.606 square inches per bolt, and a Young's modulus (E) of 28.3×10^6 psi. The hand calculations resulted in trial initial strains of 3.0×10^{-3} inch/inch for the inner lid bolts and 8.5×10^{-4} inch/inch for the outer lid bolts.

The trial initial strain values were used in the iterative procedure outlined previously. Several iterations were performed on both the two- and three-dimensional models until the initial strain values yielded bolt preload values within 5 percent of the required amount. The final values of initial strain for a cask temperature condition of 250°F were determined to be 3.034×10^{-3} inch/inch for the inner lid bolts, and 8.863×10^{-4} inch/inch for the outer lid bolts. The resulting bolt preload values are documented below:

BOLT PRELOAD

	Required Value (lb)	ANSYS Calculated 2-D Model (lb)	ANSYS Calculated 3-D Model (lb)	Difference Required 2-D	Difference Required 3-D
Outer Lid Bolts	509,316	519,280	509,7[illegible]1	2.0%	0.0%
Inner Lid Bolts	4,870,000	4,902,832	5,068,866	0.7%	4.1%

The ANSYS analyses results show good agreement with required bolt preload values. The differences between the required values and the two-dimensional ANSYS analysis values are less than 2 percent. The differences between the required values and the three-dimensional ANSYS values are less than 4.1 percent. Both the two-dimensional and three-dimensional ANSYS values are conservative; therefore, it is concluded that the final values of initial strain are adequate for modeling bolt preload.

2.10.2.3 Finite Element Analysis Procedures

The structural evaluation of the NAC-STC is performed by ANSYS analyses using three finite element models. A two-dimensional axisymmetric model is used for the axisymmetric loading cases, including bolt preload, internal pressure (high and low), thermal hot and cold, thermal fire transient, top end drop, and bottom end drop. A three-dimensional top fine mesh model is used in the non-axisymmetric loading conditions that result in high stresses on the top end of the cask, including the top corner drop and top oblique drops. The three-dimensional bottom fine mesh model is used for the non-axisymmetric loading conditions that result in high stresses on the bottom end of the cask, including the bottom corner drop, and bottom oblique drops. For the side drop analysis, both the top fine mesh model and the bottom fine mesh model are analyzed separately, in order to obtain the detailed stresses for both ends of the cask.

A number of individual and combined loading conditions are evaluated using separate ANSYS analyses. The ANSYS analyses performed for each individual loading condition are for the purpose of studying the structural effects of each individual type of load applied to the cask. The stress results of the ANSYS analysis of each individual load case are documented by nodal stress summaries (for details about finite element stress documentation procedures, see Section 2.10.2.4). The individual loading conditions considered are:

1. Bolt preload plus maximum internal pressure, 50 psig.

2. Bolt preload plus minimum internal pressure, 12 psig.

3. Gravity with 100°F ambient temperature, maximum decay heat load, and maximum insolation.

4. Gravity with -40°F ambient temperature, no decay heat load, and no insolation.

5. Thermal heat with 100°F ambient temperature, maximum decay heat load, and maximum insolation.

6. Thermal cold with -20°F ambient temperature, maximum decay heat load, and no insolation.

7. Thermal cold with -40°F ambient temperature, no decay heat load, and no insolation.

8. Thermal fire transient with 1475°F surrounding environment, 30-minute period.

9. Impact and inertial loads, 1-foot top end drop, 20 g impact load, $\phi = 0$ degrees.

10. Impact and inertial loads, 1-foot bottom end drop, 20 g impact load, $\phi = 0$ degrees.

11. Impact and inertial loads, 1-foot side drop, 20 g impact load, $\phi = 90$ degrees.

12. Impact and inertial loads, 1-foot top corner drop, 20 g impact load, $\phi = 24$ degrees.

13. Impact and inertial loads, 1-foot bottom corner drop, 20 g impact load, $\phi = 24$ degrees.

14. Impact and inertial loads, 30-foot top end drop, 56.1 g impact load, $\phi = 0$ degrees.

15. Impact and inertial loads, 30-foot bottom end drop, 56.1 g impact load, $\phi = 0$ degrees.

16. Impact and inertial loads, 30-foot side drop, 55 g impact load, $\phi = 90$ degrees.

17. Impact and inertial loads, 30-foot top corner drop, 55 g impact load, $\phi = 24$ degrees.

18. Impact and inertial loads, 30-foot bottom corner drop, 55 g impact load, $\phi = 24$ degrees.

19. Impact and interial loads, 30-foot bottom oblique drop, 55 g impact load, $\phi = 15$ degrees.

20. Impact and inertial loads, 30-foot top critical oblique drop, 55 g impact load, $\phi = 75$ Degrees. ($\phi = 75$ degrees is the angle that results in the most critical stresses for the 30-foot top oblique drops).

21. Impact and inertial loads, 30-foot bottom critical oblique drop, 55 g impact load, $\phi = 75$ degrees. ($\phi = 75$ degrees is the angle that results in the most critical stresses for the 30-foot bottom oblique drops).

Combined load cases are then evaluated by running ANSYS analyses of the combined loading conditions. For example, the 30-foot top corner drop accident condition is evaluated by a single ANSYS analysis with the following loads applied simultaneously:

> 55 g Impact and inertial loads ($\phi = 24$ degrees), 100°F ambient temperature, maximum decay heat load, maximum solar insolation, bolt preload, and 50 psig internal pressure.

A single analysis with multiple loads is used in contrast to the method of superimposing the stress results from the individual analyses, in order to more accurately evaluate the effect of the simultaneous loads on the cask structure. For combined load cases, the stresses are documented by nodal, sectional, and critical stress summaries. The following combined loads cases are considered:

1. Thermal Heat (normal condition), with bolt preload, maximum internal pressure of 50 psig, 100°F ambient temperature, maximum solar insolation, maximum decay heat, 1 g gravity load, still air, loaded and ready for shipment in the horizontal position.

2. Thermal Cold (normal condition) with bolt preload, minimum internal pressure of 12 psig, -40°F ambient temperature, no solar insolation, no decay heat load, 1 g gravity load, still air, loaded and ready for shipment in the horizontal position.

3. Thermal Fire Transient (hypothetical accident condition) with a surrounding environment of 1475°F for a 30-minute period, with bolt preload, internal pressure of 125 psig (conservative; actual internal pressure is 107.3 psig), maximum solar insolation, maximum decay heat load, and 1 g gravity load in the vertical direction.

4. 1-Foot Top End Drop (normal condition) with bolt preload, maximum internal pressure of 50 psig, 100°F ambient temperature, maximum solar insolation, maximum decay heat load, 20 g impact and inertial load (ϕ = 0 degrees), still air.

5. 1-Foot Top End Drop (normal condition) with bolt preload, minimum internal pressure of 12 psig, -20°F ambient temperature, no solar insolation, maximum decay heat load, 20 g impact and inertial load (ϕ = 0 degrees), still air.

6. 1-Foot Top End Drop (normal condition) with bolt preload, minimum internal pressure of 12 psig, -20°F ambient temperature, no solar insolation, no decay heat load, 20 g impact and inertial load (ϕ = 0 degrees), still air.

7. 1-Foot Bottom End Drop (normal condition) with bolt preload, maximum internal pressure of 50 psig, 100°F ambient temperature, maximum solar insolation, maximum decay heat load, 20 g impact and inertial load (ϕ = 0 degrees), still air.

8. 1-Foot Bottom End Drop (normal condition) with bolt preload, minimum internal pressure of 12 psig, -20°F ambient temperature, no solar insolation, maximum decay heat load, 20 g impact and inertial load (ϕ = 0 degrees), still air.

9. 1-Foot Bottom End Drop (normal condition) with bolt preload, minimum internal pressure of 12 psig, -20°F ambient temperature, no solar insolation, no decay heat load, 20 g impact and inertial load (ϕ = 0 degrees), still air.

10. 1-Foot Side Drop (normal condition) with bolt preload, maximum internal pressure of 50 psig, 100°F ambient temperature, maximum solar insolation, maximum decay heat load, 20 g impact and inertial load (ϕ = 90 degrees), still air.

11. 1-Foot Top Corner Drop (normal condition) with bolt preload, maximum internal pressure of 50 psig, 100°F ambient temperature, maximum solar insolation, maximum decay heat load, 20 g impact and inertial load (ϕ = 24 degrees), still air.

12. 1-Foot Bottom Corner Drop (normal condition) with bolt preload, maximum internal pressure of 50 psig, 100°F ambient temperature, maximum solar insolation, m imum 20 g impact and inertial load (ϕ = 24 degrees), still air.

13. 30-Foot Top End Drop (hypothetical accident condition) with bolt preload, maximum internal pressure of 50 psig, 100°F ambient temperature, maximum solar insolation, maximum decay heat load, 56.1 g impact and inertial load (ϕ = 0 degrees), still air.

14. 30-Foot Top End Drop (hypothetical accident condition) with bolt preload, minimum internal pressure of 12 psig, -20°F ambient temperature, no solar insolation, maximum decay heat load, 56.1 g impact and inertial load (ϕ = 0 degrees), still air.

15. 30-Foot Top End Drop (hypothetical accident condition) with bolt preload, minimum internal pressure of 12 psig, -20°F ambient temperature, no solar insolation, no decay heat load, 56.1 g impact and inertial load (ϕ = 0 degrees), still air.

16. 30-Foot Bottom End Drop (hypothetical accident condition) with bolt preload, maximum internal pressure of 50 psig, 100°F ambient temperature, maximum solar insolation, maximum decay heat load, 56.1 g impact and inertial load (ϕ = 0 degrees) still air.

17. 30-Foot Bottom End Drop (hypothetical accident condition) with bolt preload, minimum internal pressure of 12 psig, -20°F ambient temperature, no solar insolation, maximum decay heat load, 56.1 g impact and inertial load (ϕ = 0 degrees), still air.

18. 30-Foot Bottom End Drop (hypothetical accident condition) with bolt preload, minimum internal pressure of 12 psig, -20°F ambient temperature, no solar insolation, no decay heat load, 56.1 g impact and inertial load (ϕ = 0 degrees), still air.

19. 30-Foot Side Drop (hypothetical accident condition) with bolt preload, maximum internal pressure of 50 psig, 100°F ambient temperature, maximum solar insolation, maximum decay heat load, 55 g impact and inertial load (ϕ = 90 degrees, still air.

20. 30-Foot Top Corner Drop (hypothetical accident condition) with bolt preload, maximum internal pressure of 50 psig, 100°F ambient temperature, maximum solar insolation, maximum decay heat load, 55 g impact and inertial load (ϕ = 24 degrees), still air.

21. 30-Foot Bottom Corner Drop (hypothetical accident condition) with bolt preload, maximum internal pressure of 50 psig, 100°F ambient temperature, maximum solar insolation, maximum decay heat load, 55 g impact and inertial load (ϕ = 24 degrees), still air.

22. 30-Foot Bottom Oblique Drop (hypothetical accident condition) with bolt preload, maximum internal pressure of 50 psig, 100°F ambient temperature, maximum solar insolation, maximum decay heat load, 55 g impact and inertial load (ϕ = 15 degrees), still air.

23. 30-Foot Top Oblique Drop (hypothetical accident condition) with bolt preload, maximum internal pressure of 50 psi, 100°F ambient temperature, maximum solar insolation, maximum decay heat load, 55 g impact and inertial load (ϕ = 75°), still air. (ϕ = 75° is the angle which results in the most critical stresses for 30-foot top oblique drops).

24. 30-Foot Bottom Oblique Drop (hypothetical accident condition) with bolt preload, maximum internal pressure of 50 psi, 100°F ambient temperature, maximum solar insolation, maximum decay heat load, 55 g impact and inertial load ($\phi = 75°$), still air. ($\phi = 75°$ is the angle which results in the most critical stresses for 30-foot top oblique drops).

2.10.2.4 Finite Element Documentation Procedures

Documentation of the finite element stress calculations is performed according to the following procedure:

1. A sketch of the cask is prepared showing the points on each shell for which stresses are calculated and tabulated. At given axial locations on the cask, separate points are designated on the inside and outside of each shell. At given radial locations on the end and closure plates, separate points are designated on the inside and outside of each plate. In addition, for thick sections or thin sections at structural discontinuities, the stresses are presented for several points through the thickness in order to adequately define the stress distribution for the stress linearization calculations. Furthermore, for three-dimensional models, the stress variations around the circumference are documented at several selected circumferential locations.

2. For each stress point identified in step 1, a nodal stress summary, including stress components and principal stresses, is prepared for each individual normal and accident condition loading (e.g., internal pressure, hot and cold temperature, impact, etc.).

3. Summaries are prepared for the combined stresses at each stress point per the load combinations specified in Regulatory Guide 7.8. The combined stresses are classified in the categories of primary, and primary plus secondary stress intensities, as specified in Regulatory Guide 7.6.

4. Stress intensity summaries are prepared for the primary membrane (P_m), primary membrane plus primary bending ($P_m + P_b$), and primary plus secondary (S_n) stress categories. These stress intensity values are obtained by performing stress linearization calculations using the nodal stresses obtained from step 2. This calculation is peformed on all of the selected sections.

In order to perform steps 1 through 4, representative section cut locations were chosen based on the critical stress locations. The nodes representing the stress points used in steps 1 through 4 are located on these representative section cuts. The section locations are described in detail in Section 2.10.2.4.2.

5. Stress evaluations are then performed at every feasible cross-section of the cask. Then, the most critical cross-section within each component is determined by searching, on a component basis, for the cross section where the maximum stress intensity is located. Since the stress evaluations and the search are performed by a computer algorithm, every feasible cross-section is identified and evaluated, insuring that the maximum stress location within each component is found. Stress tables are then prepared to summarize the critical primary membrane, primary membrane plus primary bending, primary plus secondary stresses, and the margin of safety, of each cask component, for each loading condition.

In order to perform step 5, the cask is divided into components based on the physical geometry of the cask, such that each component consists of a single material. The details of the cask component identification are given in Section 2.10.2.4.1.

2.10.2.4.1 Structural Component Identification

Cask components are defined so that the qualification of the cask can be performed on a component basis. Stress evaluations are performed at every feasible cask cross-section, and then a computer search is performed to identify the section within each component which has the maximum stress intensity. Critical stress summaries are then prepared on a component basis.

The determination of critical stresses considers the stress results at a total of 3877 cross-sections on the three-dimensional top fine mesh model, and at a total of 3188 cross-sections on the three-dimensional bottom fine mesh model. For the two-dimensional axisymmetric model, stress evaluations are performed for a total of 487 cross-sections. These evaluations cover all of the feasible cross-sections of the cask.

Preparation of the critical stress summaries also requires the calculation of allowable stress values. Since allowable stress is a function of material properties (design stress intensity, yield strength and ultimate tensile strength), it is convenient that the components be defined such that each component consists of a single material. This is accomplished by designating the components in a manner consistent with the actual physical construction of the cask, i.e., the components are defined as the unique physical entities which exist prior to the final assembly of the cask.

The material properties used to determine allowable stresses are functions of temperature. If the allowable stresses for all components were determined using the maximum cask temperature, the allowable stresses will be overly conservative in those components which never experience the maximum cask temperature. Maximum temperatures determined on a component basis, rather than on a cask basis, permit the determination of more reasonable, but still conservative, allowable stresses. Therefore, the maximum component temperature is used in calculating the allowable stresses for that component.

The finite element cask components are uniquely designated as shown in Figure 2.10.2-33. Tables 2.10.2-5 through 2.10.2-7 document the name of each component, the material of which it is constructed, and an arbitrary material identification number (used in the ANSYS model). The fifth column of each table documents the maximum temperature which occurs in each individual component, as determined by the thermal analysis of the temperature conditions indicated in the table title.

The sixth and eighth columns of Tables 2.10.2-5 through 2.10.2-7 document the design stress intensity (S_m), and the ultimate tensile strength (S_u), for the component material at the maximum component temperature. The values of $1.5(S_m)$ and $0.7(S_u)$ are also provided.

2.10.2.4.2 Representative Section Locations

The entire NAC-STC body and closure lids are analyzed for structural adequacy. Representative section cut locations are defined, based on the critical stress locations, in order to illustrate the overall structural behavior of the cask. The selected section locations are identified by letters on Figure 2.10.2-34.

Each load case--pressure, thermal, and mechanical--is evaluated separately. The stress components are documented for each of the selected sections and for the nodes on the sections. The individual load cases are then combined to obtain total principal stresses and stress intensities for the primary membrane, primary membrane plus primary bending, and primary plus secondary stress categories.

Figures 2.10.2-35 and 2.10.2-36 show the distribution of nodes and elements in the circumferential direction for the three-dimensional top fine mesh model, and for the three-dimensional bottom fine mesh model, respectively. For the three-dimensional models, stress results are documented for several of the 16 circumferential planes.

The coordinates of the nodes which define the ends of the section cuts for the two-dimensional axisymmetric, three-dimensional bottom fine mesh, and three-dimensional top fine mesh models are provided in Tables 2.10.2-8 through 2.10.2-10, respectively. Tables 2.10.2-11 through 2.10.2-13 contain the node numbers and coordinates of all stress point locations on each section cut, for the three models.

Figure 2.10.2-1 ANSYS Two-Dimensional Finite Element Model - NAC-STC

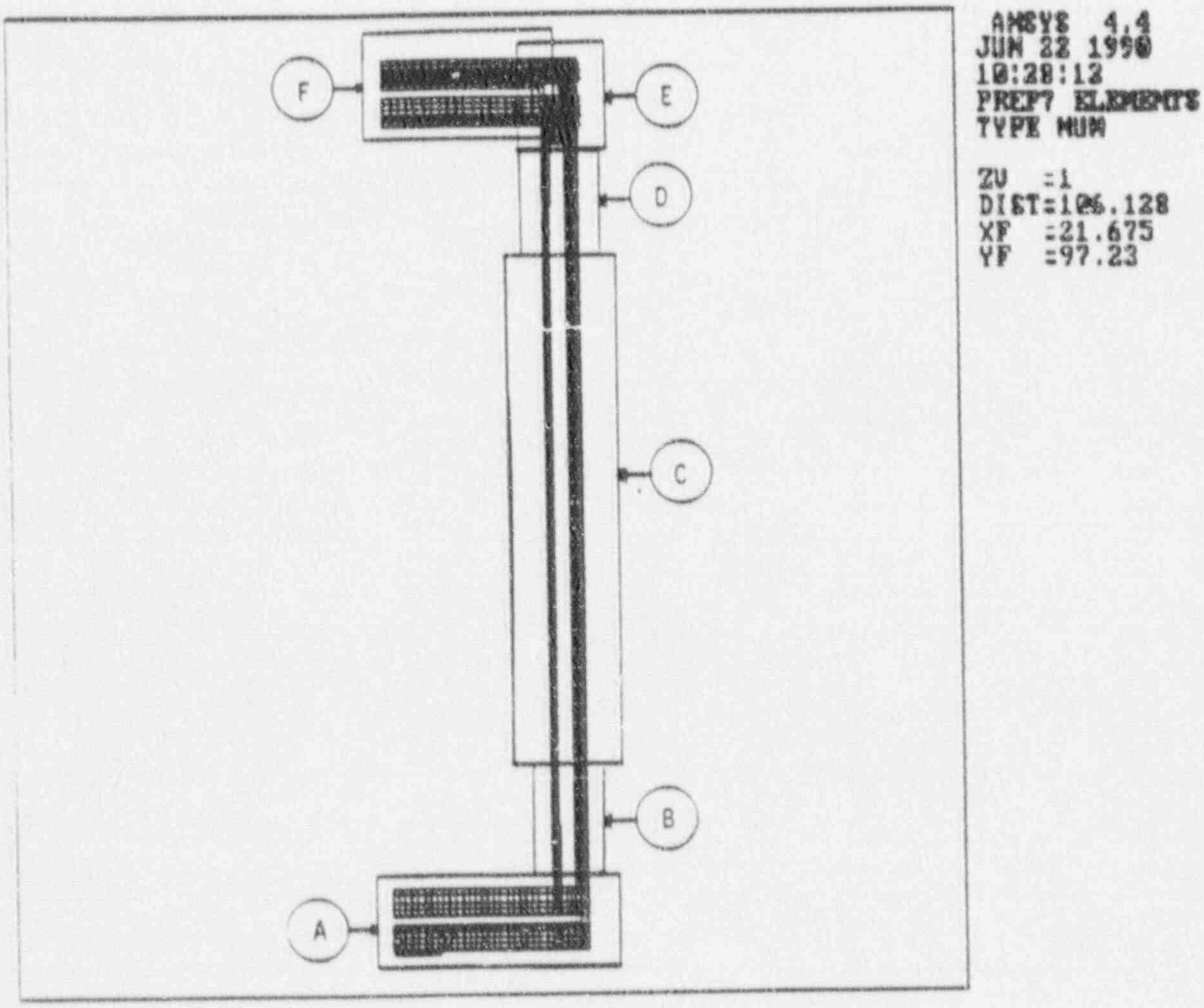

Figure 2.10.2-2 Cask Bottom (Region A) - NAC-STC ANSYS Two-Dimensional Model

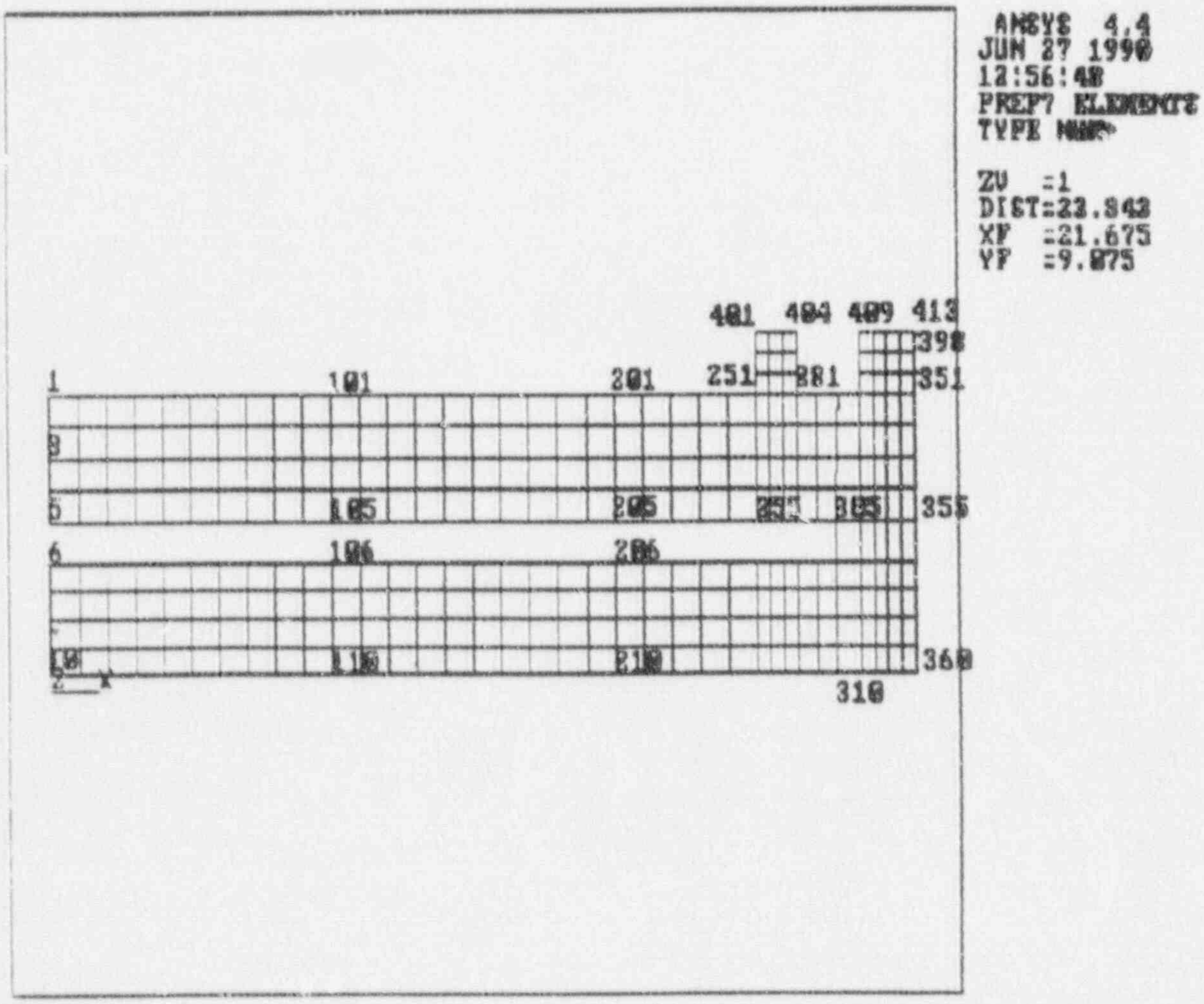

Figure 2.10.2-3 Cask Lower Transition (Region B) - NAC-STC ANSYS Two-Dimensional Model

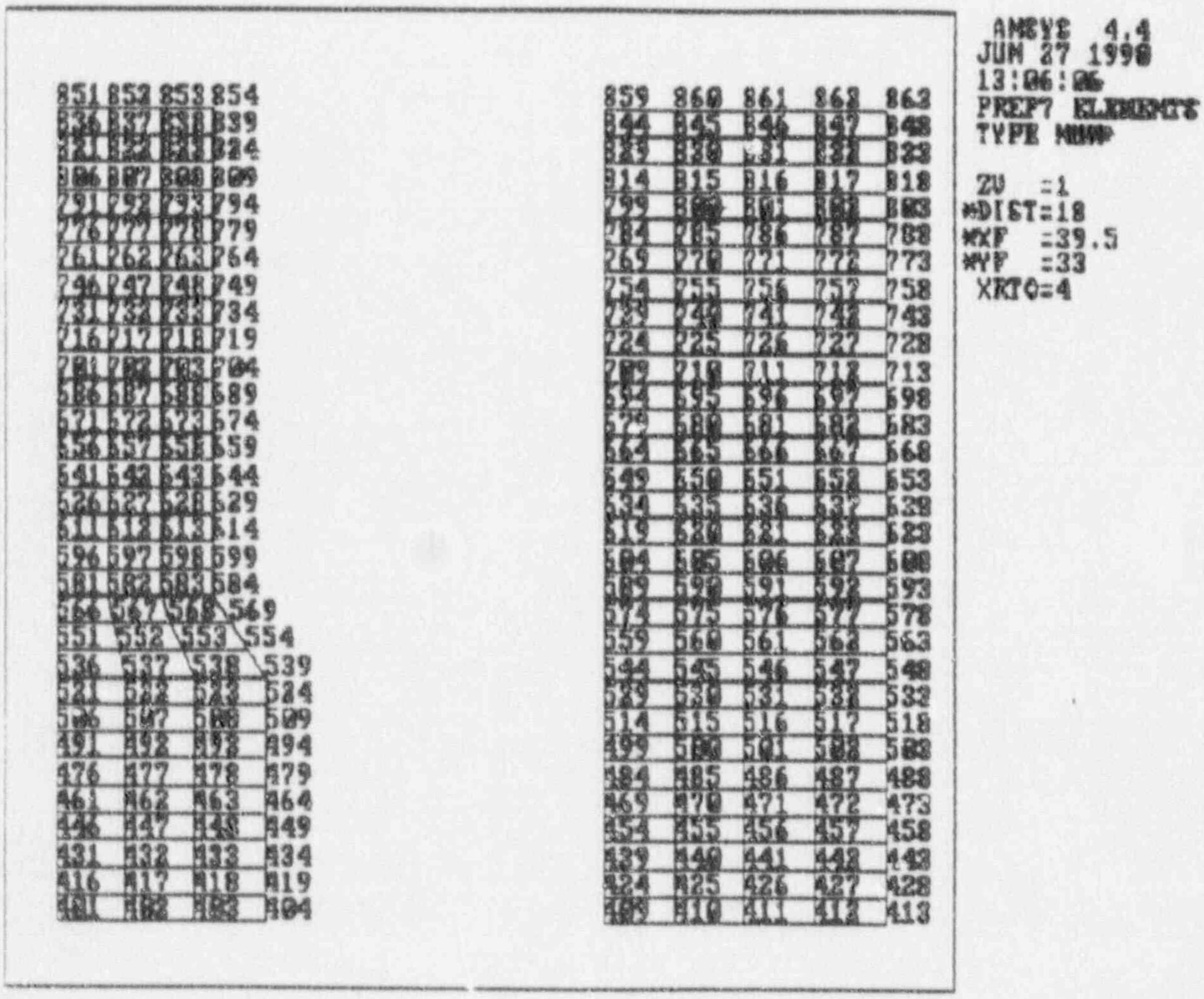

1

IMAGE EVALUATION TEST TARGET (MT-3)

150mm

6"

Figure 2.10.2-4 Cask Shells (Region C) - NAC-STC ANSYS Two-Dimensional Model

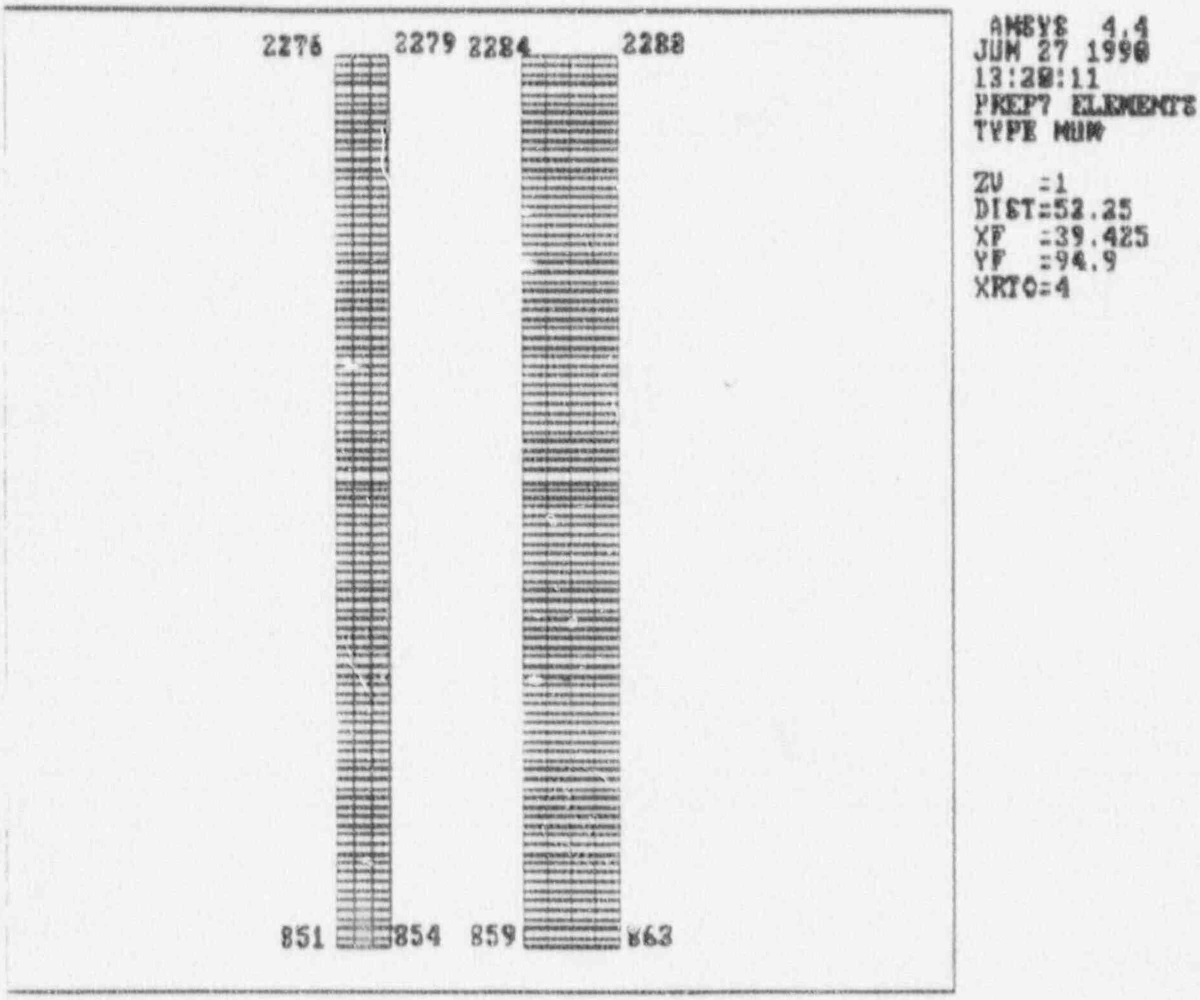

Figure 2.10.2-5 Cask Upper Transition (Region D) - NAC-STC ANSYS Two-Dimensional Model

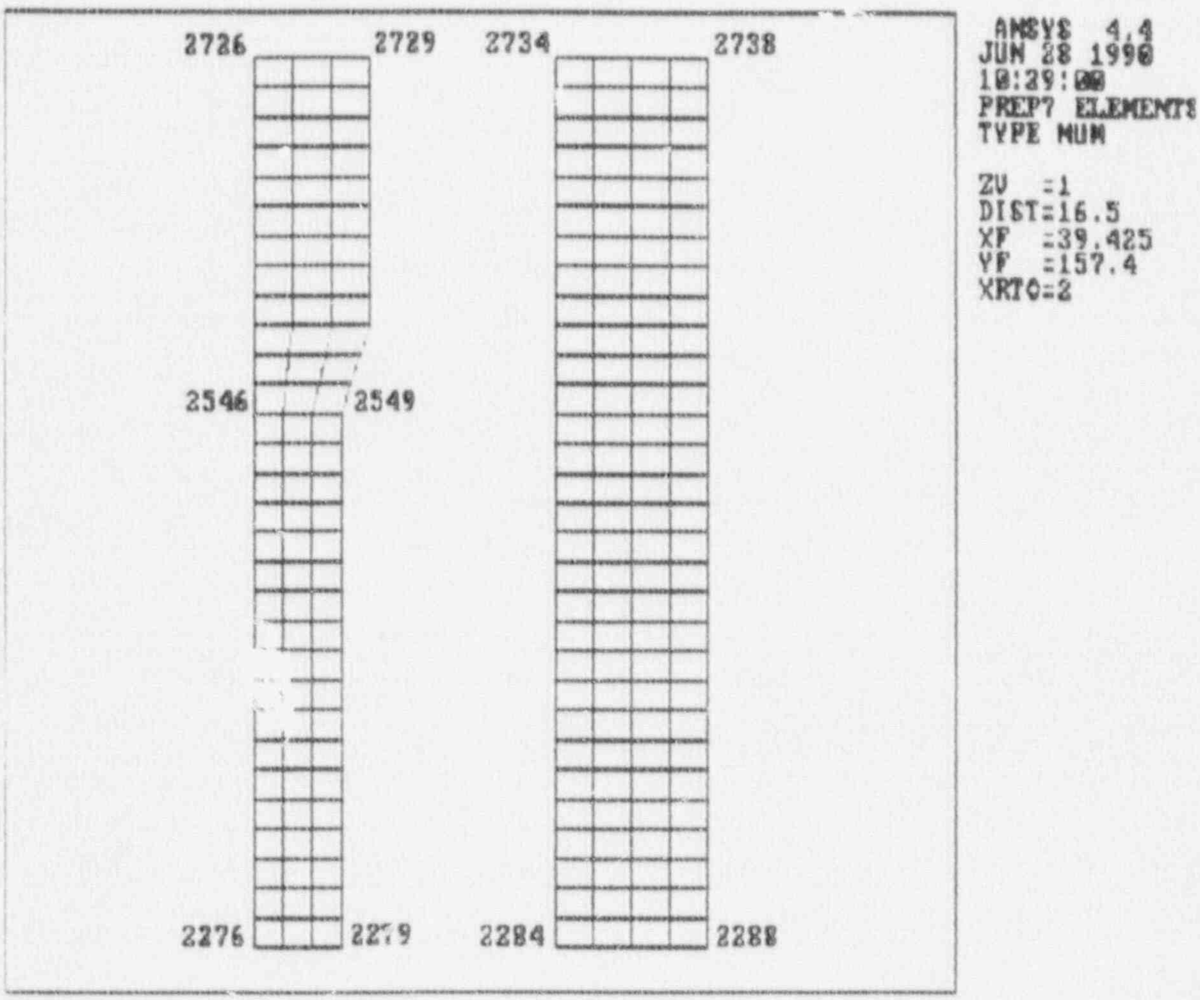

Figure 2.10.2-6 Cask Top Forging (Region E) - NAC-STC ANSYS Two-Dimensional Model

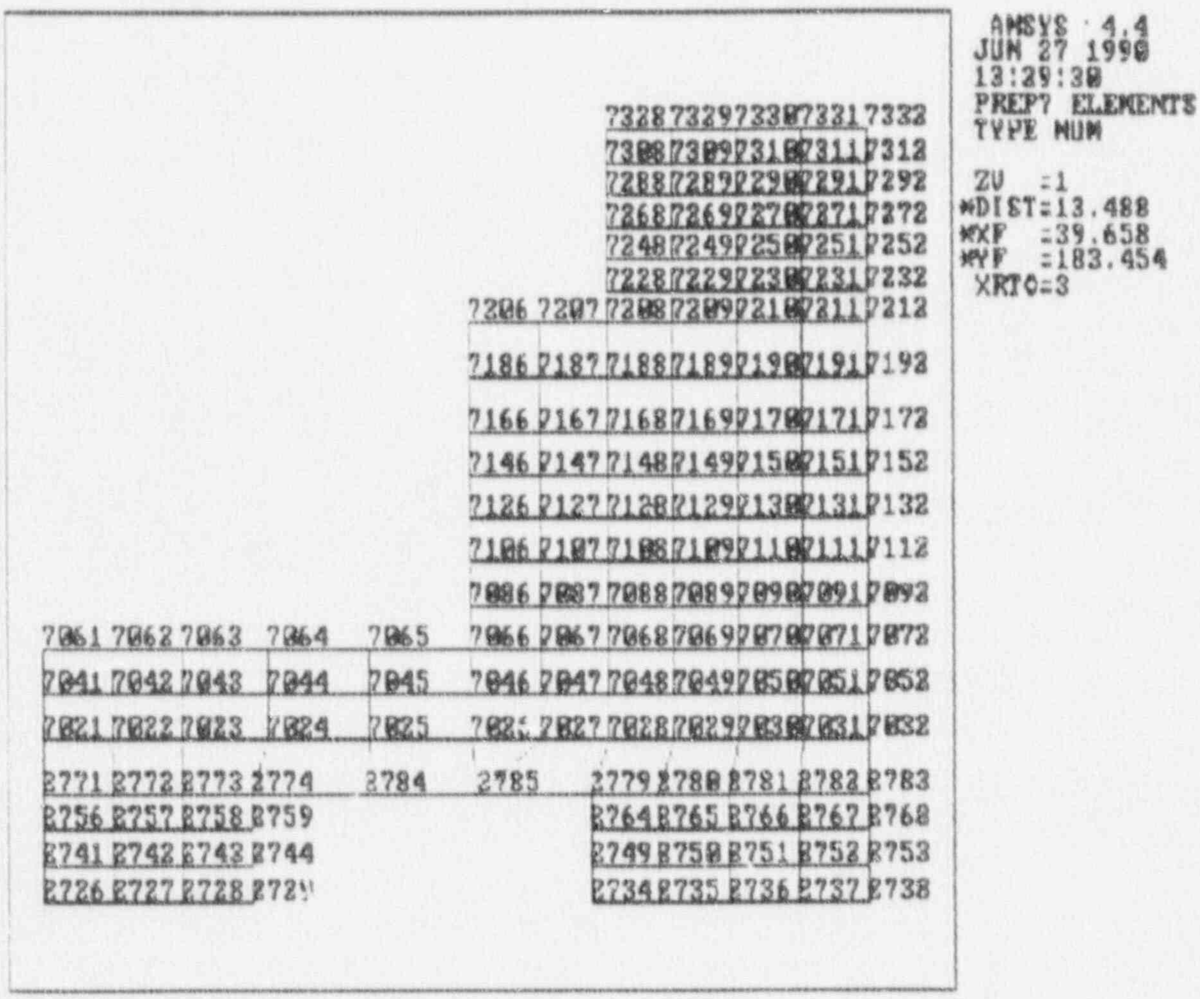

Figure 2.10.2-7 Cask Lids (Region F) - NAC-STC ANSYS Two-Dimensional Model

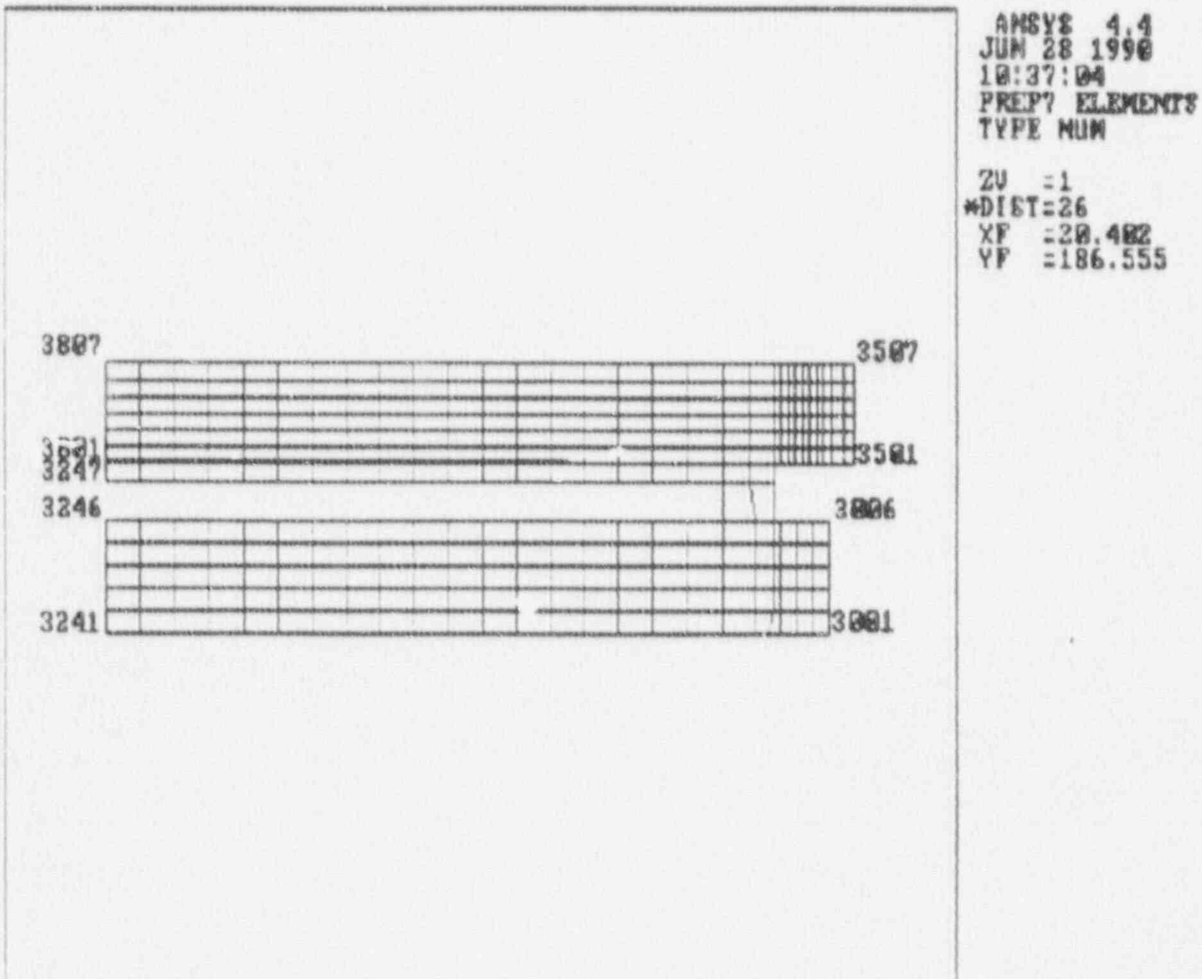

Figure 2.10.2-8 Circumferential Mesh Spacing (End View) - ANSYS Three-Dimensional Top and Bottom Fine Mesh Models

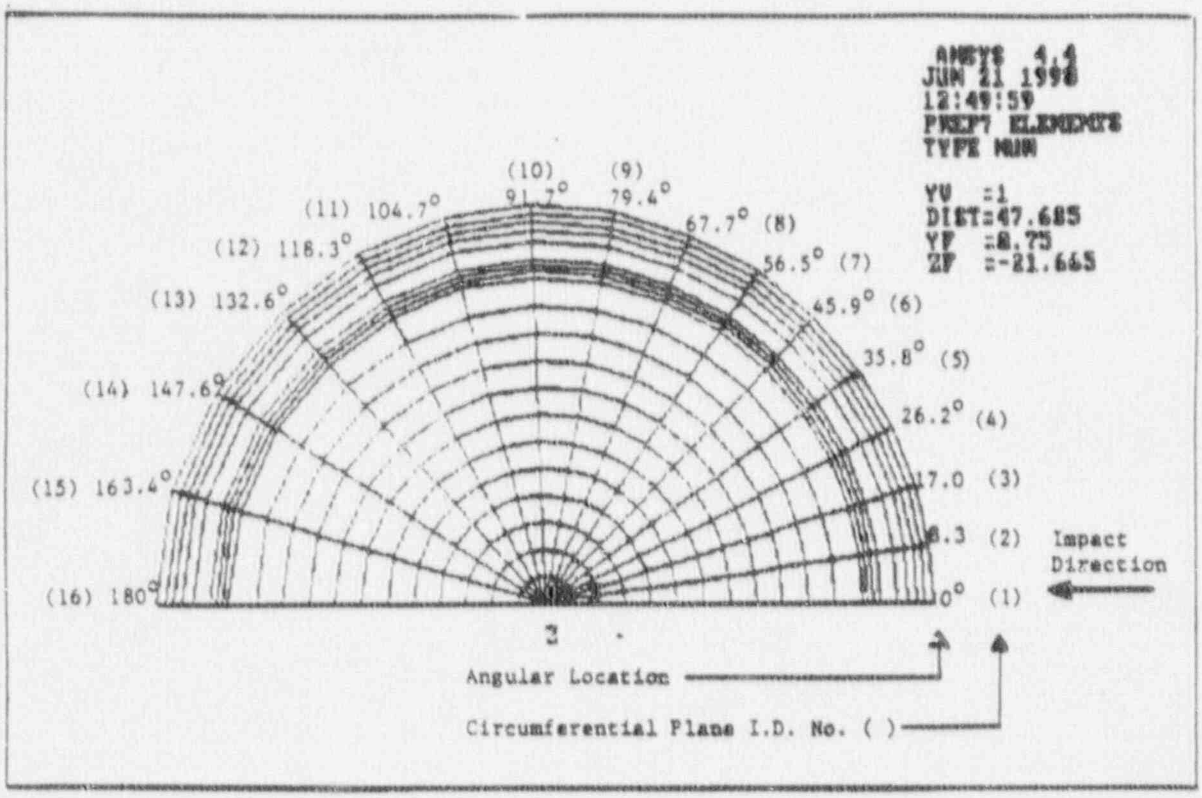

Figure 2.10.2-9 ANSYS Three-Dimensional Bottom Fine Mesh Finite Element Model - NAC-STC

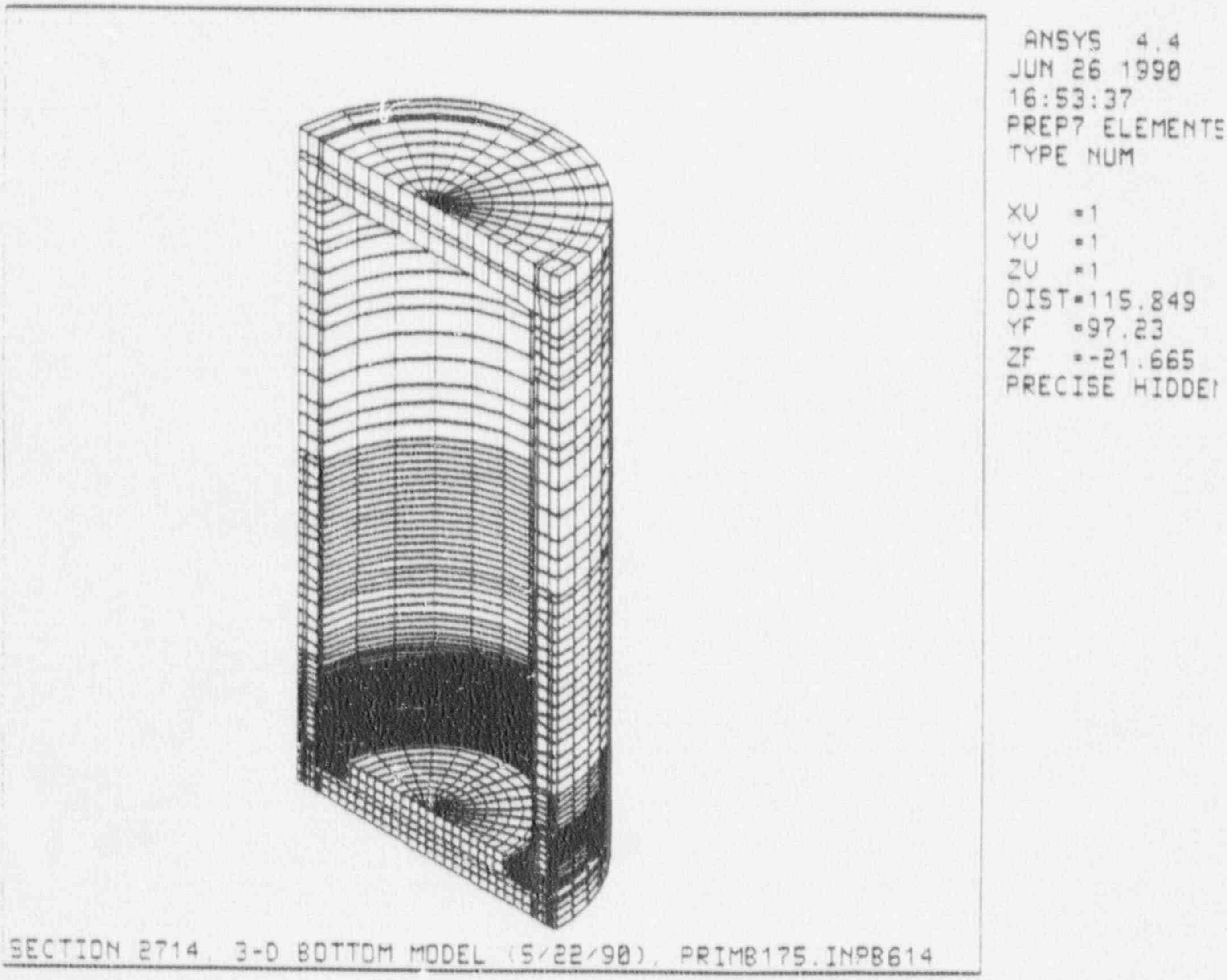

Figure 2.10.2-10 Details - NAC-STC ANSYS Three-Dimensional Bottom Fine Mesh Model

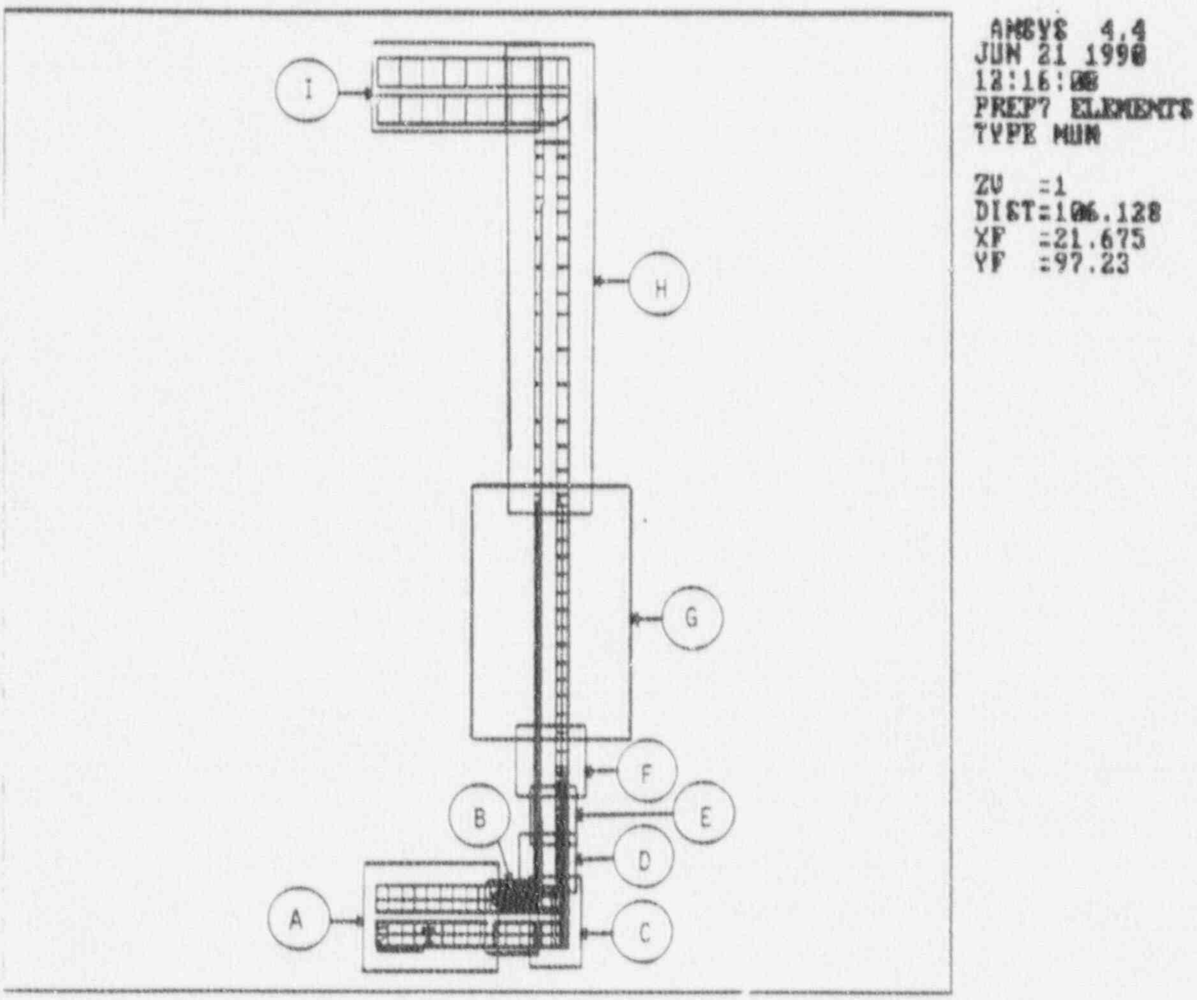

Figure 2.10.2-11 Cask Bottom (Region A) - NAC-STC ANSYS Bottom Fine Mesh Three-Dimensional Model

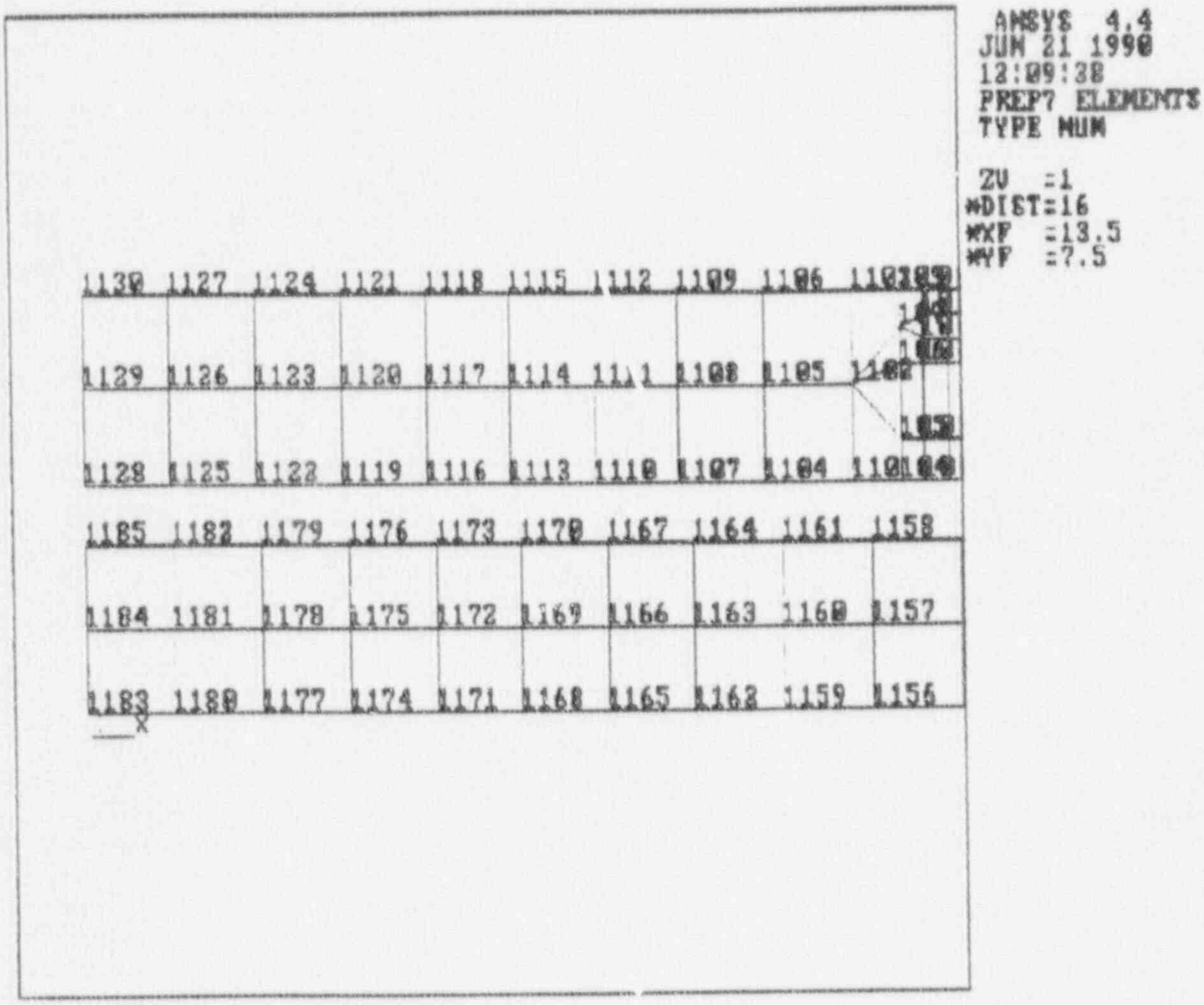

Figure 2.10.2-12 Cask Bottom (Region B) - NAC-STC ANSYS Bottom Fine Mesh Three-Dimensional Model

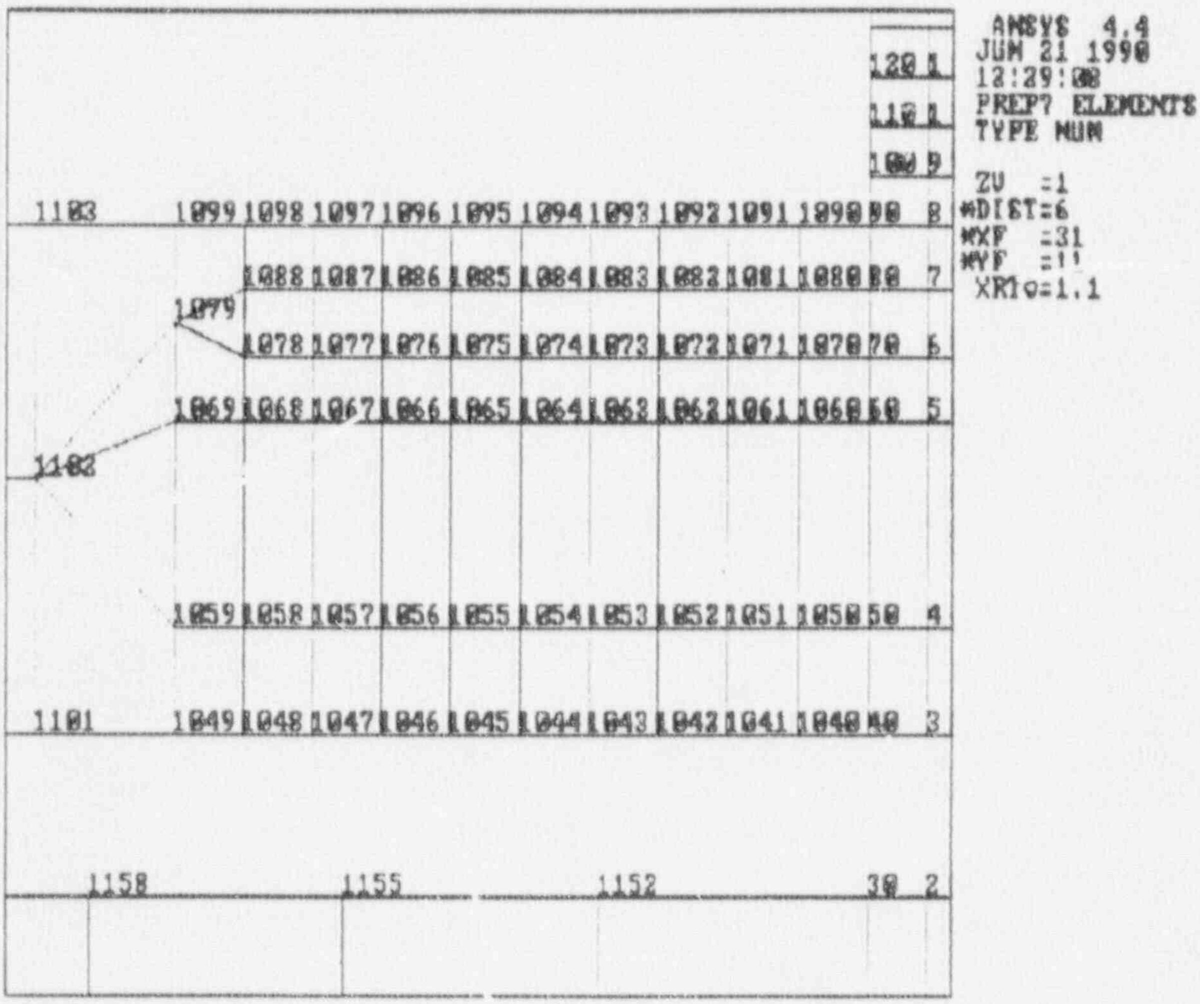

Figure 2.10.2-13 Cask Bottom (Region C) - NAC-STC ANSYS Bottom Fine Mesh Three-Dimensional Model

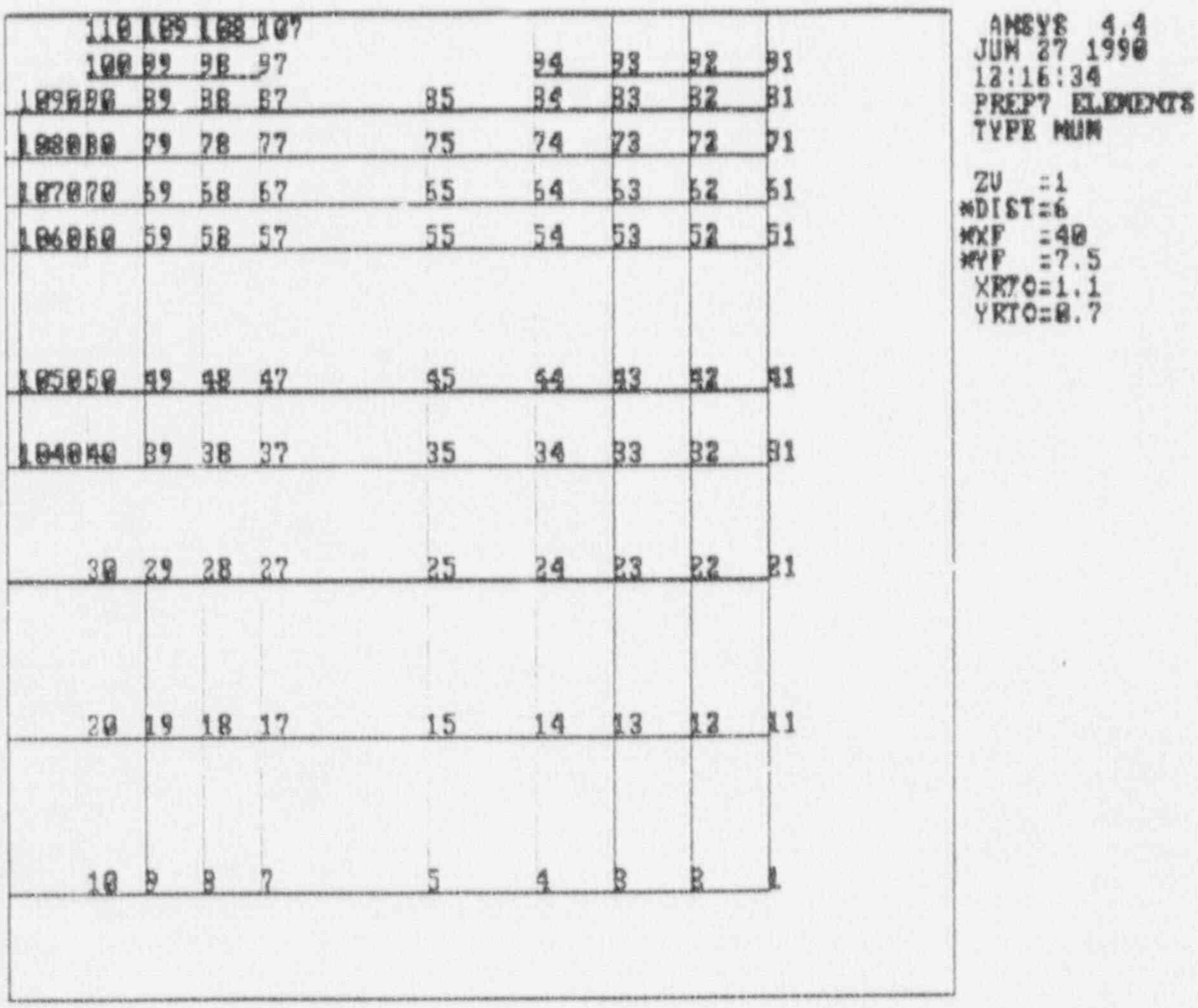

Figure 2.10.2-14 Cask Lower Transition (Region D) - NAC-STC ANSYS Bottom Fine Mesh Three-Dimensional Model

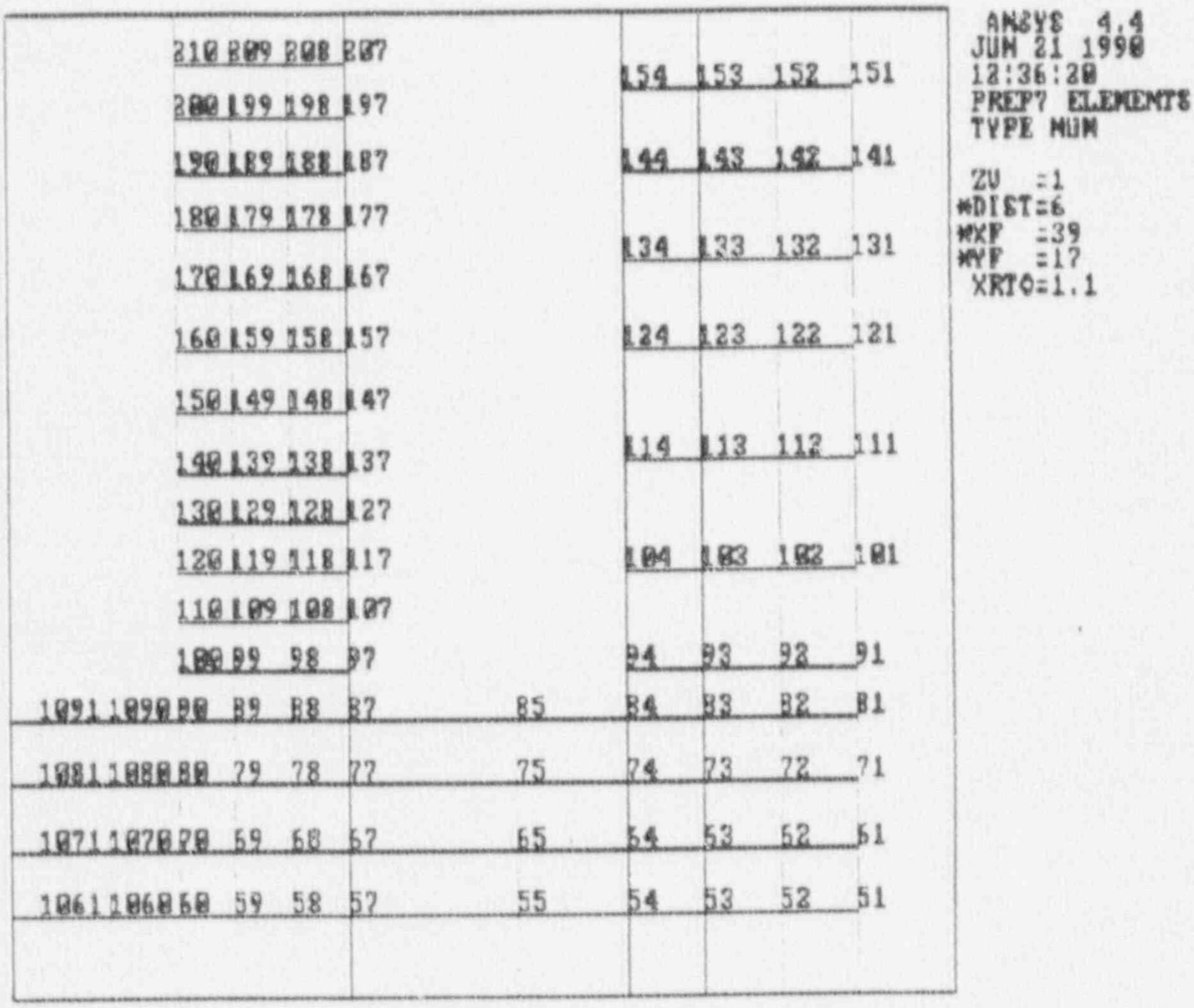

Figure 2.10.2-15 Cask Lower Transition (Region E) - NAC-STC ANSYS Bottom Fine Mesh Three-Dimensional Model

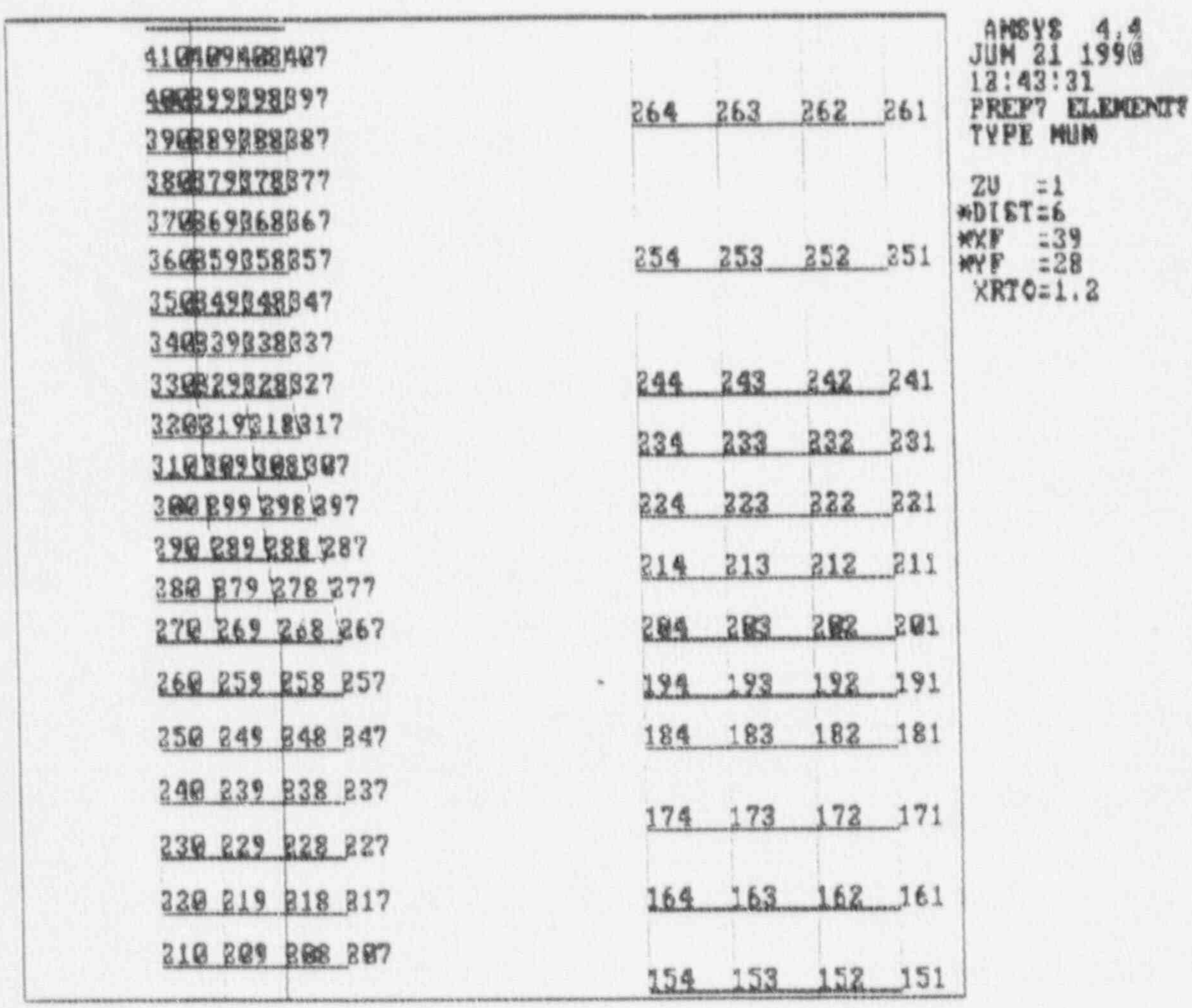

Figure 2.10.2-16 Cask Lower Shell (Region F) - NAC-STC ANSYS Bottom Fine Mesh Three-Dimensional Model

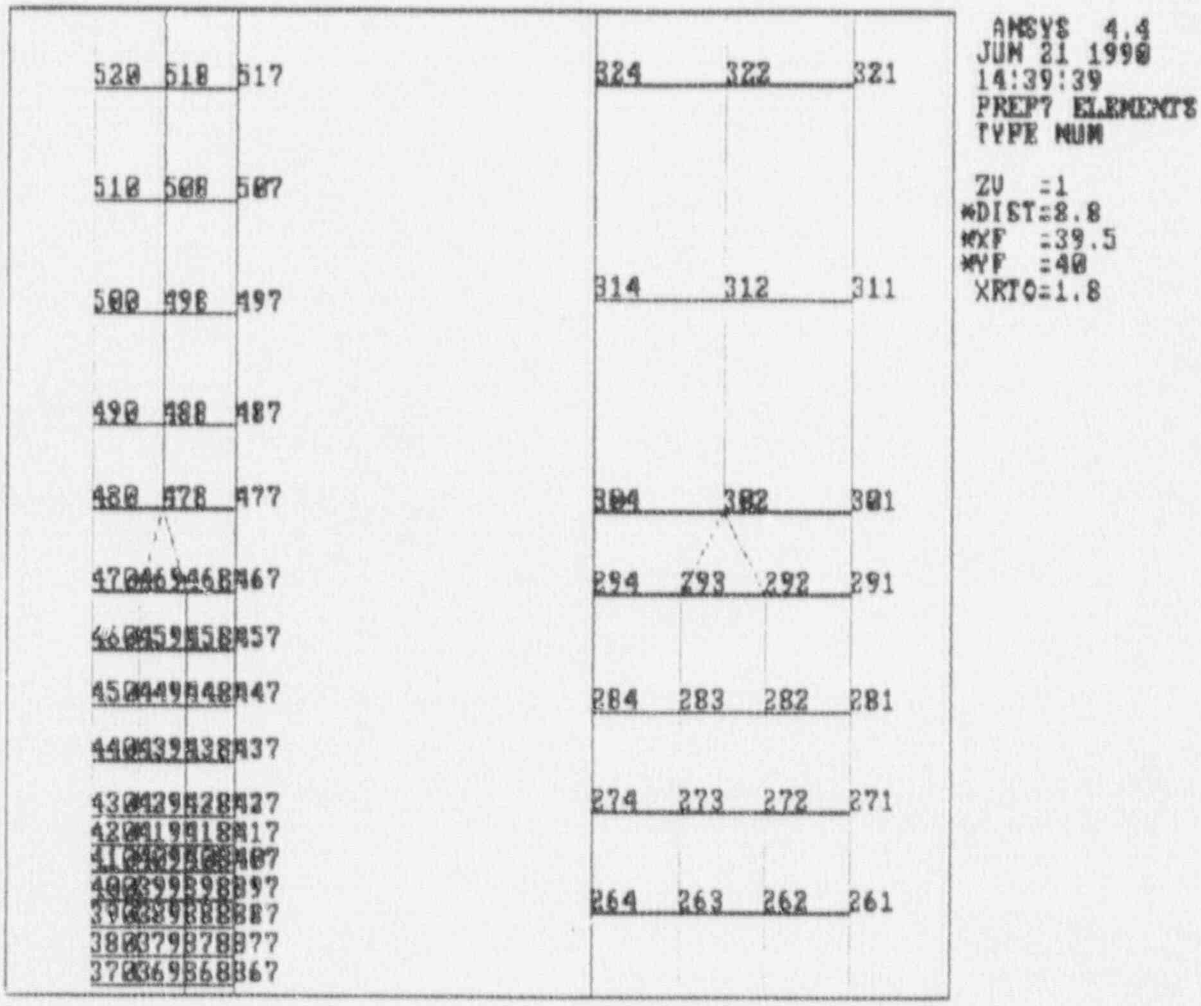

Figure 2.10.2-17 Cask Lower Shell (Region G) - NAC-STC ANSYS Bottom Fine Mesh Three-Dimensional Model

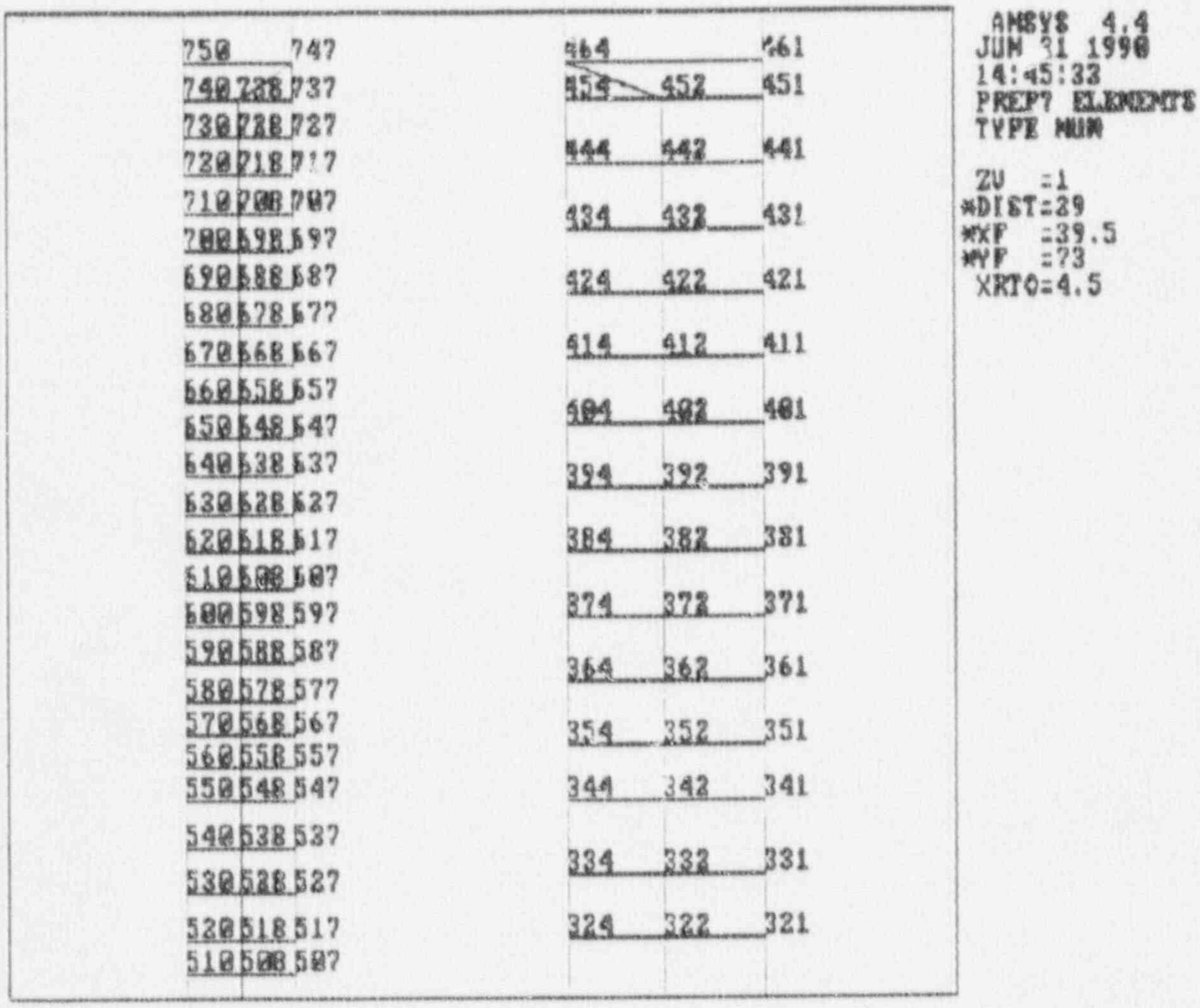

Figure 2.10.2-18 Cask Upper Shell (Region H) - NAC-STC ANSYS Bottom Fine Mesh Three-Dimensional Model

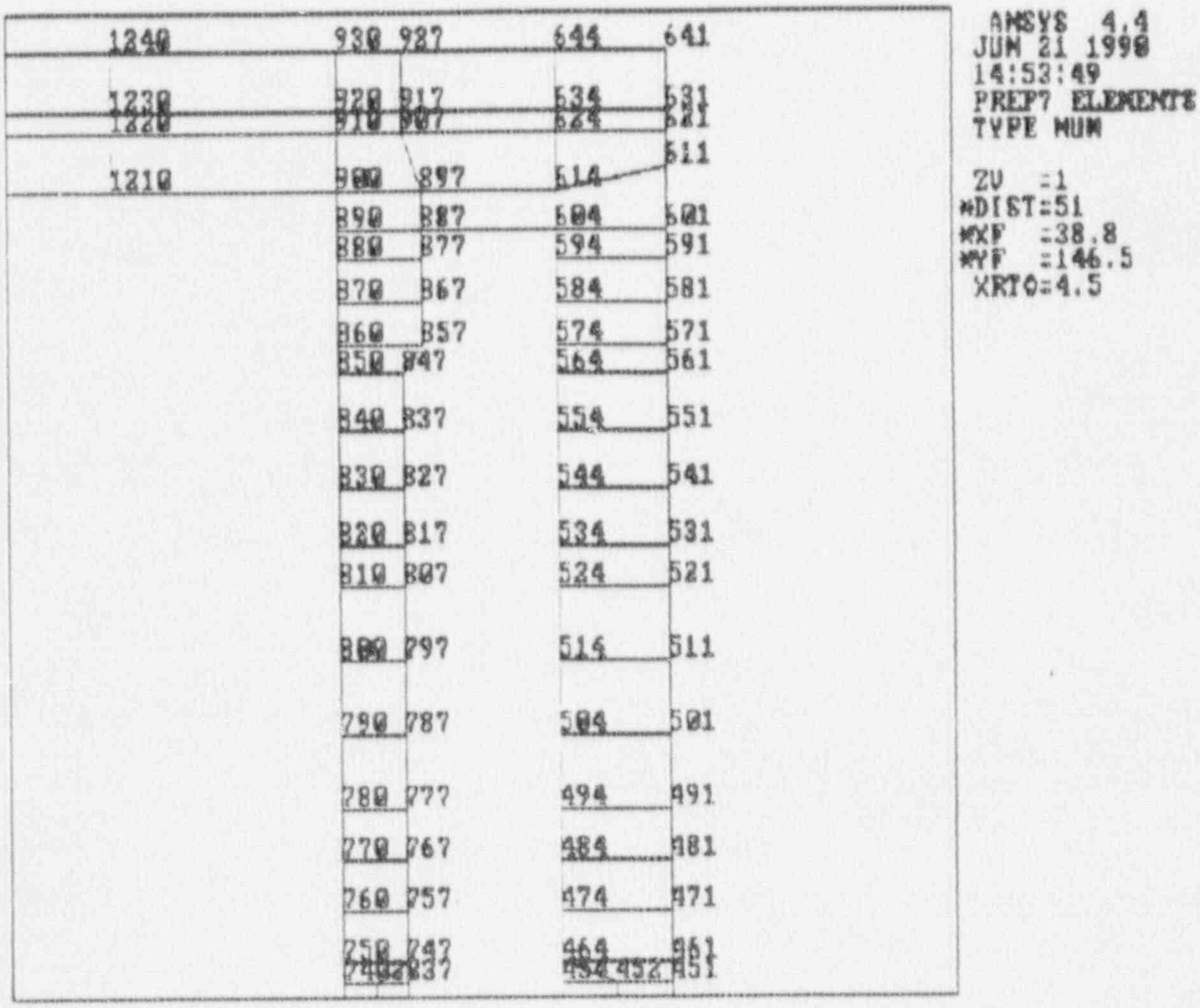

Figure 2.10.2-19 Cask Lids (Region I) - NAC-STC ANSYS Bottom Fine Mesh Three-Dimensional Model

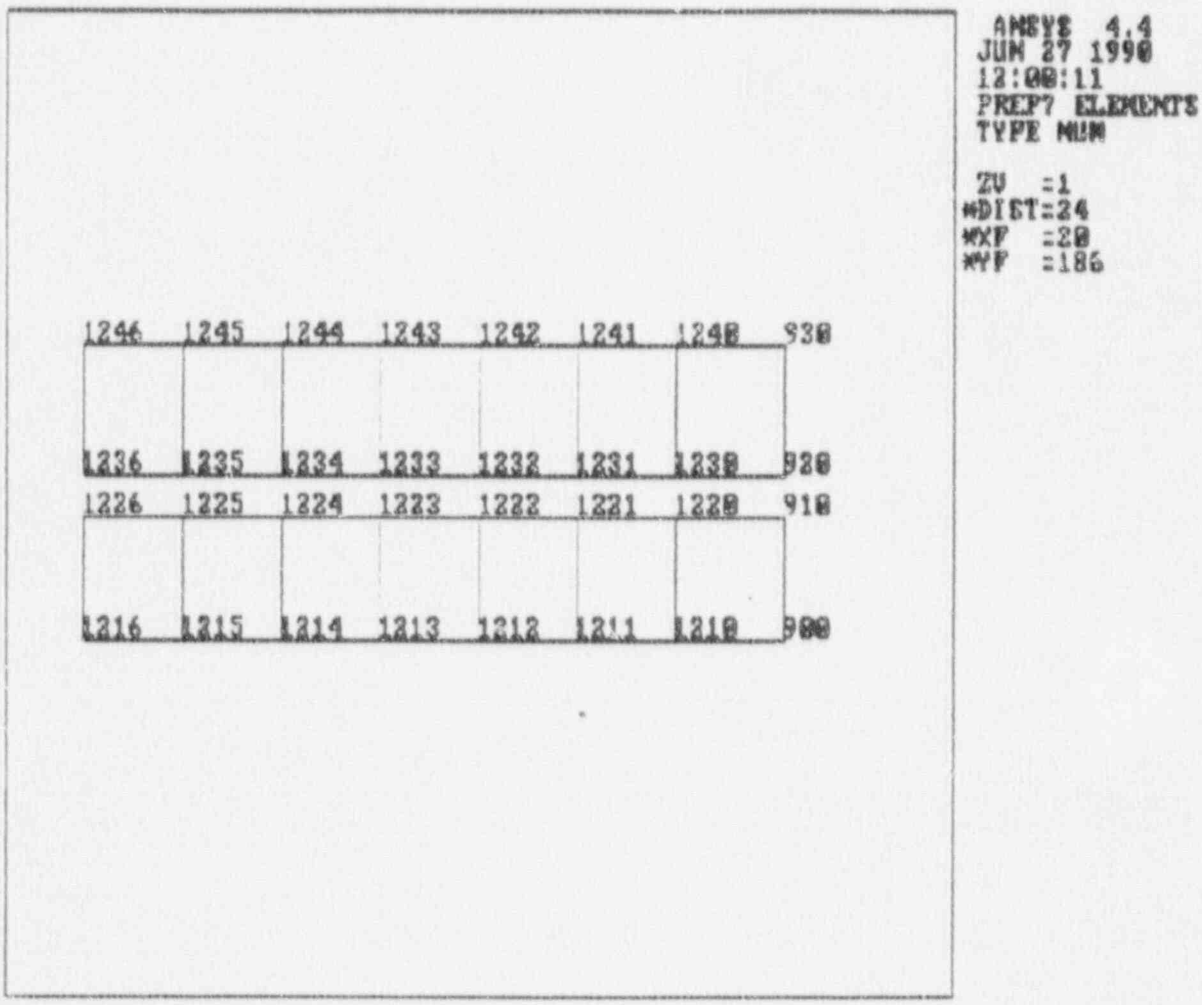

Figure 2.10.2-20 ANSYS Three-Dimensional Top Fine Mesh Finite Element Model - NAC-STC

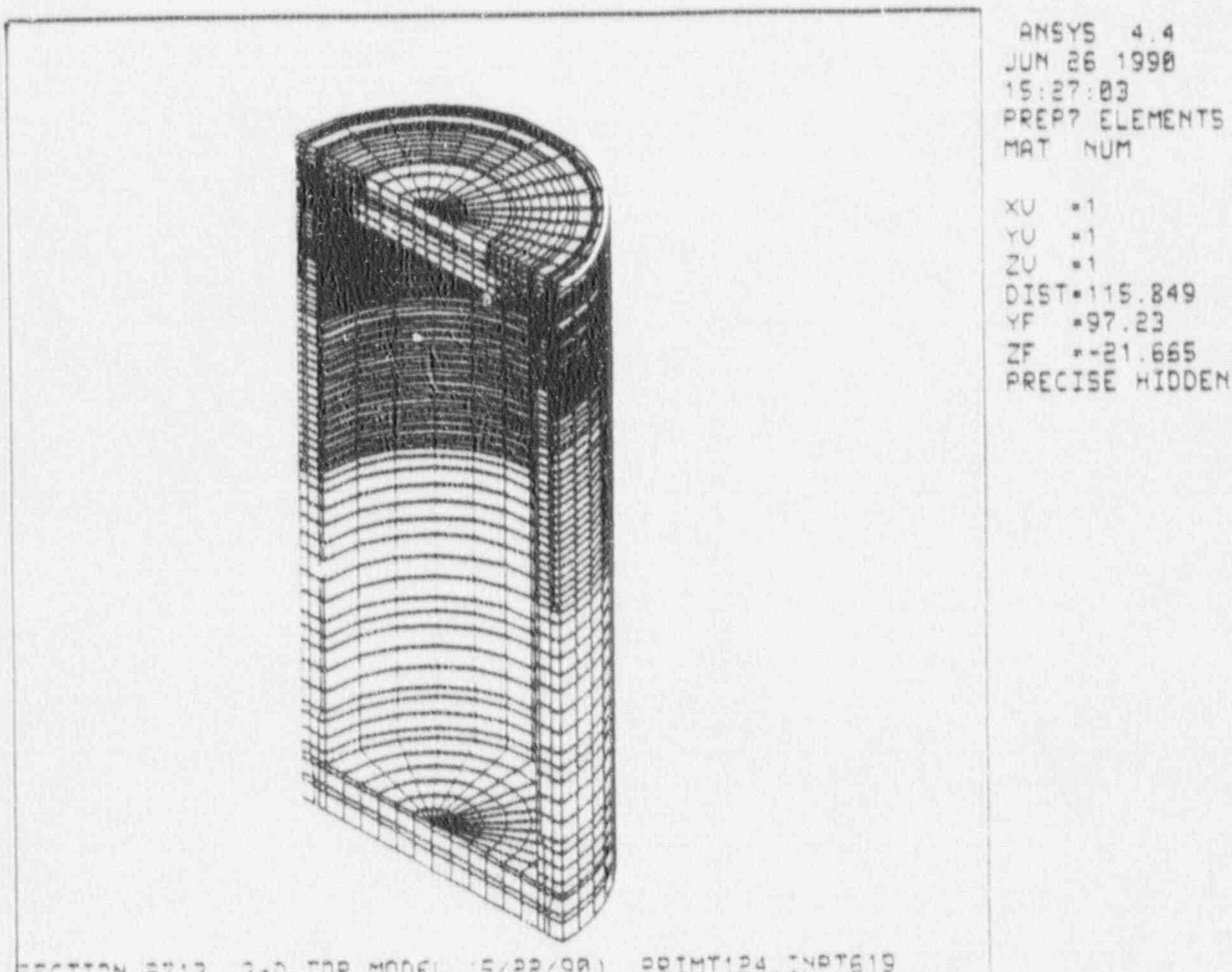

Figure 2.10.2-21 Upper Half of NAC-STC ANSYS Three-Dimensional Top Fine Mesh Finite Element Model

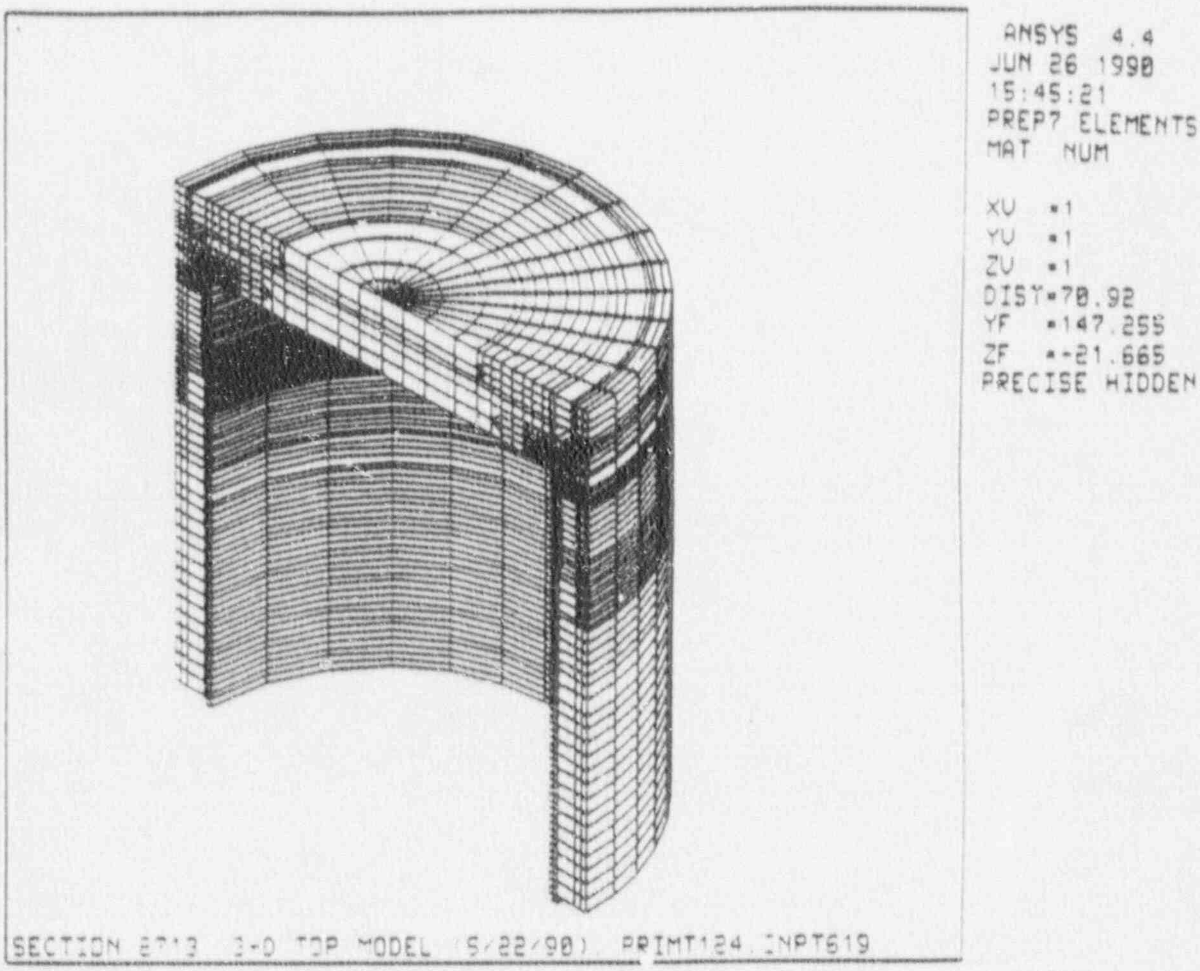

Figure 2.10.2-22 Details - NAC-STC ANSYS Three-Dimensional Top Fine Mesh Model

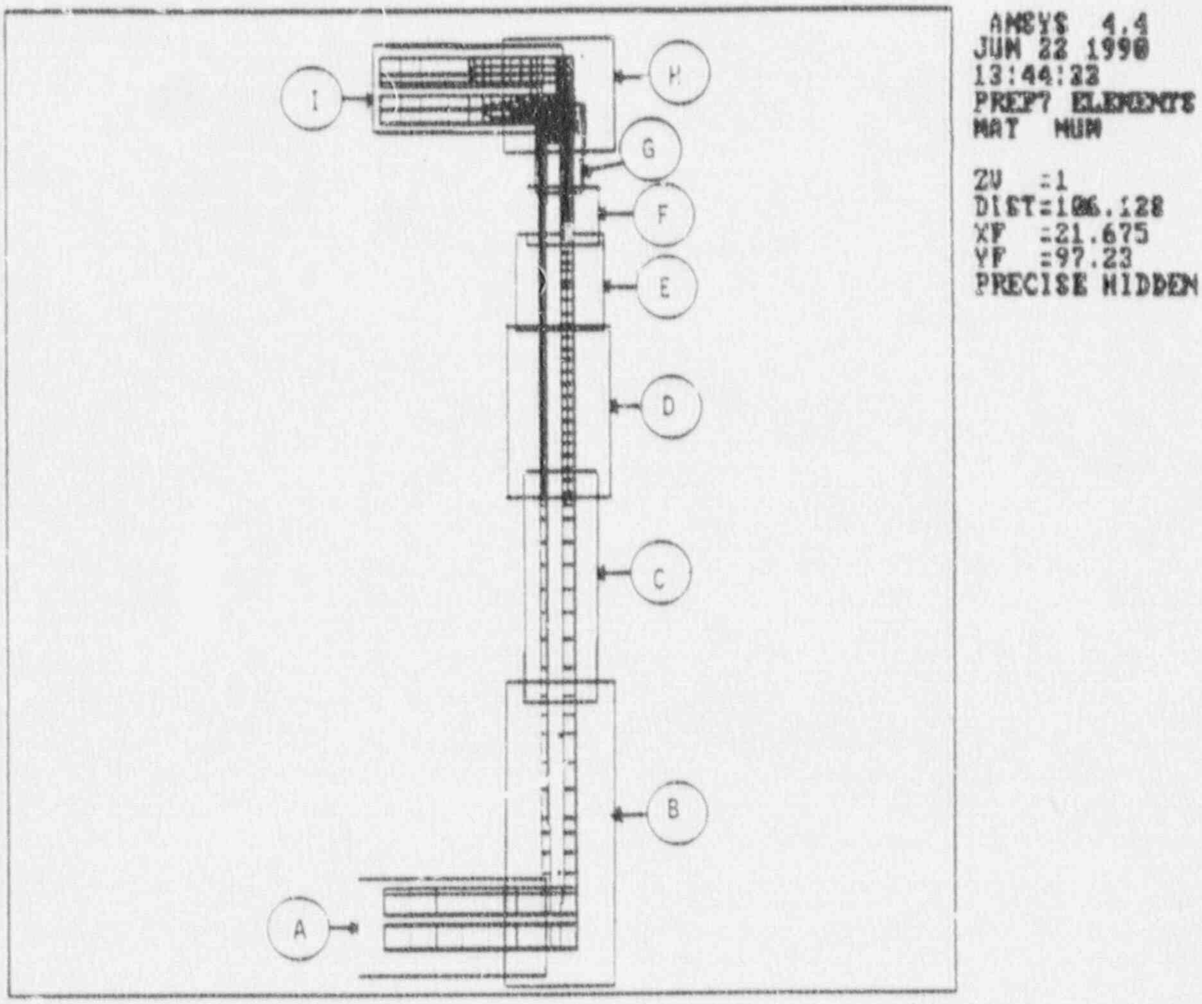

Figure 2.10.2-22 Details - NAC-STC ANSYS Three-Dimensional Top Fine Mesh Model

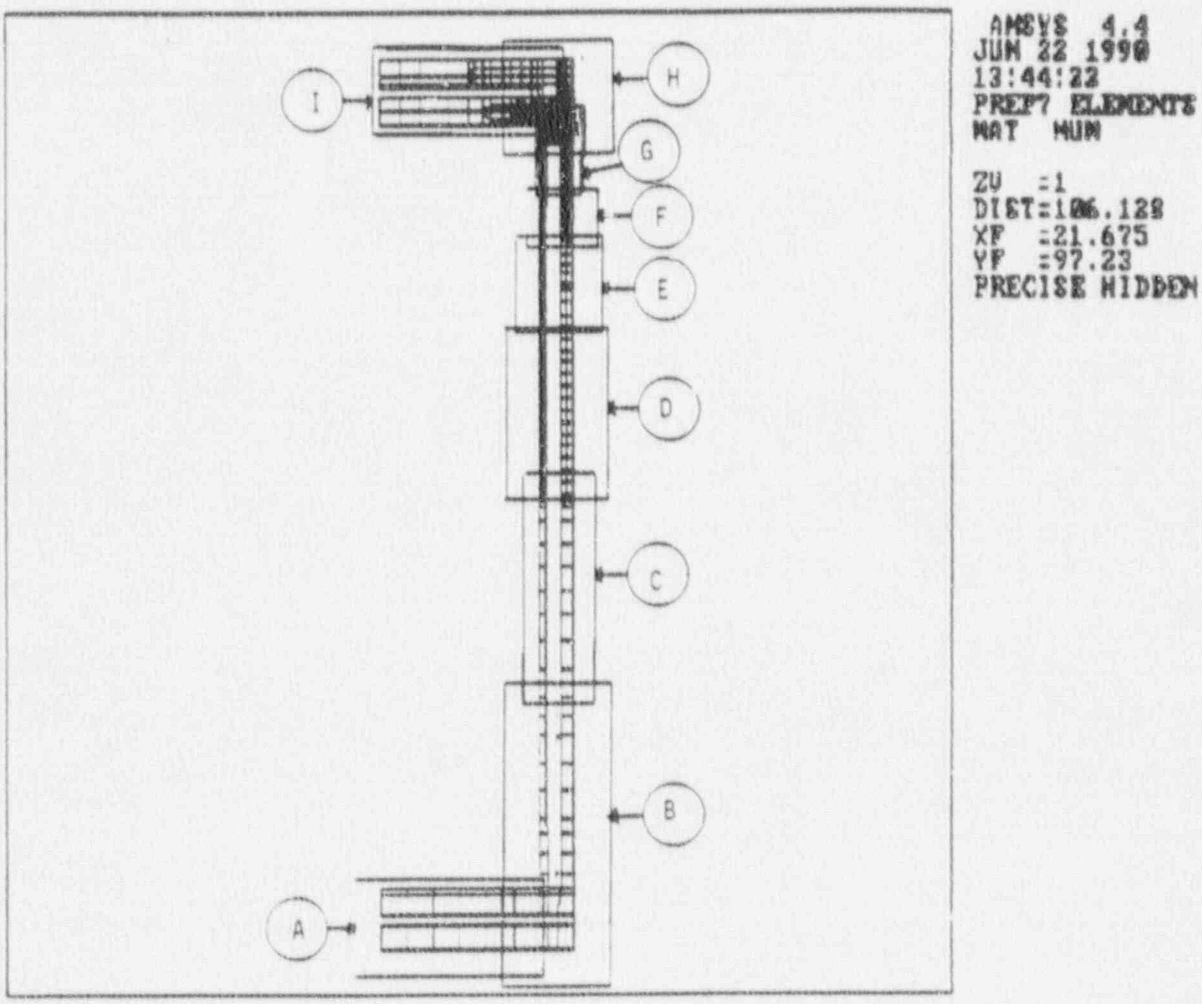

Figure 2.10.2-23 Cask Bottom (Region A) - NAC-STC ANSYS Top Fine Mesh Three-Dimensional Model

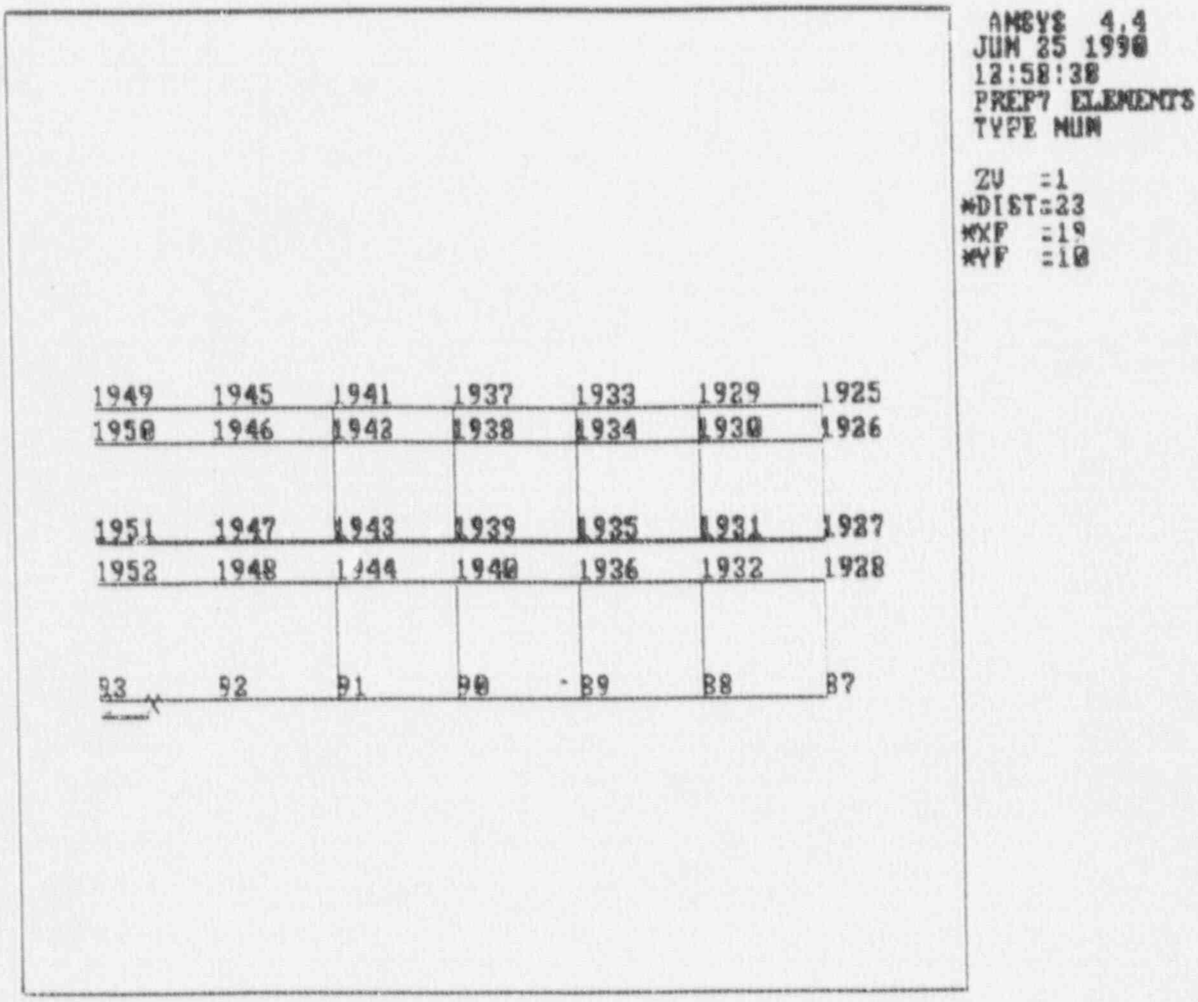

Figure 2.10.2-24 Cask Lower Transition (Region B) - NAC-STC ANSYS Top Fine Mesh Three-Dimensional Model

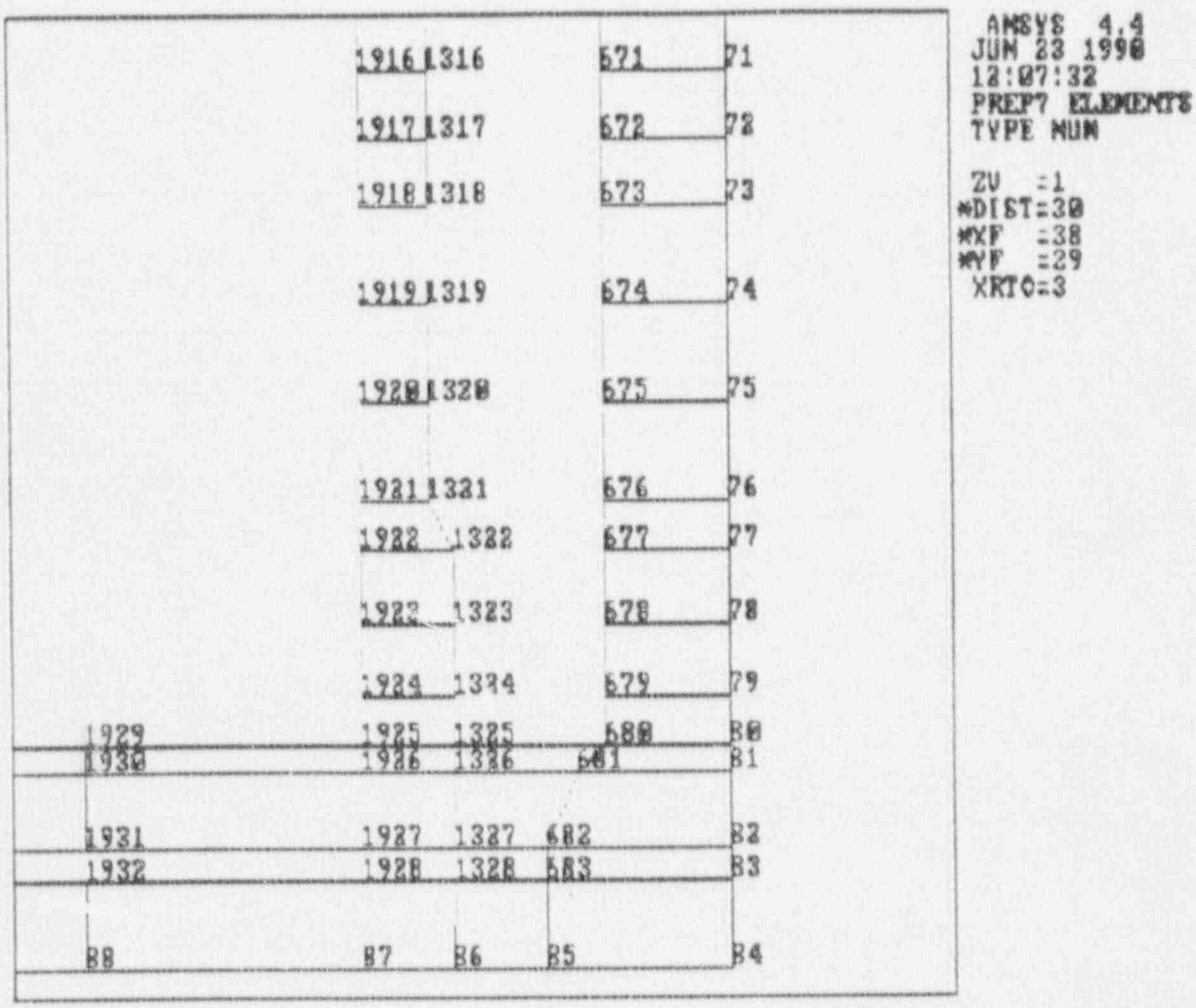

Figure 2.10.2-25 Cask Lower Shell (Region C) - NAC-STC ANSYS Top Fine Mesh Three-Dimensional Model

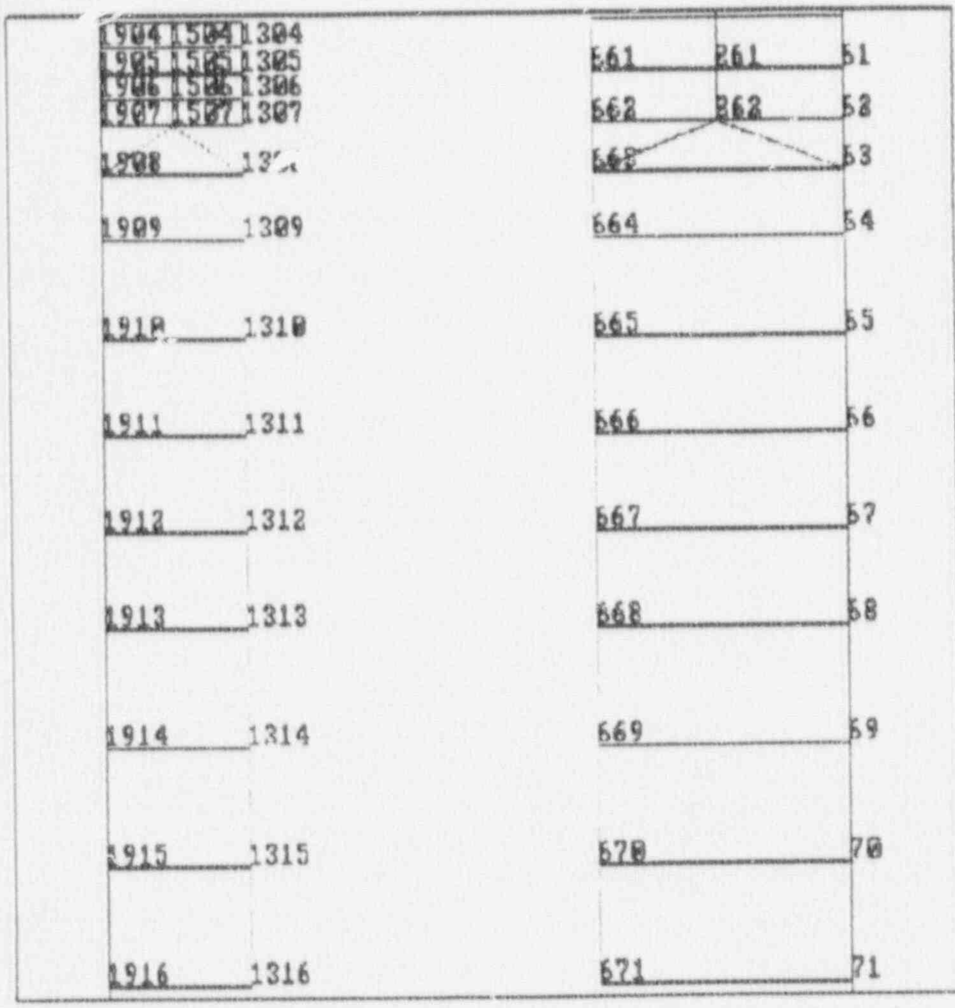

Figure 2.10.2-26 Cask Middle Shell (Region D) - NAC-STC ANSYS Top Fine Mesh Three-Dimensional Model

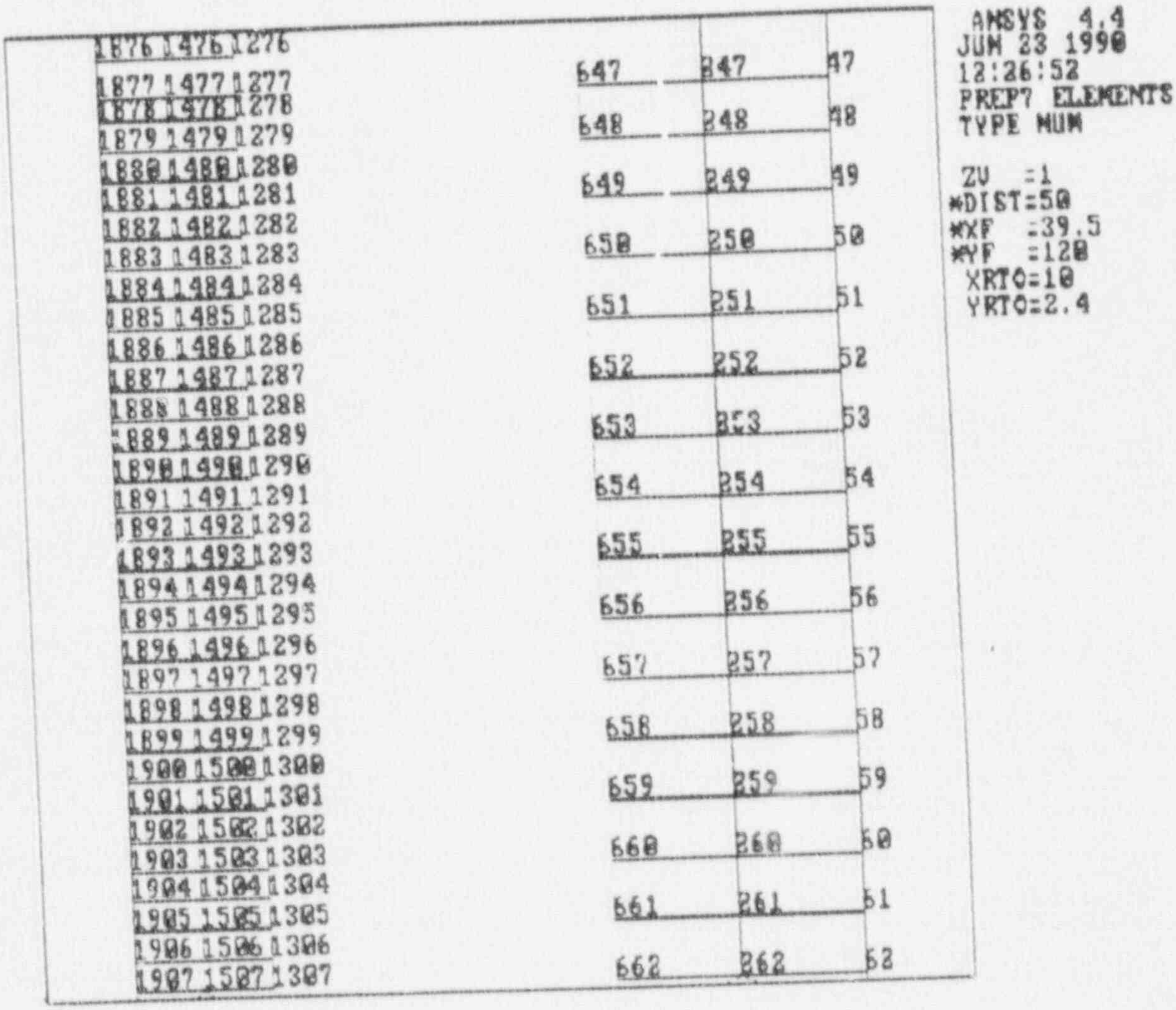

Figure 2.10.2-27 Cask Upper Shell (Region E) - NAC-STC ANSYS Top Fine Mesh Three-Dimensional Model

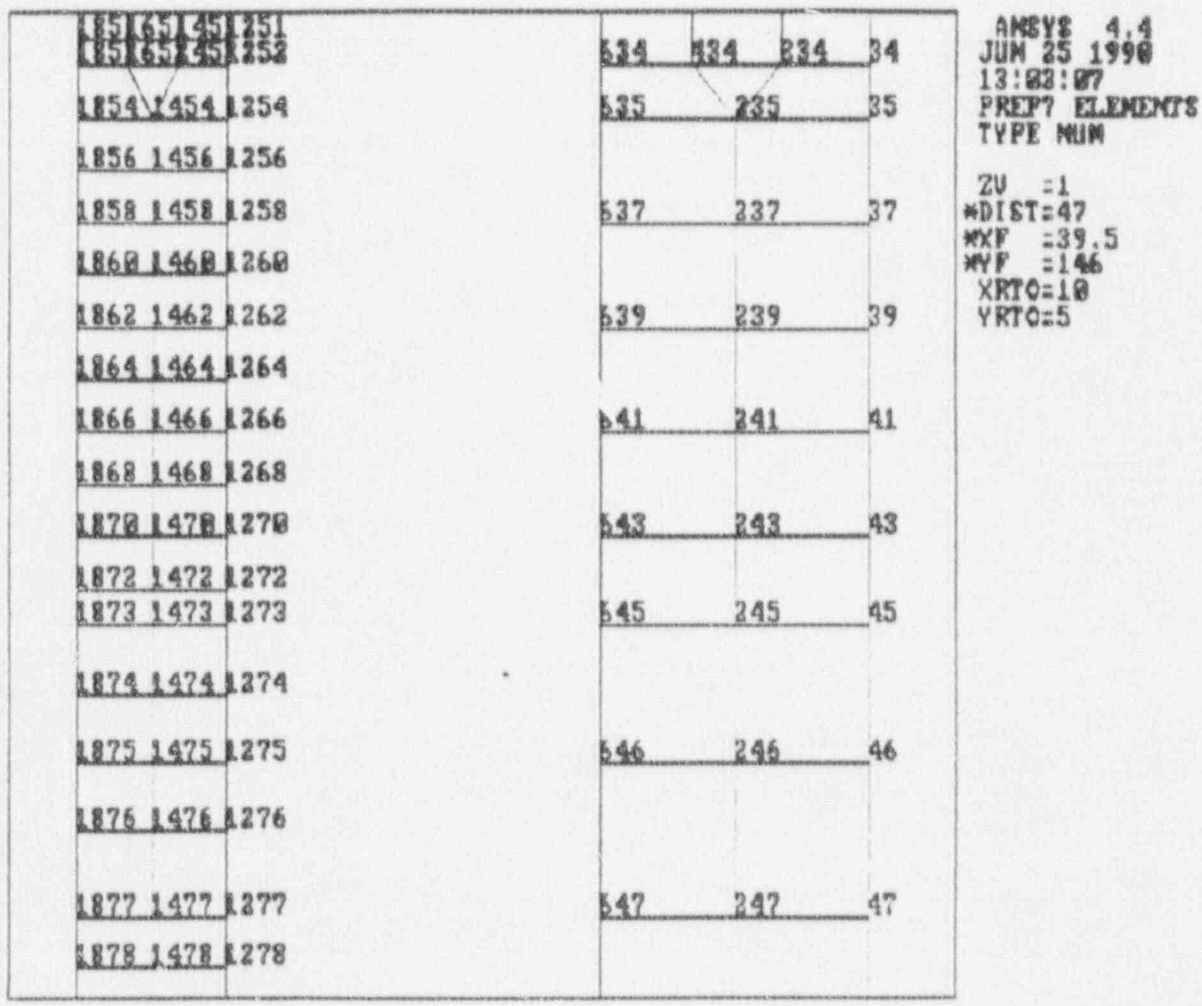

Figure 2.10.2-28 Cask Upper Transition (Region F) - NAC-STC ANSYS Top Fine Mesh Three-Dimensional Model

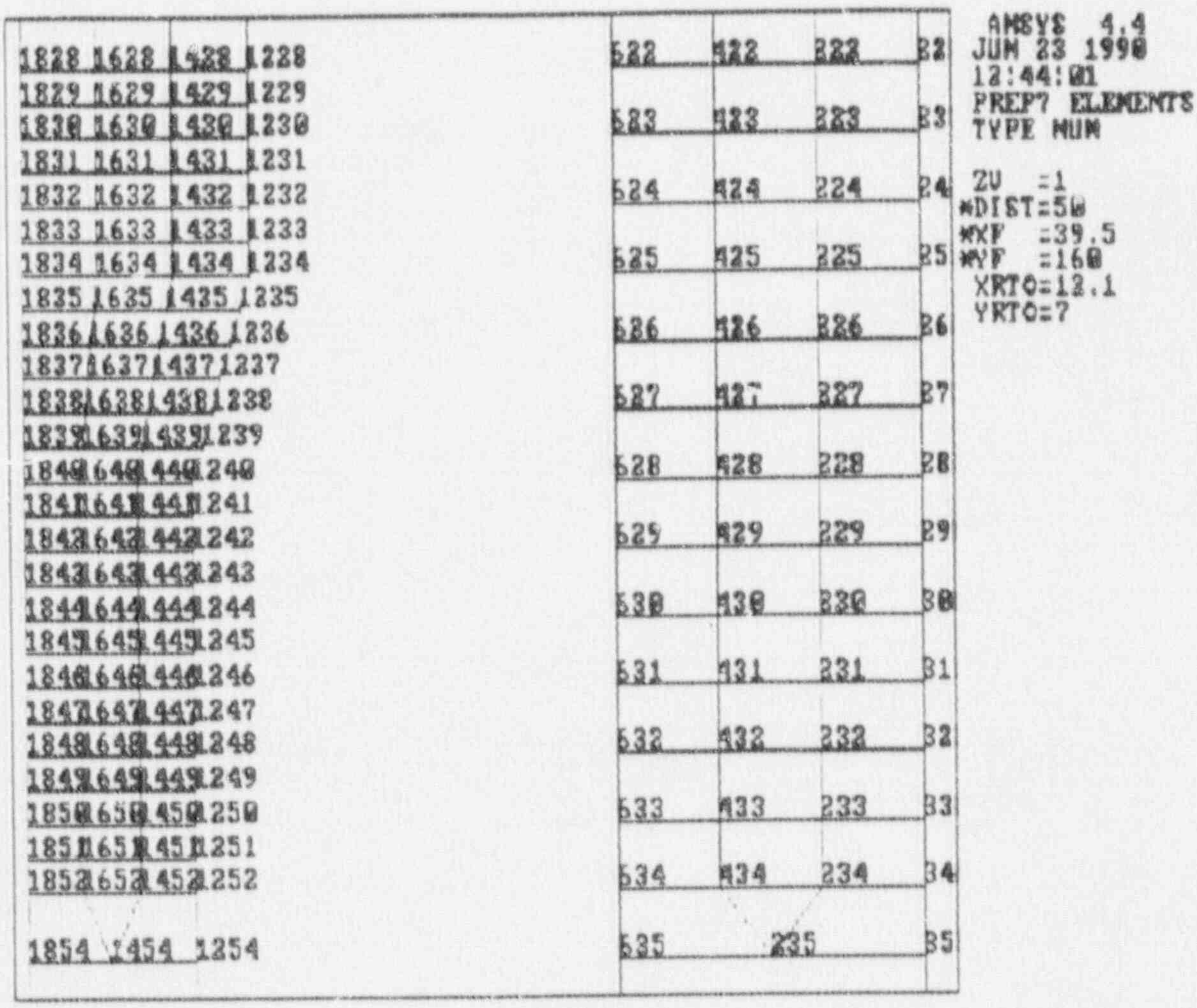

Figure 2.10.2-29 Cask Upper Transition (Region G) - NAC-STC ANSYS Top Fine Mesh Three-Dimensional Model

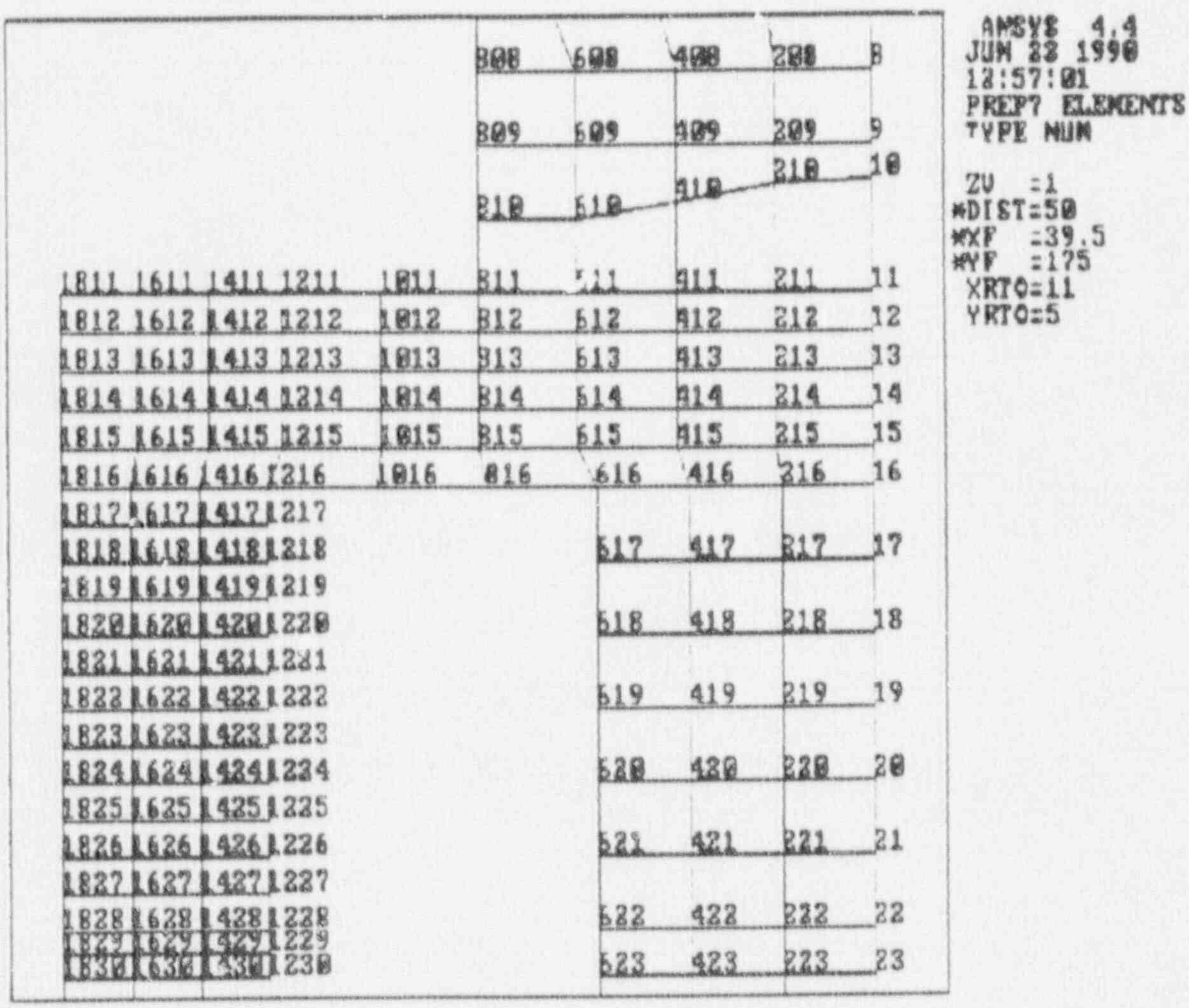

Figure 2.10.2-30 Cask Top Forging (Region H) - NAC-STC ANSYS Top Fine Mesh Three-Dimensional Model

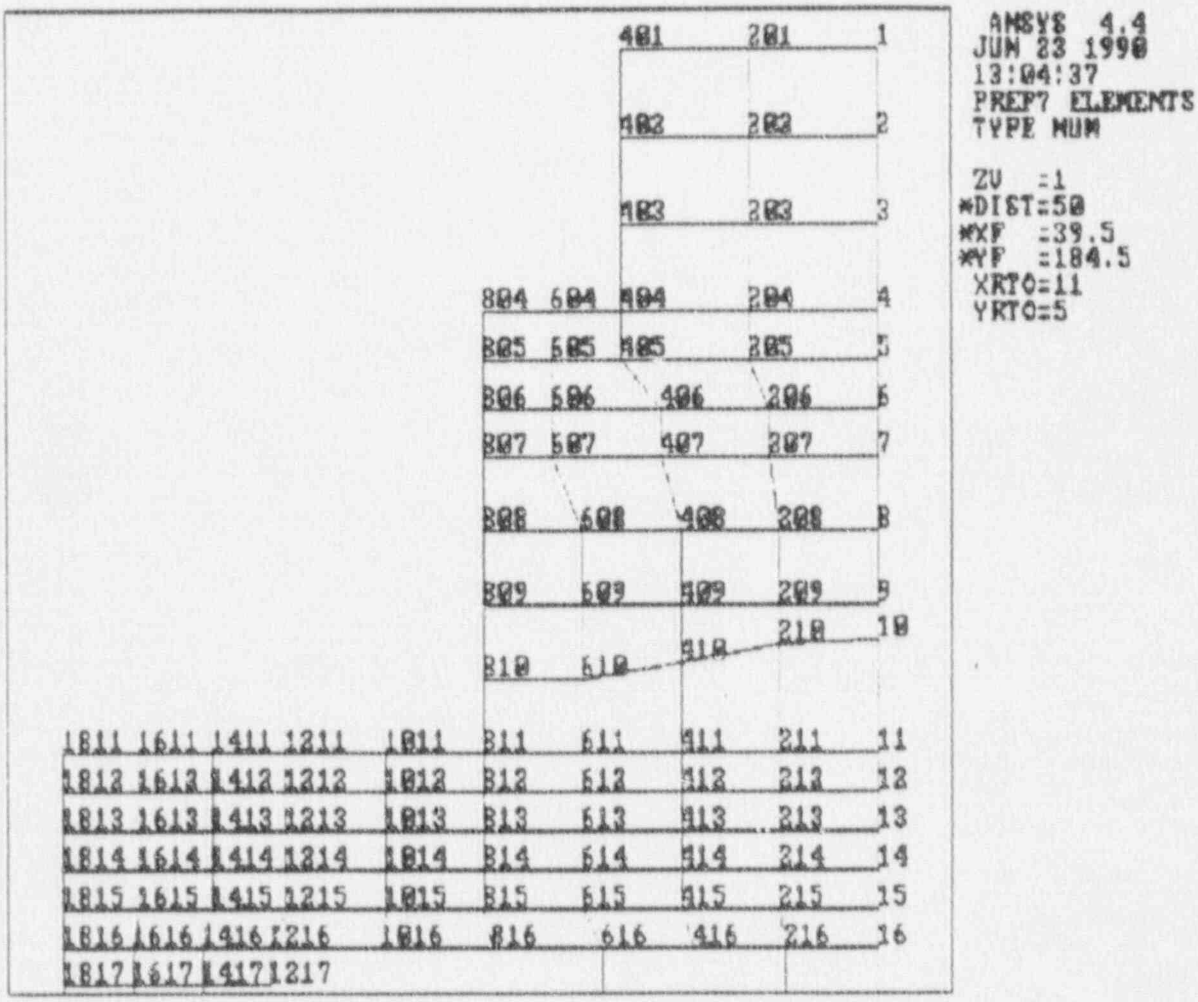

Figure 2.10.2-31 Cask Lids (Region I) - NAC-STC ANSYS Top Fine Mesh Three-Dimensional Model

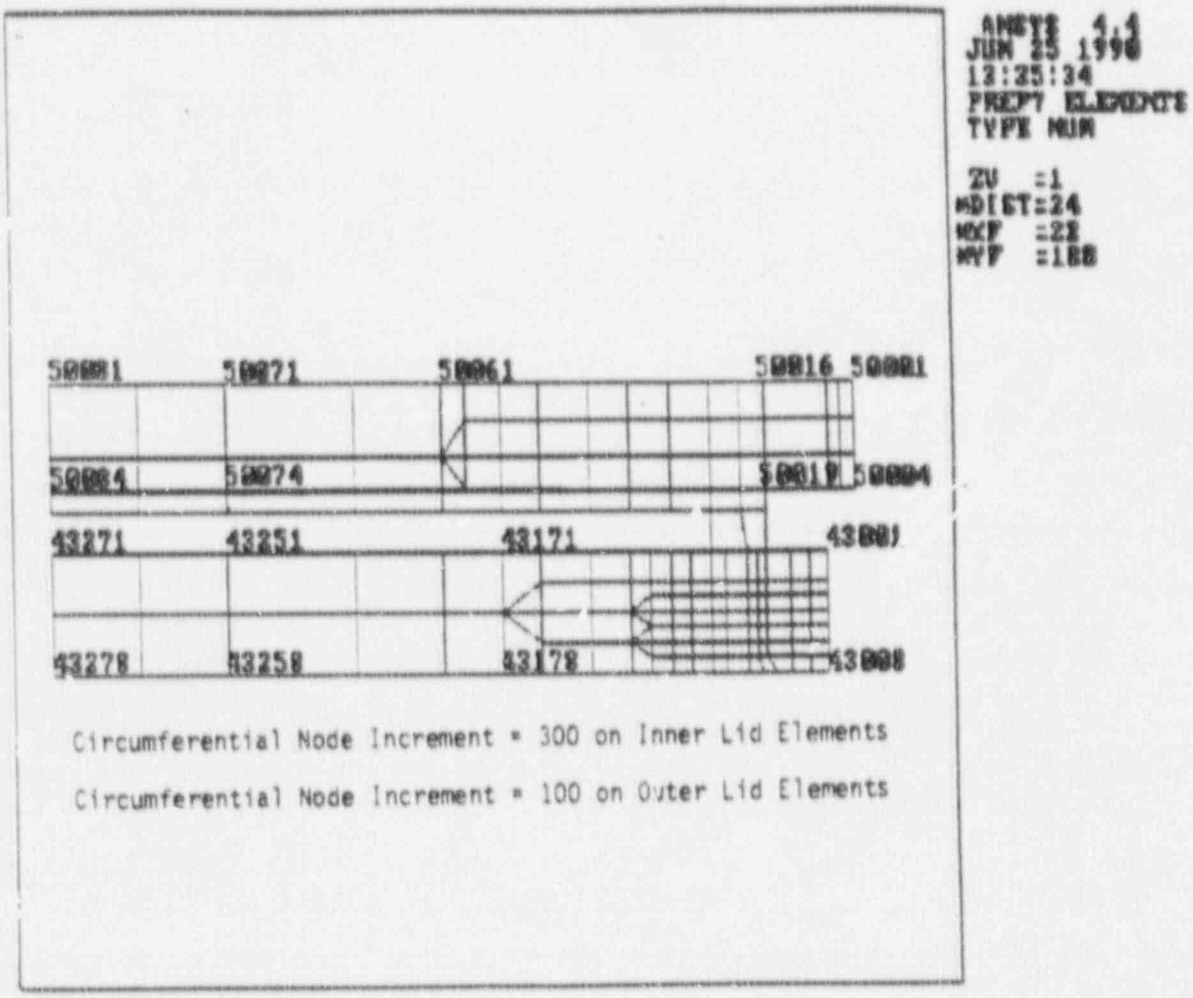

Figure 2.10.2-32 Load Distribution for Cask Side Drop Impact

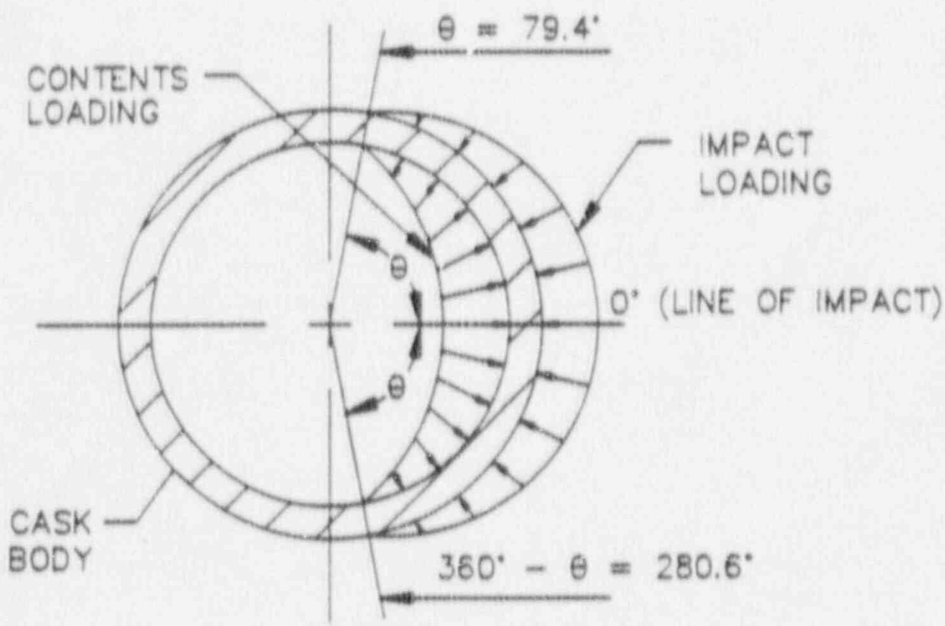

Figure 2.10.2-33 ANSYS Finite Element Model - Structural Component Identification

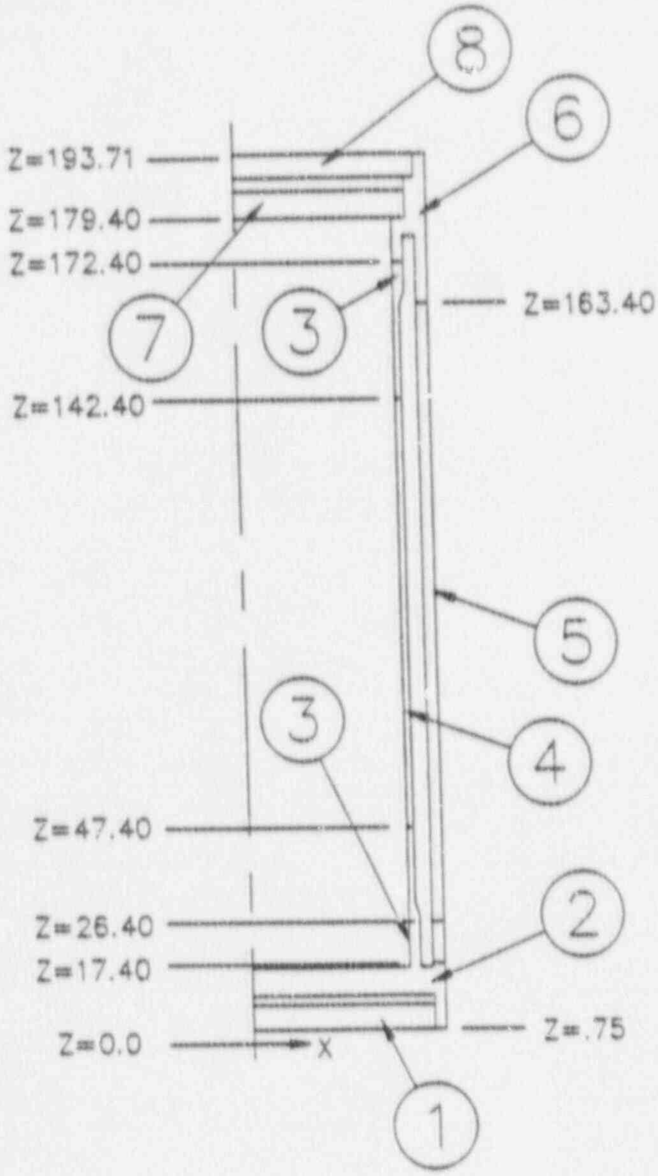

1 - Bottom Plate
2 - Bottom Forging and Bottom Ring Forging
3 - Transition Shell
4 - Inner Shell
5 - Outer Shell
6 - Top Forging
7 - Inner Lid
8 - Outer Lid

Figure 2.10.2-34 ANSYS Finite Element Model - Representative Section Locations

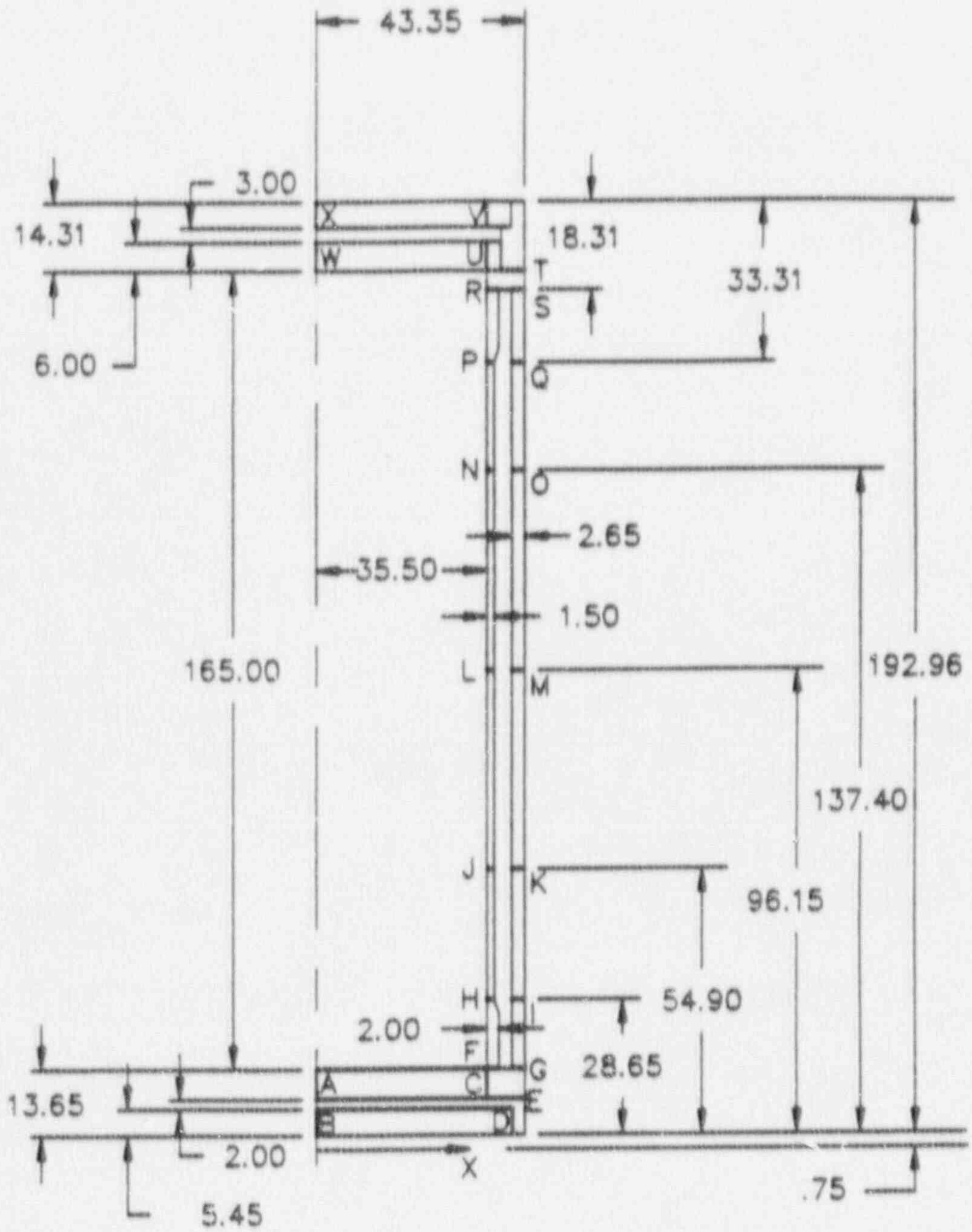

Figure 2.10.2-35 Circular Nodal Locations - NAC-STC ANSYS Three-Dimensional Model

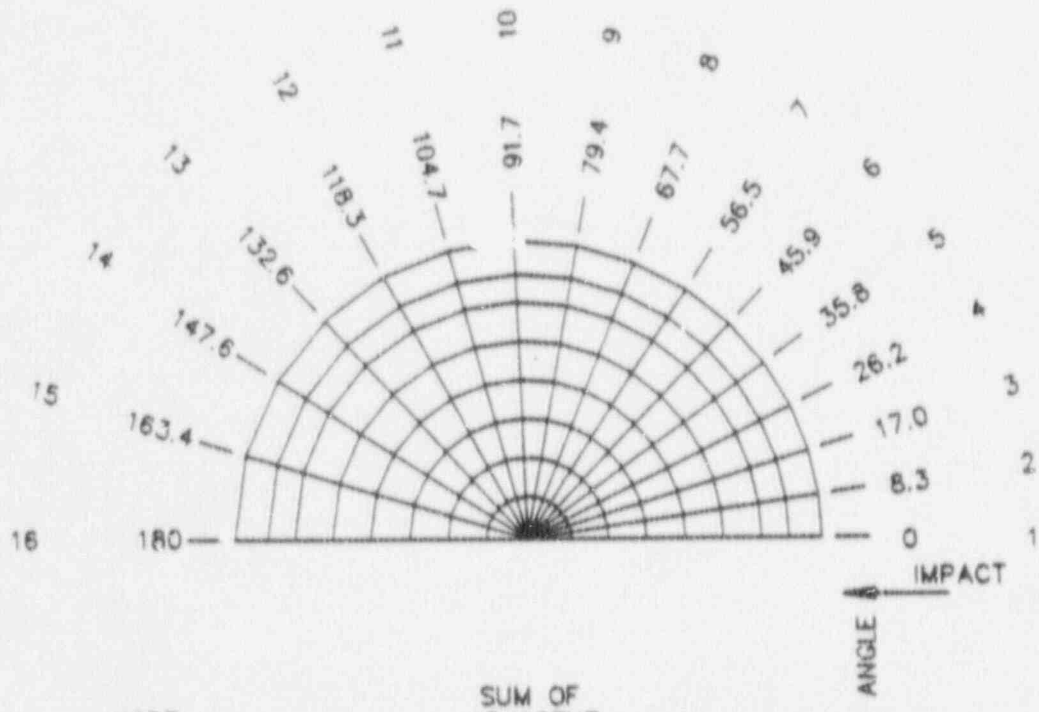

NODE LOCATION	SUM OF ADJACENT HALF ANGLES	CIRCUMFERENCE %
1	4.2	2.33
2	8.5	4.72
3	9.0	5.00
4	9.4	5.22
5	9.9	5.50
6	10.4	5.77
7	10.9	6.05
8	11.5	6.39
9	12.0	6.67
10	12.7	7.06
11	13.3	7.38
12	14.0	7.78
13	14.7	8.17
14	15.4	8.56
15	16.2	9.00
16	8.3	4.61

Figure 2.10.2-36 Nodal Identification - NAC-STC ANSYS Three-Dimensional Model

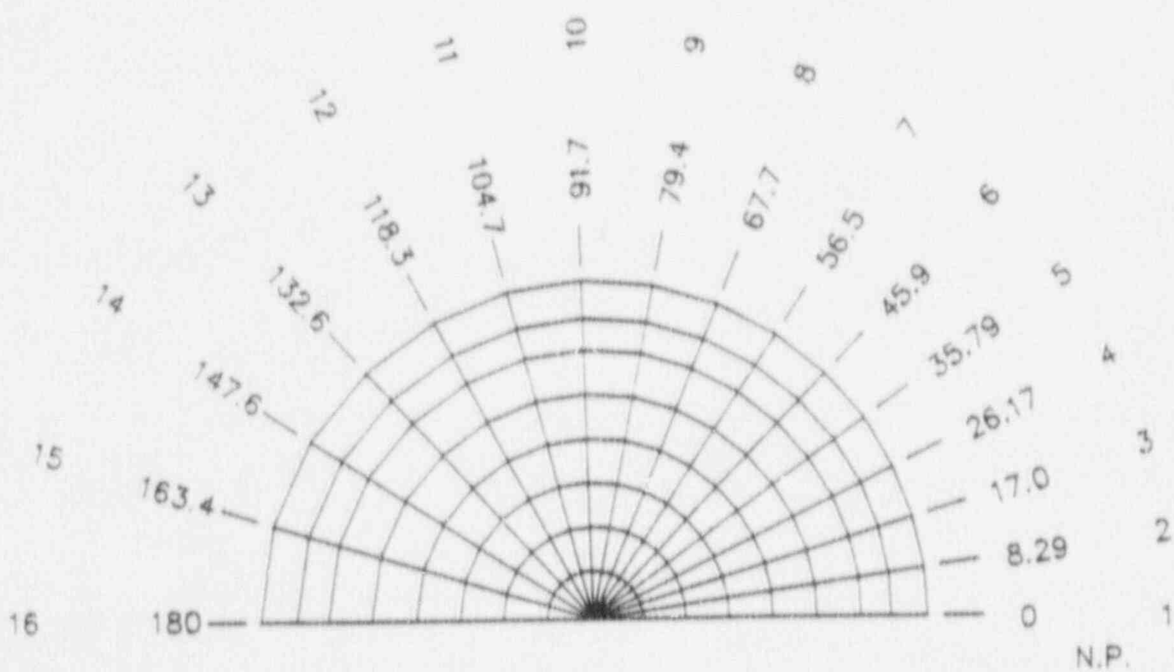

NODE LOCATION	ANGLE	NODES
1	0	1-2000
2	8.29	2001-4000
3	17.0	4001-6000
4	26.17	6001-8000
5	35.79	8001-10000
6	45.9	10001-12000
7	56.5	12001-14000
8	67.7	14001-16000
9	79.4	16001-18000
10	91.7	18001-20000
11	104.7	20001-22000
12	118.3	22001-24000
13	132.6	24001-26000
14	147.6	26001-28000
15	163.4	28001-3000
16	180.0	30001-32000

Table 2.10.2-1 Circumferential Mesh Spacing

Circumferential Plane Identification Number	Angular Location θ (degrees)	Angular Spacing Increment (degrees)
1	0.0	---
2	8.3	8.3
3	17.0	8.7
4	26.2	9.2
5	35.8	9.6
6	45.9	10.1
7	56.5	10.6
8	67.7	11.2
9	79.4	11.7
10	91.7	12.3
11	104.7	13.0
12	118.3	13.6
13	132.6	14.3
14	147.6	15.0
15	163.4	15.8
16	180.0	16.6

Table 2.10.2-2 Circumferential Plane - Percentage of 180° Arc

Circumferential Plane Identification No.	Real Constant Numbers		Sum of Adjacent Half-Angles	Percentage of 180° Arc
	Inner Bolts	Outer Bolts		
1	14	31	(1/2)(8.3) = 4.12	0.0233
2	15	32	(1/2)(8.3 + 8.7) = 8.5	0.0472
3	16	33	(1/2)(8.7 + 9.2) = 9.0	0.0500
4	17	34	(1/2)(9.2 + 9.6) = 9.4	0.0522
5	18	35	(1/2)(9.6 + 10.1) = 9.9	0.0550
6	19	36	(1/2)(10.1 + 10.6) = 10.4	0.0577
7	20	37	(1/2)(10.6 + 11.2) = 10.9	0.0605
8	21	38	(1/2)(11.2 + 11.7) = 11.5	0.0639
9	22	39	(1/2)(11.7 + 12.3) = 12.0	0.0667
10	23	40	(1/2)(12.3 + 13.0) = 12.7	0.0706
11	24	41	(1/2)(13.0 + 13.6) = 13.3	0.0738
12	25	42	(1/2)(13.6 + 14.3) = 14.0	0.0778
13	26	43	(1/2)(14.3 + 15.0) = 14.7	0.0817
14	27	44	(1/2)(15.0 + 15.8) = 15.4	0.0856
15	28	45	(1/2)(15.8 + 16.6) = 16.2	0.0900
16	29	46	(1/2)(16.6) = 8.3	0.0461

Table 2.10.2-3 Effective Inner Lid Bolt Properties

Circumferential Plane Identification No.	Real Constant Numbers	Area	Izz/Iyy	Tkz/Tky	[Shear z / Shear y]
1	14	0.7300	0.0785	1.378	1.11
2	15	1.4790	0.1590	1.378	1.11
3	16	1.5665	0.1684	1.378	1.11
4	17	1.6354	0.1758	1.378	1.11
5	18	1.723	0.1852	1.378	1.11
6	19	1.8077	0.1943	1.378	1.11
7	20	1.8955	0.2037	1.378	1.11
8	21	2.0020	0.2152	1.378	1.11
9	22	2.0897	0.2246	1.378	1.11
10	23	2.2119	0.2377	1.378	1.11
11	24	2.3122	0.2485	1.378	1.11
12	25	2.4375	0.2620	1.378	1.11
13	26	2.5500	0.2751	1.378	1.11
14	27	2.6818	0.2883	1.378	1.11
15	28	2.8197	0.3031	1.378	1.11
16	29	1.4443	0.1552	1.378	1.11

Table 2.10.2-4 Outer Lid Effective Bolt Properties

Circumferential Plane Identification No.	Real Constant Numbers	Area	Izz/Iyy	Tkz/Tky	[Shear z / Shear y]
1	31	0.2342	0.0105	0.879	1.11
2	32	0.5149	0.2124	0.879	1.11
3	33	0.5454	0.0225	0.879	1.11
4	34	0.5694	0.0235	0.879	1.11
5	35	0.5999	0.0248	0.879	1.11
6	36	0.6294	0.0260	0.879	1.11
7	37	0.6599	0.0272	0.879	1.11
8	38	0.6970	0.0288	0.879	1.11
9	39	0.7276	0.0300	0.879	1.11
10	40	0.7701	0.0318	0.879	1.11
11	41	0.8050	0.0332	0.879	1.11
12	42	0.8486	0.0350	0.879	1.11
13	43	0.8912	0.0378	0.879	1.11
14	44	0.9337	0.0385	0.879	1.11
15	45	0.9817	0.0405	0.879	1.11
16	46	0.5029	0.0207	0.879	1.11

Table 2.10.2-5 Identification of ANSYS Model Structural Components, Materials and Allowables; Condition 1

Condition 1: 100°F Ambient with Contents

Comp ID.	Description	Material	Mat ID	Max Temp.	Allowable Stress (ksi) Normal P_m (S_m)	P_m+P_b ($1.5S_m$)	Accident P_m ($0.7S_u$)	P_m+P_b (S_u)
1	Bottom Plate	304SS	5	136	28.2[1]	30.0	51.5	73.6
2	Bottom Forging	304SS	6	201	20.0	30.0	46.3	66.2
3	Transition Shell	XM-19SS	15	294	31.5	47.3	66.2	94.6
4	Inner Shell	304SS	7	356	19.5	29.2	46.0	65.7
5	Outer Shell	304SS	8	330	22.2[1]	29.6	46.0	65.8
6	Top Forging	304SS	9	233	20.0	30.0	45.2	64.6
7	Inner Lid	304SS	10	200	20.0	30.0	48.0[2]	71.0
8	Outer Lid	17-4 PH SS	11	183	45.0	67.5	94.5	135.0
9	Inner Lid Bolt	SB-637 Ni	13	210		119.4[3]		119.4[3]
10	Outer Lid Bolt	17-4 PH SS	12	184		98.4[3]		98.4[3]

Notes:

[1] S_y is used (the greater of S_m and S_y governs for nonconfinement structures).

[2] $2.4S_m$ governs.

[3] Bolt allowables based on material yield strength.

Table 2.10.2-6 Identification of ANSYS Model Structural Components, Materials and Allowables; Condition 2

Condition 2: -20°F Ambient with Contents

					Allowable Stress (ksi)			
					Normal		Accident	
Comp ID.	Description	Material	Mat ID	Max Temp.	P_m (S_m)	P_m+P_b ($1.5S_m$)	P_m ($0.7S_u$)	P_m+P_b (S_u)
1	Bottom Plate	304SS	5	9[1]	30.0[2]	30.0	52.5	75.0
2	Bottom Forging	304SS	6	80[1]	20.0	30.0	48.0[3]	70.0
3	Transition Shell	XM-19SS	15	184	33.2	49.8	69.7	99.6
4	Inner Shell	304SS	7	243	20.0	30.0	48.0[3]	68.9
5	Outer Shell	304SS	8	222	24.5[2]	30.0	48.9	69.9
6	Top Forging	304SS	9	120	20.0	30.0	48.0[3]	69.2
7	Inner Lid	304SS	10	86[1]	20.0	30.0	48.0[3]	72.0[3]
8	Outer Lid	17-4 PH SS	11	7[illegible][1]	45.0	67.5	94.5	135.0
9	Inner Lid Bolt	SB-637 Ni	13			119.4[4]		119.4[4]
10	Outer Lid Bolt	17-4 PH SS	12			98.4[4]		98.4[4]

Notes:

[1] Material properties at 100°F used for temperature less than 100°F.

[2] S_y is used (The greater of S_m and S_y governs for Nonconfinement Structure).

[3] $2.4S_m$ and $3.6S_m$ govern.

[4] Bolt allowables based on material yield strength.

Table 2.10.2-7 Identification of ANSYS Model Structural Components, Materials and Allowables; Conditions 3, 4, and 5

					Allowable Stress (ksi)			
					Normal		Accident	
Comp ID.	Description	Material	Mat ID	Max Temp.[1]	P_m (S_m)	P_m+P_b ($1.5S_m$)	P_m ($0.7S_u$)	P_m+P_b (S_u)
1	Bottom Plate	304SS	5	≤ 100	30.0[2]	30.0	52.5	75.0
2	Bottom Forging	304SS	6	≤ 100	20.0	30.0	48.0[3]	70.0
3	Transition Shell	XM-19 SS	15	≤ 100	33.3	50.0	70.0	100.0
4	Inner Shell	304SS	7	≤ 100	20.0	30.0	48.0[3]	72.0[3]
5	Outer Shell	304SS	8	≤ 100	30.0[2]	30.0	52.5	75.0
6	Top Forging	304SS	9	≤ 100	20.0	30.0	48.0[3]	70.0
7	Inner Lid	304SS	10	≤ 100	20.0	30.0	48.0[3]	72.0[3]
8	Outer Lid	17-4 PH SS	11	≤ 100	45.0	67.5	94.5	135.0
9	Inner Lid Bolt	SB-637 Ni	13	≤ 100		115.0[4]		115.0[4]
10	Outer Lid Bolt	17-4 PH SS	12	≤ 100		105.0[4]		105.0[4]

Notes:

[1] Condition 3: -20°F ambient without contents
Condition 4: -40°F ambient without contents
Condition 5: 100°F ambient without contents
(Material properties at 100°F used for -40°F and -20°F conditions.)

[2] S_y is used (the greater of S_m and S_y governs for nonconfinement structures).

[3] $2.4S_m$ and $3.6S_m$ govern.

[4] Bolt allowables based on material yield strength.

Table 2.10.2-8 Section Cut Identification - (2-D Model)

Section*	Inside Node Radial (in)	Inside Node Axial (in)	Outside Node Radial (in)	Outside Node Axial (in)
A	0.00	14.40	0.00	8.20
B	0.00	6.20	0.00	0.75
C	35.50	14.40	35.50	8.20
D	39.44	6.20	39.44	0.75
E	39.44	8.20	43.35	8.20
F	35.50	14.40	37.50	14.40
G	40.70	14.40	43.35	14.40
H	35.50	29.40	37.00	29.40
I	40.70	29.40	43.35	29.40
J	35.50	55.65	37.00	55.65
K	40.70	55.65	43.35	55.65
L	35.50	96.90	37.00	96.90
M	40.70	96.90	43.35	96.90
N	35.50	138.15	37.00	138.15
O	40.70	138.15	43.35	138.15
P	35.50	160.40	37.00	160.40
Q	40.70	160.40	43.35	160.40
R	35.50	175.40	37.00	175.40
S	40.70	175.40	43.35	175.40
T	39.56	179.40	43.35	179.40
U	35.50	179.40	35.50	185.40
V	35.21	188.40	35.21	193.71
W	0.00	179.40	0.00	185.40
X	0.00	188.46	0.00	193.71

*Refer to Figure 2.10.2-34 for the section cut locations.

Table 2.10.2-9 Section Cut Identification - (3-D Bottom Fine Mesh Model)

	Inside Node		Outside Node	
Section[1]	Radial (in)	Axial (in)	Radial (in)	Axial (in)
A	0.00	14.40	0.00	8.20
B	0.00	6.20	0.00	0.75
C	35.50	14.40	35.50	8.20
D	39.44	6.20	39.44	0.75
E	39.44	8.20	43.35	8.20
F	35.50	15.00[2]	37.50	15.00[2]
G	40.70	15.00[2]	43.35	15.00[2]
H	35.50	29.40	37.00	29.40
I	40.70	29.40	43.35	29.40
J	35.50	55.65	37.00	55.65
K	40.70	55.65	43.35	55.65
L	35.50	96.90	37.00	96.90
M	40.70	96.90	43.35	96.90
N	35.50	138.15	37.00	138.15
O	40.70	138.15	43.35	138.15
P	35.50	160.40	37.00	160.40
Q	40.70	160.40	43.35	160.40
R	35.50	175.40	37.50	175.40
S	40.70	175.40	43.35	175.40
T	40.70	179.40	43.35	181.68[3]
U	35.50	179.40	35.50	185.40
V	35.50[4]	187.40	35.50[4]	193.71
W	0.00	179.40	0.00	185.40
X	0.00	187.40	0.00	193.71

[1] Refer to Figure 2.10.2-34 for the section cut locations

[2] Moved one section up from the root (Y = 14.40") to pick up higher stresses

[3] Moved up for impact pressure specification

[4] No nodes at outer lid bolt circle for three-dimensional bottom model

Table 2.10.2-10 Section Cut Identification - (3-D Top Fine Mesh Model)

Section*	Inside Node Radial (in)	Inside Node Axial (in)	Outside Node Radial (in)	Outside Node Axial (in)
A	0.00	14.40	0.00	8.20
B	0.00	6.20	0.00	0.75
C	35.50	14.40	35.50	8.20
D	39.44	6.20	39.44	0.75
E	39.44	8.20	43.35	8.20
F	35.50	14.40	37.50	14.40
G	40.70	14.40	43.35	14.40
H	35.50	29.40	37.00	29.40
I	40.70	29.40	43.35	29.40
J	35.50	55.65	37.00	55.65
K	40.70	55.65	43.35	55.65
L	35.50	96.90	37.00	96.90
M	40.70	96.90	43.35	96.90
N	35.50	138.15	37.00	138.15
O	40.70	138.15	43.35	138.15
P	35.50	160.40	37.00	160.40
Q	40.70	160.40	43.35	160.40
R	35.50	175.40	37.50	175.40
S	40.70	175.40	43.35	175.40
T	39.56	179.40	43.35	179.40
U	35.50	179.41	35.50	185.40
V	35.21	188.40	35.21	193.71
W	0.00	179.40	0.00	185.40
X	0.00	188.46	0.00	193.71

*Refer to Figure 2.10.2-34 for the section cut locations

Table 2.10.2-11 Stress Point Locations - 2-D Model

Stress Point ID	Stress Point Node	Location Radial (in)	Location Axial (in)
A-1	1	0.00	14.40
A-2	2	0.00	12.95
A-3	3	0.00	11.30
A-4	4	0.00	9.75
A-5	5	0.00	8.20
B-1	6	0.00	6.20
B-2	7	0.00	4.84
B-3	8	0.00	3.48
B-4	9	0.00	2.11
B-5	10	0.00	0.75
C-1	251	35.50	14.40
C-2	252	35.50	12.85
C-3	253	35.50	11.30
C-4	254	35.50	9.75
C-5	255	35.50	8.20
D-1	306	39.44	6.20
D-2	307	39.44	4.84
D-3	308	39.44	3.48
D-4	309	39.44	2.11
D-5	310	39.44	0.75
E-1	305	39.44	8.20
E-2	315	40.70	8.20
E-3	325	41.36	8.20
E-4	335	42.03	8.20
E-5	345	42.69	8.20
E-6	355	43.35	8.20

Table 2.10.2-11 Stress Point Locations - 2-D Model (continued)

Stress Point ID	Node	Location Radial (in)	Location Axial (in)
F-1	251	35.50	14.40
F-2	261	36.17	14.40
F-3	271	36.83	14.40
F-4	281	37.50	14.40
G-1	311	40.70	14.40
G-2	321	41.36	14.40
G-3	331	42.03	14.40
G-4	341	42.69	14.40
G-5	351	43.35	14.40
H-1	581	35.50	29.40
H-2	582	36.00	29.40
H-3	583	36.50	29.40
H-4	584	37.00	29.40
I-1	589	40.70	29.40
I-2	590	41.36	29.40
I-3	591	42.03	29.40
I-4	592	42.69	29.40
I-5	593	43.35	29.40
J-1	971	35.50	55.65
J-2	972	36.00	55.65
J-3	973	36.50	55.65
J-4	974	37.00	55.65
K-1	979	40.70	55.65
K-2	980	41.36	55.65
K-3	981	42.03	55.65

Table 2.10.2-11 Stress Point Locations - 2-D Model (continued)

Stress Point		Location	
ID	Node	Radial (in)	Axial (in)
K-4	982	69	55.65
K-5	983	[illegible].35	55.65
L-1	1601	35.50	96.90
L-2	1602	36.00	96.90
L-3	1603	36.50	96.90
L-4	1604	37.00	96.90
M-1	1609	40.70	96.90
M-2	1610	41.36	96.90
M-3	1611	42.03	96.90
M-4	1612	42.69	96.90
M-5	1613	43.35	96.90
N-1	2216	35.50	138.15
N-2	2217	36.00	138.15
N-3	2218	36.50	138.15
N-4	2219	37.00	138.15
O-1	2224	40.70	138.15
O-2	2225	41.36	138.15
O-3	2226	42.03	138.15
O-4	2227	42.69	138.15
O-5	2228	43.35	138.15
P-1	2546	35.50	160.40
P-2	2547	36.00	160.40
P-3	2548	36.50	160.40
P-4	2549	37.00	160.40

Table 2.10.2-11 Stress Point Locations - 2-D Model (continued)

Stress Point ID	Stress Point Node	Location Radial (in)	Location Axial (in)
Q-1	2554	40.70	160.40
Q-2	2555	41.36	160.40
Q-3	2556	42.03	160.40
Q-4	2557	42.69	160.40
Q-5	2558	43.35	160.40
R-1	2771	35.50	175.40
R-2	2772	36.17	175.40
R-3	2773	36.83	175.40
R-4	2774	37.50	175.40
S-1	2779	40.70	175.40
S-2	2780	41.36	175.40
S-3	2781	42.03	175.40
S-4	2782	42.69	175.40
S-5	2783	43.35	175.40
T-1	7066	39.56	179.40
T-2	7067	40.22	179.40
T-3	7068	40.88	179.40
T-4	7069	41.50	179.40
T-5	7070	42.11	179.40
T-6	7071	42.73	179.40
T-7	7072	43.35	179.40
U-1	3051	35.50	179.40
U-2	3052	35.50	180.60
U-3	3053	35.50	181.80
U-4	3054	35.50	183.00
U-5	3055	35.50	184.20
U-6	3056	35.50	185.40

Table 2.10.2-11 Stress Point Locations - 2-D Model (continued)

Stress Point ID	Stress Point Node	Location Radial (in)	Location Axial (in)
V-1	3611	35.21	188.40
V-2	3612	35.21	189.23
V-3	3613	35.21	190.1[illegible]
V-4	3614	35.21	191.03
V-5	3615	35.21	191.90
V-6	3616	35.21	192.78
V-7	3617	35.21	193.71
W-1	3241	0.00	179.40
W-2	3242	0.00	180.60
W-3	3243	0.00	181.80
W-4	3244	0.00	183.00
W-5	3245	0.00	184.20
W-6	3246	0.00	185.40
X-1	3801	0.00	188.46
X-2	3802	0.00	189.28
X-3	3803	0.00	190.15
X-4	3804	0.00	191.03
X-5	3805	0.00	191.90
X-6	3806	0.00	192.78
X-7	3807	0.00	193.71

Table 2.10.2-12 Stress Point Locations - 3-D Bottom Fine Mesh Model

Stress Point		Location	
ID	Node	Radial (in)	Axial (in)
A-1	1130	0.00	14.40
A-2	1129	0.00	11.35
A-3	1128	0.00	8.20
B-1	1185	0.00	6.20
B-2	1184	0.00	3.48
B-3	1183	0.00	0.75
C-1	90	35.50	14.40
C-2	80	35.50	13.60
C-3	70	35.50	12.80
C-4	60	35.50	12.00
C-5	50	35.50	9.50
C-6	40	35.50	8.20
D-1	25	39.44	6.20
D-2	15	39.44	3.48
D-3	5	39.44	0.75
E-1	35	39.44	8.20
E-2	34	40.70	8.20
E-3	33	41.58	8.20
E-4	32	42.47	8.20
E-5	31	43.35	8.20
F-1	100	35.50	15.07
F-2	99	36.17	15.07
F-3	98	36.83	15.07
F-4	97	37.50	15.07

Table 2.10.2-12 Stress Point Locations - 3-D Bottom Fine Mesh Model (continued)

Stress Point ID	Stress Point Node	Location Radial (in)	Location Axial (in)
G-1	94	40.70	15.52
G-2	93	41.58	15.52
G-3	92	42.47	15.52
G-4	91	43.35	15.52
H-1	330	35.50	29.40
H-2	329	36.00	29.40
H-3	328	36.50	29.40
H-4	327	37.00	29.40
I-1	244	40.70	29.40
I-2	243	41.58	29.40
I-3	242	42.47	29.40
I-4	241	43.35	29.40
J-1	550	35.50	55.65
J-2	548	36.25	55.65
J-3	547	37.00	55.65
K-1	344	40.70	55.65
K-2	342	42.03	55.65
K-3	341	43.35	55.65
L-1	740	35.50	96.90
L-2	738	36.25	96.90
L-3	737	37.00	96.90
M-1	454	40.70	96.90
M-2	452	42.03	96.90

Table 2.10.2-12 Stress Point Locations - 3-D Bottom Fine Mesh Model (continued)

Stress Point		Location	
ID	Node	Radial (in)	Axial (in)
M-3	451	43.35	96.90
N-1	810	35.50	138.15
N-2	807	37.00	138.15
O-1	524	40.70	138.15
O-2	521	43.35	138.15
P-1	850	35.50	160.40
P-2	847	37.00	160.40
Q-1	564	40.70	160.40
Q-2	561	43.35	160.40
R-1	890	35.50	175.40
R-2	887	37.50	175.40
S-1	604	40.70	175.40
S-2	601	43.35	175.40
T-1	614	40.70	179.40
T-2	611	43.35	179.40
U-1	900	35.50	179.40
U-2	910	35.50	185.40
V-1	920	35.50	187.40
V-2	930	35.50	193.71

Table 2.10.2-12 Stress Point Locations - 3-D Bottom Fine Mesh Model (continued)

Stress Point		Location	
		Radial	Axial
ID	Node	(in)	(in)
W-1	1216	0.00	179.40
W-2	1226	0.00	185.40
X-1	1236	0.00	187.40
X-2	1246	0.00	193.71

Table 2.10.2-13 Stress Point Locations - 3-D Top Fine Mesh Model

Stress Point ID	Node	Location Radial (in)	Location Axial (in)
A-1	1949	0.00	14.40
A-2	1950	0.00	12.78
A-3	1951	0.00	8.20
B-1	1952	0.00	6.20
B-2	93	0.00	0.75
C-1	1925	35.50	14.40
C-2	1926	35.50	12.78
C-3	1927	35.50	8.20
D-1	683	39.44	6.20
D-2	85	39.44	0.75
E-1	682	39.44	8.20
E-2	82	43.35	8.20
F-1	1925	35.50	14.40
F-2	1325	37.50	14.40
G-1	680	40.70	14.40
G-2	80	43.35	14.40
H-1	1921	35.50	29.40
H-2	1321	37.00	29.40
I-1	676	40.70	29.40
I-2	76	43.35	29.40

Table 2.10.2-13 Stress Point Locations - 3-D Top Fine Mesh Model (continued)

Stress Point ID	Node	Location Radial (in)	Location Axial (in)
J-1	1916	35.50	55.65
J-2	1316	37.00	55.65
K-1	671	40.70	55.65
K-2	71	43.50	55.65
L-1	1908	35.50	96.90
L-2	1308	37.00	96.90
M-1	663	40.70	96.90
M-2	63	43.50	96.90
N-1	1877	35.50	138.15
N-2	1477	36.25	138.15
N-3	1277	37.00	138.15
O-1	647	40.70	138.15
O-2	247	42.03	138.15
O-3	47	43.35	138.15
P-1	1840	35.50	160.40
P-2	1640	36.00	160.40
P-3	1440	36.50	160.40
P-4	1240	37.00	160.40
Q-1	628	40.70	160.40
Q-2	428	41.58	160.40
Q-3	228	42.47	160.40
Q-4	28	43.35	160.40

Table 2.10.2-13 Stress Point Locations - 3-D Top Fine Mesh Model (continued)

Stress Point ID	Node	Location Radial (in)	Location Axial (in)
R-1	1816	35.50	175.40
R-2	1616	36.17	175.40
R-3	1416	36.83	175.40
R-4	1216	37.50	175.40
S-1	616	40.70	175.40
S-2	416	41.58	175.40
S-3	216	42.47	175.40
S-4	16	43.35	175.40
T-1	811	39.56	179.40
T-2	611	40.51	179.40
T-3	411	41.46	179.40
T-4	211	42.40	179.40
T-5	11	43.35	179.40
U-1	43058	35.50	179.40
U-2	43057	35.50	180.15
U-3	43056	35.50	180.90
U-4	43055	35.50	181.65
U-5	43054	35.50	182.40
U-6	43053	35.50	183.15
U-7	43052	35.50	183.90
U-8	43051	35.50	185.40
V-1	50024	35.21	188.40
V-2	50023	35.21	190.15
V-3	50022	35.21	191.90
V-4	50021	35.21	193.71

Table 2.10.2-13 Stress Point Locations - 3-D Top Fine Mesh Model (continued)

Stress Point ID	Node	Location Radial (in)	Location Axial (in)
W-1	43278	0.00	179.40
W-2	43274	0.00	182.40
W-3	43271	0.00	185.40
X-1	50084	0.00	188.46
X-2	50083	0.00	190.15
X-3	50081	0.00	193.71

2.10.4 Detailed Finite Element Stress Summaries

This section documents the finite element stress results from the different loading cases for the normal condition of transport and hypothetical accident conditions. Nodal and sectional stress summaries are presented for the representative sections as defined in Section 2.10.2.4.2. Critical stress summaries are presented for the critical component sections determined as described in Section 2.10.2.4.1.

A summary of the individual and combined loading conditions is provided, followed by the stress summary tables.

Table 2.10.4-121 Primary Stresses; 30-Foot Bottom End Drop; Drop Orientation = 0 Degrees; 2-D Model; Condition 1

Condition 1: 100°F Ambient with Contents

Stress Points		Stress Components (ksi)						Principal Stresses (ksi)		
Section*	Node	Sx	Sy	Sz	Sxy	Syz	Szx	S1	S2	S3
A1	1	21.0	-1.0	21.0	0.0	0.0	0.0	21.0	21.0	-1.0
A2	2	11.9	-1.1	11.9	0.0	0.0	0.0	11.9	11.9	-1.1
A3	3	2.9	-1.3	2.9	0.0	0.0	0.0	2.9	2.9	-1.3
A4	4	-6.1	-1.5	-6.1	0.0	0.0	0.0	-1.5	-6.1	-6.1
A5	5	-15.2	-1.6	-15.2	0.0	0.0	0.0	-1.6	-15.2	-15.2
B1	6	12.2	-1.8	12.2	0.0	0.0	0.0	12.2	12.2	-1.8
B2	7	4.3	-1.9	4.3	0.0	0.0	0.0	4.3	4.3	-1.9
B3	8	-3.6	-2.1	-3.6	0.0	0.0	0.0	-2.1	-3.6	-3.6
B4	9	-11.5	-2.2	-11.5	0.0	0.0	0.0	-2.2	-11.5	-11.5
B5	10	-19.3	-2.4	-19.3	0.0	0.0	0.0	-2.4	-19.3	-19.3
C1	251	-11.2	-13.5	-0.4	-2.3	0.0	0.0	-0.4	-9.7	-14.9
C2	252	-1.8	-5.6	2.4	-1.7	0.0	0.0	2.4	-1.2	-6.2
C3	253	3.1	-2.5	2.7	-1.8	0.0	0.0	3.6	2.7	-3.0
C4	254	9.3	-1.6	2.7	-1.4	0.0	0.0	9.4	2.7	-1.8
C5	255	16.1	-1.4	2.5	-1.0	0.0	0.0	16.2	2.5	-1.5
D1	306	-17.9	-15.3	-8.4	-5.3	0.0	0.0	-8.4	-11.1	-22.1
D2	307	-4.7	-11.0	-4.7	-2.3	0.0	0.0	-4.0	-4.7	-11.7
D3	308	-1.2	-5.6	-3.7	0.0	0.0	0.0	-1.2	-3.7	-5.6
D4	309	2.3	-3.6	-3.8	0.5	0.0	0.0	2.3	-3.7	-3.8
D5	310	6.6	-2.9	-3.9	0.5	0.0	0.0	6.6	-2.9	-3.9
E1	305	15.2	-4.7	3.5	-3.5	0.0	0.0	15.8	3.5	-5.3
E2	315	7.3	-6.9	1.0	-4.5	0.0	0.0	8.6	1.0	-8.2
E3	325	3.1	-5.4	0.3	-4.4	0.0	0.0	5.	0.3	-7.3
E4	335	1.5	-4.4	0.2	-3.4	0.0	0.0	3.1	0.2	-6.0
E5	345	0.6	-3.7	0.2	-2.0	0.0	0.0	1.4	0.2	-4.5
E6	355	0.2	-3.6	0.1	-1.2	0.0	0.0	0.6	0.1	-3.9
F1	251	-11.2	-13.5	-0.4	-2.3	0.0	0.0	-0.4	-9.7	-14.9
F2	261	-8.1	-6.1	2.2	-0.8	0.0	0.0	2.2	-5.8	-8.4
F3	271	-5.4	-0.6	4.2	0.1	0.0	0.0	4.2	-0.6	-5.4
F4	281	-5.4	4.0	5.3	-0.2	0.0	0.0	5.3	4.0	-5.4
G1	311	-7.8	-12.6	-1.0	-0.4	0.0	0.0	-1.0	-7.8	-12.6
G2	321	-5.5	-7.9	0.8	0.3	0.0	0.0	0.8	-5.4	-7.9
G3	331	-2.8	-4.7	2.3	0.9	0.0	0.0	2.3	-2.5	-5.1
G4	341	-1.1	-1.5	3.5	0.7	0.0	0.0	3.5	-0.6	-2.0
G5	351	-0.5	2.6	4.7	0.4	0.0	0.0	4.7	2.7	-0.6
H1	581	-0.1	-3.0	1.7	0.0	0.0	0.0	1.7	-0.1	-3.0
H2	582	-0.2	-4.8	1.2	0.0	0.0	0.0	1.2	-0.2	-4.8
H3	583	-0.1	-6.6	0.7	0.2	0.0	0.0	0.7	-0.1	-6.6
H4	584	0.1	-9.1	0.0	0.5	0.0	0.0	0.0	-0.1	-9.2
I1	589	0.0	-3.6	1.1	0.0	0.0	0.0	1.1	0.0	-3.6
I2	590	0.0	-4.2	0.9	0.0	0.0	0.0	0.9	0.0	-4.2
I3	591	0.0	-4.7	0.8	0.0	0.0	0.0	0.8	0.0	-4.7

Table 2.10.4-121 Primary Stresses; 30-Foot Bottom End Drop; Drop Orientation = 0 Degrees; 2-D Model; Condition 1 (continued)

Condition 1: 100°F Ambient with Contents

Stress Points		Stress Components (ksi)						Principal Stresses (ksi)		
Section*	Node	Sx	Sy	Sz	Sxy	Syz	Szx	S1	S2	S3
I4	592	0.0	-5.3	0.6	0.0	0.0	0.0	0.6	0.0	-5.3
I5	593	0.0	-5.9	0.4	0.0	0.0	0.0	0.4	0.0	-5.9
J1	971	-0.1	-5.4	1.2	0.0	0.0	0.0	1.2	-0.1	-5.4
J2	972	0.0	-5.4	1.2	0.0	0.0	0.0	1.2	0.0	-5.4
J3	973	0.0	-5.4	1.2	0.0	0.0	0.0	1.2	0.0	-5.4
J4	974	0.0	-5.4	1.2	0.0	0.0	0.0	1.2	0.0	-5.4
K1	979	0.0	-4.2	0.0	0.0	0.0	0.0	0.0	0.0	-4.2
K2	980	0.0	-4.2	0.0	0.0	0.0	0.0	0.0	0.0	-4.2
K3	981	0.0	-4.1	0.0	0.0	0.0	0.0	0.0	0.0	-4.1
K4	982	0.0	-4.1	0.0	0.0	0.0	0.0	0.0	0.0	-4.1
K5	983	0.0	-4.1	0.0	0.0	0.0	0.0	0.0	0.0	-4.1
L1	1601	-0.1	-4.4	1.2	0.0	0.0	0.0	1.2	-0.1	-4.4
L2	1602	0.0	-4.4	1.2	0.0	0.0	0.0	1.2	0.0	-4.4
L3	1603	0.0	-4.4	1.2	0.0	0.0	0.0	1.2	0.0	-4.4
L4	1604	0.0	-4.4	1.2	0.0	0.0	0.0	1.2	0.0	-4.4
M1	1609	0.0	-3.2	0.0	0.0	0.0	0.0	0.0	0.0	-3.2
M2	1610	0.0	-3.2	0.0	0.0	0.0	0.0	0.0	0.0	-3.2
M3	1611	0.0	-3.2	0.0	0.0	0.0	0.0	0.0	0.0	-3.2
M4	1612	0.0	-3.2	0.0	0.0	0.0	0.0	0.0	0.0	-3.2
M5	1613	0.0	-3.2	0.0	0.0	0.0	0.0	0.0	0.0	-3.2
N1	2216	-0.1	-3.4	1.2	0.0	0.0	0.0	1.2	-0.1	-3.4
N2	2217	0.0	-3.4	1.2	0.0	0.0	0.0	1.2	0.0	-3.4
N3	2218	0.0	-3.4	1.2	0.0	0.0	0.0	1.2	0.0	-3.4
N4	2219	0.0	-3.4	1.2	0.0	0.0	0.0	1.2	0.0	-3.4
O1	2224	0.0	-2.2	0.0	0.0	0.0	0.0	0.0	0.0	-2.2
O2	2225	0.0	-2.2	0.0	0.0	0.0	0.0	0.0	0.0	-2.2
O3	2226	0.0	-2.2	0.0	0.0	0.0	0.0	0.0	0.0	-2.2
O4	2227	0.0	-2.2	0.0	0.0	0.0	0.0	0.0	0.0	-2.2
O5	2228	0.0	-2.2	0.0	0.0	0.0	0.0	0.0	0.0	-2.2
P1	2546	-0.1	-2.1	1.1	0.0	0.0	0.0	1.1	-0.1	-2.1
P2	2547	-0.1	-2.6	1.0	0.0	0.0	0.0	1.0	-0.1	-2.6
P3	2548	-0.1	-3.0	0.9	-0.1	0.0	0.0	0.9	-0.1	-3.0
P4	2549	0.0	-3.6	0.7	-0.2	0.0	0.0	0.7	0.0	-3.7
Q1	2554	0.0	-1.4	0.3	0.0	0.0	0.0	0.3	0.0	-1.4
Q2	2555	0.0	-1.5	0.3	0.0	0.0	0.0	0.3	0.0	-1.5
Q3	2556	0.0	-1.7	0.2	0.0	0.0	0.0	0.2	0.0	-1.7
Q4	2557	0.0	-1.8	0.2	0.0	0.0	0.0	0.2	0.0	-1.8
Q5	2558	0.0	-1.9	0.1	0.0	0.0	0.0	0.1	0.0	-1.9
R1	2771	-0.3	-4.4	0.0	0.2	0.0	0.0	0.0	-0.3	-4.4
R2	2772	-0.1	-2.9	0.4	0.3	0.0	0.0	0.4	-0.1	-2.9
R3	2773	-0.2	-1.4	0.8	0.4	0.0	0.0	0.8	-0.1	-1.5
R4	2774	-0.7	1.0	1.3	0.5	0.0	0.0	1.3	1.2	-0.9

Table 2.10.4-121 Primary Stresses; 30-Foot Bottom End Drop; Drop Orientation = 0 Degrees; 2-D Model; Condition 1 (continued)

Condition 1: 100°F Ambient with Contents

Stress Points		Stress Components (ksi)						Principal Stresses (ksi)		
Section*	Node	Sx	Sy	Sz	Sxy	Syz	Szx	S1	S2	S3
S1	2779	-2.1	-2.9	-0.4	0.2	0.0	0.0	-0.4	-2.0	-2.9
S2	2780	-1.3	-1.8	0.1	0.0	0.0	0.0	0.1	-1.3	-1.8
S3	2781	-0.7	-1.1	0.4	-0.2	0.0	0.0	0.4	-0.5	-1.2
S4	2782	-0.3	-0.3	0.7	-0.2	0.0	0.0	0.7	-0.1	-0.5
S5	2783	-0.1	0.7	1.0	-0.1	0.0	0.0	1.0	0.8	-0.1
T1	7066	1.9	1.6	1.1	0.5	0.0	0.0	2.3	1.2	1.1
T2	7067	1.5	0.1	0.5	0.1	0.0	0.0	1.5	0.5	0.1
T3	7068	1.0	-0.5	0.3	0.0	0.0	0.0	1.0	0.3	-0.5
T4	7069	0.6	-0.8	0.1	-0.1	0.0	0.0	0.6	0.1	-0.8
T5	7070	0.3	-1.1	-0.1	-0.1	0.0	0.0	0.3	-0.1	-1.1
T6	7071	0.1	-1.4	-0.2	-0.1	0.0	0.0	0.1	-0.2	-1.4
T7	7072	0.1	-1.9	-0.3	-0.1	0.0	0.0	0.1	-0.3	-1.9
U1	3051	-1.2	-3.6	0.6	0.7	0.0	0.0	0.6	-1.0	-3.8
U2	3052	-0.4	-3.7	0.1	0.7	0.0	0.0	0.1	-0.2	-3.9
U3	3053	0.3	-3.5	-0.2	0.3	0.0	0.0	0.3	-0.2	-3.5
U4	3054	0.6	-2.9	-0.5	-0.3	0.0	0.0	0.6	-0.5	-2.9
U5	3055	0.4	-2.3	-0.9	-0.3	0.0	0.0	0.4	-0.9	-2.3
U6	3056	1.2	-1.0	-0.7	0.4	0.0	0.0	1.2	-0.7	-1.0
V1	3611	0.6	-0.1	1.8	-0.1	0.0	0.0	1.8	0.6	-0.1
V2	3612	0.3	-0.2	1.1	-0.1	0.0	0.0	1.1	0.3	-0.2
V3	3613	0.1	-0.4	0.5	-0.1	0.0	0.0	0.5	0.2	-0.5
V4	3614	0.0	-0.7	-0.1	-0.1	0.0	0.0	0.0	-0.1	-0.7
V5	3615	-0.1	-1.1	-0.8	0.0	0.0	0.0	-0.1	-0.8	-1.1
V6	3616	-0.3	-0.5	-1.2	0.0	0.0	0.0	-0.3	-0.5	-1.2
V7	3617	-0.8	0.4	-1.7	0.0	0.0	0.0	0.4	-0.8	-1.7
W1	3241	4.7	0.0	4.7	0.0	0.0	0.0	4.7	4.7	0.0
W2	3242	3.0	0.0	3.0	0.0	0.0	0.0	3.0	3.0	0.0
W3	3243	1.4	0.0	1.4	0.0	0.0	0.0	1.4	1.4	0.0
W4	3244	-0.2	0.0	-0.2	0.0	0.0	0.0	0.0	-0.2	-0.2
W5	3245	-1.9	0.0	-1.9	0.0	0.0	0.0	0.0	-1.9	-1.9
W6	3246	-3.5	0.0	-3.5	0.0	0.0	0.0	0.0	-3.5	-3.5
X1	3801	4.6	-0.1	4.6	0.0	0.0	0.0	4.6	4.6	-0.1
X2	3802	3.1	-0.1	3.1	0.0	0.0	0.0	3.1	3.1	-0.1
X3	3803	1.6	0.0	1.6	0.0	0.0	0.0	1.6	1.6	0.0
X4	3804	0.1	0.0	0.1	0.0	0.0	0.0	0.1	0.1	0.0
X5	3805	-1.4	0.0	-1.4	0.0	0.0	0.0	0.0	-1.4	-1.4
X6	3806	-2.9	0.1	-2.9	0.0	0.0	0.0	0.1	-2.9	-2.9
X7	3807	-4.6	0.1	-4.6	0.0	0.0	0.0	0.1	-4.6	-4.6

*Refer to Figure 2.10.2-34 for the identification of the representative sections.

Note: Sx, Sy and Sz are normal stresses corresponding to radial, longitudinal and circumferential stresses, respectively.

Table 2.10.4-122 P_m Stresses; 30-Foot Bottom End Drop; Drop Orientation = 0 Degrees; 2-D Model; Condition 1

Condition 1: 100°F Ambient with Contents

Section*	Node - Node	Sx	Sy	Sz	Sxy	Syz	Szx	S1	S2	S3	S.I.
		Stress Components (ksi)						Principal Stresses (ksi)			
A	1 - 5	2.9	-1.3	2.9	0.0	0.0	0.0	2.9	2.9	-1.3	4.2
B	6 - 10	-3.6	-2.1	-3.6	0.0	0.0	0.0	-2.1	-3.6	-3.6	1.5
C	251 - 255	3.2	-4.3	2.2	-1.6	0.0	0.0	3.6	2.2	-4.6	8.2
D	306 - 310	-2.3	-7.3	-4.6	-1.1	0.0	0.0	-2.1	-4.6	-7.5	5.4
E	305 - 355	5.1	-5.0	1.0	-3.4	0.0	0.0	6.2	1.0	-6.1	12.3
F	251 - 281	-7.3	-3.7	3.0	-0.6	0.0	0.0	3.0	-3.6	-7.4	10.3
G	311 - 351	-3.4	-4.7	2.1	0.5	0.0	0.0	2.1	-3.2	-4.9	7.0
H	581 - 584	-0.1	-5.9	0.9	0.2	0.0	0.0	0.9	-0.1	-5.9	6.8
I	589 - 593	0.0	-4.8	0.8	0.0	0.0	0.0	0.8	0.0	-4.8	5.5
J	971 - 974	0.0	-5.4	1.2	0.0	0.0	0.0	1.2	0.0	-5.4	6.6
K	979 - 983	0.0	-4.1	0.0	0.0	0.0	0.0	0.0	0.0	-4.1	4.1
L	1601 - 1604	0.0	-4.4	1.2	0.0	0.0	0.0	1.2	0.0	-4.4	5.6
M	1609 - 1613	0.0	-3.2	0.0	0.0	0.0	0.0	0.0	0.0	-3.2	3.2
N	2216 - 2219	0.0	-3.4	1.2	0.0	0.0	0.0	1.2	0.0	-3.4	4.6
O	2224 - 2228	0.0	-2.2	0.0	0.0	0.0	0.0	0.0	0.0	-2.2	2.2
P	2546 - 2549	-0.1	-2.8	0.9	-0.1	0.0	0.0	0.9	-0.1	-2.8	3.7
Q	2554 - 2558	0.0	-1.7	0.2	0.0	0.0	0.0	0.2	0.0	-1.7	1.9
R	2771 - 2774	-0.3	-2.0	0.6	0.3	0.0	0.0	0.6	-0.2	-2.0	2.7
S	2779 - 2783	-0.8	-1.0	0.4	-0.1	0.0	0.0	0.4	-0.8	-1.1	1.5
T	7066 - 7072	0.8	-0.6	0.2	0.0	0.0	0.0	0.8	0.2	-0.6	1.4
U	3051 - 3056	0.2	-3.0	-0.4	0.2	0.0	0.0	0.2	-0.4	-3.0	3.2
V	3611 - 3617	0.0	-0.4	-0.1	-0.1	0.0	0.0	0.0	-0.1	-0.4	0.4
W	3241 - 3246	0.6	0.0	0.6	0.0	0.0	0.0	0.6	0.6	0.0	0.6
X	3801 - 3807	0.0	0.0	0.0	0.0	0.0	0.0	0.0	0.0	0.0	0.0

*Refer to Figure 2.10.2-34 for the identification of the representative sections.

Note: Sx, Sy and Sz are normal stresses corresponding to radial, longitudinal and circumferential stresses, respectively.

Table 2.10.4-123 $P_m + P_b$ Stresses; 30-Foot Bottom End Drop; Drop Orientation = 0 Degrees; 2-D Model; Condition 1

Condition 1: 100°F Ambient with Contents

			Stress Components (ksi)						Principal Stresses (ksi)			
Section*	Node - Node		Sx	Sy	Sz	Sxy	Syz	Szx	S1	S2	S3	S.I.
A I	1 -	5	21.0	-1.0	21.0	0.0	0.0	0.0	21.0	21.0	-1.0	22.0
B O	6 -	10	-19.4	-2.4	-19.4	0.0	0.0	0.0	-2.4	-19.4	-19.4	17.0
C O	251 -	255	15.9	-1.4	3.2	-1.6	0.0	0.0	16.1	3.2	-1.6	17.7
D O	306 -	310	7.9	-2.9	-2.8	-1.1	0.0	0.0	8.0	-2.8	-3.0	11.0
E I	305 -	355	15.2	-6.4	2.5	-3.4	0.0	0.0	15.7	2.5	-7.0	22.7
F I	251 -	281	-11.2	-12.4	0.1	-0.6	0.0	0.0	0.1	-10.9	-12.7	12.7
G I	311 -	351	-7.8	-11.9	-0.7	0.5	0.0	0.0	-0.7	-7.8	-12.0	11.3
H O	581 -	584	-0.1	-8.8	0.1	0.2	0.0	0.0	0.1	-0.1	-8.8	8.9
I O	589 -	593	0.0	-5.9	0.4	0.0	0.0	0.0	0.4	0.0	-5.9	6.3
J I	971 -	974	-0.1	-5.4	1.2	0.0	0.0	0.0	1.2	-0.1	-5.4	6.6
K I	979 -	983	0.0	-4.2	0.0	0.0	0.0	0.0	0.0	0.0	-4.2	4.2
L I	1601 -	1604	-0.1	-4.4	1.2	0.0	0.0	0.0	1.2	-0.1	-4.4	5.6
M O	1609 -	1613	0.0	-3.2	0.0	0.0	0.0	0.0	0.0	0.0	-3.2	3.2
N I	2216 -	2219	-0.1	-3.4	1.2	0.0	0.0	0.0	1.2	-0.1	-3.4	4.6
O I	2224 -	2228	0.0	-2.2	0.0	0.0	0.0	0.0	0.0	0.0	-2.2	2.2
P O	2546 -	2549	0.0	-3.5	0.7	-0.1	0.0	0.0	0.7	0.0	-3.5	4.2
Q O	2554 -	2558	0.0	-1.9	0.1	0.0	0.0	0.0	0.1	0.0	-1.9	2.1
R I	2771 -	2774	-0.3	-4.6	0.0	0.3	0.0	0.0	0.0	-0.2	-4.6	4.6
S I	2779 -	2783	-2.1	-2.8	-0.3	-0.1	0.0	0.0	-0.3	-2.0	-2.8	2.5
T O	7066 -	7072	0.1	-2.0	-0.4	0.0	0.0	0.0	0.1	-0.4	-2.0	2.1
U I	3051 -	3056	-0.7	-11.2	0.3	0.2	0.0	0.0	0.3	-0.7	-11.2	11.4
V O	3611 -	3617	-0.6	0.4	-1.8	-0.1	0.0	0.0	0.4	-0.6	-1.8	2.2
W I	3241 -	3246	4.7	0.0	4.7	0.0	0.0	0.0	4.7	4.7	0.0	4.7
X O	3801 -	3807	-4.5	0.1	-4.5	0.0	0.0	0.0	0.1	-4.5	-4.5	4.7

*Refer to Figure 2.10.2-34 for the identification of the representative sections.

Note: Sx, Sy and Sz are normal stresses corresponding to radial, longitudinal and circumferential stresses, respectively.

Table 2.10.4-124 Critical P_m Stress Summary: 30-Foot Bottom End Drop; Drop Orientation = 0 Degrees; 2-D Model; Condition 1

Condition 1: 100°F Ambient with Contents

Comp. No.*	Section Cut Node-Node	P_m Stresses (ksi) Sx	Sy	Sz	Sxy	Syz	Szx	Principal Stresses (ksi) S1	S2	S3	S.I.	Allow. Stress	Margin of Safety
1	306- 310	-2.3	-7.3	-4.6	-1.1	0.0	0.0	-2.1	-4.6	-7.5	5.4	51.5	8.5
2	305- 355	5.1	-5.0	1.0	-3.4	0.0	0.0	6.2	1.0	-6.1	12.3	46.3	2.8
3	416- 419	-0.1	-4.7	5.6	-0.6	0.0	0.0	5.6	0.0	-4.8	10.4	66.2	5.4
4	851- 854	0.0	-5.6	1.2	0.0	0.0	0.0	1.2	0.0	-5.6	6.8	46.0	5.8
5	544- 548	0.0	-4.8	1.4	-0.1	0.0	0.0	1.4	0.0	-4.8	6.2	46.0	6.4
6	7064- 2774	0.0	3.8	1.7	0.4	0.0	0.0	3.8	1.7	0.0	3.9	45.2	10.7
7	3021- 3026	0.2	-8.0	-1.7	-0.2	0.0	0.0	0.2	-1.7	-8.0	8.3	48.0	4.8
8	3621- 3627	0.0	-0.6	-0.2	-0.1	0.0	0.0	0.0	-0.2	-0.6	0.6	94.5	144.7

Locations of the most critical sections for each component are provided in the following:

Comp. No.*	Section Location: Inside Node X (in)	Inside Node Y (in)	Outside Node X (in)	Outside Node Y (in)
1	39.44	6.20	39.44	0.75
2	39.44	8.20	43.35	8.20
3	35.50	18.40	37.50	18.40
4	35.50	47.40	37.00	47.40
5	40.70	26.40	43.35	26.40
6	37.655	179.40	37.50	175.40
7	37.655	179.40	37.655	185.40
8	33.705	188.40	33.705	193.71

*Refer to Figure 2.10.2-33 for cask component identification.

Note: The X (radial) and Y (longitudinal) are global cartesian coordinate axes. Sx, Sy and Sz are normal stresses corresponding to radial, longitudinal and the circumferential stresses, respectively.

Table 2.10.4-125 Critical $P_m + P_b$ Stress Summary; 30-Foot Bottom End Drop; Drop Orientation = 0 Degrees; 2-D Model; Condition 1

Condition 1: 100°F Ambient with Contents

Comp. No.*	Section Cut Node-Node	$P_m + P_b$ Stresses (ksi) Sx	Sy	Sz	Sxy	Syz	Szx	Principal Stresses (ksi) S1	S2	S3	S.I.	Allow. Stress	Margin of Safety
1	16- 20	-19.3	-2.2	-19.3	-0.1	0.0	0.0	-2.2	-19.3	-19.3	17.1	73.6	3.3
2	305- 355	15.2	-6.4	2.5	-3.4	0.0	0.0	15.7	2.5	-7.0	22.7	66.2	1.9
3	416- 419	-0.1	-10.5	4.2	-0.6	0.0	0.0	4.2	-0.1	-10.5	14.7	94.6	5.4
4	851- 854	-0.1	-5.7	1.2	0.0	0.0	0.0	1.2	-0.1	-5.7	6.9	65.7	8.5
5	544- 548	0.0	-5.6	1.1	-0.1	0.0	0.0	1.1	0.0	-5.6	6.7	65.8	8.8
6	7064- 2774	2.6	12.2	3.3	0.4	0.0	0.0	12.2	3.3	2.6	9.6	64.6	5.7
7	3021- 3026	0.1	12.2	-0.1	-0.2	0.0	0.0	12.2	0.1	-0.1	12.3	71.0	4.8
8	3801- 3807	-4.5	0.1	-4.5	0.0	0.0	0.0	0.1	-4.5	-4.5	4.7	135.0	28.0

Locations of the most critical sections for each component are provided in the following:

Section Location

Comp. No.*	Inside Node X (in)	Inside Node Y (in)	Outside Node X (in)	Outside Node Y (in)
1	1.42	6.20	1.42	0.75
2	39.44	8.20	43.35	8.20
3	35.50	18.40	37.50	18.40
4	35.50	47.40	37.00	47.40
5	40.70	26.40	43.35	26.40
6	37.655	179.40	37.50	175.40
7	37.655	179.40	37.655	185.40
8	0.0	188.46	0.0	193.71

*Refer to Figure 2.10.2-33 for cask component identification.

Note: The X (radial) and Y (longitudinal) are global cartesian coordinate axes. Sx, Sy Sz are normal stresses corresponding to radial, longitudinal and the circumferential stresses, respectively.

Table 2.10.4-130 Primary Stresses; 30-Foot Side Drop; Drop Orientation = 90 Degrees; 3-D Model; 0-Degree Circumferential Location; Condition 1

Condition 1: 100°F Ambient with Contents

Stress Points		Stress Components (ksi)						Principal Stresses (ksi)		
Section*	Node	Sx	Sy	Sz	Sxy	Syz	Szx	S1	S2	S3
A1	1130	-0.8	-1.9	-0.3	-0.1	0.1	0.0	-0.3	-0.7	-1.9
A2	1129	-1.0	-3.2	0.0	-0.1	0.1	0.0	0.0	-1.0	-3.2
A3	1128	-1.3	-4.4	0.3	0.0	0.1	0.0	0.3	-1.3	-4.4
B1	1185	-1.1	-5.3	0.0	-0.1	0.0	-0.2	0.0	-1.1	-5.3
B2	1184	-0.3	-6.0	0.0	-0.1	0.0	-0.2	0.1	-0.4	-6.0
B3	1183	0.4	-6.7	0.0	-0.1	0.1	-0.2	0.5	-0.1	-6.7
C1	90	5.9	-2.4	15.3	0.0	-0.8	1.5	15.6	5.7	-2.5
C2	80	-2.4	-7.0	6.6	-0.1	-0.5	0.0	6.6	-2.4	-7.0
C3	70	-3.5	-8.6	2.2	0.1	-0.4	-0.8	2.3	-3.6	-8.6
C4	60	-4.6	-9.5	0.3	0.2	-0.2	-0.5	0.4	-4.7	-9.5
C5	50	-9.8	-11.5	-0.1	0.2	-0.1	-0.1	-0.1	-9.8	-11.6
C6	40	-12.0	-12.5	-0.1	0.2	0.0	0.0	-0.1	-12.0	-12.6
D1	25	-4.9	-9.6	5.6	0.3	-0.1	0.1	5.6	-4.9	-9.6
D2	15	-9.8	-11.4	1.8	0.1	-0.1	-0.5	1.9	-9.8	-11.4
D3	5	-10.8	-11.6	0.4	0.2	0.0	-0.4	0.4	-10.8	-11.7
E1	35	-10.5	-11.4	4.9	0.2	-0.2	1.6	5.0	-10.6	-11.5
E2	34	-7.5	-11.5	2.1	0.3	0.0	1.8	2.5	-7.8	-11.5
E3	33	-8.0	-12.4	-0.3	0.3	0.0	1.5	0.0	-8.2	-12.4
E4	32	-8.6	-13.4	-2.8	0.4	0.0	0.9	-2.7	-8.7	-13.4
E5	31	-8.8	-14.3	-5.4	0.4	0.0	0.5	-5.3	-8.8	-14.3
F1	100	-1.3	-2.3	23.1	0.0	-1.2	2.3	23.4	-1.5	-2.4
F2	99	-1.5	-8.1	2.3	0.4	-0.9	2.5	3.5	-2.6	-8.2
F3	98	-0.5	-11.3	-11.0	0.8	-0.7	3.3	0.5	-10.7	-12.6
F4	97	0.6	-17.8	-36.7	1.3	-0.7	3.9	1.1	-17.8	-37.1
G1	94	0.8	-2.3	21.3	0.2	-0.5	3.3	21.8	0.3	-2.3
G2	93	1.5	-5.9	7.1	0.5	-0.3	2.4	8.0	0.6	-6.0
G3	92	1.5	-7.1	2.4	0.6	-0.3	1.0	3.1	0.9	-7.1
G4	91	0.7	-8.6	-3.1	0.7	-0.2	0.4	0.8	-3.1	-8.7
H1	330	-0.3	7.3	-4.6	-0.5	-1.6	0.1	7.6	-0.3	-4.8
H2	329	-0.1	9.1	-0.8	-0.6	-1.5	0.0	9.4	-0.2	-1.0
H3	328	0.1	10.8	2.9	-0.7	-1.5	-0.2	11.1	2.7	0.0
H4	327	0.2	12.8	7.4	-0.8	-1.4	-0.5	13.1	7.1	0.1
I1	244	-0.2	-0.4	4.8	0.0	-0.8	0.0	5.0	-0.2	-0.5
I2	243	-0.1	1.2	7.4	-0.1	-0.7	0.0	7.5	1.2	-0.1
I3	242	-0.1	2.8	10.0	-0.2	-0.5	0.0	10.0	2.7	-0.1
I4	241	0.0	4.2	12.5	-0.3	-0.4	0.0	12.6	4.3	0.0
J1	550	-0.3	7.9	10.8	-0.6	-0.8	0.0	11.0	7.7	-0.4
J2	548	-0.2	10.3	12.7	-0.8	-0.8	0.0	12.9	10.2	-0.2
J3	547	-0.1	12.7	14.5	-0.9	-0.7	0.0	14.8	12.5	-0.1
K1	344	-0.1	-1.3	11.2	0.0	-0.5	0.0	11.2	-0.1	-1.3
K2	342	-0.1	2.5	13.0	-0.2	-0.4	0.0	13.0	2.5	-0.1
K3	341	0.0	6.0	14.7	-0.5	-0.3	0.0	14.7	6.0	-0.1

Table 2.10.4-130 Primary Stresses; 30-Foot Side Drop; Drop Orientation = 90 Degrees; 3-D Model; 0-Degree Circumferential Location; Condition 1 (continued)

Stress Points		Stress Components (ksi)						Principal Stresses (ksi)		
Section*	Node	Sx	Sy	Sz	Sxy	Syz	Szx	S1	S2	S3
L1	740	-0.1	4.8	16.7	0.3	0.0	-0.2	16.7	4.8	-0.1
L2	738	-0.6	7.7	18.3	-1.2	0.0	0.0	18.3	7.8	-0.7
L3	737	0.2	10.7	20.0	-2.6	0.0	0.0	20.0	11.3	-0.4
M1	663	-1.3	-2.5	13.9	0.1	0.0	0.0	13.9	-1.3	-2.5
M2	63	0.5	9.3	19.3	2.2	0.0	0.0	19.3	9.8	0.0
N1	1877	-0.3	7.6	9.2	-0.6	1.0	0.0	9.6	7.2	-0.4
N2	1477	-0.2	10.4	10.9	-0.8	0.9	0.0	11.6	9.7	-0.2
N3	1277	-0.1	13.0	12.7	-1.0	0.9	0.0	13.8	12.0	-0.1
O1	647	-0.1	-1.7	12.7	0.1	0.4	0.0	12.7	-0.1	-1.7
O2	247	-0.1	2.4	14.6	-0.2	0.3	0.0	14.6	2.4	-0.1
O3	47	0.0	6.1	16.5	-0.5	0.2	0.0	16.5	6.2	-0.1
P1	1840	-0.3	7.6	-4.4	-0.5	1.6	0.0	7.8	-0.3	-4.6
P2	1640	-0.2	9.5	-1.2	-0.7	1.6	0.0	9.8	-0.2	-1.4
P3	1440	0.0	11.4	1.9	-0.7	1.5	0.1	11.7	1.7	0.0
P4	1240	0.2	13.5	5.6	-0.9	1.5	0.4	13.8	5.4	0.1
Q1	628	-0.3	0.4	8.4	-0.1	0.7	0.1	8.5	0.3	-0.3
Q2	428	-0.2	2.3	10.7	-0.2	0.6	0.1	10.7	2.3	-0.2
Q3	228	-0.1	4.1	12.9	-0.3	0.4	0.1	12.9	4.2	-0.1
Q4	28	0.0	5.9	15.2	-0.4	0.3	0.1	15.2	5.9	-0.1
R1	1816	-1.0	-7.5	5.9	0.5	1.1	-0.2	6.0	-1.0	-7.6
R2	1616	-2.0	-9.2	-1.2	0.6	1.0	-0.5	-0.9	-2.1	-9.4
R3	1416	-4.8	-11.1	-7.4	0.7	0.7	-2.1	-3.6	-8.2	-11.4
R4	1216	-6.4	-13.1	-15.7	0.8	0.4	-4.3	-4.6	-13.1	-17.5
S1	616	2.8	-4.3	1.3	0.2	0.6	-0.2	2.8	1.3	-4.4
S2	416	0.4	-3.3	6.4	0.2	0.5	-0.1	6.4	0.4	-3.4
S3	216	0.4	-1.7	11.1	0.1	0.3	0.3	11.1	0.4	-1.7
S4	16	0.2	-0.2	15.6	0.0	0.2	0.2	15.6	0.2	-0.2
T1	811	-19.4	-21.7	-19.3	0.9	0.5	-5.4	-13.9	-21.4	-25.0
T2	611	-9.6	-14.7	-5.4	0.7	0.4	-4.5	-2.5	-12.2	-14.9
T3	411	-4.5	-10.8	2.5	0.5	0.3	-3.3	3.8	-5.7	-10.8
T4	211	-1.0	-7.6	9.5	0.5	0.2	-1.8	9.8	-1.3	-7.6
T5	11	0.2	-4.2	20.0	0.3	0.1	-0.9	20.0	0.2	-4.2
U1	43058	6.9	0.4	-0.1	0.2	0.0	-0.1	6.9	0.4	-0.1
U2	43057	3.3	-0.9	-0.4	0.2	0.0	-0.1	3.3	-0.4	-0.9
U3	43056	1.0	-2.0	-1.0	0.1	0.0	-0.1	1.0	-1.1	-2.0
U4	43055	-0.6	-2.9	-1.9	0.1	0.0	-0.4	-0.4	-2.0	-3.0
U5	43054	-2.3	-3.9	-2.7	0.1	-0.1	-1.3	-1.1	-3.8	-3.9
U6	43053	-4.1	-4.9	-3.2	0.1	-0.2	-2.7	-0.9	-4.9	-6.4
U7	43052	-7.0	-5.6	-1.6	0.0	-0.3	-3.4	0.0	-5.6	-8.6
U8	43051	-13.1	-7.3	0.2	-0.1	0.0	-0.1	0.2	-7.3	-13.1
V1	50024	2.4	-1.4	0.1	0.1	0.0	0.0	2.4	0.1	-1.4
V2	50023	-3.7	-4.3	-0.8	0.1	0.0	0.1	-0.8	-3.7	-4.3
V3	50022	-6.9	-6.0	-0.6	0.1	0.0	0.1	-0.6	-6.0	-6.9

Table 2.10.4-130 Primary Stresses; 30-Foot Side Drop; Drop Orientation = 90 Degrees; 3-D Model; 0-Degree Circumferential Location; Condition 1 (continued)

Stress Points		Stress Components (ksi)						Principal Stresses (ksi)		
Section*	Node	Sx	Sy	Sz	Sxy	Syz	Szx	S1	S2	S3
V4	50021	-17.1	-9.5	0.6	-0.1	0.0	0.0	0.6	-9.5	-17.1
W1	43278	-2.1	-2.8	0.1	-0.1	-0.2	0.2	0.1	-2.1	-2.8
W2	43274	-1.4	-3.2	0.0	0.0	-0.2	0.2	0.0	-1.4	-3.2
W3	43271	-0.3	-1.8	0.0	0.0	-0.3	0.1	0.0	-0.4	-1.9
X1	50084	-0.7	-5.6	0.0	-0.1	0.0	0.2	0.1	-0.7	-5.6
X2	50083	-0.3	-5.9	0.0	-0.1	0.0	0.2	0.1	-0.4	-5.9
X3	50081	0.4	-6.6	0.0	0.0	-0.1	0.2	0.5	-0.1	-6.6

*Refer to Figure 2.10.2-34 for the identification of the representative sections.

Note: Stresses are in the cylindrical coordinate system.

Table 2.10.4-131 P_m Stresses; 30-Foot Side Drop; Drop Orientation = 90 Degrees; 3-D Model; 0-Degree Circumferential Location; Condition 1

Condition 1: 100°F Ambient with Contents

			Stress Components (ksi)						Principal Stresses (ksi)			
Section*	Node	- Node	Sx	Sy	Sz	Sxy	Syz	Szx	S1	S2	S3	S.I.
A	1130	- 1128	-1.0	-3.2	0.0	-0.1	0.1	0.0	0.0	-1.0	-3.2	3.1
B	1185	- 1183	-0.3	-6.0	0.0	-0.1	0.0	-0.2	0.1	-0.4	-6.0	6.0
C	90	- 40	-5.9	-9.5	2.2	0.1	-0.3	-0.2	2.2	-5.9	-9.5	11.7
D	25	- 5	-8.8	-11.0	2.4	0.2	-0.1	-0.3	2.4	-8.8	-11.0	13.4
E	35	- 31	-8.5	-12.4	0.1	0.3	0.0	1.4	0.3	-8.6	-12.5	12.7
F	100	- 97	-0.8	-9.8	-5.2	0.6	-0.8	3.0	0.7	-6.4	-10.1	10.8
G	94	- 91	1.2	-6.2	6.2	0.5	-0.3	1.8	6.8	0.7	-6.2	13.0
H	330	- 327	0.0	10.0	1.2	-0.7	-1.5	-0.1	10.3	1.0	-0.1	10.4
I	244	- 241	-0.1	2.0	8.7	-0.1	-0.6	0.0	8.8	1.9	-0.1	8.9
J	550	- 547	-0.2	10.3	12.7	-0.8	-0.8	0.0	12.9	10.1	-0.2	13.2
K	344	- 341	-0.1	2.4	13.0	-0.2	-0.4	0.0	13.0	2.4	-0.1	13.1
L	740	- 737	-0.3	7.7	18.3	-1.2	0.0	0.0	18.3	7.9	-0.4	18.8
M	663	- 63	-0.4	3.4	16.6	1.1	0.0	0.0	16.6	3.7	-0.7	17.3
N	1877	- 1277	-0.2	10.3	10.9	-0.8	0.9	0.0	11.6	9.7	-0.2	11.9
O	647	- 47	-0.1	2.3	14.6	-0.2	0.3	0.0	14.6	2.3	-0.1	14.7
P	1840	- 1240	-0.1	10.5	0.4	-0.7	1.5	0.1	10.8	0.3	-0.2	11.0
Q	628	- 28	-0.2	3.2	11.8	-0.3	0.5	0.1	11.8	3.2	-0.2	12.0
R	1816	- 1216	-3.5	-10.2	-4.5	0.7	0.8	-1.6	-2.3	-5.5	-10.4	8.1
S	616	- 16	0.8	-2.4	8.6	0.1	0.4	0.1	8.7	0.8	-2.5	11.1
T	811	- 11	-6.2	-11.5	1.7	0.6	0.3	-3.2	2.9	-7.2	-11.6	14.5
U	43058	- 43051	-2.9	-3.8	-1.4	0.1	-0.1	-1.2	-0.7	-3.6	-3.8	3.0
V	50024	- 50021	-6.1	-5.2	-0.3	0.1	0.0	0.0	-0.3	-5.2	-6.1	5.7
W	43278	- 43271	-1.3	-2.7	0.0	0.0	-0.2	0.2	0.1	-1.3	-2.8	2.8
X	50084	- 50081	-0.1	-6.1	0.0	0.0	0.0	0.2	0.1	-0.3	-6.1	6.2

*Refer to Figure 2.10.2-34 for the identification of the representative sections.

Note: Stresses are in the cylindrical coordinate system.

Table 2.10.4-132 $P_m + P_b$ Stresses; 30-Foot Side Drop; Drop Orientation = 90-Degrees; 3-D Model; 0-Degree Circumferential Location; Condition 1

Condition 1: 100°F Ambient with Contents

Section*	Node - Node	Stress Components (ksi) Sx	Sy	Sz	Sxy	Syz	Szx	Principal Stresses (ksi) S1	S2	S3	S.I.
A O	1130 - 1128	-1.3	-4.4	0.3	0.0	0.1	0.0	0.3	-1.3	-4.4	4.7
B O	1185 - 1183	0.4	-6.7	0.0	-0.1	0.1	-0.2	0.5	-0.1	-6.7	7.2
C I	90 - 40	1.0	-5.7	7.3	0.0	-0.6	0.0	7.3	1.0	-5.7	13.1
D I	25 - 5	-5.9	-10.0	5.0	0.2	-0.1	-0.1	5.0	-5.9	-10.0	15.0
E I	35 - 31	-8.8	-10.8	5.3	0.3	-0.1	2.0	5.5	-9.1	-10.9	16.4
F O	100 - 97	0.3	-16.9	-32.8	1.2	-0.6	3.8	0.8	-16.9	-33.3	34.1
G I	94 - 91	1.3	-3.3	17.2	0.3	-0.5	3.4	17.9	0.6	-3.3	21.2
H O	330 - 327	0.2	12.7	7.1	-0.8	-1.4	-0.4	13.0	6.8	0.1	12.9
I O	244 - 241	0.0	4.3	12.6	-0.3	-0.4	0.0	12.6	4.3	0.0	12.6
J O	550 - 547	-0.1	12.7	14.6	-0.9	-0.7	0.0	14.8	12.5	-0.1	14.9
K O	344 - 341	0.0	6.1	14.7	-0.5	-0.3	0.0	14.7	6.1	-0.1	14.8
L O	740 - 737	-0.1	10.6	20.0	-2.6	0.0	0.0	20.0	11.2	-0.7	20.7
M O	663 - 63	0.5	9.3	19.3	2.2	0.0	0.0	19.3	9.8	0.0	19.3
N O	1877 - 1277	-0.1	13.0	12.7	-1.0	0.9	0.0	13.8	12.0	-0.1	13.9
O O	647 - 47	0.0	6.2	16.5	-0.5	0.2	0.0	16.5	6.2	-0.1	16.6
P O	1840 - 1240	0.2	13.4	5.4	-0.8	1.5	0.3	13.7	5.2	0.1	13.6
Q O	628 - 28	0.0	6.0	15.2	-0.4	0.3	0.1	15.2	6.0	0.0	15.2
R I	1816 - 1216	-0.5	-7.4	5.9	0.5	1.2	0.5	6.1	-0.5	-7.5	13.6
S O	616 - 16	-0.3	-0.3	15.8	0.0	0.2	0.4	15.8	-0.2	-0.3	16.1
T O	811 - 11	3.2	-3.4	19.6	0.3	0.1	-0.8	19.6	3.1	-3.4	23.0
U O	43058 - 43051	-11.9	-7.5	-1.7	-0.1	-0.2	-2.5	-1.1	-7.5	-12.5	11.4
V O	50024 - 50021	-14.8	-9.0	0.0	0.0	0.0	0.1	0.0	-9.0	-14.8	14.7
W I	43278 - 43271	-2.2	-3.2	0.1	-0.1	-0.1	0.2	0.1	-2.2	-3.3	3.4
X O	50084 - 50081	0.4	-6.6	0.0	0.0	-0.1	0.2	0.5	0.1	-6.6	7.1

*Refer to Figure 2.10.2-34 for the identification of the representative sections.

Note: Stresses are in the cylindrical coordinate system.

Table 2.10.4-133 Critical P_m Stress Summary; 30-Foot Side Drop; Drop Orientation = 90 Degrees 3-D Model; Condition 1

Condition 1: 100°F Ambient with Contents

Comp. No.*	Section Cut Node-Node	P_m Stresses (ksi) Sx	Sy	Sz	Sxy	Syz	Szx	Principal Stresses (ksi) S1	S2	S3	S.I.	Allow. Stress	Margin of Safety
1	25- 5	-8.8	-11.0	2.4	0.2	-0.1	-0.3	2.4	-8.8	-11.0	13.4	51.5	2.8
2	16140-16137	0.0	1.5	1.1	0.0	-12.4	-0.2	13.7	0.0	-11.1	24.[illegible]	46.3	0.9
3	14340-14337	-0.1	3.9	0.7	0.2	-15.4	-0.1	17.8	-0.1	-13.2	31.0	66.2	1.1
4	14520-14517	-0.1	3.7	0.9	0.0	-10.7	0.0	13.1	-0.1	-8.5	21.6	46.0	1.1
5	662- 62	0.2	2.9	16.7	-2.6	0.0	0.1	16.7	4.5	-1.4	18.0	46.0	1.6
6	401- 1	-10.7	-35.5	0.1	1.8	0.2	1.6	0.4	-10.8	-35.6	36.0	45.2	0.3
7	43071-43031	-12.0	-6.9	-0.5	-0.1	-0.2	-2.0	-0.1	-6.9	-12.3	12.2	49.7	3.1
8	51501-51504	-4.5	-3.3	3.2	0.2	0.1	0.1	3.2	-3.3	-4.6	7.8	94.5	11.[illegible]

Locations of the most critical sections for each component are provided in the following:

Comp. No.*	Section Location: Inside Node x (in)	y (deg)	z (in)	Outside Node x (in)	y (deg)	z (in)
1	39.44	0.0	6.20	39.44	0.0	0.75
2	35.50	79.4	17.40	37.50	79.4	17.40
3	35.50	67.7	29.90	37.00	67.7	29.90
4	35.50	67.7	47.40	37.00	67.7	47.40
5	40.70	0.0	99.50	43.35	0.0	99.50
6	40.88	0.0	193.71	43.35	0.0	193.71
7	33.71	0.0	185.40	36.46	0.0	185.40
8	40.88	180.0	193.71	40.88	180.0	188.40

*Refer to Figure 2.10.2-33 for cask component identification.

Note: The x (radial), y (circumferential) and z (longitudinal) are global cylindrical coordinate axes. Stresses are in the cylindrical coordinate system.

Table 2.10.4-134 Critical $P_m + P_b$ Stress Summary; 30-Foot Side Drop; Drop Orientation = 90 Degrees; 3-D Model; Condition 1

Condition 1: 100°F Ambient with Contents

Comp. No.*	Section Cut Node-Node	$P_m + P_b$ Stresses (ksi) Sx	Sy	Sz	Sxy	Syz	Szx	Principal Stresses (ksi) S1	S2	S3	S.I.	Allow. Stress	Margin of Safety
1	25- 5	-5.9	-10.0	5.0	0.2	-0.1	-0.1	5.0	-5.9	-10.0	15.0	73.6	3.9
2	100- 97	0.3	-16.9	-32.8	1.2	-0.6	3.8	0.8	-16.9	-33.3	34.1	66.2	0.9
3	12350-12347	-0.2	6.0	-0.7	0.0	-16.0	-0.1	18.9	-0.2	-13.7	32.6	94.6	1.9
4	14520-14517	-0.2	6.4	1.9	0.0	-11.4	0.0	15.7	-0.2	-7.5	23.2	65.7	1.8
5	662- 62	0.5	8.5	19.6	-2.9	0.0	0.0	19.6	9.5	-0.4	20.0	65.8	2.3
6	403- 3	-7.4	-27.7	21.2	1.5	0.5	3.4	21.6	-7.7	-27.8	49.4	64.6	0.3
7	43001-43008	-20.3	-7.0	10.0	-0.7	0.3	1.0	10.1	-7.0	-20.3	30.4	71.0	1.3
8	51501-51504	-13.3	-7.9	4.9	0.7	0.0	0.8	4.9	-7.8	-13.5	18.4	135.0	6.3

Locations of the most critical sections for each component are provided in the following:

Section Location

Comp. No.*	Inside Node x (in)	Inside Node y (deg)	Inside Node z (in)	Outside Node x (in)	Outside Node y (deg)	Outside Node z (in)
1	39.44	0.0	6.20	39.44	0.0	0.75
2	35.50	0.0	15.00	37.50	0.0	15.00
3	35.50	56.5	30.40	37.00	56.5	30.40
4	35.50	67.7	142.40	37.00	67.7	142.40
5	40.70	0.0	99.50	43.35	0.0	99.50
6	40.88	0.0	190.15	43.35	0.0	190.15
7	39.53	0.0	185.40	39.53	0.0	179.40
8	40.88	180.0	193.71	40.88	180.0	188.40

*Refer to Figure 2.10.2-33 for cask component identification.

Note: The x (radial), y (circumferential) and z (longitudinal) are global cylindrical coordinate axes. Stresses are in the cylindrical coordinate system.

Table 2.10.4-152 Primary Stresses: 30-Foot Bottom Corner Drop; Drop Orientation = 24 Degrees; 3-D Bottom Model; 0-Degree Circumferential Location; Condition 1

Condition 1: 100°F Ambient with Contents

Stress Points		Stress Components (ksi)						Principal Stresses (ksi)		
Section*	Node	Sx	Sy	Sz	Sxy	Syz	Szx	S1	S2	S3
A1	1130	17.5	13.4	-6.5	-0.5	2.1	2.1	17.7	13.6	-6.9
A2	1129	2.2	-0.1	-1.2	0.0	1.5	2.1	3.3	0.5	-2.9
A3	1128	-13.0	-13.6	4.1	0.5	2.0	2.1	4.6	-13.2	-13.9
B1	1185	10.1	3.3	-6.5	-0.5	2.5	2.3	10.4	3.9	-7.3
B2	1184	-3.6	-7.8	-1.9	0.0	1.8	2.3	0.0	-4.9	-8.4
B3	1183	-17.5	-18.8	2.7	0.4	1.9	2.3	3.1	-17.8	-19.0
C1	90	-19.6	-5.7	-24.9	-1.2	-0.7	-5.1	-5.6	-16.6	-28.1
C2	80	-8.8	-1.6	-14.4	-1.0	-0.5	-4.2	-1.4	-6.7	-16.7
C3	70	-5.7	-1.1	-9.1	-0.5	-0.4	-3.8	-1.1	-3.3	-11.6
C4	60	-3.0	-1.2	-5.4	-0.1	-0.4	-3.6	-0.3	-1.2	-8.1
C5	50	6.5	-4.1	-3.5	1.0	-0.2	-2.5	7.2	-4.1	-4.2
C6	40	13.7	-5.5	-3.5	1.6	-0.1	-1.5	14.0	-3.7	-5.6
D1	25	-30.3	-22.9	-31.9	-0.4	-0.6	-8.4	-22.6	-23.0	-39.5
D2	15	-6.7	-18.5	-14.8	0.6	-0.3	-3.8	-5.1	-16.3	-18.5
D3	5	0.5	-22.3	-7.5	1.4	-0.1	-1.2	0.7	-7.6	-22.4
E1	35	10.5	-8.3	-21.9	1.3	-0.4	-3.8	11.0	-8.4	-22.4
E2	34	1.8	-8.9	-17.5	0.7	-0.8	-7.4	4.3	-9.0	-20.0
E3	33	-5.2	-9.1	-11.1	0.3	-0.7	-7.8	0.2	-9.1	-16.5
E4	32	-6.7	-8.4	-6.7	0.1	-0.4	-4.8	1.9	-8.4	-11.5
E5	31	-7.3	-7.6	-2.5	0.0	-0.3	-2.9	-1.1	-7.6	-8.6
F1	100	-0.1	-2.1	-32.9	-0.1	-0.9	-3.2	0.2	-2.1	-33.2
F2	99	-2.8	1.0	-18.9	-0.4	-0.8	-1.6	1.1	-2.7	-19.1
F3	98	-2.8	2.3	-13.4	-0.5	-0.4	1.0	2.4	-2.7	-13.6
F4	97	0.1	4.6	-8.0	-0.4	-0.4	2.0	4.6	0.5	-8.5
G1	94	0.3	-2.6	-24.2	0.1	-0.4	-1.1	0.4	-2.6	-24.3
G2	93	-0.6	-0.3	-14.8	-0.1	-0.4	-0.5	-0.2	-0.6	-14.9
G3	92	-1.1	1.3	-8.4	-0.2	-0.2	0.1	1.3	-1.1	-8.4
G4	91	-0.5	3.5	-0.7	-0.3	-0.1	0.1	3.5	-0.5	-0.8
H1	330	-0.3	4.0	-13.1	-0.3	-1.0	-0.1	4.1	-0.3	-13.2
H2	329	-0.5	3.8	-16.1	-0.3	-0.9	0.0	3.9	-0.5	-16.1
H3	328	-0.5	3.7	-18.8	-0.3	-0.8	0.6	3.8	-0.5	-18.9
H4	327	-0.5	2.9	-24.3	-0.2	-0.7	1.3	3.0	-0.4	-24.4
I1	244	0.0	1.8	-10.1	-0.1	-0.4	-0.1	1.8	0.0	-10.1
I2	243	0.0	2.3	-10.1	-0.2	-0.4	-0.1	2.3	0.0	-10.1
I3	242	0.0	2.7	-9.9	-0.2	-0.3	-0.1	2.8	0.0	-9.9
I4	241	0.0	3.2	-9.9	-0.2	-0.2	-0.1	3.2	0.0	-9.9
J1	550	-0.1	2.5	-10.8	-0.2	-0.7	0.0	2.5	-0.2	-10.8
J2	548	-0.1	4.9	-9.9	-0.4	-0.6	0.0	4.9	-0.1	-9.9
J3	547	0.0	7.1	-9.0	-0.5	-0.6	0.0	7.2	-0.1	-9.0
K1	344	-0.1	-0.3	-7.6	0.0	-0.3	0.0	-0.1	-0.3	-7.6
K2	342	0.0	1.2	-7.0	-0.1	-0.3	0.0	1.2	0.0	-7.0
K3	341	0.0	2.5	-6.4	-0.2	-0.2	0.0	2.6	0.0	-6.5

Table 2.10.4-152 Primary Stresses; 30-Foot Bottom Corner Drop; Drop Orientation = 24 Degrees; 3-D Bottom Model; 0-Degree Circumferential Location; Condition 1 (continued)

Stress Points		Stress Components (ksi)						Principal Stresses (ksi)		
Section*	Node	Sx	Sy	Sz	Sxy	Syz	Szx	S1	S2	S3
L1	740	0.1	2.4	-2.9	0.4	-0.2	-0.1	2.4	0.0	-2.9
L2	738	-0.3	4.7	-2.0	-0.9	-0.2	0.0	4.8	-0.5	-2.0
L3	737	0.3	7.2	-0.9	-2.1	-0.2	0.0	7.8	-0.3	-0.9
M1	454	-0.1	-0.9	-3.9	-0.6	-0.2	0.0	0.2	-1.2	-3.9
M2	452	0.2	0.9	-3.2	-0.3	-0.2	0.0	1.0	0.1	-3.2
M3	451	-0.2	2.4	-2.7	0.0	-0.2	-0.1	2.4	-0.2	-2.7
N1	810	-0.1	3.5	-1.4	-0.2	0.2	0.0	3.5	-0.1	-1.4
N2	807	-0.1	6.3	-0.1	-0.4	0.1	0.0	6.3	-0.1	-0.1
O1	524	0.0	-0.7	-1.2	0.0	-0.1	0.0	0.0	-0.6	-1.2
O2	521	0.0	2.0	0.1	-0.1	-0.1	0.0	2.0	0.1	0.0
P1	850	0.0	3.5	-4.0	-0.2	0.4	-0.1	3.6	0.0	-4.0
P2	847	-0.1	5.3	-1.3	-0.3	0.3	0.0	5.4	-0.1	-1.3
Q1	564	0.0	-0.2	-0.2	0.0	0.0	0.0	0.0	-0.2	-0.3
Q2	561	0.0	1.5	0.7	-0.1	0.0	0.0	1.5	0.7	0.0
R1	890	-1.0	-0.2	1.5	0.0	0.2	-0.2	1.5	-0.2	-1.0
R2	887	-1.2	-1.7	-5.2	0.1	0.1	-0.5	-1.1	-1.7	-5.2
S1	604	-0.4	0.3	0.4	0.0	0.0	-0.4	0.6	0.3	-0.6
S2	601	0.0	0.7	0.5	-0.1	-0.1	-0.1	0.7	0.5	0.0
T1	897	0.5	-0.3	-1.6	0.0	0.1	-0.2	0.6	-0.3	-1.6
T2	614	0.3	0.2	0.0	0.0	0.0	-0.4	0.5	0.3	-0.3
T3	611	-0.1	0.1	0.0	0.0	-0.1	-0.2	0.2	0.1	-0.3
U1	900	0.7	0.1	-0.4	0.0	0.1	0.1	0.7	0.1	-0.5
U2	910	0.5	-0.2	-0.4	0.0	0.0	0.1	0.5	-0.2	-0.4
V1	920	-0.2	-0.4	-0.3	0.1	0.0	0.1	-0.1	-0.4	-0.4
V2	930	-0.5	-1.0	-0.2	0.2	0.0	0.1	-0.1	-0.5	-1.0
W1	1216	1.2	2.3	-1.0	0.0	0.0	-0.2	2.3	1.2	-1.0
W2	1226	-0.3	-0.1	0.5	0.0	-0.1	-0.1	0.5	-0.1	-0.3
X1	1236	0.1	0.0	-0.6	0.0	-0.1	-0.1	0.1	0.0	-0.6
X2	1246	-1.5	-2.4	1.1	-0.1	0.0	-0.2	1.1	-1.5	-2.5

*Refer to Figure 2.10.2-34 for the identification of the representative sections.

Note: The x (radial), y (circumferential) and z (longitudinal) are global cylindrical coordinate axes. Stresses are in the cylindrical coordinate system.

Table 2.10.4-153 P_m Stresses; 30-Foot Bottom Corner Drop; Drop Orientation = 24 Degrees; 3-D Bottom Model; 0-Degree Circumferential Location; Condition 1

Condition 1: 100°F Ambient with Contents

			Stress Components (ksi)						Principal Stresses (ksi)			
Section*	Node - Node		Sx	Sy	Sz	Sxy	Syz	Szx	S1	S2	S3	S.I.
A	1130 -	1128	2.2	-0.1	-1.2	0.0	1.8	2.1	3.4	0.6	-3.1	6.4
B	1185 -	1183	-3.7	-7.8	-1.9	0.0	2.0	2.3	0.0	-4.9	-8.5	8.5
C	90 -	40	-0.5	-2.9	-7.6	0.2	-0.4	-3.2	0.8	-2.9	-8.8	9.6
D	25 -	5	-10.8	-20.5	-17.2	0.5	-0.3	-4.3	-8.6	-19.4	-20.6	12.0
E	35 -	31	-1.3	-8.6	-12.6	0.5	-0.6	-5.8	1.2	-8.6	-15.1	16.3
F	100 -	97	-1.9	1.5	-17.6	-0.4	-0.6	-0.4	1.6	-1.9	-17.6	19.2
G	94 -	91	-0.[illegible]	0.5	-11.9	-0.1	-0.3	-0.3	0.5	-0.6	-11.9	12.4
H	330 -	327	-0.[illegible]	3.7	-17.9	-0.3	-0.9	0.4	3.7	-0.5	-17.9	21.6
I	244 -	241	0.[illegible]	2.5	-10.0	-0.2	-0.3	-0.1	2.5	0.0	-10.0	12.5
J	550 -	547	-0.1	4.8	-9.9	-0.4	-0.6	0.0	4.9	-0.1	-9.9	14.8
K	344 -	341	0.0	1.1	-7.0	-0.1	-0.3	0.0	1.2	0.0	-7.0	8.2
L	740 -	737	-0.1	4.7	-1.9	-0.9	-0.2	0.0	4.9	-0.2	-1.9	6.8
M	454 -	451	0.0	0.9	-3.2	-0.3	-0.2	0.0	0.9	-0.1	-3.2	4.2
N	810 -	807	-0.1	4.9	-0.8	-0.3	0.2	0.0	4.9	-0.1	-0.8	5.7
O	524 -	521	0.0	0.7	-0.6	0.0	-0.1	0.0	0.7	0.0	-0.6	1.3
P	850 -	847	0.0	4.4	-2.6	-0.2	0.4	0.0	4.5	-0.1	-2.6	7.1
Q	564 -	561	0.0	0.6	0.2	0.0	0.0	0.0	0.6	0.2	0.0	0.7
R	890 -	887	-1.1	-1.0	-1.8	0.0	0.2	-0.3	-0.9	-1.0	-2.0	1.1
S	604 -	601	-0.2	0.5	0.4	0.0	0.0	-0.2	0.5	0.5	-0.3	0.8
T	614 -	611	0.1	0.2	0.0	0.0	-0.1	-0.3	0.4	0.2	-0.3	0.6
U	900 -	910	0.6	-0.1	-0.4	0.0	0.1	0.1	0.6	-0.1	-0.5	1.1
V	920 -	930	-0.4	-0.7	-0.2	0.1	0.0	0.1	-0.1	-0.4	-0.7	0.6
W	1216 -	1226	0.5	1.1	-0.3	0.0	0.0	-0.2	1.1	0.5	-0.3	1.4
X	1236 -	1246	-0.7	-1.2	0.3	-0.1	0.0	-0.2	0.3	-0.7	-1.2	1.5

*Refer to Figure 2.10.2-34 for the identification of the representative sections.

Note: The x (radial), y (circumferential) and z (longitudinal) are global cylindrical coordinate axes. Stresses are in the cylindrical coordinate system.

Table 2.10.4-154 $P_m + P_b$ Stresses; 30-Foot Bottom Corner Drop; Drop Orientation = 24 Degrees; 3-D Bottom Model; 0-Degree Circumferential Location; Condition 1

Condition 1: 100°F Ambient with Contents

		Stress Components (ksi)						Principal Stresses (ksi)			
Section*	Node - Node	Sx	Sy	Sz	Sxy	Syz	Szx	S1	S2	S3	S.I.
A I	1130 - 1128	17.5	13.4	-6.5	-0.5	1.8	2.1	17.7	13.5	-6.8	24.5
B O	1185 - 1183	-17.5	-18.8	2.7	0.4	1.7	2.3	3.1	-17.7	-19.0	22.1
C I	90 - 40	-14.1	-1.4	-15.6	-1.3	-0.6	-4.7	-1.3	-10.1	-19.7	18.5
D O	25 - 5	4.6	-20.3	-5.0	1.4	0.0	-0.7	4.7	-5.1	-20.3	25.1
E I	35 - 31	8.2	-8.9	-23.1	1.2	-0.7	-6.6	9.6	-9.0	-24.4	34.1
F I	100 - 97	-2.0	-1.5	-29.1	-0.2	-1.0	-3.3	-1.4	-1.7	-29.5	28.1
G I	94 - 91	-0.1	-2.4	-23.2	0.0	-0.5	-1.0	-0.1	-2.4	-23.2	23.2
H O	330 - 327	-0.6	3.2	-23.1	-0.2	-0.7	1.1	3.3	-0.5	-23.2	26.5
I O	244 - 241	0.0	3.2	-9.8	-0.2	-0.2	-0.1	3.2	0.0	-9.9	13.1
J O	550 - 547	0.0	7.1	-9.0	-0.5	-0.6	0.0	7.2	-0.1	-9.0	16.2
K O	344 - 341	0.0	2.6	-6.4	-0.2	-0.2	0.0	2.6	0.0	-6.4	9.0
L O	740 - 737	0.0	7.1	-0.9	-2.1	-0.2	0.0	7.7	-0.5	-0.9	8.6
M O	454 - 451	-0.1	2.5	-2.6	0.0	-0.2	0.0	2.5	-0.1	-2.6	5.1
N O	810 - 807	-0.1	6.3	-0.1	-0.4	0.1	0.0	6.3	-0.1	-0.1	6.4
O O	524 - 521	0.0	2.0	0.1	-0.1	-0.1	0.0	2.0	0.1	0.0	2.1
P I	850 - 847	0.0	3.5	-4.0	-0.2	0.4	-0.1	3.6	0.0	-4.0	7.6
Q O	564 - 561	0.0	1.5	0.7	-0.1	0.0	0.0	1.5	0.7	0.0	1.5
R O	890 - 887	-1.2	-1.7	-5.2	0.1	0.1	-0.5	-1.1	-1.7	-5.2	4.1
S I	604 - 601	-0.4	0.3	0.4	0.0	0.0	-0.4	0.6	0.3	-0.6	1.1
T I	614 - 611	0.3	0.2	0.0	0.0	0.0	-0.4	0.5	0.3	-0.3	0.8
U I	900 - 910	0.7	0.1	-0.4	0.0	0.1	0.1	0.7	0.1	-0.5	1.2
V O	920 - 930	-0.5	-1.0	-0.2	0.2	0.0	0.1	-0.1	-0.5	-1.0	0.9
W I	1216 - 1226	1.2	2.3	-1.0	0.0	0.0	-0.2	2.3	1.2	-1.0	3.3
X O	1236 - 1246	-1.5	-2.4	1.1	-0.1	0.0	-0.2	1.1	-1.5	-2.5	3.6

*Refer to Figure 2.10.2-34 for the identification of the representative sections.

Note: The x (radial), y (circumferential) and z (longitudinal) are global cylindrical coordinate axes. Stresses are in the cylindrical coordinate system.

Table 2.10.4-155 Critical P_m Stress Summary; 30-Foot Bottom Corner Drop; Drop Orientation = 24 Degrees; 3-D Bottom Model; Condition 1

Condition 1: 100°F Ambient with Contents

Comp. No.*	Section Cut Node-Node	P_m Stresses (ksi) Sx	Sy	Sz	Sxy	Syz	Szx	Principal Stresses (ksi) S1	S2	S3	S.I.	Allow. Stress	Margin of Safety
1	27- 7	-13.0	-17.0	-3.7	0.1	-0.5	-6.2	-0.6	-16.1	-17.0	16.4	51.5	2.1
2	10140-10137	0.0	6.4	-12.9	0.0	-6.6	-0.8	8.5	0.0	-14.9	23.4	46.3	1.0
3	10160-10157	0.0	6.9	-12.5	0.0	-6.6	-0.6	8.9	0.0	-14.6	23.5	66.2	1.8
4	12520-12517	-0.1	3.0	-9.7	0.0	-7.6	0.0	6.5	-0.1	-13.3	19.8	46.0	1.3
5	12204-12201	-0.2	2.6	-9.7	0.0	-4.4	-0.2	4.0	-0.2	-11.1	15.1	46.0	2.0
6	14880-14877	-0.1	1.7	-0.8	-0.1	3.3	0.1	4.0	-0.1	-3.1	7.1	45.2	5.3
7	16900-16910	-0.2	0.5	-0.8	-0.1	0.6	0.2	0.7	-0.1	-1.1	1.8	48.0	25.2
8	1236- 1246	-0.7	-1.2	0.3	-0.1	0.0	-0.2	0.3	-0.7	-1.2	1.5	94.5	60.7

Locations of the most critical sections for each component are provided in the following:

Section Location

Comp. No.*	Inside Node x (in)	y (deg)	z (in)	Outside Node x (in)	y (deg)	z (in)
1	37.50	0.0	6.20	37.50	0.0	0.75
2	35.50	45.9	17.40	37.50	45.9	17.40
3	35.50	45.9	18.90	37.50	45.9	18.90
4	35.50	56.5	47.40	37.00	56.5	47.40
5	40.70	56.5	26.40	43.35	56.5	26.40
6	35.50	67.7	172.40	37.50	67.7	172.40
7	35.50	79.4	179.40	35.50	79.4	185.40
8	0.0	0.0	187.40	0.0	0.0	193.71

*Refer to Figure 2.10.2-33 for cask component identification.

Note: The x (radial), y (circumferential) and z (longitudinal) are global cylindrical coordinate axes. Stresses are in the cylindrical coordinate system.

Table 2.10.4-156 Critical $P_m + P_b$ Stress Summary; 30-Foot Bottom Corner Drop; Drop Orientation = 24 Degrees; 3-D Bottom Model; Condition 1

Condition 1: 100°F Ambient with Contents

		$P_m + P_b$ Stresses (ksi)						Principal Stresses (ksi)					Margin
Comp. No.*	Section Cut Node-Node	Sx	Sy	Sz	Sxy	Syz	Szx	S1	S2	S3	S.I.	Allow. Stress	of Safety
1	1170- 1168	-44.2	-33.1	-4.6	-0.1	-0.1	-0.1	-4.6	-33.1	-44.2	39.6	73.6	0.9
2	14035-14031	9.1	-3.6	-21.0	5.2	-8.6	-5.2	12.9	-3.6	-24.8	37.7	66.2	0.8
3	10150-10147	-0.1	4.6	-21.5	0.0	-7.9	-0.7	6.8	-0.1	-23.7	30.5	94.6	2.1
4	12520-12517	-0.1	5.0	-9.1	0.0	-8.0	0.0	8.6	-0.1	-12.8	21.4	65.7	2.1
5	10204-10201	-0.3	2.9	-10.6	0.0	-4.3	-0.2	4.2	-0.3	-11.9	16.0	65.8	3.1
6	14880-14877	-0.1	1.7	-1.8	-0.1	4.0	0.1	4.3	-0.1	-4.4	8.7	64.6	6.4
7	1216- 1226	1.2	2.3	-1.0	0.0	0.0	-0.2	2.3	1.2	-1.0	3.3	71.0	20.3
8	1236- 1246	-1.5	-2.4	1.1	-0.1	0.0	-0.2	1.1	-1.5	-2.5	3.6	135.0	36.5

Locations of the most critical sections for each component are provided in the following:

Section Location

	Inside Node			Outside Node		
Comp. No.*	x (in)	y (deg)	z (in)	x (in)	y (deg)	z (in)
1	14.73	0.0	6.20	14.73	0.0	0.75
2	39.44	67.7	8.20	43.35	67.7	8.20
3	35.50	45.9	18.15	37.50	45.9	18.15
4	35.50	56.5	47.40	37.00	56.5	47.40
5	40.70	45.9	26.40	43.35	45.9	26.40
6	35.50	67.7	172.40	37.50	67.7	172.40
7	0.0	0.0	179.40	0.0	0.0	185.40
8	0.0	0.0	187.40	0.0	0.0	193.71

*Refer to Figure 2.10.2-33 for cask component identification.

Note: The x (radial), y (circumferential) and z (longitudinal) are global cylindrical coordinate axes. Stresses are in the cylindrical coordinate system.

11.2.4.6.1 Buckling Analysis

U.S. NRC Comment

The effects of the lead slump stress needs to be included in all of the load conditions. This requires the use of the unbonded SCANS analyses for all accident load cases. The inner shell stress levels will be higher than the values given in the TSAR when the correct lead modulus is used in the accident analyses. If SCANS is not used with the built-in lead properties for this analysis, an elastic-plastic analysis using the lead stress-strain curve of NUREG/CR-0481 and an acceptable finite element program will be required.

NAC Response

As discussed in the response to Comment 11.2.4.3.2, rigorous finite element analyses using the ANSYS computer program have been prepared for the NAC-STC. The effects of the lead slump stress are calculated in all of the ANSYS evaluations. The axial, hoop, and in-plane shear components of the primary plus secondary stresses, as determined by the ANSYS analyses, are the input data for the buckling evaluation of the NAC-STC. The ANSYS analysis results are compared to those from the quarter-scale model drop tests for the outer shell in the NAC Response to Comment 11.2.4.9. The buckling evaluation of the NAC-STC inner shell and transition sections is performed by an NAC proprietary computer program in accordance with ASME Code Case N-284. The documentation of the NAC-STC adequacy in satisfying the buckling criteria is presented in the NAC-STC SAR Section 2.10.5. The results of the buckling evaluation are summarized in Table 2.10.5-1 of the SAR.

Appendix B

Pertinent pages copied from the NAC-STC SAR for reference purposes.

2.10.5 Inner Shell Buckling Analysis

Code Case N-284 (Metal Containment Shell Buckling Design Methods) of the "ASME Boiler and Pressure Vessel Code" is used to analyze the NAC-STC inner shell and transition sections for structural stability. Structural stability ensures that the inner shell and transition sections do not buckle during cask fabrication, normal conditions of transport, or hypothetical accident conditions. The buckling evaluation requirements of Regulatory Guide 7.6, Paragraph C.5, are shown to be satisfied by the results of the interaction equation calculations of Code Case N-284.

The inner shell buckling design criteria, specifically the criteria of Code Case N-284, are described in detail in Section 2.1.3.4.

2.10.5.1 Buckling Analysis

The structural stability analysis of the NAC-STC inner shell and transition sections is performed by an NAC proprietary computer program in accordance with the ASME Code Case N-284. The data considered for an ASME Code Case N-284 buckling evaluation includes shell geometry parameters, shell fabrication tolerances, shell material properties, theoretical elastic buckling stress values for the shell, and primary plus secondary (P + Q) stresses at the sections of the shell to be evaluated. The axial, hoop, and in-plane shear components of the P + Q stresses in the inner shell and in the transition sections are obtained from the ANSYS finite element analyses for each of the normal conditions of transport and hypothetical accident conditions. Since the inner shell and the transition sections of the primary containment vessel are different materials and have different operating temperatures, a separate buckling evaluation is performed for the inner shell and for the transition sections. The fixity provided by the thick end forgings precludes buckling in the regions of the inner shell immediately adjacent to the forgings.

Nodal P + Q stress components are conservatively used for the buckling evaluation of the inner shell and the transition sections of the NAC-STC for the heat condition, the cold condition, all of the 1-foot drop conditions, the 30-foot top and bottom end drops, the 30-foot side drop, and the 30-foot top and bottom corner drops (nodal stresses include any peaking effects that are present at the node location). Sectional P + Q stress components, as required by ASME Code Case N-284, are used for the buckling evaluation of the inner shell and the transition sections of the NAC-STC for the 30-foot top and bottom 75-degree oblique drops and for the 30-foot bottom 15-degree oblique drop. For each load condition evaluated, the maximum compressive axial stress component calculated anywhere in the inner shell is combined with the maximum compressive hoop stress component calculated anywhere in the inner shell and the maximum in-plane shear stress component calculated anywhere in the inner shell; this produces a grossly conservative, bounding case buckling evaluation of the inner shell. The same analysis is used in the buckling evaluation of the transition sections. The stress component values used in the buckling evaluations are documented in Table 2.10.5-1.

The maximum normal conditions transport temperature in the inner shell is determined to be 356°F. The maximum temperature in the transition sections is determined to be 306°F. Therefore, a temperature of 356°F is used to determine the values of the modulus of elasticity and yield stress to be used in the buckling evaluation of the Type 304 stainless steel inner shell. Similarily, a temperature of 306°F is used for the transition sections.

2.10.5.2 Analysis Results

The results of the buckling evaluation of the NAC-STC inner shell and transition sections are summarized in Table 2.10.5-1. All interaction equations yield values less than 1.0. Also, there are no concentrated loads on the inner shell or transition sections that would lead to localized buckling. Therefore, the buckling criteria of Code Case N-284 are satisfied and it is concluded that buckling of the NAC-STC inner shell and transition sections will not occur.

2.10.5.3 Verification of the Code Case N-284 Buckling Evaluation of the NAC-STC Inner Shell and Transition Sections

The results of the proprietary NAC computer program that performs the Code Case N-284 buckling evaluation are verified by a hand calculation of load case "J_T" (Table 2.10.5-1). This step-by-step analysis procedure reflects the procedure diagrammed in paragraph-1800 of Code Case N-284. The geometry parameters for the NAC-STC inner shell and transition sections are defined in Table 2.10.5-2.

Step 1

For load case "J_T", the compressive stresses from Table 2.10.5-1 are:

$$S_\phi = 16{,}445 \text{ psi}$$

$$S_\theta = 10{,}356 \text{ psi}$$

$$S_{\phi\theta} = 14{,}515 \text{ psi}$$

Step 2

For accident conditions, the factor of safety (FS) is 1.34. Multiplying the stress components by this factor of safety yields:

$$FS\left(S_\phi\right) = 22{,}036 \text{ psi}$$

$$FS\left(S_\theta\right) = 13{,}877 \text{ psi}$$

$$FS\left(S_{\phi\theta}\right) = 19{,}450 \text{ psi}$$

Step 3

Capacity reduction factors, calculated per Section 2.1.3.4.3, are provided in Table 2.10.5-3, and are as follows for the load case "J_T" transition section temperature of 300°F:

$\alpha_{\phi L} = 0.403$

$\alpha_{\theta L} = 0.8$

$\alpha_{\phi\theta L} = 0.8$

In order to directly use the capacity reduction factors from Table 2.10.5-3, the tolerance requirements of Article NE-4220 of the "ASME Boiler and Pressure Vessel Code," Subsection NE must be satisfied. Article NE-4221.1 and Article NE-4221.2 set forth the "maximum difference in cross-sectional diameters" and "maximum deviation from true theoretical form for external pressure". Table 2.10.5-4 shows that the requirements of Articles NE-4221.1 and NE-4221.2 are satisfied, as long as the maximum tolerances and configuration constraints are met during manufacturing.

Step 4

Plasticity reduction factors are determined using the equations presented in Section 2.1.3.4.4 as follows (S_y available from Table 2.10.5-5):

1. Axial Compression

$S_\phi(FS)/S_y = (22,036)/(43,620) = 0.5052$

$\eta_\phi = 1.0$

2. Hoop Compression

$S_\theta(FS)/S_y = (13,877)/(43,620) = 0.3181$

$\eta_\theta = 1.0$

3. Shear

$S_{\phi\theta}(FS)/S_y = (19,450)/(43,620) = 0.4459$

$\eta_{\phi\theta} = 1.0$

From Section-1600 of Code Case N-284, as an upper limit, the compressive stresses, S_i ($i = \phi$ or θ), must be less than the yield strength, S_y, divided by the appropriate factor of safety ($S_i < S_y/FS$). Similarly, for shear, $S_{\phi\theta}$ must be less than or equal to 0.6 S_y divided by the appropriate factor of safety ($S_{\phi\theta} \leq 0.6\ S_y/FS$). As stated in Section 2.1.3.4.1, there is a factor of safety of 2.0 for normal transport conditions and a factor of safety of 1.34 for hypothetical accident conditions. Table 2.10.5-6 presents the elastic upper bound compressive and shear stresses, evaluated using normal and accident condition factors of safety. Under no circumstances can the elastic values presented in the table be exceeded. However, satisfying these limits alone is not sufficient to demonstrate that buckling will not occur. As stated in Section 2.1.3.4.1, the interaction equations must also be satisfied.

Step 5

Compute elastic stress components per the following equation:

$$S_{is} = S_i(FS)/\alpha_{iL}$$

$$S_{\phi s} = S_\phi(FS)/\alpha_{\phi L} = (22{,}036)/(0.403) = 54{,}680 \text{ psi}$$

$$S_{\theta s} = S_\theta(FS)/\alpha_{\theta L} = (13{,}877)/(0.8) = 17{,}346 \text{ psi}$$

$$S_{\phi\theta s} = S_{\phi\theta}(FS)/\alpha_{\phi\theta L} = (19{,}450)/(0.8) = 24{,}313 \text{ psi}$$

Step 6

Compute inelastic stress components per the following equation:

$$S_{ip} = S_{is}/\eta_i$$

$$S_{\phi p} = S_{\phi s}/\eta_\phi = (54{,}680)/(1.0) = 54{,}680 \text{ psi}$$

$$S_{\theta p} = S_{\theta s}/\eta_\theta = (17{,}346)/(1.0) = 17{,}346 \text{ psi}$$

$$S_{\phi\theta p} = S_{\phi\theta s}/\eta_{\phi\theta} = (24{,}313)/(1.0) = 24{,}313 \text{ psi}$$

Step 7

For the NAC-STC, the buckling evaluation approach, consistent with the vessel design and method of analysis, is that of paragraph-1710 of Code Case N-284.

Step 8

Theoretical uniaxial buckling values are available from Section 2.1.3.4.2. For the transition section at 300°F, these theoretical values are as follows (Table 2.10.5-7 and Table 2.10.5-8):

$S_{\phi eL}$ = 368,435 psi

$S_{\theta eL} = S_{reL}$ = 49,155 psi

S_{heL} = 47,927 psi

$S_{\phi\theta eL}$ = 176,487 psi

Applicable elastic and inelastic interaction equations in paragraph-1713.1.1 and paragraph-1713.2.1 of Code Case N-284 are checked as follows:

1. Elastic Buckling (Paragraph-1713.1.1, Code Case N-284)

   a. Axial Compression Plus Hoop Compression

   $\left(S_{\phi s} < 0.5\ S_{\theta s}\right)$

   54,680 > (0.5)(17,346); therefore, not applicable.

   b. Axial Compression Plus Hoop Compression

   $\left(S_{\phi s} \geq 0.5\ S_{\theta s}\right)$

   $\left[\left(S_{\phi s} - 0.5\ S_{heL}\right)/\left(S_{\phi eL} - 0.5\ S_{heL}\right)\right] + \left(S_{\theta s}/S_{heL}\right)^2 \leq 1.0$

$$\frac{54,680 - (0.5)(48,465)}{668,435 - (0.5)(48,465)} + (17,346/48,465)^2 \le 1.0$$

$$0.1754 \le 1.0$$

therefore,

$$Q1 = 0.1754 < 1.0.$$

c. Axial Compression Plus Shear

$$\left(S_{\phi s}/S_{\phi eL}\right) + \left(S_{\phi\theta s}/S_{\phi\theta eL}\right)^2 \le 1.0$$

$$(54,680/668,435) + (24,313/176,487)^2 \le 1.0$$

$$0.101 \le 1.0$$

therefore,

$$Q2 = 0.101 < 1.0$$

d. Hoop Compression Plus Shear

$$\left(S_{\theta s}/S_{reL}\right) + \left(S_{\phi\theta s}/S_{\phi\theta eL}\right)^2 \le 1.0$$

$$(17,346/49,165) + (24,313/176,487)^2 \le 1.0$$

$$0.372 \le 1.0$$

therefore,

$$Q3 = 0.372 < 1.0$$

e. Axial Compression Plus Hoop Compression Plus Shear

$$K = 1 - \left(S_{\phi\theta s}/S_{\phi\theta eL}\right)^2 = 1 - (24,313/176,487)^2 = 0.981$$

and, therefore, Equation B (above) becomes:

$$\frac{54,680 - (0.5)(0.981)(48,465)}{(668,435)(0.981) - (0.5)(0.981)(48,465)} + [(17,346/(0.981)(48,465)]^2 = 0.182$$

therefore,

$Q4 = 0.182 < 1.0$

2. Inelastic Buckling (Paragraph-1713.2.1, Code Case N-284)

a. Axial Compression Plus Shear

$$\left(S_{\phi p}/S_{\phi eL}\right)^2 + \left(S_{\phi\theta p}/S_{\phi\theta eL}\right)^2 \le 1.0$$

$$(54,680/668,435)^2 + (24,313/176,487)^2 \le 1.0$$

$$0.026 \le 1.0$$

therefore,

$Q5 = 0.026 < 1.0$

b. Hoop Compression Plus Shear

$$\left(S_{\theta p}/S_{reL}\right)^2 + \left(S_{\phi\theta p}/S_{\phi\theta eL}\right)^2 \le 1.0$$

$$(17,346/49,155)^2 + (24,313/176,487)^2 \le 1.0$$

$$0.144 \le 1.0$$

therefore,

$Q6 = 0.144 < 1.0$

The results of the hand calculation of load case "J_T" are identical to the results in Table 2.10.5-1 that were calculated by the NAC proprietary computer program, which performs the Code Case N-284 buckling evaluation. Thus, the computer program results in Table 2.10.5-1 and the buckling stability of the NAC-STC inner shell are verified.

Table 2.10.5-1 Buckling Evaluation Results NAC-STC Inner Shell

Load Case	Load Condition	Analysis Section Location	Axial Stress (psi)	Hoop Stress (psi)	Inplane Shear Stress (psi)	Elastic Buckling Interaction Equations Q1	Q2	Q3	Q4	Plastic Buckling Interactions Equations Q5	Q6
A_{IS}	Heat	Inner Shell	-1634	-830	322	.00	.02	.04	.00	.00	.00
B_{IS}	Cold	Inner Shell	-321	-3838	315	.00	.00	.19	.00	.00	.04
C_{IS}	1-Ft Top End	Inner Shell	-5755	-2867	0	.09	.04	.29	.09	.00	.08
D_{IS}	1-Ft Bottom End	Inner Shell	-5938	-2864	0	.10	.04	.30	.10	.00	.09
E_{IS}	1-Ft Side	Inner Shell	-4911	-1829	4338	04	.07	.10	.04	.01	.01
F_{IS}	1-Ft Top Corner	Inner Shell	-6729	-937	3029	.06	.10	.05	.07	.02	.00
G_{IS}	1-Ft Bottom Corner	Inner Shell	-6819	-847	-2945	.07	.10	.04	.07	.02	.00
H_{IS}	30-Ft Top End	Inner Shell	-10409	-2705	0	.07	.10	.09	.07	.03	.01
I_{IS}	30-Ft Bottom End	Inner Shell	-10649	-2679	0	.08	.10	.09	.08	.03	.01
J_{IS}	30-Ft Side	Inner Shell	-9836	-7346	9724	.12	.10	.26	.13	.08	.13
K_{IS}	30-Ft Top Corner	Inner Shell	-16021	-2484	8083	.13	.16	.09	.13	.72	.02
L_{IS}	30-Ft Bottom Corner	Inner Shell	-15916	-2154	-7853	.13	.16	.08	.13	.65	.01
M_{IS}	30-Ft Top Obliq. (75°)	Inner Shell	-9659	-6848	9460	.11	.10	.24	.12	.07	.11
N_{IS}	30-Ft Bott. Obliq. (15°)	Inner Shell	-16170	-1595	-6427	.13	.16	.06	.13	.81	.01
O_{IS}	30-Ft Bott. Obliq. (75°)	Inner Shell	-10161	-5650	-9286	.10	.10	.20	.10	.07	.08

Table 2.10.5-1 Buckling Evaluation Results NAC-STC Inner Shell - Continued

Load Case	Load Condition	Analysis Section Location	Axial Stress (psi)	Hoop Stress (psi)	Inplane Shear Stress (psi)	Elastic Buckling Interaction Equations Q1	Q2	Q3	Q4	Plastic Buckling Interactions Equations Q5	Q6
A_T	Heat	Transition	-2956	-5218	-694	.00	.02	.26	.00	.00	.07
B_T	Cold	Transition	-2988	-4135	503	.00	.02	.21	.00	.00	.04
C_T	1-Ft Top End	Transition	-2960	-5727	0	.00	.02	.29	.00	.00	.08
D_T	1-Ft Bottom End	Transition	-2955	-6581	0	.00	.02	.33	.00	.00	.11
E_T	1-Ft Side	Transition	-7482	-3994	6037	.06	.06	.21	.06	.01	.05
F_T	1-Ft Top Corner	Transition	-9626	-1473	3679	.04	.08	.07	.04	.01	.01
G_T	1-Ft Bottom Corner	Transition	-10422	-1704	-3467	.05	.08	.09	.05	.01	.01
H_T	30-Ft Top End	Transition	-2984	-14144	0	.00	.01	.48	.00	.00	.23
I_T	30-Ft Bottom End	Transition	-2973	-14362	0	.00	.01	.48	.00	.00	.23
J_T	30-Ft Side	Transition	-16445	-10356	14515	.17	.16	.37	.18	.03	.14
K_T	30-Ft Top Corner	Transition	-26632	-898	9400	.10	.14	.04	.10	.13	.01
L_T	30-Ft Bottom Corner	Transition	-27565	-2122	-9183	.11	.14	.08	.11	.17	.01
M_T	30-Ft Top Obliq. (75°)	Transition	-13488	-9023	15240	.13	.09	.32	.13	.02	.11
N_T	30-Ft Bott. Obliq. (15°)	Transition	-30799	-1935	-7402	.12	.16	.07	.13	.47	.01
O_T	30-Ft Bott. Obliq. (75°)	Transition	-17164	-10107	-15101	.17	.10	.36	.18	.03	.14

Table 2.10.5-2 Geometry Parameters for the NAC-STC Inner Shell and Transition Sections

Parameter	Inner Shell	Transition Section*
R = radius (in) [to centerline of shell]	36.25	36.25
t = thickness (in)	1.5	1.50
$(Rt)^{0.5}$	7.37	7.37
L_ϕ = length (in)	161.00	161.00
$L_\theta = 2\pi R$ = circumference (in)	227.8	227.8
$M_\phi = L_\phi/(Rt)^{0.5}$	21.83	21.83
$M_\theta = L_\theta/(Rt)^{0.5}$	30.89	30.89
M = lesser of M_ϕ or M_θ	21.83	21.83
ν = Poisson's Ratio	0.275	0.275

*Conservatively consider the thinner portion of the Transition Section.

Table 2.10.5-3 Capacity Reduction Factors for the NAC-STC Inner Shell and Transition Sections

Capacity Reduction Factor	Temperature (°F) 70	300	356
(SA-240, Type 304 Stainless Steel)			
$\alpha_{\phi L}$ (axial)	0.267	0.207	0.207
$\alpha_{\theta L}$ (hoop)	0.8	0.8	0.8
$\alpha_{\phi\theta L}$ (shear)	0.8	0.8	0.8
(SA-240, Type XM-19 Stainless Steel)			
$\alpha_{\phi L}$ (axial)	0.517	0.403	0.392
$\alpha_{\theta L}$ (hoop)	0.8	0.8	0.8
$\alpha_{\phi\theta L}$ (shear)	0.8	0.8	0.8

Table 2.10.5-4 Fabrication Tolerances for the NAC-STC Inner Shell

Requirement	Parameter	Inner Shell Data (in)
	Maximum Inside Diameter (I.D.)	71.06
	Minimum I.D.	70.96
	Nominal I.D.	71.00
NE-4221.1	a) (Max I.D. - Min I.D.)	0.10
	b) (0.01) x (Nominal I.D.)	0.710
	Tolerance Check (a < b)	Yes (0.10 in < 0.710 in)
	Nominal Shell Thickness	1.50
	Minimum Shell Thickness	1.48
	Shell Length	161.00
	Nominal Shell Outside Diameter (O.D.)	74.00
	Minimum Shell O.D.	73.92
NE-4221.2	c) Permissible Deviation, e (Figure -4221.2-1)	0.54
	d) Actual Deviation*	0.04
	Tolerance Check (d < c)	Yes (0.04 in < 0.54 in)

* (Nominal O.D. - Minimum O.D.)/2 = (74.00 - 73.92)/2 = 0.04

Table 2.10.5-5 Material Properties for Buckling Analysis Input

Parameter*/Temperature (°F)	70	300	356
(SA-240, Type 304 Stainless Steel)			
E (psi)	28.3×10^6	27.0×10^6	26.7×10^6
S_y (psi)	30.0×10^3	22.7×10^3	21.9×10^3
(SA-240, Type XM-19 Stainless Steel)			
E (psi)	28.3×10^6	27.0×10^6	26.7×10^6
S_y (psi)	55.0×10^3	43.6×10^3	42.6×10^3

* Section 2.3.2

Table 2.10.5-6 Upper Bound Buckling Stress

Load Condition		70°F	300°F	356°F
(SA-240, Type 304 Stainless Steel)				
Elastic, Upper Bound Compressive Stress S_θ or S_ϕ (psi)	Normal	15,000	11,320	10,960
	Accident	22,390	16,900	16,343
Elastic, Upper Bound In-Plane Shear Stress $S_{\theta\phi}$ (psi)	Normal	9,000	6,795	6,580
	Accident	13,434	10,140	9,806
(SA-240, Type XM-19 Stainless Steel)				
Elastic, Upper Bound Compressive Stress S_θ or S_ϕ (psi)	Normal	27,500	21,800	21,300
	Accident	41,040	32,550	31,790
Elastic, Upper Bound In-Plane Shear Stress $S_{\theta\phi}$ (psi)	Normal	16,500	13,080	12,780
	Accident	24,620	19,530	19,070

Table 2.10.5-7 Theoretical Elastic Buckling Stress Values (Temperature Independent Form)

Elastic Buckling Stress	Inner Shell	Load Description
$S_{\phi eL}$	0.025035E	axial
$S_{\theta eL} = S_{reL}$	0.001841E	hoop, without end pressure
S_{heL}	0.001795E	hoop, with end pressure
$S_{\phi\theta eL}$	0.00661E	shear

Table 2.10.5-8 Theoretical Elastic Buckling Stresses for Selected Temperatures (SA-240, Type 304 and SA-240, Type XM-19 Stainless Steel)

Parameter	Theoretical Elastic Buckling Stress (psi)	Transition Section	Inner Shell
Modulus of Elasticity	T = 70°F $E = 28.3 \times 10^6$	T = 300°F $E = 27.0 \times 10^6$	T = 356°F $E = 26.7 \times 10^6$
$S_{\phi eL}$	708,490	675,945	668,435
$S_{\theta eL} = S_{reL}$	52,100	49,710	49,155
S_{heL}	50,800	48,465	47,927
$S_{\phi\theta eL}$	187,060	178,470	176,487

11.2.4.7.2 Analysis Consideration

U.S. NRC Comment

(a) The statement: "The fuel assembly loads are transmitted in direct compression through the tube wall to the web structure of each support disk", indicates that the borated aluminum tubes play a structural role in the basket. Please include the tubes in all basket structural analyses.

(b) If the borated aluminum tubes fail, are there criticality concerns due to the exposed fuel rods between the support disks?

(c) Although the side drop is probably the most critical load case for the basket support disks, the end and corner drops should be addressed. Reasons for omitting the analyses should be provided.

NAC Response

(a) Refer to the NAC Response to Comment 3.3.1; based on the requirement of the Transportation Branch of the U.S. NRC that no credit be taken for the strength of "borated aluminum alloy" because no code, standard, or specification for its fabrication exists, the fuel tubes are conservatively not considered in the structural evaluation of the NAC-STC fuel basket, other than to transmit direct compressive load through the wall of the tube. As documented in the NAC Response to Comment 3.3.1, the "borated aluminum alloy" fuel tubes do possess good strength characteristics; the following classical stress analyses are presented to conservatively demonstrate the substantial margins of safety that exist for the fuel tubes for the 10 CFR 71 30-foot drop accident conditions (the storage drop accident conditions are much less severe).

30-Foot Bottom End Drop

During a 30-foot bottom end drop accident, the fuel tubes are loaded axially by their own weight. The direct compressive stresses will develop in the fuel tubes. The design load for analysis is the tube weight multiplied by an equivalent static deceleration factor of 56.1g (Table 2.6.7.4-3, NAC-STC SAR).

It is noted that the lateral pressures, produced by the fuel assembly and the support disks, will restrain the fuel tube wall from buckling. Only the direct compressive stresses are evaluated.

Tube Weight: $W = [(9.073)^2 - (8.653)^2](160.0)(0.102) = 121.50$ lb

Design Load: $W_d = (121.50)(56.1) = 6816.2$ lb

Cross-Sectional Area of Tube: $A = (9.073)^2 - (8.653)^2 = 7.44\ in^2$

The calculated compressive stress is:

$$S_c = \frac{W_d}{A} = 916 \text{ psi}$$

The allowable compressive stress is equal to the yield stress of "borated" 6351-T54 aluminum alloy at 450°F (NAC Response to Comment 3.3.1).

$$S_c' = S_{cy} = 12900 \text{ psi}$$

$$M.S. = \frac{S_c'}{S_c} - 1 = \underline{\underline{+Large}}$$

Therefore, the fuel tubes are structurally adequate for a 30-foot drop bottom end impact accident condition.

30-Foot Side Drop

During a 30-foot side drop accident, the impact load on a tube due to the contained fuel assembly may be supported by the wall of the aluminum tube in the direction of the impact. Each fuel assembly weighs 1500 pounds. The impact load on a tube is determined by multiplying the fuel assembly weight by an equivalent static deceleration factor of 55g. The impact load is considered as a uniformly distributed pressure over the entire surface of the tube wall. The impact pressure is dete ned as:

$$w = (55)(1500\ \text{lb})/(160\ \text{in} \times 9.0\ \text{in}) = 57.3\ \text{psi}$$

Assuming that the loaded tube wall is simply supported on two sides by the disks, which are at a 3.5-inch edge-to-edge distance, and on the other two sides by the vertical side walls of the tube, Reference 2, page 386, case 1, is used to calculate the maximum bending stress in the tube wall as:

$$(S_b)_{max} = \beta\ w\ b^2/t^2 = 10{,}648\ \text{psi}$$

where

$\beta = 0.669$ ($a/b = 9/3.5 = 2.57$)
$w = 57.3$ psi
$a = 9$ in = width of aluminum tube
$b = 3.5$ in = edge-to-edge spacing between adjacent disks
$t = 0.21$ in = wall thickness of aluminum tube

The margin of safety is:

$$\text{M.S.} = (12{,}900/10{,}648) - 1 = \underline{+0.21}$$

The maximum shear stress in the loaded tube wall is:

$$(S_s)_{max} = \frac{F}{A} = \frac{57.3 \times 9 \times 3.5}{2 \times 9 \times 0.21} = 477.5\ \text{psi}$$

The margin of safety is

$$\text{M.S.} = [(12900/2)/(477.5)] - 1 = \underline{+\text{Large}}$$

Therefore, the fuel tubes are structurally adequate for a 30-foot side drop accident condition.

Corner Drop

Reviewing the stress results in the tube for the side and end drop analyses, the side drop condition is much more critical. The stresses that occur during a 30-foot corner drop condition are close to, but less than, the stresses resulting from the 30-foot end drop condition. Therefore, the corner drop condition is not evaluated.

(b) Should the "borated aluminum alloy" tubes in the NAC-STC fuel basket rupture and there was leakage of water into the cask, there would be a criticality concern. The containment boundary of the NAC-STC is demonstrated to remain intact for all storage and transport load conditions, so in-leakage of water to the cask will not occur; Paragraph (a) of this response demonstrates that the tube material yield strength at operating temperature for the critical drop accident load conditions provides a minimum margin of safety of +0.21 (the margin of safety against ultimate rupture is +0.51, where S_u = 15.0 ski). Therefore, there is no criticality concern for the NAC-STC fuel basket.

(c) The stresses developed in the support disk for an end drop loading condition are calculated in the following analysis. Comparing the stress results for the side drop analyses in Section 11.2.4.7.5 of the TSAR and these end drop analyses, the calculated maximum stresses (impact + thermal) in the support disk are nearly the same; 15.8 ksi for a side drop condition and 16.4 ksi for an end drop condition with the thermal stress dominating (12.6 ksi). It is expected that the impact stress value for the corner drop condition is of the same order of magnitude as the impact stress value for the side and end drop conditions and the thermal stresses are identical. Therefore, the corner drop condition is not evaluated in detail.

End Drop

The support disks of the NAC-STC fuel basket are supported by threaded rods and spacer nuts positioned at four locations near the periphery of each disk. An ANSYS structural analysis is performed to evaluate the effect of a 30-foot end drop impact (out-of-plane loading) on the support disks in the NAC-STC with the cask in the vertical position. The ANSYS 11 element (STIF43) is used in the model as shown in Figure 1. This shell element is selected because it can accurately calculate the shear deformation effect on thick plate bending. The end drop impact loading is applied in the cask longitudinal direction (perpendicular to the plane of the support disk). A load factor of 56.1g is applied to the mass of the support disk. The value of 56.1g is the maximum deceleration of the NAC-STC for a 30-foot end drop impact. Displacement restraints are applied in the ANSYS model at the nodes where the four threaded rods with spacer nuts are located.

The 20 highest nodal stresses in the support disk resulting from thermal expansion (Table 1) are used as a basis to determine the critical combined thermal and 30-foot end drop impact stresses because the thermal expansion stresses are dominant. The maximum SIGE nodal stress (3.7 ksi, Table 2) resulting from the end impact loading, is conservatively used in the calculation of the combined thermal expansion plus end impact stresses for each of the 20 nodes with the maximum thermal expansion stresses. The absolute summation method is used to combine the thermal expansion and impact stresses. Table 3 documents the 20 nodal locations with the highest total stresses (thermal expansion stresses plus maximum end drop impact stress) at normal operation temperatures, and documents the associated margins of safety. The minimum margin of safety is +0.67. Therefore, the structural adequacy of the NAC-STC fuel basket support disk design for the 30-foot end drop accident condition is demonstrated.

Figure 1   Basket Support Disk Finite Element Model - End Impact Analysis

Figure 11.2.4-15 Finite Element Model - Gravity Analysis
(NAC-STC 26 PWR Basket Support Disk)

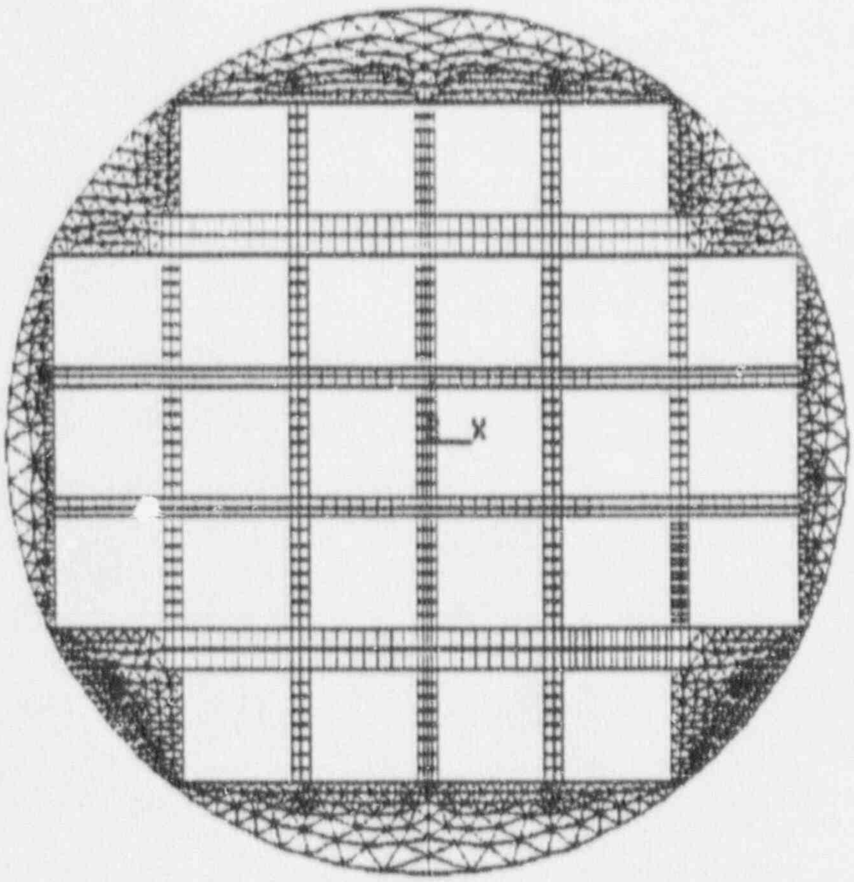

Figure 2 Location of the 20 Maximum SIGE Nodal Stresses in the NAC-STC Fuel Basket Support Disk - Thermal Condition

Figure 3.4.10-4 Location of the 20 Maximum SIGE Nodal Stresses in the NAC-STC Fuel Basket Support Disk - Thermal Condition

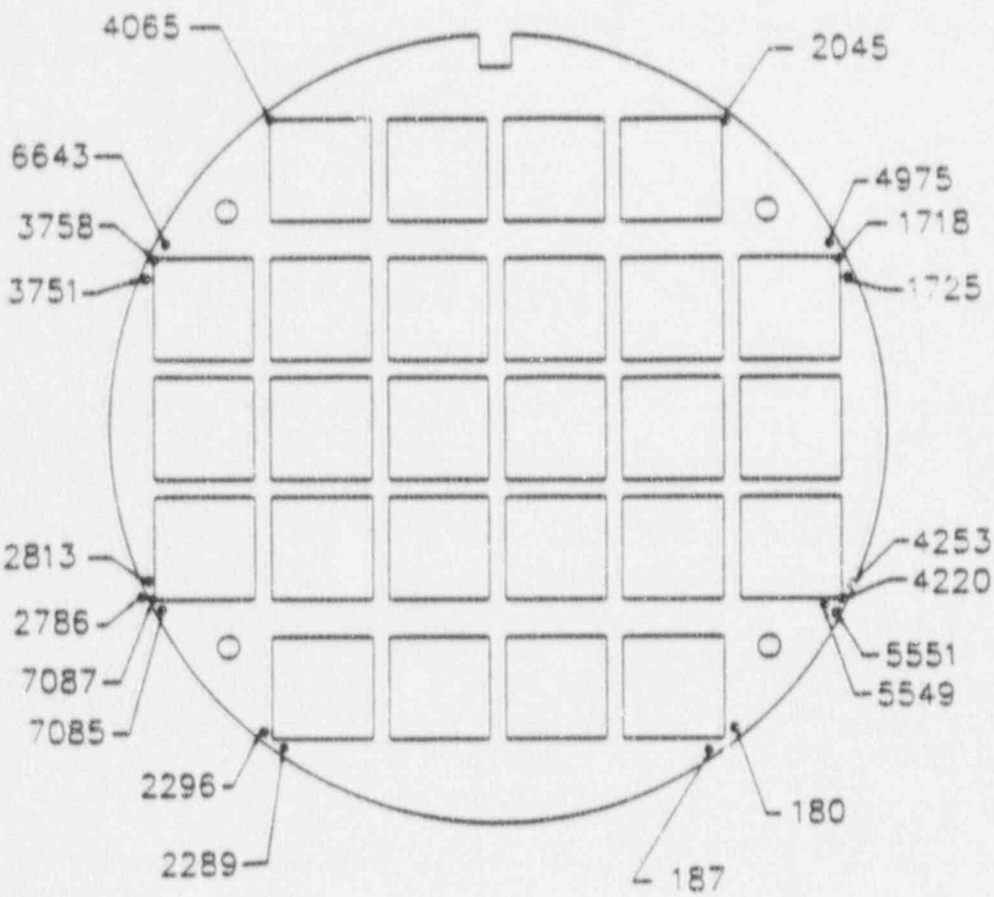

Table 1 Basket Support Disk Thermal Expansion Stresses

Location of 20 Highest Stresses[1]	Node Number	S_x (ksi)	S_y (ksi)	S_{xy} (ksi)	SIGE[2] (ksi)	Temperature (°F)
1	4220	0.3	12.6	-1.5	12.7	376
2	4065	3.6	13.5	0.7	12.2	376
3	2289	2.9	13.3	-0.6	12.1	376
4	2045	3.6	13.5	-0.7	12.1	376
5	180	2.9	13.2	0.5	12.1	376
6	3751	0.6	11.0	-0.9	10.8	376
7	1718	0.6	10.9	0.9	10.7	376
8	2786	0.7	10.6	1.1	10.5	376
9	5551	-0.8	9.7	0.1	10.1	376
10	2813	2.0	8.5	3.4	9.7	376
11	3758	2.2	8.1	-3.2	9.2	376
12	1725	2.2	8.1	3.2	9.1	376
13	6543	-0.7	8.7	-0.2	9.1	376
14	4975	-0.7	8.6	0.2	9.0	376
15	4253	0.9	7.9	-2.7	8.8	376
16	5549	0.0	8.8	0.2	8.8	376
17	7085	0.0	8.3	-0.1	8.3	376
18	7087	-0.8	7.9	0.2	8.3	376
19	2296	2.7	4.7	-4.2	8.3	377
20	187	2.7	4.7	4.1	8.3	377

[1] Stress components are listed for the nodes with the 20 highest thermal stresses. (See Figure 2 for locations of these nodes.) Note that S_x is the stress in the radial direction, S_y is the stress in circumferential direction and S_{xy} is the shearing stress.

[2] SIGE (Von Mises) Stress = (0.707) $\left[(S_x - S_y)^2 + S_x^{\,2} + S_y^{\,2} + 6\,S_{xy}^{\,2}\right]^{0.5}$

Note that the terms of S_z, S_{yz}, and S_{xz} are zero for a two-dimensional stress analysis and, therefore, are not shown in the Von Mises stress formula.

Table 2 End Drop Impact (56.1 g) Basket Support Disk Stresses

Location of 20 Highest Stresses	Node Number	S_x (ksi)	S_y (ksi)	S_{xy} (ksi)	SIGE[1] (ksi)
1	13532	-3.3	-1.4	-1.3	3.7
2	13493	-4.1	-1.7	-0.3	3.6
3	18497	-0.1	3.5	0.0	3.6
4	18122	0.1	-3.5	0.0	3.6
5	15576	0.2	3.6	0.0	3.5
6	13476	-0.2	-3.6	0.0	3.5
7	18516	0.0	3.4	-0.1	3.5
8	18141	0.0	-3.4	-0.1	3.5
9	18545	-0.2	3.3	0.3	3.4
10	18170	0.2	-3.3	0.3	3.4
11	18415	3.2	2.9	-0.8	3.4
12	18032	-3.2	-2.9	-0.8	3.4
13	18498	-0.1	3.4	0.1	3.4
14	18123	0.1	-3.4	0.1	3.4
15	18517	0.0	3.3	0.3	3.3
16	18142	0.0	-3.3	0.3	3.3
17	14097	-1.6	-1.9	1.5	3.2
18	13677	-0.5	2.9	0.0	3.2
19	18042	0.2	-3.0	-0.4	3.1
20	18425	-0.2	3.0	-0.4	3.1

[1] SIGE (Von Mises) Stress - $(0.707)\left[(S_x - S_y)^2 + S_x^{\,2} + S_y^{\,2} + 6\,S_{xy}^{\,2}\right]^{0.5}$

Table 3 Combined Thermal + End Drop Impact (56.1 g) Basket Support Disk Stresses

Node Number	Thermal SIGE Stress[1] (ksi)	End Drop SIGE Stress[2] (ksi)	Combined SIGE Stress[3] (ksi)	Temperature (°F)	Allow. Stress[4] (ksi)	Margin of Safety
4220	12.7	3.7	16.4	376	27.4	+0.67
4065	12.2	3.7	15.9	376	27.4	+0.72
2289	12.1	3.7	15.8	376	27.4	+0.73
2045	12.1	3.7	15.8	376	27.4	+0.73
180	12.1	3.7	15.8	376	27.4	+0.73
3751	10.8	3.7	14.5	376	27.4	+0.89
1718	10.7	3.7	14.4	376	27.4	+0.90
2786	10.5	3.7	14.2	376	27.4	+0.93
5551	10.1	3.7	13.8	376	27.4	+0.99
2813	9.7	3.7	13.4	376	27.4	+1.04
3758	9.2	7.7	12.9	376	27.4	+1.12
1725	9.1	3.7	12.8	376	27.4	+1.14
6543	9.1	3.7	12.8	376	27.4	+1.14
4975	9.0	3.7	12.7	376	27.4	+1.16
4253	8.8	3.7	12.5	376	27.4	+1.19
5549	8.8	3.7	12.5	376	27.4	+1.19
7085	8.3	3.7	12.0	376	27.4	+1.28
7087	8.3	3.7	12.0	376	27.4	+1.28
2296	8.3	3.7	12.0	377	27.3	+1.28
187	8.3	3.7	12.0	377	27.3	+1.28

[1] The 20 highest nodal thermal stresses (Table 1) are used as a basis for the calculation of the combined thermal + end drop impact stresses because the thermal stresses are dominant.

[2] The maximum SIGE nodal stress (3.7 ksi, Table 2) resulting from the 56.1g end drop impact loading, is conservatively used to determine the critical combined thermal and end drop impact stresses.

[3] The absolute summation method is used to calculate the combined thermal and end drop impact stresses.

[4] The allowable stresses is S_y. S_y is the yield strength of 2219-T87 aluminum alloy, including consideration of elevated temperature aging effects at operating temperature.

11.2.4.7.3 Methodology

U.S. NRC Comment

The analysis in Section 11.2.3.2 used a side drop impact force corresponding to 27.5g, while the side drop in this section uses a force corresponding to 23.5g. Please review.

NAC Response

The 27.5g side drop impact force used in Section 11.2.3.2 for each impact limiter represents the assumed design impact force of 55g for the NAC-STC for the 30-foot side drop load condition specified by 10 CFR 71; that design impact force, which is used in the 30-foot side drop analysis in Section 2.7.1.2 of the NAC-STC SAR, is used in Section 11.2.3.2 to demonstrate that the 30-foot side drop load condition analysis envelopes the storage cask tipover load condition. In this section, 11.2.4.7.3, the upper side impact limiter force for the storage cask tipover load condition is calculated in Section 3.4.9 and tabulated in Table 3.4.9-1 (2.94E06 pounds of 11.76g), is multiplied by 2 to obtain an "equivalent" total side impact force of 5.88E06 pounds (23.5g) for the analysis of the fuel basket.

11.2.4.7.4.3 Model Description

U.S. NRC Comment

(a) In the ANSYS model, what type of displacement restraints were assumed at the rod locations, hinged, fixed, or other?

(b) Please provide the basis for the gap element stiffness of 1×10^6 pound/inch.

(c) What is the contact area between the basket disk and the inner cask shell at the maximum load? Was this area used in determining the gap element stiffness?

NAC Response

(a) Different displacement restraints were used at the rod locations in the ANSYS model of the support disk depending on the type of analysis, thermal, differential thermal expansion, end drop and side drop. For the end drop analysis, roller-type displacement restraints were assumed at the rod locations; to be specific, displacement is restrained in the disk lateral direction. For the other analyses, no displacement restraint was assumed at the rod locations in the ANSYS model of the support disk.

(b) ANSYS gap elements are used to model the interface between the support disk and the inner shell. The gap elements maintain the physical boundary, and ensure no excessive overlapping between the support disk and the inner shell.

The initial trial stiffness of the gap elements is first determined by performing hand calculations using the formula:

$P = (K_g)(u)$,

where P = force
u = displacement
K_g = gap element stiffness

and $K_g = AE/L$,

where A = Unit contact area at the interface between the support disk and the cask inner shell
= 2.5 square inches
E = Young's Modulus of Aluminum
= 10×10^6 psi
L = support disk diameter
= 70.85 inch

The value of $K_g = AE/L$ is 3.5×10^5 pounds/inch. Therefore, a trial value of 1.0×10^6 pounds/inch is used as the gap element stiffness in the initial ANSYS analysis run. The analysis results are then examined to ensure that any overlapping between the deformed support disk and the cask inner shell in the ANSYS model is less than 5 percent of the thickness of the inner shell; the actual overlap is only 0.5 percent; therefore, the gap element stiffness of 1.0×10^6 psi is appropriate for use in the basket support disk side drop evaluations.

(c) The contact area is essentially the 180° arc surface between the basket support disk and the cask inner shell resulting from the most critical loading condition, thermal plus side drop. The contact surface ranges from 140° to 180° for other loading conditions. This data was not used to determine the gap element stiffness.

11.2.4.7.5 Analysis Results

U.S. NRC Comment

(a) Why were the 23.5g results not directly scaled from the 55g results? The 23.5g results appear to be calculated by first adding the 55g results to the thermal stress values and then subtracting the thermal stress results. The difference is then scaled to 23.5g.

(b) Since the Von Mises Stress is not direction dependent, it should not be used for load combinations. The combination of load cases should be done using the stress components referring to the same coordinate system.

NAC Response

(a) The stress results for the combined thermal plus 55g impact loading condition are obtained from the analysis considering the combined thermal and impact effects. No analysis was performed for the impact load only. Therefore, the stress results for the combined thermal plus 23.5g impact loading condition are calculated by:

(1) subtracting the thermal stresses from the combined stresses for the thermal plus 55g impact loading,

(2) ratioing the 55g impact stresses by 5/55); and

(3) adding back the thermal stresses to the 23.5g side impact stresses to obtain the combined stresses for the thermal plus 23.5g impact loading condition.

More than 80 percent of the combined thermal plus 55g impact stresses are thermal stresses; therefore, no significant inaccuracy is introduced by the use of a ratio to scale the impact stresses from 55g to 23.5g.

(b) NAC agrees that for the most accurate results, the combination of load cases should be done using the stress components referring to the same coordinate system. However, NAC has determined that for the fuel basket support disk analysis, the direction addition of the Von Mises SIGE stresses for the thermal and the impact load conditions produces higher (conservative) total stress values than does the combination of the stress components for the same load conditions. Thus, the simpler direct addition method is used in this analysis.

11.2.4.7.6.4 Threaded Rods and Spacer Nuts - Accident Conditions

U.S. NRC Comment

(a) After computing the average compressive stress, was a buckling analysis done for the rods? For the end drop, buckling is a critical concern.

(b) Although the end drop is thought to be the most critical load case for the basket threaded rods, please explicitly address the side and corner drops and provide reasons for omitting the analyses for these drop cases.

NAC Response

(a) The classical Euler buckling equation is used to determine the critical buckling load for the threaded rods:

$$P_{cr} = \pi^2 E I / L^2$$

where E = Young's Modulus for the 2024-T351 aluminum alloy at 360°F.
= 9.6×10^6 psi
I = the moment of inertia for the threaded rod
= $\pi d^4 / 64$
where d = 1.378 inches is the rod diameter derived from the rod tensile area (tensile area = 1.492 in^2 = $\pi d^2 /4$)
= 0.177 inch^4
L = the length of the threaded rod between the bottom plate and the first adjacent support disk
= 6.4 inch

The calculated P_{cr} (critical buckling load) for a threaded rod is 409,768 pound, which is much greater than the maximum calculated load, P = 649,715/4 = 162,480 pounds on each rod. Therefore, the buckling of the threaded rods is not a concern. The structural rigidity of the spacer nuts is conservatively not included in these buckling calculations.

(b) For the side drop case, the fuel assembly loads are transmitted in direct compression through the tube wall to the web structure of each support disk. The loads are transmitted to the inner shell of the cask by the series of 25 support disks and the top and bottom plates. Therefore, the threaded rods are not subjected to the weight of the support disks or fuel assembly for a side drop condition. The threaded rods are loaded in shear by the weight of the spacer nuts for a side drop condition. The larger spacer nuts weigh approximately 5 pounds each; using a 55g impact load factor and the rod tensile area multiplied by 2 (double shear), the shear stress on the threaded rod is only 93 psi, which is negligible. For an end drop condition, the threaded rods are loaded with the full weight of the support disks and one of the top and bottom plates as shown in the analysis in Section 11.2.4.7.6.4. For the corner drop condition the threaded rods only take the cosine component of the full weight used for the end drop condition. Therefore, the threaded rods are evaluated only for the most critical load case, which is the end drop condition.

11.2.4.8.1 Geometry and Loads

U.S. NRC Comment

Is the analysis for the top end drop included in the TSAR? How were the corresponding 37.0g and 48.6g decelerations calculated?

NAC Response

No, the analysis for the top end drop condition is not included in the TSAR. The top end drop event is not a credible occurance for a storage cask.

The 37.0g and 48.6g decelerations are calculated for the NAC-STC transport impact limiter using the RBCUBED computer program (Section 2.6.7.4 of the NAC-SAR).

11.2.4.9 Accident Dose Calculations

U.S. NRC Comment

The lead slump analysis should include the additional lead slump caused by radial displacements. The radial displacements are the results of the high hydrostatic pressure existing in the slumping lead shield. What is the amount of the lead slump calculated with the formula given in ORNL-NSIC-68 (Cask Design Guide by L. Shappert)?

NAC Response

As discussed in Section 11.2.4.9, the lead slump calculation for the NAC-STC very conservatively assumes that lead movement completely fills the 0.0324-inch radial gap that exists between the outer shell and the lead as a result of the lead contraction following lead pour. Based on SCANS analyses, the calculated lead slump is essentially zero, primarily because of the relatively soft NAC-STC impact limiters that permit the lead to remain elastic during a 30-foot drop impact. (Refer to Paragraph (a) of the NAC Response to Comment 3.3.6.1). The formula given in ORNL-NSIC-68 (Cask Design Guide by L. Shappert) is not applicable, since it was developed based on the hard impact incurred by casks without impact limiters (ORNL TM-1312, Volume 6).

The lead in the NAC-STC remains elastic during a 30-foot drop impact; thus, the moduli of elasticity tabulated in Tables 3.3.6-1 and 3.3.6-2 of the NAC-STC TSAR are appropriate for use in the 6-foot drop and the tipover impact analyses in the TSAR and in the 1-foot and 30-foot drop analyses in the SAR. The elastic behavior of the lead is verified by the comparison of the outer shell stresses measured during the 30-foot top end drop test of the NAC-STC quarter-scale model with those calculated by the SCANS 30-foot top end drop analyses using the elastic modulus of lead (refer to Table 1 in the NAC Response to Comments 3.3.6.1). A SCANS analysis was also performed for a 30-foot top end drop using the elastic-plastic modulus of elasticity for lead as defined in the SCANS program documentation; the calculated outer shell stresses are also tabulated in the attached table. Since the measured hoop (S_t) and axial (S_z) stresses in the outer shell for the quarter-scale model top end drop compare favorably with those SCANS calculated values using the elastic lead modulus and are greatly different than those values calculated by SCANS using the elastic-plastic lead modulus, it is evident that the lead remains elastic during a 30-foot drop impact.

Based on the elastic lead modulus, the calculated and measured maximum hoop stress in the outer shell is 2.0 ksi, which results from an internal pressure in the lead of 126 psi; this pressure produces an outward radial deflection of the outer shell of 0.0026 inch and an inward radial deflection of the inner shell of 0.0022 inch; incorporating these deflections into the lead slump calculation, which very conservatively assumes that the lead moves to completely fill the annulus between the inner and outer shells, yields a lead slump of 1.957 inches. As stated at the top of page 11.2.4-92, the lead slump is approximately one-half of the height of the end-fitting, but the dose rate calculation very conservatively assumes that the full height of the end-fitting is exposed; therefore, the calculated dose rates are unchanged and the shielding consequences of the accident remain bounded by the complete loss of radial neutron shield accident.

11.2.13.1.2 Accident Analysis (15-Inch Bottom End Drop Onto a Concrete Pad)

U.S. NRC Comment

The soil and concrete model presented in the TSAR needs proof that the analytical model is conservative and that it envelopes all possible site conditions; otherwise separate action must be taken for each site. Use of an unyielding surface model is approved in a more timely manner than a soil and concrete model. The 15-inch bottom end drop analysis should be redone with a finite element model of the cask impacting an unyielding surface.

NAC Response

The soil and concrete model presented in the TSAR describes the configurations and specifications for a typical dry-storage concrete pad. If the pad at a specific site is more rigid than that analyzed in this section, a bottom impact limiter is required; a statement to that effect will be added to the last paragraph in Section 11.2.13.1.2 of the TSAR.